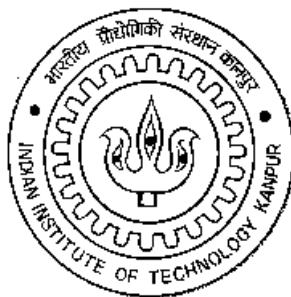


h-p spectral element methods for three dimensional elliptic problems on non-smooth domains using parallel computers

Akhlaq Husain¹



DEPARTMENT OF MATHEMATICS AND STATISTICS
INDIAN INSTITUTE OF TECHNOLOGY KANPUR

June, 2010

¹This is a reprint of the PhD thesis of the author, which was submitted on 11th June, 2010 and defended on 14th January, 2011 at IIT Kanpur, India

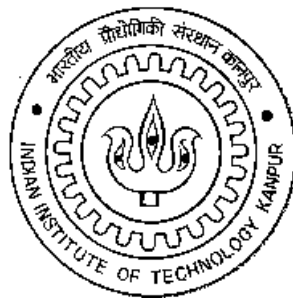
h-p spectral element methods for three dimensional elliptic problems on non-smooth domains using parallel computers

A Thesis Submitted
in Partial Fulfillment of the Requirements
for the Degree of

Doctor of Philosophy

by

Akhlaq Husain²



to the

DEPARTMENT OF MATHEMATICS AND STATISTICS
INDIAN INSTITUTE OF TECHNOLOGY KANPUR

June, 2010

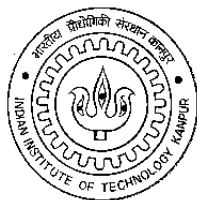
1 2

¹This is a reprint of the PhD thesis of the author, which was submitted on 11th June, 2010 and defended on 14th January, 2011 at IIT Kanpur, India

²Dr. Akhlaq Husain

LNM Institute of Information Technology

Rupa ki Nangal, Post-Sumel, Via-Jamdoli, Jaipur-302031, Rajasthan, INDIA



CERTIFICATE

It is certified that the work contained in the thesis entitled “ **$h - p$ spectral element methods for three dimensional elliptic problems on non-smooth domains using parallel computers**” by Akhlaq Husain, has been carried out under our supervision and that this work has not been submitted elsewhere for a degree.

Pravir Dutt
(Professor)
Department of Mathematics
and Statistics
Indian Institute of Technology
Kanpur

A.S. Vasudeva Murthy
(Professor)
TIFR Centre for Applicable
Mathematics
Tata Institute of Fundamental Research
Bangalore

June, 2010

ABSTRACT

Elliptic partial differential equations arise in many fields of science and engineering such as steady state distribution of heat, fluid dynamics, structural/mechanical engineering, aerospace engineering, medical science and seismology etc.

In three dimensions it is well known that the solutions of elliptic boundary value problems have singular behaviour near the corners and edges of the domain. The singularities which arise are known as vertex, edge, and vertex-edge singularities. Due to the presence of singularities the conventional numerical methods are unable to provide accurate numerical solutions and the rate of convergence of these methods degrades. In order to improve efficiency of computations and accuracy of the solutions, it is desirable to find efficient methods along with standard numerical techniques such as finite element method (FEM), spectral element method (SEM) and so on.

We propose a nonconforming $h-p$ spectral element method to solve three dimensional elliptic boundary value problems on non-smooth domains to exponential accuracy.

To overcome the singularities which arise in the neighbourhoods of the vertices, vertex-edges and edges we use local systems of coordinates. Away from these neighbourhoods standard Cartesian coordinates are used. In each of these neighbourhoods we use a *geometrical mesh* which becomes finer near the corners and edges. The geometrical mesh becomes a *quasi-uniform mesh* in the new system of coordinates. Hence *Sobolev's embedding theorems* and the *trace theorems* for Sobolev spaces are valid for spectral element functions defined on mesh elements in the new system of variables with a uniform constant. We then derive *differentiability estimates* in these new sets of variables and a *stability estimate*, on which our method is based, for a non-conforming $h-p$ spectral element method.

We choose as our approximate solution the spectral element function which minimizes the sum of a weighted squared norm of the residuals in the partial differential equations and the squared norm of the residuals in the boundary conditions in fractional Sobolev spaces and enforce continuity by adding a term which measures the jump in the function

and its derivatives at inter-element boundaries in fractional Sobolev norms, to the functional being minimized. The Sobolev spaces in vertex-edge and edge neighbourhoods are anisotropic and become singular at the corners and edges.

The method is essentially a *least-squares collocation* method and a solution can be obtained using *Preconditioned Conjugate Gradient Method (PCGM)*. To solve the minimization problem we need to solve the *normal equations* for the *least-squares* problem. The residuals in the normal equations can be obtained without computing and storing *mass* and *stiffness* matrices.

We solve the normal equations using a block diagonal preconditioner where each block corresponds to the square of H^2 norm of the SEF defined on a particular element. Moreover it is shown that there exists a diagonal preconditioner using separation of variables technique. Let N denote the number of refinements in the geometrical mesh. We shall assume that N is proportional to W .

For problems with Dirichlet boundary conditions the condition number of the preconditioned system is $O((\ln W)^2)$, provided $W = O(e^{N^\alpha})$ for $\alpha < 1/2$. Moreover there exists a new preconditioner which can be diagonalized in a new set of basis functions, using separation of variables techniques, in which each diagonal block corresponds to a different element, and hence it can easily be inverted on each element. For Dirichlet problems the method requires $O(N \ln N)$ iterations of the PCGM to obtain solution to exponential accuracy and it requires $O(N^5 \ln(N))$ operations on a parallel computer with $O(N^2)$ processors to compute the solution. For mixed problems with Neumann and Dirichlet boundary conditions the condition number of the preconditioned system is $O(N^4)$, provided $W = O(e^{N^\alpha})$ for $\alpha < 1/2$. Hence, it requires $O(N^3)$ iterations of the PCGM to obtain solution to exponential accuracy and requires $O(N^7)$ operations on a parallel computer with $O(N^2)$ processors to compute the solution.

Computational results for a number of model problems confirm the theoretical estimates obtained for the error and computational complexity.

Synopsis

Name of the Student	: Akhlaq Husain
Roll Number	: Y4108061
Degree for which submitted	: Ph.D.
Department	: Mathematics
Thesis Title	: $h - p$ Spectral Element Methods for Three Dimensional Elliptic Problems on Non-smooth Domains using Parallel Computers
Thesis Supervisors	: Dr. Pravir K. Dutt and Dr. A. S. Vasudeva Murthy
Month and year of submission	: June, 2010

Elliptic partial differential equations arise in many fields of science and engineering such as steady state distribution of heat, fluid dynamics, structural/mechanical engineering, aerospace engineering, medical science and seismology etc. Elliptic boundary value problems in polygonal and polyhedral domains have been studied in many works in the literature. Among these, problems on polyhedral domains with corners and edges have become increasingly important in the last two decades. In many practical situations, the physical domain often has corners and edges either due to its geometry or created by unions and intersections of simpler objects such as cylinders, cones and spheres. Hence singularities of the solutions occur at the corners and edges, and severely affect the regularity of the solutions.

In three dimensions it is well known that the solutions of elliptic boundary value problems have singular behaviour near the corners and edges of the domain. The singularities which arise are known as vertex, edge, and vertex-edge singularities. Due to the presence of singularities the conventional numerical methods are unable to provide accurate numerical solutions and the rate of convergence of these methods degrades. In order to improve efficiency of computations and accuracy of the solutions, it is desirable to find efficient methods along with standard numerical techniques such as finite element method (FEM), spectral element method (SEM) and so on. Different approaches and methods have been attempted over the years to find accurate solutions to the elliptic boundary value problems on polyhedrons containing singularities.

We propose a nonconforming $h-p$ spectral element method to solve three dimensional elliptic boundary value problems on non-smooth domains to exponential accuracy.

To overcome the singularities which arise in the neighbourhoods of the vertices, vertex-edges and edges we use local systems of coordinates. These local coordinates are modified versions of spherical and cylindrical coordinate systems in their respective neighbourhoods. Away from these neighbourhoods standard Cartesian coordinates are used. In each of these neighbourhoods we use a *geometrical mesh* which becomes finer near the corners and edges. The geometrical mesh becomes a *quasi-uniform mesh* in the new system of coordinates. Hence *Sobolev's embedding theorems* and the *trace theorems* for Sobolev spaces are valid for spectral element functions defined on mesh elements in the new system of variables with a uniform constant. We then derive *differentiability estimates* in these new sets of variables and a *stability estimate*, on which our method is based, for a non-conforming $h-p$ spectral element method.

We choose as our approximate solution the spectral element function which minimizes the sum of a weighted squared norm of the residuals in the partial differential equations and the squared norm of the residuals in the boundary conditions in fractional Sobolev spaces and enforce continuity by adding a term which measures the jump in the function and its derivatives at inter-element boundaries in fractional Sobolev norms, to the functional being minimized. The Sobolev spaces in vertex-edge and edge neighbourhoods are anisotropic and become singular at the corners and edges.

The spectral element functions are represented by a uniform constant at all the corner elements in vertex neighborhoods and on the corner-most elements in vertex-edge neighbourhoods which are in the angular direction to the edges. At corner elements which are in the direction of edges in vertex-edge neighbourhoods and at all the corner elements in edge neighbourhoods the spectral element functions are represented as one dimensional polynomials of degree W in the modified coordinates. In all other elements in edge neighbourhoods and vertex-edge neighbourhoods the spectral element functions are a sum of tensor products of polynomials of degree W in their respective modified coordinates. The remaining elements in the vertex neighbourhoods and the regular region are mapped to the master cube and the spectral element functions are represented as a sum of tensor products of polynomials of degree W in λ_1, λ_2 , and λ_3 , the transformed variables on the master cube.

The method is essentially a *least-squares collocation* method and a solution can be obtained using *Preconditioned Conjugate Gradient Method (PCGM)*. To solve the minimization problem we need to solve the *normal equations* for the *least-squares* problem. The residuals in the normal equations can be obtained without computing and storing *mass* and *stiffness* matrices.

We choose spectral element functions (SEF) which are non-conforming. We solve the normal equations using a block diagonal preconditioner where each block corresponds to the square of H^2 norm of the SEF defined on a particular element. Let N denote the number of refinements in the geometrical mesh. We shall assume that N is proportional to W .

For problems with Dirichlet boundary conditions the condition number of the preconditioned system is $O((\ln W)^2)$, provided $W = O(e^{N^\alpha})$ for $\alpha < 1/2$. Moreover there exists a new preconditioner which can be diagonalized in a new set of basis functions, using separation of variables techniques, in which each diagonal block corresponds to a different element, and hence it can easily be inverted on each element. For Dirichlet problems the method requires $O(N \ln N)$ iterations of the PCGM to obtain solution to exponential accuracy and it requires $O(N^5 \ln(N))$ operations on a parallel computer with $O(N^2)$ processors to compute the solution. For mixed problems with Neumann and Dirichlet

boundary conditions the condition number of the preconditioned system is $O(N^4)$, provided $W = O(e^{N^\alpha})$ for $\alpha < 1/2$. Hence, it requires $O(N^3)$ iterations of the PCGM to obtain solution to exponential accuracy and requires $O(N^7)$ operations on a parallel computer with $O(N^2)$ processors to compute the solution.

We mention that once we have obtained our approximate solution consisting of non-conforming spectral element functions we can make a correction to it so that the corrected solution is conforming and is an exponentially accurate approximation to the actual solution in the H^1 norm over the whole domain.

Our method works for non self-adjoint problems too. Computational results for a number of model problems on non-smooth domains with constant and variable coefficients having smooth and singular solutions are presented which confirm the theoretical estimates obtained for the error and computational complexity.

For mixed problems rapid growth of the factor N^4 creates difficulty in parallelizing the numerical scheme. To overcome this difficulty another version of the method may be defined in which we choose spectral element functions to be conforming only on the wirebasket of the elements and non-conforming elsewhere. The values of the spectral element functions at the wirebasket of the elements constitute the set of common boundary values and an accurate approximation to the Schur complement matrix can be computed. We plan to consider this in future work.

Contents

Synopsis	vii
Contents	xi
List of Figures	xv
List of Tables	xix
1 Introduction	1
1.1 Spectral Methods	2
1.2 Types of Spectral Methods	4
1.2.1 Collocation method	4
1.2.2 Galerkin method	5
1.2.3 Tau method	6
1.3 Spectral Methods on Non-smooth Domains	6
1.3.1 Gradual h refinement	8
1.3.2 Method of auxiliary or conformal mapping	8
1.3.3 Advantages and applications of spectral methods: A survey	16
1.3.4 Limitations of spectral methods	18
1.4 Finite Element Method	18
1.4.1 Method of weighted residuals	20
1.4.2 Advantages of FEM	22
1.4.3 Disadvantages of FEM	23
1.4.4 Spectral vs. finite element methods	23

1.5	Non-conforming Methods	24
1.6	$h - p$ /Spectral Element Methods on Parallel Computers	25
1.7	Review of Existing Work	26
1.8	Review and Outline of the Thesis	28
2	Differentiability and Stability Estimates	33
2.1	Introduction	33
2.2	Differentiability Estimates in Modified Coordinates	35
2.2.1	Differentiability estimates in modified coordinates in vertex neighbourhoods	36
2.2.2	Differentiability estimates in modified coordinates in edge neighbourhoods	38
2.2.3	Differentiability estimates in modified coordinates in vertex-edge neighbourhoods	39
2.2.4	Differentiability estimates in standard coordinates in the regular region of the polyhedron	41
2.2.5	Function spaces	42
2.3	The Stability Theorem	44
3	Proof of the Stability Theorem	63
3.1	Introduction	63
3.2	Estimates for the Second Derivatives of Spectral Element Functions	64
3.2.1	Estimates for the second derivatives in the interior	64
3.2.2	Estimates for second derivatives in vertex neighbourhoods	71
3.2.3	Estimates for second derivatives in vertex-edge neighbourhoods	78
3.2.4	Estimates for second derivatives in edge neighbourhoods	83
3.3	Estimates for Lower Order Derivatives	87
3.4	Estimates for Terms in the Interior	88
3.4.1	Estimates for terms in the interior of Ω^r	88
3.4.2	Estimates for terms in the interior of Ω^e	89
3.4.3	Estimates for terms in the interior of Ω^v	90

3.4.4	Estimates for terms in the interior of Ω^{v-e}	91
3.5	Estimates for Terms on the Boundary	93
3.5.1	Estimates for terms on the boundary of Ω^r	93
3.5.2	Estimates for terms on the boundary of Ω^e	95
3.5.3	Estimates for terms on the boundary of Ω^v	96
3.5.4	Estimates for terms on the boundary of Ω^{v-e}	96
3.6	Proof of the Stability Theorem	97
4	The Numerical Scheme and Error Estimates	101
4.1	Introduction	101
4.2	The Numerical Scheme	102
4.3	Error Estimates	108
5	Solution Techniques on Parallel Computers	117
5.1	Introduction	117
5.2	Preconditioning	118
5.2.1	Preconditioners on the regular region	118
5.2.2	Preconditioners on singular regions	123
5.3	Parallelization Techniques	129
5.3.1	Integrals on the element domain	130
5.3.2	Integrals on the boundary of the elements	134
6	Numerical Results	139
6.1	Introduction	139
6.2	Test Problems in Regular Regions	141
6.3	Test Problems in Singular Regions	157
6.4	Conclusions and Future Work	170
6.4.1	Summary and conclusions	170
6.4.2	Proposed future work	172
	Appendix A	173

Appendix B	181
Appendix C	197
Appendix D	215
Bibliography	245

List of Figures

1.1	Computational domain Ω containing a corner of angle $\theta = \alpha\pi$	7
1.2	Auxiliary mapping of a domain containing a corner to a domain with no corners.	9
1.3	Typical three-dimensional singularities.	10
2.1	Polyhedral domain Ω in R^3	36
2.2	Vertex neighbourhood Ω^v	36
2.3	Edge neighbourhood Ω^e	39
2.4	Vertex-edge neighbourhood Ω^{v-e}	40
2.5	Division of a tetrahedron into hexahedrons.	45
2.6	Elements in Ω^r	46
2.7	Mesh imposed on the spherical boundary S^v	48
2.8	Geometrical mesh imposed on Ω^v	48
2.9	Geometrical mesh imposed on Ω^{v-e}	51
2.10	Geometrical mesh imposed on Ω^e	56
3.1	The element Ω_l^r	66
3.2	Boundary terms.	94
5.1	κ vs. W	123
6.1	The domain $\Omega = Q$ = standard cube with uniform mesh refinements. . . .	141
6.2	Mesh imposed on $\Omega = (0, 1)^3$ with mesh size $h = 0.5$	142
6.3	Error vs. p , Iterations vs. p , Error vs. DOF and Error vs. Iterations for Laplace equation.	143

6.4	Error vs. p , Iterations vs. p , Error vs. DOF and Error vs. Iterations for Poisson equation.	145
6.5	Error vs. p , Iterations vs. p , Error vs. DOF and Error vs. Iterations for Poisson equation with mixed boundary conditions.	146
6.6	Error vs. p , Iterations vs. p , Error vs. DOF and Error vs. Iterations for Helmholtz problem.	149
6.7	Comparison between h and p versions: Error vs. DOF.	149
6.8	Error vs. p , Iterations vs. p , Error vs. DOF and Error vs. Iterations for elliptic problem with variable coefficients.	151
6.9	Mesh imposed on domain Ω containing 24 brick elements	152
6.10	Error vs. p , Iterations vs. p , Error vs. DOF and Error vs. Iterations for elliptic problem on L-shaped domain.	153
6.11	Error as a function of W for different values of h for general elliptic (non self-adjoint) problem.	155
6.12	Error vs. p , Iterations vs. p , Error vs. DOF and Error vs. Iterations for general elliptic (non self-adjoint) problem.	156
6.13	The domain $\Omega^{(v)}$ containing a vertex singularity.	158
6.14	Geometric mesh imposed on $\Omega^{(v)}$ and elements after mapping.	158
6.15	Error vs. p , Iterations vs. N , Error vs. N_{dof} and Error vs. Iterations for Poisson equation containing a vertex singularity.	160
6.16	Error vs. p , Iterations vs. N , Error vs. N_{dof} and Error vs. Iterations for mixed problem containing a vertex singularity.	162
6.17	The domain $\Omega_1^{(e)}$ containing an edge singularity.	163
6.18	Error vs. p , Iterations vs. N , Error vs. N_{dof} and Error vs. Iterations for Laplace equation containing an edge singularity.	164
6.19	The domain $\Omega_2^{(e)}$ containing an edge singularity.	165
6.20	Geometric mesh imposed on $\Omega_2^{(e)}$	166
6.21	Error vs. p , Iterations vs. N , Error vs. N_{dof} and Error vs. Iterations for mixed problem containing an edge singularity.	167
6.22	The domain $\Omega^{(v-e)}$	168

6.23	Geometrical mesh imposed on $\Omega^{(v-e)}$ and the elements after mapping. . . .	168
6.24	Error vs. p , Iterations vs. N , Error vs. N_{dof} and Error vs. Iterations for Poisson equation containing a vertex-edge singularity.	169
B.1	Interior common boundary face $\Gamma_{k,i}^v = \Gamma_{q,r}^{v-e}$	181
B.2	The face $\tilde{\Gamma}_{k,i}^v$	184
B.3	The face $\tilde{\Gamma}_{q,r}^{v-e}$	185
B.4	Interior common boundary face $\Gamma_{u,k}^e = \Gamma_{n,l}^{v-e}$	188
B.5	The face $\tilde{\Gamma}_{u,k}^e$	190
B.6	The face $\tilde{\Gamma}_{n,l}^{v-e}$	191
C.1	The element Ω_l^r and the master cube.	198
C.2	Image of Ω_l^{v-e} in y -variables.	201
C.3	The function $r(y_3)$	202
C.4	The function $s(y_3)$	202
C.5	The element $\hat{\Omega}_l^{v-e}$	206
C.6	Faces f_1 and f_2	207
C.7	Sides $s_i, i = 1, \dots, 12$ and faces $f_i, i = 1, \dots, 6$ of a typical element in vertex-edge neighbourhood.	208
D.1	A common face in the interior of the edge neighbourhood in $x_1^e - x_2^e$ plane.	226
D.2	$\hat{\gamma}$, image of $\tilde{\gamma}$, in z -coordinates.	227
D.3	A common face in the interior of the edge neighbourhood in $x_1^e - x_3^e$ plane.	228
D.4	$\hat{\gamma}$, image of $\tilde{\gamma}$, in z -coordinates.	229
D.5	Division of $\hat{\Omega}_m^e$ into smaller rectangles.	229
D.6	The face $\Gamma_{m,j}^r$ of the boundary element Ω_m^r	234
D.7	The face $\Gamma_{m,p}^e$ of the boundary element Ω_m^e	239
D.8	The edge $\tilde{\gamma}$	241
D.9	The edge $\hat{\gamma}$	242

List of Tables

1.1	Weight functions $w_j(\mathbf{x})$ used in the method of residual and the method produced.	21
5.1	Condition number κ as a function of W	123
6.1	Performance of the p –version for Laplace equation with Dirichlet boundary conditions	143
6.2	Performance of the p –version for Poisson equation with homogeneous boundary conditions	144
6.3	Performance of the p –version for Poisson equation with mixed boundary conditions	146
6.4	Performance of the h –version for Helmholtz problem	148
6.5	Performance of the p –version for Helmholtz problem on Mesh 2	148
6.6	Performance of the p –version for elliptic problem with variable coefficients	150
6.7	Performance of the p –version for elliptic problem on L-shaped domain . .	153
6.8	Performance of the p –version on different meshes for general elliptic (non self-adjoint) problem with variable coefficients	155
6.9	Performance of the p –version for non self-adjoint problem.	156
6.10	Performance of the $h - p$ version for Dirichlet problem on $\Omega^{(v)}$ containing a vertex singularity	159
6.11	Performance of the $h - p$ version for mixed problem on $\Omega^{(v)}$ containing a vertex singularity	161
6.12	Performance of the $h - p$ version for Laplace equation on $\Omega_1^{(e)}$	163

6.13	Performance of the method for Laplace equation with mixed boundary conditions on $\Omega_2^{(e)}$ containing an edge singularity	166
6.14	Performance of the method for Poisson equation on $\Omega^{(v-e)}$ containing a vertex-edge singularity	169

Chapter 1

Introduction

Many stationary phenomena in science and engineering are modelled by elliptic boundary value problems for instance, the elasticity problem on polyhedral domains. Usually we do not have a closed form solution of the problem. So we frequently require the numerical solution of these problems. In structural mechanics the physical domain often has edges, vertices, cracks and interface between different materials. It is well known that the solutions of these problems develop singularities due to the presence of corners and edges in a three-dimensional domain. In the presence of singularities, the standard numerical methods such as finite element method (FEM) and finite difference method (FDM) fail to provide accurate solutions and efficiency of computations. The situation is even worse if the singularity is more severe, for example, a vertex-edge singularity. As a result the approximation becomes difficult and inefficient and the conventional numerical methods yield poor convergence results for solutions to these problems. In order to have reliable and economical approximate solutions with optimal rate of convergence, it is desirable to find efficient and accurate numerical techniques.

We propose $h - p$ **Spectral Element Methods for Three Dimensional Elliptic Problems on Non-smooth Domains using Parallel Computers**. In this chapter, we give a brief review of the existing numerical methods for such problems and discuss their computational complexity.

1.1 Spectral Methods

Spectral Element Methods (SEM) are a class of spatial discretizations that can be utilized for solving partial differential equations. Spectral methods are one of the most accurate methods for solving partial differential equations, among others namely Finite Difference Methods (FDM) and Finite Element Methods (FEM).

Spectral methods are considered as higher order finite element methods due to their so called *spectral/exponential* accuracy and use of high order polynomials for computing numerical solution. The very high accuracy of spectral methods allows us to treat problems which would require an enormous number of grid points by finite difference or finite element methods with much fewer degrees of freedom.

Spectral methods were proposed by Blinova [25] and first implemented by Silberman [80], but abandoned in the mid-1960s. Orszag [70] and Eliassen *et al.* [40] resurrected them again. The formulation of the theory of modern spectral methods was first presented in the monograph by Gottlieb and Orszag [44] for the numerical solution of partial differential equations. Multi-dimensional discretizations were formulated as tensor products of one-dimensional constructs in separable domains. Since then spectral methods were extended to a broader class of problems and thoroughly analyzed in the 1980s and entered the mainstream of scientific computation in the 1990s. The text book of Canuto *et al.* [27] focuses on fluid dynamics algorithms and includes both practical as well as theoretical aspects of global spectral methods. A companion book *Spectral Methods, Fundamentals in Single Domains* by Canuto *et al.* [28] is focused on the essential aspects of spectral methods on separable domains. The book *Spectral/hp Element Methods for Computational Fluid dynamics*, by Karniadakis and Sherwin [55], deals with many important practical aspects of computations using spectral methods and summarizes the recent research in the subject. In the latest book by Bochev and Gunzburger [26] the least-squares finite element method (LSFEM) for elliptic problems have been described.

The first practitioners of spectral methods were meteorologists studying global weather modelling and fluid dynamicists investigating isotropic turbulence. The original idea was to use truncated Fourier series to approximate the (smooth) solution when the problem

was specified with (mostly) periodic boundary conditions. In order to tackle problems with more general boundary conditions (Dirichlet or Neumann type), the set of (algebraic) polynomials replaced the set of truncated series, but the characterization of the unique discrete function that would provide the numerical solution was still achieved following the original strategy.

The key components for spectral methods are the *trial functions* (also called the expansion or approximating functions) and the *test functions* (also known as weight functions). The trial functions, which are linear combinations of suitable trial basis functions, are used to provide the approximate representation of the solution. The test functions are used to ensure that the differential equation and some boundary conditions are satisfied as closely as possible by the truncated series expansion. This is achieved by minimizing, with respect to a suitable norm, the residual produced by using the truncated expansion instead of the exact solution. For this reason they may be viewed as a special case of the method of weighted residuals (Finlayson and Scriven, [41]). An equivalent requirement is that the residual satisfy a suitable orthogonality condition with respect to each of the test functions. From this perspective, spectral methods may be viewed as a special case of Petrov-Galerkin methods (Zienkiewicz and Cheung [93], Babuška and Aziz [6]).

The most frequently used approximation functions (trial functions) are trigonometric polynomials, Chebyshev polynomials, and Legendre polynomials. Generally, trigonometric polynomials are used for periodic problems whereas Chebyshev and Legendre polynomials for non-periodic problems. Laguerre polynomials are used for problems on semi-infinite domains and Hermite polynomials for problems on infinite domains.

Boyd [24] contains a wealth of detail and advice on spectral algorithms and is an especially good reference for problems on unbounded domains and in cylindrical and spherical co-ordinate systems. A thorough analysis of the theoretical aspect of spectral methods for elliptic equations was provided by Bernardi and Maday [23].

1.2 Types of Spectral Methods

Spectral methods can be broadly classified into two categories: the pseudo-spectral or collocation methods and the Galerkin methods [55]. The choice of the trial functions distinguishes between the three early versions of spectral methods, namely, the *collocation*, *Galerkin* and *tau* versions [28].

1.2.1 Collocation method

In the collocation approach the test functions are translated Dirac delta-functions centered at special, so-called *collocation points*. This approach requires the differential equation to be satisfied exactly at the collocation points. Of course the choice of the set of collocation points is of fundamental importance for the accuracy of the method and the number of collocation points must be equal to the dimension of the space of approximation. Otherwise, the problem could, in general, be over- or under-specified. The collocation points for both the differential equations and the boundary conditions are usually the same as the physical grid points. The most effective choice for the grid points are those that correspond to quadrature formulae of maximum precision.

The collocation approach appears to have been first used by Slater [83] and by Kantorovic [54] in specific applications. Frazer *et al.* [42] developed it as a general method for solving ordinary differential equations. They used a variety of trial functions and an arbitrary distribution of collocation points. The work of Lanczos [62] established for the first time that a proper choice of trial functions and distribution of collocation points is crucial to the accuracy of the solution. The earliest applications of the spectral collocation method to partial differential equations were made for spatially periodic problems by Kreiss and Oliger [59] (who called it the Fourier method) and Orszag [71] (who termed it pseudo-spectral). Here we choose different spaces of test functions and trial functions. We approximate u by

$$u_N(x) = \sum_{i=0}^N a_i \phi_i(x) \tag{1.1}$$

where $\{\phi_i\}_i$ is the space of trial functions.

We let the space of test functions $\{\psi_i\}_i$ be different and impose the orthogonality condition

$$(\mathcal{L}u_N, \psi_i) = 0 \quad \text{for all } i. \quad (1.2)$$

Now if we choose $\psi_i = \delta(x - x_i)$ for a suitably chosen set of points $\{x_i\}_i$ we obtain the set of equations

$$(\mathcal{L}u_N)(x_i) = 0 \quad \text{for all } i. \quad (1.3)$$

The points x_i are chosen as the quadrature points of a Gaussian integration formula.

1.2.2 Galerkin method

The Galerkin approach [43], enjoys the aesthetically pleasing feature that the trial and the test functions are the same, and the discretization is derived from a weak form of the mathematical problem. The test functions are, therefore, infinitely smooth functions that individually satisfy some or all of the boundary conditions. The differential equation is enforced by requiring that the integral of the residual times each test function be zero, after some integration-by-parts, accounting in the process for any remaining boundary conditions. Finite element methods customarily use this approach. Moreover, the first serious application of spectral methods to PDE's – that of Silberman [80] for meteorological modeling – was a Galerkin method. The basic idea is to assume that the unknown function $u(x)$ can be approximated by a sum of $N + 1$ basis functions $\phi_n(x)$:

$$u_N(x) = \sum_{i=0}^N a_i \phi_i(x). \quad (1.4)$$

When this series is substituted into the equation

$$\mathcal{L}u(x) = f(x) \quad (1.5)$$

where \mathcal{L} is a differential (or integral) operator, the result is the so-called *residual function* defined by

$$\mathcal{R}^N(x) = \mathcal{L}u_N(x) - f(x). \quad (1.6)$$

Since the residual function $\mathcal{R}^N(x; a_i)$ is identically equal to zero for the exact solution, the challenge is to choose the series coefficients $\{a_n\}$ so that the residual function is minimized.

1.2.3 Tau method

The spectral tau methods, introduced by Lanczos [62], are similar to Galerkin methods in the way differential equation is enforced. However, none of the test functions need satisfy the boundary conditions. Hence, a supplementary set of equations is used to apply boundary conditions. Tau methods may be viewed as a special case of the so-called Petrov-Galerkin method and are applicable to problems with nonperiodic boundary conditions.

1.3 Spectral Methods on Non-smooth Domains

We now present a brief summary of the Section *Non-Smooth Domains* in the Chapter *Diffusion Equation* of [55].

Unlike finite element and finite difference methods, the order of convergence of spectral methods is not fixed and it is related to the maximum regularity (smoothness) of the solution. Spectral methods give exponential or *spectral convergence* if the solution is very smooth, i.e. possessing a high degree of regularity. In practice, exponential convergence implies that as the number of collocation points is doubled, the error in the numerical solution decreases by at least two orders of magnitude and not a fixed factor as in low-order methods. However, this fast convergence is easily lost if the solution has finite regularity or if the domain is irregular. For example, the solution of a Helmholtz/Poisson's equation may be singular [46].

This singularity in the solution may arise due to non-smooth domains or due to discontinuity in the boundary conditions, or in the specified data (e.g. forcing). Here as in [46], we assume that all the data, as well as the boundary conditions, are smooth/analytic and that singularities are only due to non-smoothness of the domain. First derivatives are unbounded when the angle is reflexive or convex, and the second derivatives are unbounded when the angle is acute or obtuse. In this case, not only the fast convergence of spectral/*hp* discretization be destroyed, but also the numerical solution obtained (with any standard method) may be erroneous. In general, theoretical results in three dimen-

sions for vertex, edge and combined vertex-edge singularities are more difficult to obtain, but work by Guo, Babuška and others [12–16, 51, 52] has addressed these issues.

To proceed further, we consider the domain shown in Figure 1.1 with the corner located at the origin and with one side of the corner aligned along x_1 axis, while the other is at an angle $\alpha\pi$, $0 < \alpha < 2$, in the counterclockwise direction. The solution in polar coordinates may be expressed as

$$u(r, \theta) \propto r^\beta \zeta(\theta) \chi(r).$$

Here $\zeta(\theta)$ is an analytic function and $\chi(r)$ is a smooth cut-off function. In this case, it

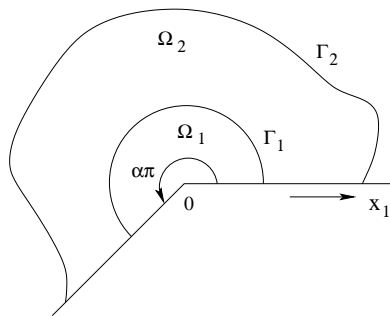


Figure 1.1: Computational domain Ω containing a corner of angle $\theta = \alpha\pi$.

is known that the spectral element solution $\tilde{u}(r, \theta)$ computed with polynomial order p in each element, satisfies

$$\|u(r, \theta) - \tilde{u}(r, \theta)\|_1 \leq Cp^{-2\beta-\epsilon},$$

where $\epsilon > 0$ and the exponent β depends on the angle. For many problems $\beta = 1/\alpha$ (where $\theta = \alpha\pi$), and thus the convergence rate lies between $\mathcal{O}(p^{-1})$ and $\mathcal{O}(p^{-2})$.

There are three main methods that allow us to recover, if not exponential, at least very high accuracy for most elliptic problems. They make use of the following:

1. The method of gradual h -refinement.
2. The Method of Auxiliary Mapping (MAM) or Conformal mapping to smooth out the singularity.
3. Use of extra basis functions that contain the form of singularity referred to as *space enrichment methods*. These require knowledge of eigenpair representation of the

solution.

1.3.1 Gradual h refinement

This approach requires the application of good discretization strategy which is usually done using radial or geometrically refined meshes (see [19]) and *quasi-uniform meshing*. A geometric progression has been found to be effective with a ratio of $(\sqrt{2} - 1)^2 \approx 0.17$, independent of the strength β of the singularity [48, 81]. However, in practice a value of 0.15 is typically adopted.

1.3.2 Method of auxiliary or conformal mapping

Babuška and Oh [17] introduced a new approach called the Method of Auxiliary Mapping (MAM), to deal with two dimensional elliptic boundary value problems containing corner singularities. In two dimensions the method adopts an auxiliary mapping of the type $\phi(z) = z^{1/\alpha}$ that maps a region where the solution is singular to a region where the transformed solution has a higher regularity. Thus, on the mapped domain true solution has better approximation properties. The method gives highly accurate numerical solutions without destroying the standard band structure of FEM and without increasing the number of degrees of freedom. The mapping is determined by the known nature of the singularity in such a way that the exact solution of lower regularity can be transformed to a function of higher regularity. The MAM, implemented in the p -version of the FEM, has proven to be successful in dealing with all prominent singularities arising in the two dimensional case [17, 65, 68, 69]. Benchmark comparisons with other well known numerical methods, reported in [65], show that MAM is more efficient than other numerical methods.

The MAM was successfully extended and implemented for elliptic PDEs on non-smooth domains in \mathbb{R}^3 by Guo and Oh [52] and Lee *et al.* [63]. However, unlike the two dimensional case, in \mathbb{R}^3 there are three different types of singularities, the vertex, the edge and the vertex-edge. The solutions of three dimensional elliptic problems are anisotropic in the neighbourhoods of edges and vertex-edges. Thus, the MAM techniques

in three dimensions are different from the two dimensional counterpart in theory as well as computation strategies. The numerical results for the Poisson equations containing the vertex, the edge and the vertex-edge singularities provided in [52, 63] show the effectiveness of the MAM in three dimensions.

We will now describe the method of auxiliary mapping for three different equations, namely *Laplace*, *Poisson* and *Helmholtz* equation in two and three dimensional domains.

Laplace equation in two-dimensional domains

Let us consider Laplace's equation $\Delta u = 0$ with homogeneous boundary conditions, i.e. $u = 0$ on $\partial\Omega$. In general, in the neighbourhood of the corner, the solution can be expressed as [57]

$$u(r, \theta) = \sum_{k=0}^{\infty} a_k \phi_k(r, \theta) \quad (1.7)$$

where the coefficients a_k are determined by the boundary conditions and

$$\phi_k(r, \theta) = \begin{cases} r^{k/\alpha} \sin\left(\frac{k}{\alpha}\theta\right), & \frac{k}{\alpha} \text{ is not an integer} \\ r^{k/\alpha} \left[\ln r \sin\left(\frac{k}{\alpha}\theta\right) + \theta \cos\left(\frac{k}{\alpha}\theta\right) \right], & \frac{k}{\alpha} \text{ is an integer.} \end{cases} \quad (1.8)$$

For homogeneous Neumann boundary conditions the sin term is replaced by $\cos(k/\alpha\theta)$, and for a problem with Dirichlet condition on one side and Neumann condition on the other side, it is replaced by $\sin\{(k/\alpha)(\theta/2)\}$. Assuming that the logarithmic term does not contribute to the solution, the mapping $z = \xi^\alpha$, where $z = re^{i\theta}$, $\alpha = \pi/\omega$ (here ω =sectoral angle), shown in Figure 1.2, makes the transformed solution analytic in terms of the new variables, thus

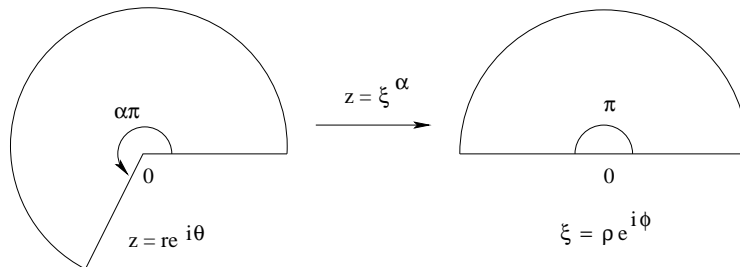


Figure 1.2: Auxiliary mapping of a domain containing a corner to a domain with no corners.

$$u(r, \theta) = \sum_{k=0}^{\infty} a_k r^{k/\alpha} \sin\left(\frac{k}{\alpha\theta}\right) \mapsto u(\rho, \phi) = \sum_{k=0}^{\infty} a_k \rho^k \sin(k\phi).$$

For the spectral/*hp* element discretization this method was first implemented in [17].

Laplace equation in three-dimensional domains

The solution of the Laplace equation in three dimensions, in the vicinity of the singularities, can be decomposed into three different forms, depending whether it is in the neighbourhood of a *vertex*, an *edge* or *vertex-edge* (an intersection of the vertex and edge). A three dimensional domain Ω , is shown in Figure 1.3, which contains typical three-dimensional singularities. Vertex singularities arise in the neighbourhoods of the

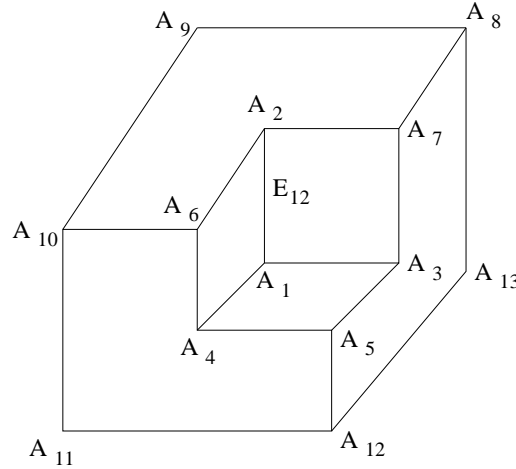


Figure 1.3: Typical three-dimensional singularities.

vertices A_i , and edge singularities arise in the neighbourhoods of the edges E_{ij} (E_{ij} is the edge joining vertices A_i and A_j). Close to the vertex-edge intersection, vertex-edge singularities arise. We assume that Ω contains only straight edges, for curved edges, we refer to [32].

Neighbourhoods of singularities caused by non-smoothness of domain

First, we give a brief introduction to the neighbourhoods of vertices, edges and vertex-edges. We shall give a complete description of each of them in Chapter 2. Throughout, we shall assume that, (x_1, x_2, x_3) , (ρ, θ, ϕ) and (r, θ, z) denote the usual Cartesian, spherical and cylindrical coordinates respectively of points in Ω .

Let Γ_i , $i \in \mathcal{I} = \{1, 2, \dots, I\}$ be the (open) faces, $E_{ij} = \Gamma_i \cap \Gamma_j$ be the edges and A_k ,

$k \in \mathcal{K} = \{1, 2, \dots, K\}$ be the vertices of Ω . We also denote a vertex by v and an edge by e . Without loss of generality, we assume that the vertex v is located at the origin and the edge coincides with the positive z -axis.

By Ω^e we denote an *edge-neighbourhood* of the edge $e = \{(r, \theta, z) | r = 0, 0 < z < l_e\}$ of length l_e , which is defined by

$$\Omega^e = \{(r, \theta, z) \in \Omega | 0 < r < \epsilon, \delta_v < z < l_e - \delta_v\}. \quad (1.9)$$

Here $\epsilon < 1$ and $\delta_v < 1$ are selected so that $\Omega^e \cap \bar{\Gamma}_i = \emptyset$ for those faces Γ_i which do not contain the edge e .

Consider a *neighbourhood* $\Omega_{\rho_v}^v$ of the vertex v (=the origin) defined by

$$\Omega_{\rho_v}^v = \{(\rho, \phi, \theta) \in \Omega | \rho < \rho_v\}.$$

Here $0 < \rho_v < 1$ is chosen so that $\Omega_{\rho_v}^v$ has a void intersection with those edges which do not pass through the vertex v . Now we decompose $\Omega_{\rho_v}^v$ into a vertex neighbourhood and several vertex-edge neighbourhoods. We define, a *vertex-edge neighbourhood* of the vertex v and edge e as:

$$\Omega^{v-e} = \{(\rho, \phi, \theta) \in \Omega_{\rho_v}^v | 0 < \phi < \phi_v\}$$

where, $0 < \phi_v$ and $\rho_v < 1$ are selected so that $\bar{\Omega}^{v-e_1} \cap \bar{\Omega}^{v-e_2} = v$ for distinct edges e_1 and e_2 having v as a common vertex.

A *vertex-neighbourhood*, Ω^v , of the vertex v is defined by

$$\Omega^v = \Omega_{\rho_v}^v \setminus \bigcup_{e \in \mathcal{E}^v} \Omega^{v-e}, \quad (1.10)$$

where, \mathcal{E}^v denote the set of all edges passing through the vertex v .

Intensities of vertex, edge and vertex-edge singularities

We now give a short outline of the singular solution decomposition in the neighbourhood of a vertex, an edge, or at a vertex-edge intersection. For corresponding computational results see [52, 63, 91]. For simplicity, we assume that in the vicinity of vertices or edges of interest, homogeneous boundary conditions are imposed. The following asymptotic expansions of the true solution are known:

Vertex singularities

In a vertex neighbourhood Ω^v of the vertex v , the solution has the vertex singularity and admits an expansion of the form

$$u(\rho, \phi, \theta) = \sum_{l=1}^L a_l \rho^{\gamma_l} h_l(\phi, \theta) + v(\rho, \phi, \theta), \quad (1.11)$$

where (ρ, ϕ, θ) denotes usual spherical coordinates with origin at the vertex v , $v(\rho, \phi, \theta) \in H^2(\Omega^v)$, $h_l(\phi, \theta)$ are analytic functions of ϕ and θ and are referred to as vertex eigenfunctions, and γ_l is a positive real number (see [21, 45, 46]). In other words, in Ω^v , the true solution has a singularity of type ρ^{λ_1} , where $\lambda_1 < 1$.

Edge singularities

In an edge neighbourhood Ω^e of the edge e , the solution has the edge singularity and can be decomposed as follows:

$$u(r, \theta, z) = \sum_{m=1}^M a_m(z) r^{\beta_m} h_m(\theta) + v(r, \theta, z), \quad (1.12)$$

where (r, θ, z) denotes usual cylindrical coordinates, and the functions $a_m(z)$ are analytic in z . The functions $v(r, \theta, z) \in H^2(\Omega^e)$, $h_m(\theta)$ are also analytic and $h_m(\theta)$ are referred to as edge eigenfunctions (see [21, 45, 88]). In other words, in Ω^e , the true solution has a singularity of type r^{λ_2} , where $\lambda_2 < 1$.

Vertex-edge singularities

The most complicated decomposition of the solution arises in the case of a vertex-edge intersection. For example, let us consider the neighbourhood where the edge e approaches the vertex v . The resulting vertex-edge neighbourhood is denoted by Ω^{v-e} , and the solution has a singularity caused by the combination of edges and a vertex and has an expansion of the form

$$\begin{aligned} u(\rho, \phi, \theta) = & \sum_{m=1}^M \left(\sum_{l=1}^L a_{ml} \rho^{\gamma_l} + f_m(\rho) \right) (\sin \phi)^{\beta_m} g_m(\theta) \\ & + \sum_{l=1}^L a_l \rho^{\gamma_l} h_l(\phi, \theta) + v(\rho, \phi, \theta), \end{aligned} \quad (1.13)$$

where the functions $f_m(\rho)$ are analytic in ρ , and $g_m(\theta)$, $h_l(\phi, \theta)$ and $v(\rho, \phi, \theta) \in H^2(\Omega^{v-e})$ are also analytic (see [45–47, 88]). That is, in Ω^{v-e} , the true solution has a singularity of

type $\rho^{\lambda_3}(\sin \phi)^{\lambda_4}$, where $\lambda_3 < 1$ and $\lambda_4 < 1$.

Poisson equation

The situation becomes more complicated when a forcing function is introduced as in Poisson's equation

$$-\Delta u = f(x) .$$

The convergence achieved through auxiliary mapping is no better than algebraic because the solution may not be analytic after the mapping. Typically, we decompose the solution into a homogeneous part $u^{\mathcal{H}}$, which has the singularity, and a particular part $u^{\mathcal{P}}$, which depends on the forcing. Complications arise due to particular part since, even if it is smooth in the original domain, it may be singular after the transformation. For instance, consider the following transformed equation which has a singular forcing function

$$\Delta u = \alpha^2 \rho^{2\alpha-2} f(\rho, \phi) .$$

Given the $\mathcal{O}(\rho^{-2\alpha})$ singularity, the spectral element convergence is of the order $\mathcal{O}(\rho^{-4\alpha-\epsilon})$ for any $\epsilon > 0$. In order to enhance the convergence, we separate the two contributions so that we have an analytic contribution in the z -plane and an analytic contribution in the ξ -plane.

Helmholtz equation

For the Helmholtz equation

$$\Delta u - \lambda u = f(x), \lambda > 0 ,$$

the conformal mapping is an effective way of improving convergence, although exponential convergence cannot be fully recovered. The auxiliary mapping $z = \xi^\alpha$, $\alpha = \omega/\pi$, $0 < \alpha < 2$ converts the Helmholtz equation to

$$\Delta u - \lambda \alpha^2 \rho^{2\alpha-2} u = \alpha^2 \rho^{2\alpha-2} f .$$

In terms of the original variables, the solution around the corner is

$$u(r, \theta) = \sum_{k=0}^{\infty} a_k I_{k/\alpha}(\sqrt{\lambda} r) \sin \left(\frac{k}{\alpha} \theta \right) ,$$

for k/α not an integer, where $I(z)$ represent the modified Bessel function of the first kind. After application of the mapping, the solution has the form

$$u(r, \theta) = \sum_{k=0}^{\infty} a_k \rho^k \sin(k\theta) \sum_{j=0}^{\infty} c_j \rho^{2j\alpha},$$

with a leading singular term of order $\rho^{1+2\alpha}$. Therefore, the estimated convergence rate is $\mathcal{O}(\rho^{-2-4\alpha-\epsilon})$, which in practise, is adequately fast, though algebraic.

Similar to the Poisson equation, in three dimension there are three different types of singularities namely, the vertex, the edge and the combined vertex-edge. Furthermore, solutions of elliptic problems are anisotropic in the neighbourhood of edges and vertex-edges. However, it is possible to obtain explicitly the form of such singularities [51], and thus the auxiliary mapping technique can be effectively used in three dimensions. The difference is that specific auxiliary mappings are required to handle each type of singularity. Lee *et al.* [63] have obtained and implemented these mappings successfully for treating all three types of singularities. The effectiveness of this method was demonstrated on two polyhedral domains. The results with the mapping method were superior to those obtained with the p -version of FEM [81] or other low-order methods.

Singular Basis

An alternative approach to using the auxiliary mapping is to use a set of supplementary basis functions which have the leading behavior of the singularity in conjunction with the smooth basis $\Phi_k(x)$. For the Helmholtz equation the leading-order singular terms are

$$r^{1/\alpha}, r^{2/\alpha}(\alpha > 1/2), r^{3/\alpha}(\alpha > 1), \dots,$$

which can be included into the expansion basis. However, we can do even better by supplementing the standard basis in the *mapped* domain. The transformed solution is then

$$u(\rho, \phi) = \sum_{k=1}^{\infty} a_k I_{k/\alpha}(\sqrt{\lambda}\rho^\alpha) \sin(k\phi) = \sum_{k=1}^{\infty} \sum_{l=0}^{\infty} b_{kl} \rho^{k+2l\alpha} \sin(k\phi), \quad (1.14)$$

and thus the leading singularities are weaker, i.e.,

$$\rho^{1+2\alpha}, \rho^{2+2\alpha}(\alpha > 1/2), \rho^{1+4\alpha}, \dots$$

A comparison of the effect of adding supplementary basis terms in the original and the transformed domain is given in [55, 73]. It has been shown in [73] that with one or two terms included in the transformed domain, a very fast convergence is obtained. To achieve the exponential accuracy we need to include higher order terms but in the limiting case the system becomes ill-conditioned as the augmented basis $\{\Phi_1, \Phi_2, \dots, \Phi_N, \varphi_1, \varphi_2, \dots, \varphi_M\}$ is nearly linearly dependent if many singular functions are used and as a result the stiffness matrix is ill-conditioned.

Eigenpair representation: Steklov formulation

A more recent method that treats singular solutions of both scalar and vector elliptic problems in the neighbourhood of corners was presented for two-dimensional domains by Yosibash and Szabó [82, 92] and for three-dimensional domains by Yosibash in [90, 91]. As we have already seen, such singular solutions are characterized by the form $u = r^\beta h(\theta)$ close to the corner.

Let us illustrate the basic characteristics of the solution to the Laplace problem over a two-dimensional domain as shown in Figure 1.2. The Laplace equation over Ω_2 , with Dirichlet boundary conditions on its boundary, is cast in cylindrical coordinates as follows:

$$\Delta u = \frac{\partial^2 u}{\partial r^2} + \frac{1}{r} \frac{\partial u}{\partial r} + \frac{1}{r^2} \frac{\partial^2 u}{\partial \theta^2} \quad \text{in } \Omega_2. \quad (1.15)$$

The solution in the vicinity of the singular point is sought by separation of variables. We denote by $h^+(\theta)$ and $h^-(\theta)$ the functions associated with the positive and negative values of β respectively. Although for the Laplace equation $h^+(\theta) \equiv h^-(\theta)$, for a general elliptic equation this is not the case. Thus, the solution to (1.15) admits the expansion

$$u = \sum_{i=1}^{\infty} a_i r^{\beta_i} h_i^+(\theta), \quad h_i^+(\theta) = \sin(\beta_i \theta), \quad \text{with } \beta_i = \frac{i}{\alpha}, \quad (1.16)$$

where β_i and $h_i(\theta)$ denote *eigenpairs*, and these are determined uniformly by the geometry and boundary conditions in the neighbourhood of the singular point. Notice that if $\beta_i < 1$ then the corresponding i th term in the expansion (1.16) for ∇u is unbounded as $r \rightarrow 0$. We say that u is singular at 0 if ∇u tends to infinity as $r \rightarrow 0$. The solution u in (1.16) is therefore singular at 0 if $\alpha > 1$ for $i = 1, \dots, \text{finitely many}$. The coefficients a_i depend

on the boundary conditions away from the singular points as well as the forcing term in the Poisson equation.

For general singular points, analytical computation of eigenpairs is not practical, and numerical approximations are usually sought. One of the most robust and efficient methods for the computation of eigenpairs is the modified Steklov method, developed by Yosibash [91] and Yosibash and Szabó [92].

1.3.3 Advantages and applications of spectral methods: A survey

We now briefly describe important features of spectral methods that should be considered in their formulation and application [44].

1. *Rate of convergence* : If the solution to a problem is analytic then a properly designed spectral method gives exponential accuracy in contrast to FDM and FEM which yield finite-order rates of convergence. The important consequence is that spectral methods can achieve high accuracy with little more resolution than is required to achieve moderate accuracy in FDM and FEM.
2. *Efficiency* : In order to be useful the spectral method should be as efficient as difference methods with comparable number of degrees of freedom. The development of collocation (pseudospectral) and Galerkin methods permits spectral methods to be implemented with comparable efficiency to that of FDM with the same number of independent degrees of freedom. As the required accuracy increases, the attractiveness of spectral methods increase.
3. *Boundary conditions* : The mathematical features of spectral methods follow very closely those of the partial differential equation being solved. Thus the boundary conditions imposed on spectral approximations are normally the same as those imposed on the differential equation. In contrast, FDM of higher order than the differential equation require additional “boundary conditions”. Many of the com-

plications of finite-order FDM disappear with the infinite-order-accurate spectral methods.

Another aspect of the treatment of boundary conditions by spectral methods is their high resolution of boundary layers. For details we refer to [44, 72].

4. *Bootstrap estimation of accuracy* : It is often possible to estimate the accuracy of spectral computations by examination of the shape of the spectrum. Thus, in computations of three-dimensional incompressible flows at high Reynolds numbers, the mean-square vorticity spectrum must not increase abruptly at large wave numbers. If the vorticity spectrum decreases smoothly to zero as wave number increases, it is safe to infer that the calculation is accurate. On the other hand, similar criteria for finite-difference methods can be misleading.

Let us now survey some applications of spectral methods. We shall classify the method according to geometry and boundary conditions.

1. *Periodic boundary conditions in Cartesian coordinates* : Here Fourier series should be used. Spectral methods have been regularly used in three-dimensions to simulate homogeneous turbulence using high resolution codes. Most operational codes now use pseudospectral methods because aliasing errors are usually small.
2. *Rigid boundary conditions in Cartesian coordinates* : Use of Chebyshev or Legendre polynomials is appropriate in this case. Typical applications include numerical studies of turbulent shear flows and boundary layer transition.
3. *Rigid boundary conditions in Cylindrical geometry* : Chebyshev or Legendre polynomials should be used in radial, Fourier series in angular, and either Fourier or Chebyshev series in the axial direction (depending on boundary conditions).
4. *Problems in spherical geometry* : Here surface harmonic expansions, generalized Fourier series, and “associated” Chebyshev expansions all have attractive features.
5. *Semi-infinite or infinite geometry* : In this case Chebyshev expansions are best if the domain can be mapped or truncated to a finite domain without serious error.

There are two cases to be considered: additional boundary conditions may or may not be required at “infinity”. If additional boundary conditions, such as radiation or outflow boundary conditions, must be imposed on the truncated domain, then they should also be applied to the spectral method. On the other hand, if mapping without additional boundary conditions does not introduce a singularity in the exact equations, no boundary conditions at “infinity” are required in the spectral approximation.

1.3.4 Limitations of spectral methods

The drawbacks of spectral methods are four fold.

1. The main drawback is their inability to handle complex geometries. Different strategies are, however, possible to overcome this difficulty. The idea to couple domain decomposition techniques to the spectral discretization has been successful in overcoming this drawback (S. A. Orszag [72]).
2. They are usually more difficult to program than finite difference methods.
3. They are more costly per degrees of freedom than other low-order methods.

1.4 Finite Element Method

The Finite Element Method (FEM) is one of the most widely used numerical methods for obtaining approximate solutions to a large variety of engineering problems. Although originally developed for numerical solution of complex problems in structural mechanics, it has since been extended and applied to the broad field of continuum mechanics. Though the term finite element was first coined by Clough [30] in 1960 in a paper on plane elasticity problems, the ideas of finite element analysis date back much further and can be traced back to the work by Alexander Hrennikoff (1941) and Richard Courant (1942). In the early 1960s, engineers used the method for approximate solutions of problems in a wide

variety of engineering problems such as stress analysis, fluid flow, heat transfer, and other areas. The first book on the FEM by Zienkiewicz and Chung [93] was published in 1967.

The underlying premise of the method states that a complicated domain can be subdivided into a series of smaller regions in which the differential equations are approximately solved. By assembling the set of equations for each region, the behavior over the entire problem domain is determined. Each region is referred to as an *element* and the process of subdividing a domain into a finite number of elements is referred to as *discretization*. Elements are connected at specific points, called *nodes*, and the assembly process requires that the solution be continuous along common boundaries of adjacent elements.

When more accuracy is needed, the finite element method has three different versions, namely h version, p version and $h - p$ version. In the h version, mesh size h is reduced and polynomials of fixed degree p are used to increase accuracy. In the p version mesh size h is kept fixed while polynomial degree p is raised. In the $h - p$ version the mesh size h is reduced and the polynomial degree p is raised simultaneously within the elements either uniformly over the entire computational domain or selectively depending on the resolution requirements.

Finite element method is a variational method of approximation, making use of global or variational statements of physical problems and employing the Rayleigh-Ritz-Galerkin philosophy of constructing co-ordinate functions whose linear combinations represent the unknown solutions. It took approximately a decade before the method was recognized as a form of the Rayleigh-Ritz method. The relation between these two techniques comes from considering the variational form of a given problem. For instance, the quadratic functional

$$\mathcal{F}(u) = \int_0^1 [p(x)(u'(x))^2 + q(x)(u(x))^2 - 2f(x)u(x)]dx \quad (1.17)$$

has a minimum with respect to a variation in $u(x)$ given by the Euler equation

$$-\frac{d}{dx} \left(p(x) \frac{du(x)}{dx} \right) + q(x)u(x) = f(x). \quad (1.18)$$

Therefore, instead of solving for (1.18) to determine $u(x)$, an alternative but equivalent

way is to find $u(x)$ which minimizes the functional (1.17).

The Rayleigh-Ritz idea approximates the solution by a finite number of functions $u(x) = \sum_{i=1}^N \alpha_i \Phi_i(x)$ to determine the unknown weights α_i , which minimize the functional (1.17). In the FEM the solution is also approximated by a finite number of functions, which are typically local in nature as opposed to the global functions used in the Rayleigh-Ritz approach. However, the starting point for a finite element method is the differential equation (1.18), which is formulated into an integral form (also known as Galerkin formulation) so that the problem reduces to an algebraic system of equations which can be solved numerically. This connection between the two methods was made when it was realized that the integral form of the FEM was exactly same as the functional form used in the Rayleigh-Ritz method.

This relation between the FEM and Rayleigh-Ritz method was very significant and it made the finite element technique mathematically respectable. A more general formulation is possible using the method of weighted residuals which leads to the standard Galerkin formulation.

1.4.1 Method of weighted residuals

The origin of the *Method of Weighted Residuals* (MWR) dates back prior to development of the finite element method. The method illustrates how the choice of different test (or weight) functions may be used to produce many commonly used numerical methods for solving differential equations.

Suppose we have a linear differential operator \mathcal{L} acting on a function u as follows:

$$\mathcal{L}(u(\mathbf{x})) = f(\mathbf{x}) \text{ for } \mathbf{x} \in \Omega.$$

We wish to approximate u by a function \tilde{u} , which is a linear combination of basis functions chosen from a linearly independent set. That is,

$$u \approx \tilde{u} = \sum_{j=1}^n a_j \Phi_j. \quad (1.19)$$

Now, when substituted into the differential operator, \mathcal{L} , the result of the operations is

not, in general, $f(x)$. Hence an error or residual will exist. Define

$$R(\mathbf{x}) = \mathcal{L}(\tilde{u}(\mathbf{x})) - f(\mathbf{x}). \quad (1.20)$$

The notion in the MWR is to force the residual to zero in some average sense over the domain Ω . That is,

$$\int_{\Omega} R(\mathbf{x}) w_j(\mathbf{x}) d\mathbf{x} = 0, j = 1, 2, \dots, n \quad (1.21)$$

where the number of test functions $w_j(\mathbf{x})$ is exactly equal to the number of unknown constants a_j in \tilde{u} . The result is a set of n algebraic equations for the unknown constants a_j . Different choices of test (or weight) functions w_j 's give rise to different methods. A list of most commonly used test functions and the computational method they produce is given in Table 1.1. We shall describe two of them namely the Least Squares method and the Galerkin method below. For further details of these methods we refer to [55].

Table 1.1: Weight functions $w_j(\mathbf{x})$ used in the method of residual and the method produced.

Test/weight function	Type of method
$w_j(\mathbf{x}) = \delta(\mathbf{x} - \mathbf{x}_j)$	Collocation
$w_j(\mathbf{x}) = 1$, inside Ω^j 0, outside Ω^j	Finite volume (sub-domain)
$w_j(\mathbf{x}) = \frac{\partial R}{\partial u_j}$	Least-squares
$w_j(\mathbf{x}) = \Phi_j$	Galerkin
$w_j(\mathbf{x}) = \Psi_j \neq \Phi_j$	Petrov-Galerkin

Least-squares method

The least-squares method originates from the idea of least-squares estimation developed by Gauss. If the integral of the square of residuals is minimized, the rationale behind the name can be seen. In other words, a minimum of

$$\int_{\Omega} R^2(\mathbf{x}) d\mathbf{x}$$

is achieved. Therefore the weight functions for the least-squares method are just the derivatives of the residual with respect to the unknown constants:

$$w_j(\mathbf{x}) = \frac{\partial R}{\partial a_j}.$$

This formulation using a spectral/*hp* element discretization has recently increased in popularity [53, 74, 75].

Galerkin method

This method (also known as Bubnov-Galerkin method) may be viewed as a modification of the least-squares method. Rather than using the derivative of the residual with respect to the unknown a_j , the derivative of the approximating function is used. It turns out that the weight/test functions are same as the trial functions. That is,

$$w_j(\mathbf{x}) = \frac{\partial \tilde{u}}{\partial a_j} = \Phi_j(\mathbf{x}).$$

1.4.2 Advantages of FEM

1. Finite element methods convert differential equations into matrix equations that are *sparse* because only a handful of basis functions are non-zero in a given sub-interval. Sparsity of matrix equations allows the stiffness matrix to be stored and inverted easily thus saving a lot of computational cost.
2. In multi-dimensional problems, the sub-intervals become triangles (in 2D) or tetrahedra (in 3D) which can be fitted to irregularly-shaped geometries such as the shell of an automobile etc.
3. The major advantages of the FEM over FDM and other low-order methods are its built-in abilities to handle unstructured meshes, a rich family of element choices, and natural handling of boundary conditions.
4. FEM can handle a wide variety of engineering problems such as problems in solid mechanics, dynamics, fluids, heat conduction and electrostatics.

1.4.3 Disadvantages of FEM

1. Finite element methods are not well suited for open region problems.
2. They suffer low accuracy (for a given number of degrees of freedom N) because each basis function is a polynomial of low degree.

1.4.4 Spectral vs. finite element methods

Spectral methods are similar to finite element methods in philosophy; the major difference is that in finite element methods we choose $\Phi_n(x)$ to be *local* functions which are polynomials of fixed degree and are non-zero only over a couple of sub-intervals. In contrast, spectral methods use *global* basis functions in which $\Phi_n(x)$ is a polynomial (or trigonometric polynomial) of high degree which is non-zero, except at isolated points, over the entire computational domain.

Finite element methods convert differential equations into matrix equations that are *sparse* because only a handful of basis functions are non-zero in a given sub-interval. Spectral methods generate algebraic equations with full matrices, but in compensation, the higher order of the basis functions give high accuracy for a given N . When fast iterative matrix solvers are used, spectral methods can be much more efficient than FEM or FDM methods for many classes of problems. However, they are most useful when the *geometry* of the problem is fairly smooth and regular.

Spectral Element Methods gain the best of both worlds by hybridizing spectral and finite element methods. The domain is subdivided into elements, as in finite elements, to gain the flexibility and matrix sparsity of finite elements. At the same time, the degree of the polynomial p in each sub-domain is sufficiently high to retain the high accuracy and low storage of spectral methods.

1.5 Non-conforming Methods

The formulations presented so far deal with conforming elements where vertices of adjoining elements coincide, and correspondingly a C^0 continuity condition is satisfied at the element interfaces. However, design over complex domains often require to refine the mesh locally. For example, to resolve the geometric singularity in a flow past a half-cylinder it is desirable to contain the mesh refinement locally as needed and not propagate the mesh changes globally. Such local refinement is particularly useful in increasing the computational efficiency of direct and large eddy simulations of turbulent flows.

Non-conforming methods can be used to decompose and recompose such complex domains into sub-domains without requiring the compatibility between the meshes on the separate components. That is, we will no longer require that the vertices of the adjoining elements coincide. Instead, we will develop a framework that allows for arbitrary connection between elements. An added advantage of this idea is that the mesh refinement can be imposed selectively on the components where it is required. We now present a brief summary of commonly used non-conforming methods which allow for arbitrary connection between elements and are highly suitable for parallel implementation (for details see [55]):

Iterative patching

This formulation employs geometrically non-conforming elements but maintains C^0 continuity of the global polynomial expansion.

Constrained approximation

The method of constrained approximation was introduced by Oden and his associates [34, 67, 76] to deal with geometrically non-conforming discretizations introduced by refinement. The main idea is to maintain C^0 continuity across elemental interfaces by modifying the unconstrained basis functions appropriately. In other words, the approximation space is a constrained space which is a subset of $H^1(\Omega)$ for second order elliptic problems.

Mortar element method

In this method C^0 continuity is no longer imposed and new weak forms of the problem are developed. This method was first introduced by Patera and co-workers [2, 22, 66], who coined the term ‘*mortar element methods*’ because the discretization introduces a set of functions that mortar the brick-like elements together. The method generalizes the SEM to geometrically nonconforming partitions, to sub-domains with different resolutions (polynomial degrees) on sub-domain interfaces and allows for the coupling of variational discretizations of different types in non-overlapping domains, that is, the non-conformity may be due to geometry, approximation spaces, or both.

Discontinuous Galerkin method

Similar to mortar element method we do not require C^0 continuity in this method. Although original application of most discontinuous Galerkin methods (DGM) was in solving hyperbolic problems, more recent work has led to formulations for parabolic and elliptic problems [31]. In an effort to classify all contributions made toward the use of discontinuous Galerkin methods for elliptic problems, Arnold *et al.*, first in [4] and then in more generality in [5], published a unified analysis of discontinuous Galerkin methods for elliptic problems.

1.6 $h - p$ /Spectral Element Methods on Parallel Computers

Spectral element methods function very well on massively parallel machines. One can assign a single large element with a high order polynomial approximation within it to a single processor. A three dimensional element of degree N roughly has N^3 internal degrees of freedom, but the number of grid points on its boundary is $\mathcal{O}(6N^2)$. It is these boundary values that must be shared with other elements i.e., other processors, so that the numerical solution is continuous everywhere. As N increases, the ratio of internal grid points to the boundary grid points increases, implying that more and more of the compu-

tations are internal to the element, and the shared boundary values become smaller and smaller compared to the total number of unknowns. This in turn implies inter-processor communication to be small. To do the same calculation with lower order methods, one would need roughly eight times as many degrees of freedom in three dimensions. That would increase the inter-processor communication load by at least a factor of four.

An exponentially accurate $h - p$ /spectral element method for solving two dimensional general elliptic problems with mixed Neumann and Dirichlet boundary conditions on non-smooth domains using parallel computers was proposed in [37–39, 84–86]. To resolve the singularities which arise at the corners an auxiliary map of the form $z = \log \xi$ is used along with a geometric mesh at the corners. In a neighbourhood of the corners, modified polar coordinates (τ_k, θ_k) are used, where $\tau_k = \ln r_k$ and (r_k, θ_k) denote polar coordinates with origin at the vertex A_k . Away from the sectoral neighbourhoods of the corners the usual coordinate system (x_1, x_2) is used.

With this mesh a numerical method was proposed as follows:

Find a solution which minimizes “*the sum of the weighted squared norm of the residuals in the partial differential equation and the squared norm of the residuals in the boundary conditions in fractional Sobolev norms and enforce continuity by adding a term which measures the jump in the function and its derivatives at inter-element boundaries, in appropriate Sobolev norms.*”

The method is a least-squares method and the solution can be obtained by solving the normal equations using the preconditioned conjugate gradient method (PCGM) without computing the mass and stiffness matrices [38, 39, 86]. Let N denote the number of layers in the geometric mesh. Then the method requires $O(N \ln N)$ iterations of the PCGM to obtain the solution to exponential accuracy.

1.7 Review of Existing Work

The $h - p$ version of the finite element method (FEM) for elliptic problems was proposed by Babuška and his coworkers in the mid 80ies. They unified the hitherto largely separate

developments of fixed order “ h -version FEM” in the sense of Ciarlet, which achieve convergence through reduction of the mesh size h , and the so-called “*spectral* (or p -version) FEM” achieving convergence through increasing polynomial order p on a fixed mesh. Apart from unifying these two approaches, a key new feature of hp -FEM was the possibility to achieve *exponential convergence* in terms of number of degrees of freedom N . A method for obtaining a numerical solution to exponential accuracy for elliptic problems in one dimension was first proposed by Babuška and Gui in [48] within the framework of hp -FEM. Exponential convergence results were shown for the model singular solution $u(x) = x^\alpha - x \in H_0^1(\Omega)$ in $\Omega = (0, 1)$. Specifically, the error was shown to be bounded by $e^{-b\sqrt{N_{dof}}}$, N_{dof} is the number of degrees of freedom. This result required σ -geometric meshes with a *fixed mesh ratio* $\sigma \in (0, 1)$ while the constant b in the convergence estimate depends on the singularity exponent α as well as on σ . Among all $\sigma \in (0, 1)$, the optimal value was shown to be $\sigma_{opt} = (\sqrt{2} - 1)^2 \approx 0.17$.

In two dimensions, exponential convergence (an upper bound $Ce^{-b\sqrt[3]{N_{dof}}}$) on the error for elliptic problems posed on polygonal domains was obtained by Babuška and Guo in the mid 80ies in a series of landmark papers [8–10]. Key ingredients in the proof were *geometric mesh* refinements towards the corners and *nonuniform elemental polynomial degrees* which increase linearly with the elements’ distance from corners. We remark that the proof of *elliptic regularity* results in terms of *countably normed spaces*, which constitutes an essential component of the exponential convergence proof, has been a major technical achievement. This problem has also been examined by Karniadakis and Sherwin in [55] and Pathria and Karniadakis in [55, 73] in the frame work of spectral/ $h - p$ element methods. In [37–39, 84–86] $h - p$ spectral element methods for solving general elliptic problems to exponential accuracy on polygonal domains using parallel computers were proposed. More recently the case of elliptic systems was analyzed in [60] for non-conforming spectral element functions. Key ingredients were use of geometric mesh at the corners and use of auxiliary mapping to remove the singularity at the corners. Computational results for least-squares $h - p$ /spectral element method for elliptic problems on non-smooth domains with monotone singularities of the type r^α and $r^\alpha \log^\delta r$ as well

as the oscillating singularities of the type $r^\alpha \sin(\epsilon \log r)$ have been obtained in [61].

Starting in the 90ies, efforts to extend the analytic regularity and the hp -convergence analysis of two dimensional problems to three dimensions in the frame work of finite element methods were undertaken in [13–15, 49] and the references therein which include related works in the subject. hp -version of discontinuous Galerkin finite element method (hp -DGFEM) for second order elliptic problems with piecewise analytic data in three dimensional polyhedral domains has been analyzed by Schötzau *et al.* [77, 78]. The method is shown to be exponentially accurate.

1.8 Review and Outline of the Thesis

As discussed earlier, current formulations of spectral methods to solve elliptic problems on non-smooth domains allow us to recover only algebraic convergence [28, 55]. The method of auxiliary mapping, which yields relatively fast convergence makes use of a conformal mapping of the form $\xi = z^{1/\alpha}$ that maps a neighbourhood of the singularity point (where the true solution is singular) onto a domain where the true solution is smooth and has better approximation properties, i.e. we smooth out the singularity that occurs at the corners [55] using auxiliary map.

In this thesis, we propose an exponentially accurate $h - p$ spectral element method for elliptic problems on non-smooth polyhedral domains in \mathbb{R}^3 .

In contrast to the two dimensional case, in three dimensions the character of the singularities is much more complex, not only because of higher dimension but also due to the different nature of the singularities which are the vertex singularity, the edge singularity and the vertex-edge singularity. Thus we have to distinguish between the behaviour of the solution in the neighbourhoods of the vertices, edges and vertex-edges. Unlike the two dimensional case where weighted isotropic spaces are used, in three dimensions we have to utilize weighted anisotropic spaces because the solution is smooth along the edges but singular in the direction perpendicular to the edges [13]. Behaviour of the solution is even more complex at the vertices where the edges are joined together and the solution

is not smooth along the edges too.

To overcome the singularities which arise in the neighbourhoods of the vertices, vertex-edges and edges we use local systems of coordinates. These local coordinates are modified versions of spherical and cylindrical coordinate systems in their respective neighbourhoods. Away from these neighbourhoods standard Cartesian coordinates are used in the regular region of the polyhedron. In each of these neighbourhoods we use a *geometrical mesh* which becomes finer near the corners and edges.

With this mesh we choose our approximate solution as the spectral element function which minimizes the sum of a weighted squared norm of the residuals in the partial differential equations and the squared norm of the residuals in the boundary conditions in fractional Sobolev spaces and enforce continuity by adding a term which measures the jump in the function and its derivatives at inter-element boundaries in fractional Sobolev norms, to the functional being minimized. The Sobolev spaces in vertex-edge and edge neighbourhoods are anisotropic and become singular at the corners and edges.

We then derive *differentiability estimates* with respect to these new coordinates in the neighbourhoods of vertices, edges and vertex-edges and in the regular region of the polyhedron where we retain standard Cartesian coordinate system.

The spectral element functions are represented by a uniform constant at all the corner elements in vertex neighborhoods and on the corner-most elements in vertex-edge neighbourhoods which are in the direction transverse to the edges of the polyhedron. At corner elements which are in the direction of edges in vertex-edge neighbourhoods and at all the corner elements in edge neighbourhoods the spectral element functions are represented as one dimensional polynomials of degree W in the modified coordinates. In all other elements in edge neighbourhoods and vertex-edge neighbourhoods the spectral element functions are a sum of tensor products of polynomials of degree W in their respective modified coordinates. The remaining elements in the vertex neighbourhoods and the regular region are mapped to the master cube and the spectral element functions are represented as a sum of tensor products of polynomials of degree W in λ_1 , λ_2 , and λ_3 , the transformed variables on the master cube.

A *stability estimate* is then derived for the functional we minimize. We use the stability estimate to obtain *parallel preconditioners* and *error estimates* for the solution of the minimization problem. Let N denote the number of refinements in the geometrical mesh. We shall assume that N is proportional to W . Then for problems with Dirichlet boundary conditions the condition number of the preconditioned system is $O((\ln W)^2)$ provided $W = O(e^{N^\alpha})$ for $\alpha < 1/2$. Moreover it is shown that there exists a new preconditioner which can be diagonalized in a new set of basis functions using separation of variables techniques in which each diagonal block corresponds to a different element, and hence it can easily be inverted on each element. Moreover, if the data is analytic then the error is *exponentially small* in N .

For mixed problems the condition number grows like $O(N^4)$. The rapid growth of the factor N^4 creates difficulties in parallelizing the numerical scheme. To overcome this difficulty another version of the method may be defined in which we choose our spectral element functions to be conforming on the wirebasket (union of vertices and edges) of elements. It can be shown that a probing parallel preconditioner can be defined for the minimization problem using the stability estimates which allows the problem to decouple. We intend to study this in the future.

The method is essentially a *least-squares* collocation method and a solution can be obtained using *Preconditioned Conjugate Gradient Method (PCGM)*. To solve the minimization problem we need to solve the *normal equations* for the *least-squares* problem. The residuals in the normal equations can be obtained without computing and storing *mass* and *stiffness* matrices.

For Dirichlet problems we use spectral element functions which are non-conforming and hence there are no common boundary values. For problems with mixed boundary conditions the spectral element functions are essentially non-conforming except that they are continuous only at the wirebasket of the elements. Hence the cardinality of the set of common boundary values which is equal to the values of the function at the wirebasket of the elements is much smaller than the cardinality of the common boundary values for the standard finite element method and so we can compute an accurate approximation

to the Schur complement matrix. In this dissertation we examine the non-conforming version of the method. The case when the spectral element functions are conforming on the wirebasket will be examined in future work.

The method requires $O(N \ln N)$ iterations of the PCGM to obtain the solution to exponential accuracy and requires $O(N^5 \ln(N))$ operations on a parallel computer with $O(N^2)$ processors for Dirichlet problems. However, for mixed problems it would require $O(N^3)$ iterations of the PCGM to obtain solution to exponential accuracy and $O(N^7)$ operations on a parallel computer with $O(N^2)$ processors.

Our method works for non self-adjoint problems too. Results of numerical simulations for a number of model problems on non-smooth domains are presented with constant and variable coefficients including the non self-adjoint case which confirm the theoretical estimates obtained for the error and computational complexity.

We remark here that once we have obtained our approximate solution, consisting of non-conforming spectral element functions, we can make a correction to the approximate solution so that the corrected solution is conforming and the error between the corrected and exact solution is exponentially small in N in the H^1 norm over the whole domain.

We now briefly describe the contents of the thesis which is divided into six chapters.

Chapter 1 provides brief descriptions of different methods, namely spectral and finite element methods, with advantages and disadvantages. Basic properties of these methods are discussed. An overview of the existing work is also provided.

Chapter 2 introduces the problem under consideration. We define various neighbourhoods of vertices, edges and vertex-edges and then derive the differentiability estimates and introduce the function spaces in these neighbourhoods which will be needed in what follows. The main stability estimates are stated here.

Chapter 3 gives the proof of the stability theorem on which our method is based.

Chapter 4 presents the numerical scheme which is based on the stability estimates of Chapter 2 and error estimates for the approximate solution are obtained.

Chapter 5 provides preconditioning and parallelization techniques. It is shown that a preconditioner can be defined for the quadratic form corresponding to the minimization problem which allows the problem to decouple. It is also shown that there exists another preconditioner which can be diagonalized in a new basis using the separation of variables technique. Lastly, it briefly describes the steps to compute the residual.

Chapter 6 gives numerical results to validate the error estimates and bounds on computational complexity. We also briefly outline our plan for future work here.

Chapter 2

Differentiability and Stability Estimates

2.1 Introduction

In this chapter we shall obtain differentiability estimates and stability estimates for a general elliptic boundary value problem posed on a polyhedral domain with mixed Dirichlet and Neumann boundary conditions. To resolve the singularities which arise at the corners and edges namely, the vertex, vertex-edge and edge singularities we use geometrical meshes which become finer near corners and edges. In the neighbourhood of vertices, vertex-edges and edges we switch to local systems of coordinates (auxiliary mappings). In doing this the geometrical mesh is reduced to a quasi-uniform mesh and hence Sobolev's embedding theorems and trace theorems for Sobolev spaces apply for functions defined on mesh elements in these new variables with a uniform constant. Away from these neighbourhoods we retain standard Cartesian coordinates in the regular region of the polydehron. The use of auxiliary mappings together with geometrical meshes to overcome the singularities along corners and edges allows us to obtain the solution with exponential accuracy. We remark that the local systems of coordinates which we use are modified versions of spherical and cylindrical coordinates in the vertex and edge neighbourhoods respectively and a hybridization of the two coordinate systems in the vertex-edge neighbourhoods.

We now seek a solution as in [37, 38, 84–86] which minimizes the sum of the squares of a weighted squared norm of the residuals in the partial differential equation and a fractional Sobolev norm of the residuals in the boundary conditions and enforce continuity across inter-element boundaries by adding a term which measures the sum of the squares of the jump in the function and its derivatives at inter-element boundaries in appropriate Sobolev norms to the functional being minimized. Since the residuals in the partial differential equation blow up in the neighbourhoods of vertices, vertex-edges and edges, we have to multiply these residuals by appropriate weights in various neighbourhoods. Anisotropic Sobolev norms are used in the neighbourhoods of edges and vertex-edges. All these computations are done using modified system of coordinates in the neighbourhoods of corners and edges and a global coordinate system elsewhere.

The differentiability estimates are now obtained with respect to these new coordinates in the neighbourhoods of vertices, edges and vertex-edges and in the regular region where standard Cartesian coordinate system is used.

We use spectral element functions which are *non-conforming*. Let N denote the number of layers in the geometric mesh. The spectral element functions are represented by a uniform constant at all the corner elements in vertex neighborhoods and on the corner-most elements in vertex-edge neighbourhoods which are in the angular direction from the edges of the domain. At remaining corner elements which are in the direction of the edges in edge neighbourhoods and vertex-edge neighbourhoods the spectral element functions are represented as polynomials which are functions of one variable. On elements away from corners and edges in edge neighbourhoods and vertex-edge neighbourhoods these spectral element functions are a sum of tensor products of polynomials in the modified coordinates. The remaining elements in the vertex neighbourhoods and the regular region are mapped to the master cube Q and the approximate solution is represented as a sum of tensor products of polynomials of degree W in λ_1, λ_2 and λ_3 , the transformed variables. Here W is chosen proportional to N , the number of layers. A stability estimate is obtained on which our method is based.

2.2 Differentiability Estimates in Modified Coordinates

We consider an elliptic boundary value problem posed on a polyhedron Ω in R^3 with mixed Neumann and Dirichlet boundary conditions:

$$\begin{aligned} Lw &= F \text{ in } \Omega, \\ w &= g^{[0]} \text{ for } x \in \Gamma^{[0]}, \\ \left(\frac{\partial w}{\partial \nu} \right)_A &= g^{[1]} \text{ for } x \in \Gamma^{[1]}. \end{aligned} \quad (2.1)$$

It is assumed that the differential operator

$$Lw(x) = \sum_{i,j=1}^3 -\frac{\partial}{\partial x_i}(a_{i,j}w_{x_j}) + \sum_{i=1}^3 b_i w_{x_i} + cw \quad (2.2)$$

is a strongly elliptic differential operator which satisfies the *Lax-Milgram* conditions. Moreover $a_{i,j} = a_{j,i}$ for all i, j and the coefficients of the differential operator are analytic. Let Γ_i , $i \in \mathcal{I} = \{1, 2, \dots, I\}$, be the faces of the polyhedron. Let \mathcal{D} be a subset of \mathcal{I} and $\mathcal{N} = \mathcal{I} \setminus \mathcal{D}$. We impose Dirichlet boundary conditions on the faces Γ_i , $i \in \mathcal{D}$ and Neumann boundary conditions on the faces Γ_j , $j \in \mathcal{N}$. The data F , $g^{[0]}$ and $g^{[1]}$ are analytic on each open face and $g^{[0]}$ is continuous on $\bigcup_{i \in \mathcal{D}} \bar{\Gamma}_i$.

By $H^m(\Omega)$, we denote the usual Sobolev space of integer order $m \geq 0$ furnished with the norm

$$||u||_{H^m(\Omega)}^2 = \sum_{|\alpha| \leq m} ||D^\alpha u||_{L^2(\Omega)}^2$$

where $\alpha = (\alpha_1, \alpha_2, \alpha_3)$, $|\alpha| = \alpha_1 + \alpha_2 + \alpha_3$, and $D^\alpha u = D_{x_1}^{\alpha_1} D_{x_2}^{\alpha_2} D_{x_3}^{\alpha_3} u = u_{x_1^{\alpha_1} x_2^{\alpha_2} x_3^{\alpha_3}}$ is the distributional (weak) derivative of u . As usual, $H^0(\Omega) = L^2(\Omega)$, $H_0^1(\Omega) = \{u \in L^2(\Omega) : Du \in L^2(\Omega), u = 0 \text{ on } \partial\Omega\}$. A seminorm on $H^m(\Omega)$ is given by

$$|u|_{H^m(\Omega)}^2 = \sum_{|\alpha|=m} ||D^\alpha u||_{L^2(\Omega)}^2.$$

2.2.1 Differentiability estimates in modified coordinates in vertex neighbourhoods

Let Ω denote a polyhedron in R^3 , as shown in Figure 2.1. Let $\Gamma_i, i \in \mathcal{I} = \{1, 2, \dots, I\}$, be

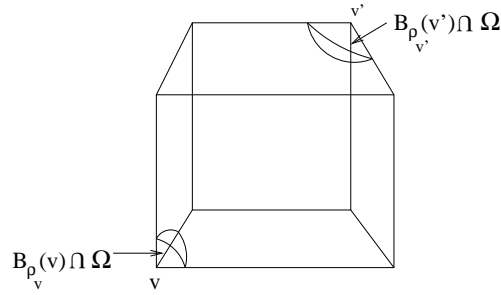


Figure 2.1: Polyhedral domain Ω in R^3 .

the faces (open), $S_j, j \in \mathcal{J} = \{1, 2, \dots, J\}$, be the edges and $A_k, k \in \mathcal{K} = \{1, 2, \dots, K\}$, be the vertices of the polyhedron.

We shall also denote an edge by e , where $e \in \mathcal{E} = \{S_1, S_2, \dots, S_J\}$, the set of edges, and a vertex by v where $v \in \mathcal{V} = \{A_1, A_2, \dots, A_K\}$, the set of vertices. Let $B_{\rho_v}(v) = \{x :$

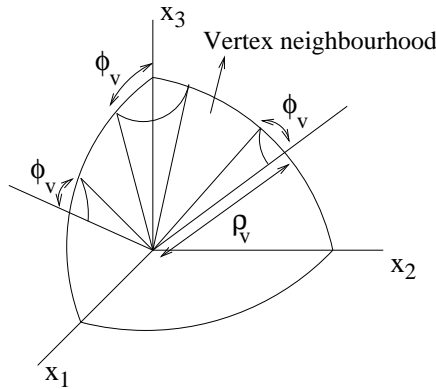


Figure 2.2: Vertex neighbourhood Ω^v .

$dist(x, v) < \rho_v\}$. For every vertex v , ρ_v is chosen so small that $B_{\rho_v}(v) \cap B_{\rho_{v'}}(v') = \emptyset$ if the vertices v and v' are distinct.

Now consider a vertex v which has n_v edges passing through it. We shall let the x_3 axis denote one of these edges. Consider first the edge e which coincides with the x_3 axis.

Let ϕ denote the angle which $x = (x_1, x_2, x_3)$ makes with the x_3 axis. Let

$$\mathcal{V}_{\rho_v, \phi_v}(v, e) = \{x \in \Omega : 0 < \text{dist}(x, v) < \rho_v, 0 < \phi < \phi_v\}$$

where ϕ_v is a constant. Let us choose ϕ_v sufficiently small so that

$$\mathcal{V}_{\rho_v, \phi_v}(v, e') \cap \mathcal{V}_{\rho_v, \phi_v}(v, e'') = \emptyset$$

if e' and e'' are distinct edges which have v as a common vertex. Now we define Ω^v , the vertex neighbourhood of the vertex v . Let \mathcal{E}^v denote the subset of \mathcal{E} , the set of edges, such that $\mathcal{E}^v = \{e \in \mathcal{E} : v \text{ is a vertex of } e\}$. Then

$$\Omega^v = \left(B_{\rho_v}(v) \setminus \bigcup_{e \in \mathcal{E}^v} \overline{\mathcal{V}_{\rho_v, \phi_v}(v, e)} \right) \cap \Omega.$$

Here ρ_v and ϕ_v are chosen so that $\rho_v \sin(\phi_v) = Z$, a constant for all $v \in \mathcal{V}$, the set of vertices. We now introduce a set of modified coordinates in the vertex neighbourhood Ω^v . Let

$$\begin{aligned} \rho &= \sqrt{x_1^2 + x_2^2 + x_3^2} \\ \phi &= \cos^{-1}(x_3/\rho) \\ \theta &= \tan^{-1}(x_2/x_1) \end{aligned}$$

denote the usual spherical coordinates in Ω^v . Define

$$\begin{aligned} x_1^v &= \phi \\ x_2^v &= \theta \\ x_3^v &= \chi = \ln \rho. \end{aligned} \tag{2.3}$$

Let $w_v = w(v)$, denote the value of w at the vertex v . By $\tilde{\Omega}^v$ is denoted the image of Ω^v in x^v coordinates. We can now state the differentiability estimates in these modified coordinates in vertex neighbourhoods. The proof is based on the regularity results proved by Babuška and Guo in [14]. These estimates are obtained when the differential operator is the Laplacian. However they are valid for the more general situation examined in this work.

Unless otherwise stated, as in Babuška and Guo [14–16] we let $w(x^v)$, $w(x^{v-e})$, $w(x^e)$ denote $w(x(x^v))$, $w(x(x^{v-e}))$, $w(x(x^e))$ respectively. We shall use the same notation for the spectral element functions $u(x^v)$, $u(x^{v-e})$, $u(x^e)$ etc. as well in the ensuing sections and chapters.

Proposition 2.2.1. *There exists a constant $\beta_v \in (0, 1/2)$ such that for all $0 < \nu \leq \rho_v$ the estimate*

$$\int_{\tilde{\Omega}^v \cap \{x^v: x_3^v \leq \ln(\nu)\}} \sum_{|\alpha| \leq m} e^{x_3^v} |D_{x^v}^\alpha (w(x^v) - w_v)|^2 dx^v \leq C (d^m m!)^2 \nu^{(1-2\beta_v)} \quad (2.4)$$

holds for all integers $m \geq 1$. Here C and d denote constants and dx^v denotes a volume element in x^v coordinates.

Proof. The proof is provided in Appendix A.1. □

2.2.2 Differentiability estimates in modified coordinates in edge neighbourhoods

Let e denote an edge, which for convenience we assume to coincide with the x_3 axis, whose end points are the vertices v and v' as shown in Figure 2.3.

Assume that the vertex v coincides with the origin. Let the length of the edge e be l_e , $\delta_v = \rho_v \cos(\phi_v)$ and $\delta_{v'} = \rho_{v'} \cos(\phi_{v'})$. Let (r, θ, x_3) denote the usual cylindrical coordinates

$$\begin{aligned} r &= \sqrt{x_1^2 + x_2^2} \\ \theta &= \tan^{-1}(x_2/x_1) \end{aligned}$$

and Ω^e the edge neighbourhood

$$\Omega^e = \{x \in \Omega : \delta_v < x_3 < l_e - \delta_{v'}, 0 < r < Z\}$$

as shown in Figure 2.3. We introduce the modified system of coordinates

$$\begin{aligned} x_1^e &= \tau = \ln r \\ x_2^e &= \theta \\ x_3^e &= x_3. \end{aligned} \quad (2.5)$$

Let $\tilde{\Omega}^e$ denote the image of Ω^e in x^e coordinates. The differentiability estimates for the

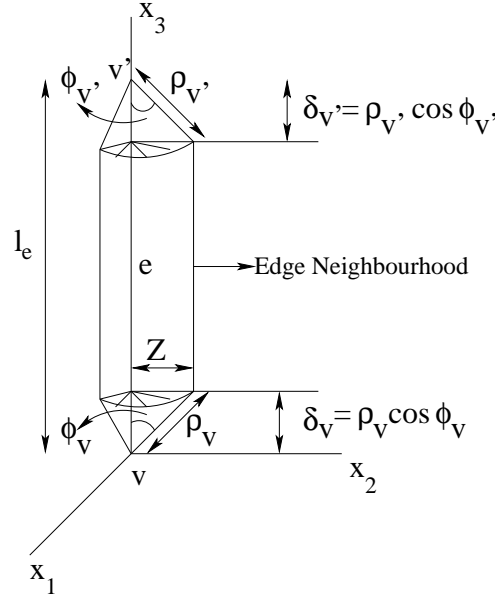


Figure 2.3: Edge neighbourhood Ω^e .

solution w in edge neighbourhoods in these modified coordinates can now be stated.

Proposition 2.2.2. *Let $s(x_3) = w(x_1, x_2, x_3)|_{(x_1=0, x_2=0)}$. Then*

$$\int_{\delta_v}^{l_e - \delta_{v'}} \sum_{k \leq m} \left| D_{x_3^e}^k s(x_3^e) \right|^2 dx_3^e \leq C (d^m m!)^2 \quad (2.6)$$

for all integers $m \geq 1$.

Moreover there exists a constant $\beta_e \in (0, 1)$ such that for $\mu \leq Z$

$$\int_{\tilde{\Omega}^e \cap \{x^e: x_1^e < \ln \mu\}} \sum_{|\alpha| \leq m} |D_{x^e}^\alpha (w(x^e) - s(x_3^e))|^2 dx^e \leq C (d^m m!)^2 \mu^{2(1-\beta_e)} \quad (2.7)$$

for all integers $m \geq 1$. Here dx^e denotes a volume element in x^e coordinates.

Proof. The proof is provided in Appendix A.2. □

2.2.3 Differentiability estimates in modified coordinates in vertex-edge neighbourhoods

Let e denote an edge, which for convenience we assume coincides with the x_3 axis, and v a vertex which coincides with the origin.

Then the vertex-edge neighbourhood Ω^{v-e} , shown in Figure 2.4, is defined as

$$\Omega^{v-e} = \{x \in \Omega : 0 < \phi < \phi_v, 0 < x_3 < \delta_v = \rho_v \cos \phi_v\}.$$

We thus obtain a set of vertex-edge neighbourhoods Ω^{v-e} where $v - e \in \mathcal{V} - \mathcal{E}$, the set

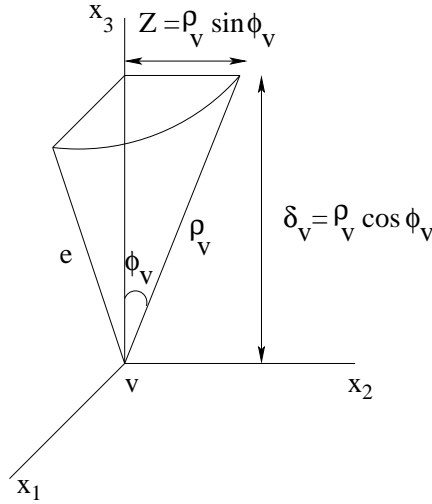


Figure 2.4: Vertex-edge neighbourhood Ω^{v-e} .

of vertex-edges.

Let us introduce a set of modified coordinates in the vertex-edge neighbourhood Ω^{v-e}

$$\begin{aligned} x_1^{v-e} &= \psi = \ln(\tan \phi) \\ x_2^{v-e} &= \theta \\ x_3^{v-e} &= \zeta = \ln x_3. \end{aligned} \tag{2.8}$$

Let $\tilde{\Omega}^{v-e}$ denote the image of Ω^{v-e} in x^{v-e} coordinates. We can now state the differentiability estimates in modified coordinates in vertex-edge neighbourhoods.

Proposition 2.2.3. *Let $w_v = w(v)$, the value of w evaluated at the vertex v , and $s(x_3) = w(x_1, x_2, x_3)|_{(x_1=0, x_2=0)}$. Then there exists a constant $\beta_v \in (0, 1/2)$ such that for any $0 < \nu \leq \delta_v$*

$$\int_{-\infty}^{\ln \nu} e^{x_3^{v-e}} \sum_{k \leq m} \left| D_{x_3^{v-e}}^k (s(x_3^{v-e}) - w_v) \right|^2 dx_3^{v-e} \leq C (d^m m!)^2 \nu^{(1-2\beta_v)}. \tag{2.9}$$

Moreover there exists a constant $\beta_e \in (0, 1)$ such that for any $0 < \alpha \leq \tan \phi_v$ and $0 < \nu \leq \delta_v$

$$\begin{aligned} \int_{\tilde{\Omega}^{v-e} \cap \{x^{v-e}: x_1^{v-e} < \ln \alpha, x_3^{v-e} < \ln \nu\}} e^{x_3^{v-e}} \sum_{|\gamma| \leq m} |D_{x^{v-e}}^\gamma (w(x^{v-e}) - s(x_3^{v-e}))|^2 dx^{v-e} \\ \leq C (d^m m!)^2 \alpha^{2(1-\beta_e)} \nu^{(1-2\beta_v)} \end{aligned} \quad (2.10)$$

for all integers $m \geq 1$. Here dx^{v-e} denotes a volume element in x^{v-e} coordinates.

Proof. The proof is provided in Appendix A.3. \square

2.2.4 Differentiability estimates in standard coordinates in the regular region of the polyhedron

Let Ω^r denote the portion of the polyhedron Ω obtained after the closure of the vertex neighbourhoods, edge neighbourhoods and vertex-edge neighbourhoods have been removed from it.

Thus let

$$\Delta = \left\{ \bigcup_{v \in \mathcal{V}} \overline{\Omega}^v \right\} \cup \left\{ \bigcup_{e \in \mathcal{E}} \overline{\Omega}^e \right\} \cup \left\{ \bigcup_{v-e \in \mathcal{V}-\mathcal{E}} \overline{\Omega}^{v-e} \right\}.$$

Then

$$\Omega^r = \Omega \setminus \Delta.$$

We denote the regular region of the polyhedron, in which the solution w is analytic, by Ω^r . In Ω^r the standard coordinate system $x = (x_1, x_2, x_3)$ is retained. The differentiability estimates in these coordinates in the regular region of the polyhedron, are now stated.

Proposition 2.2.4. *The estimate*

$$\int_{\Omega^r} \sum_{|\alpha| \leq m} |D_x^\alpha w(x)|^2 dx \leq C (d^m m!)^2 \quad (2.11)$$

holds for all integers $m \geq 1$. Here dx denotes a volume element in x coordinates.

Proof. The proof is provided in Appendix A.4. \square

2.2.5 Function spaces

We need to review a set of function spaces described in [14].

Let Ω^v denote the vertex neighbourhood of the vertex v and $\rho = \rho(x) = \text{dist}(x, v)$ for $x \in \Omega^v$ and $\beta_v \in (0, 1/2)$. We introduce a weight function as in [14] as follows: Define

$$\Phi_{\beta_v}^{\alpha, l}(x) = \begin{cases} \rho^{\beta_v + |\alpha| - l}, & \text{for } |\alpha| \geq l \\ 1, & \text{for } |\alpha| < l \end{cases}$$

as in (2.3) of [14]. Let

$$\mathbf{H}_{\beta_v}^{k, l}(\Omega^v) = \left\{ u \mid \|u\|_{\mathbf{H}_{\beta_v}^{k, l}(\Omega^v)}^2 = \sum_{|\alpha| \leq k} \left\| \Phi_{\beta_v}^{\alpha, l} D^\alpha u \right\|_{L^2(\Omega^v)}^2 < \infty \right\}$$

and

$$\mathbf{B}_{\beta_v}^l(\Omega^v) = \left\{ u \mid u \in \mathbf{H}_{\beta_v}^{k, l}(\Omega^v) \text{ for all } k \geq l \text{ and } \left\| \Phi_{\beta_v}^{\alpha, l} D^\alpha u \right\|_{L^2(\Omega^v)}^2 \leq C d^\alpha \alpha! \right\}$$

denote the weighted Sobolev space and countably normed space defined on Ω^v as in [14].

Let us denote by $\mathbf{C}_{\beta_v}^2(\Omega^v)$ a countably normed space as in [14, 51] which is the set of functions $u(x) \in \mathbf{C}^0(\bar{\Omega}^v)$ such that for all α , $|\alpha| \geq 0$

$$|D_x^\alpha(u(x) - u(v))| \leq C d^\alpha \alpha! \rho^{-(\beta_v + |\alpha| - 1/2)}(x).$$

Here $\bar{\Omega}^v$ denotes the closure of Ω^v . Then by Theorem 5.6 of [14], $\mathbf{B}_{\beta_v}^2(\Omega^v) \subseteq \mathbf{C}_{\beta_v}^2(\Omega^v)$.

We now cite an important regularity result, viz. Theorem 5.1 of [51] for the solution of (2.1).

There exists a unique (weak) solution $u \in H^1(\Omega^v)$ of (2.1) which belongs to $\mathbf{C}_{\beta_v}^2(\Omega^v)$ with $\beta_v \in (0, 1/2)$ satisfying

$$\beta_v \geq 1/2 - \lambda_v, \lambda_v = \frac{1}{2} \sqrt{1 + 4\nu_{\min}^v} - 1 \quad (2.12)$$

where ν_{\min}^v is the smallest positive eigenvalue of the Laplace-Beltrami operator on the spherical boundary S^v .

Next, let Ω^e denote an edge neighbourhood of Ω and $r = r(x) = \text{dist}(x, e)$ for $x \in \Omega^e$ and $\beta_e \in (0, 1)$. Define the weight function by

$$\Phi_{\beta_e}^{\alpha, l}(x) = \begin{cases} r^{\beta_e + |\alpha'| - l}, & \text{for } |\alpha'| = \alpha_1 + \alpha_2 \geq l \\ 1, & \text{for } |\alpha| < l \end{cases}$$

as in (2.1) of [14]. Let

$$\mathbf{H}_{\beta_e}^{k,l}(\Omega^e) = \left\{ u \mid \|u\|_{\mathbf{H}_{\beta_e}^{k,l}(\Omega^e)}^2 = \sum_{|\alpha| \leq k} \left\| \Phi_{\beta_e}^{\alpha,l} D^\alpha u \right\|_{L^2(\Omega^e)}^2 < \infty \right\}$$

and

$$\mathbf{B}_{\beta_e}^l(\Omega^e) = \left\{ u \mid u \in \mathbf{H}_{\beta_e}^{k,l}(\Omega^e) \text{ for all } k \geq l \text{ and } \left\| \Phi_{\beta_e}^{\alpha,l} D^\alpha u \right\|_{L^2(\Omega^e)}^2 \leq C d^\alpha \alpha! \right\}$$

denote the weighted Sobolev space and countably normed space defined on Ω^e as in [14].

We denote by $\mathbf{C}_{\beta_e}^2(\Omega^e)$, $\beta_e \in (0, 1)$ a countably normed space as in [14, 51], the set of functions $u \in \mathbf{C}^0(\bar{\Omega}^e)$ such that for $|\alpha| \geq 0$

$$\left\| r^{\beta_e + \alpha_1 + \alpha_2 - 1} D_x^\alpha (u(x) - u(0, 0, x_3)) \right\|_{\mathbf{C}^0(\bar{\Omega}^e)} \leq C d^\alpha \alpha!$$

and for $k \geq 0$

$$\left\| \frac{d^k}{(dx_3)^k} u(0, 0, x_3) \right\|_{\mathbf{C}^0(\bar{\Omega}^e \cap \{x: x_1=x_2=0\})} \leq C d^k k!,$$

where $\bar{\Omega}^e$ denotes the closure of Ω^e . Then by Theorem 5.3 of [14], $\mathbf{B}_{\beta_e}^2(\Omega^e) \subseteq \mathbf{C}_{\beta_e}^2(\Omega^e)$.

We now cite another important regularity result, viz. Theorem 3.1 of [51] for the solution of (2.1).

There exists a unique (weak) solution $u \in H^1(\Omega^e)$ of (2.1) which belongs to $\mathbf{C}_{\beta_e}^2(\Omega^e)$ with $\beta_e \in (0, 1)$ satisfying

$$\beta_e \geq 1 - \kappa_e, \kappa_e = \begin{cases} \frac{\pi}{2\omega_e} & \text{if } \Gamma_s \subset \Gamma^{[0]}, \Gamma_t \subset \Gamma^{[1]} \\ \frac{\pi}{\omega_e}, & \text{otherwise} \end{cases} \quad (2.13)$$

where Γ_s and Γ_t are such that $\Gamma_s \cap \Gamma_t = e$.

Finally, let $\rho = \rho(x)$ and $\phi = \phi(x)$ for $x \in \Omega^{v-e}$. We define a weight function by

$$\Phi_{\beta_{v-e}}^{\alpha,l}(x) = \begin{cases} \rho^{\beta_v + |\alpha| - l} (\sin(\phi))^{\beta_e + |\alpha'| - l}, & \text{for } |\alpha'| = \alpha_1 + \alpha_2 \geq l \\ \rho^{\beta_v + |\alpha| - l}, & \text{for } |\alpha'| < l \leq |\alpha| \\ 1, & \text{for } |\alpha| < l \end{cases}$$

as in (2.2) of [14]. Let

$$\mathbf{H}_{\beta_{v-e}}^{k,l}(\Omega^{v-e}) = \left\{ u \mid \|u\|_{\mathbf{H}_{\beta_{v-e}}^{k,l}(\Omega^{v-e})}^2 = \sum_{|\alpha| \leq k} \left\| \Phi_{\beta_{v-e}}^{\alpha,l} D^\alpha u \right\|_{L^2(\Omega^{v-e})}^2 < \infty \right\}$$

and

$$\mathbf{B}_{\beta_{v-e}}^l(\Omega^{v-e}) = \left\{ u \mid u \in \mathbf{H}_{\beta_{v-e}}^{k,l}(\Omega^{v-e}) \ \forall k \geq l \text{ and } \left\| \Phi_{\beta_{v-e}}^{\alpha,l} D^\alpha u \right\|_{L^2(\Omega^{v-e})}^2 \leq C d^\alpha \alpha! \right\}$$

denote the weighted Sobolev space and countably normed space defined on Ω^{v-e} as in [14].

Let us denote by $\mathbf{C}_{\beta_{v-e}}^2(\Omega^{v-e})$, where $\beta_{v-e} = (\beta_v, \beta_e)$, $\beta_v \in (0, 1/2)$ and $\beta_e \in (0, 1)$, the set of functions $u(x) \in \mathbf{C}^0(\bar{\Omega}^{v-e})$ such that

$$\left\| \rho^{\beta_v+|\alpha|-1/2} (\sin \phi)^{\beta_e+\alpha_1+\alpha_2-1} D_x^\alpha (u(x) - u(0, 0, x_3)) \right\|_{\mathbf{C}^0(\bar{\Omega}^{v-e})} \leq C d^\alpha \alpha!$$

and

$$\left| |x_3|^{\beta_v+k-1/2} \frac{d^k}{dx_3^k} (u(0, 0, x_3) - u(v)) \right|_{\mathbf{C}^0(\bar{\Omega}^{v-e} \cap \{x: x_1=x_2=0\})} \leq C d^k k!$$

as described in [14, 51]. Here $\bar{\Omega}^{v-e}$ denotes the closure of Ω^{v-e} . Now by Theorem 5.9 of [14], $\mathbf{B}_{\beta_{v-e}}^2(\Omega^{v-e}) \subseteq \mathbf{C}_{\beta_{v-e}}^2(\Omega^{v-e})$.

We cite one last Theorem 4.1 of [51] for the solution of (2.1).

There exists a unique (weak) solution $u \in H^1(\Omega^{v-e})$ of (2.1) which belongs to $\mathbf{C}_{\beta_{v-e}}^2(\Omega^{v-e})$, where $\beta_{v-e} = (\beta_v, \beta_e)$, $\beta_v \in (0, 1/2)$ and $\beta_e \in (0, 1)$ satisfying (2.12) and (2.13).

2.3 The Stability Theorem

Ω is divided into a regular region Ω^r , a set of vertex neighbourhoods Ω^v , where $v \in \mathcal{V}$, a set of edge neighbourhoods Ω^e , where $e \in \mathcal{E}$ and a set of vertex-edge neighbourhoods Ω^{v-e} , where $v-e \in \mathcal{V}-\mathcal{E}$. In the regular region Ω^r standard coordinates $x = (x_1, x_2, x_3)$ are used and in the remaining regions modified coordinates are used as has been described in Section 2. Ω^r is divided into a set of curvilinear hexahedrons, tetrahedrons and prisms. We impose a geometrically graded mesh in the remaining regions which is described in this section. We remark that a tetrahedron can always be divided into four hexahedrons [77], in the same way that a triangle can be divided into three quadrilaterals by joining the centre of the triangle to the midpoints of the sides (Figure 2.5). Moreover a prism can be divided into three hexahedral elements. Hence we can choose all our elements to be hexahedrons. A set of spectral element functions are defined on the elements. In edge

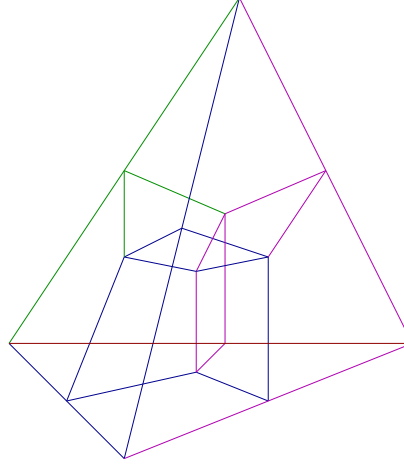


Figure 2.5: Division of a tetrahedron into hexahedrons.

neighbourhoods and vertex-edge neighbourhoods these spectral element functions are a sum of tensor products of polynomials in the modified coordinates. Let $\{\mathcal{F}_u\}$ denote the spectral element representation of the function u . We shall examine two cases. The first case is when the spectral element functions are nonconforming. The second case is when the spectral element functions are conforming on the wirebasket WB of the elements, i.e. the union of the edges and vertices of the elements. In both these cases the spectral element functions are nonconforming on the faces (open) of the elements.

To state the stability theorem we need to define some quadratic forms. Let N denote the number of refinements in the geometrical mesh and W denote an upper bound on the degree of the polynomial representation of the spectral element functions. We shall define two quadratic forms $\mathcal{V}^{N,W}(\{\mathcal{F}_u\})$ and $\mathcal{U}^{N,W}(\{\mathcal{F}_u\})$.

Now

$$\begin{aligned} \mathcal{V}^{N,W}(\{\mathcal{F}_u\}) &= \mathcal{V}_{regular}^{N,W}(\{\mathcal{F}_u\}) + \mathcal{V}_{vertices}^{N,W}(\{\mathcal{F}_u\}) + \mathcal{V}_{vertex-edges}^{N,W}(\{\mathcal{F}_u\}) \\ &\quad + \mathcal{V}_{edges}^{N,W}(\{\mathcal{F}_u\}). \end{aligned} \quad (2.14)$$

In the same way

$$\begin{aligned} \mathcal{U}^{N,W}(\{\mathcal{F}_u\}) &= \mathcal{U}_{regular}^{N,W}(\{\mathcal{F}_u\}) + \mathcal{U}_{vertices}^{N,W}(\{\mathcal{F}_u\}) + \mathcal{U}_{vertex-edges}^{N,W}(\{\mathcal{F}_u\}) \\ &\quad + \mathcal{U}_{edges}^{N,W}(\{\mathcal{F}_u\}). \end{aligned} \quad (2.15)$$

Let us first consider the regular region Ω^r of Ω and define the two quadratic forms $\mathcal{V}_{regular}^{N,W}(\{\mathcal{F}_u\})$ and $\mathcal{U}_{regular}^{N,W}(\{\mathcal{F}_u\})$. The regular region Ω^r is divided into N_r curvilinear hexahedrons, tetrahedrons and prisms. In Ω^r the standard coordinates $x = (x_1, x_2, x_3)$ are used. Let Ω_l^r be one of the elements into which Ω^r is divided, which we shall assume is a curvilinear hexahedron to keep the exposition simple. Let Q denote the standard cube $Q = (-1, 1)^3$. Then there is an analytic map M_l^r from Q to Ω_l^r which has an analytic inverse. Let Ω_l^r be as shown in Figure 2.6 and let $\{\Gamma_{l,i}^r\}_{1 \leq i \leq n_l^r}$ denote its faces. Now the

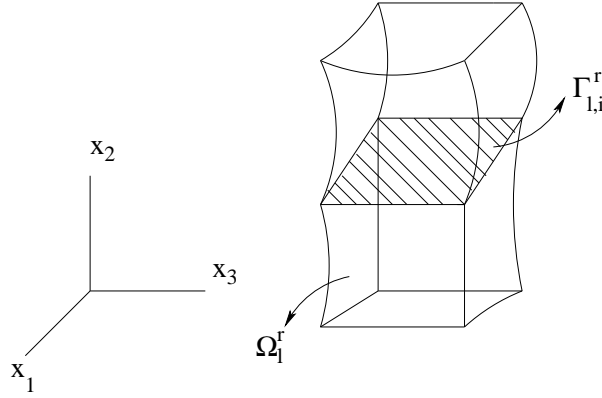


Figure 2.6: Elements in Ω^r .

map M_l^r is of the form

$$x = X_l^r(\lambda_1, \lambda_2, \lambda_3)$$

where $(\lambda_1, \lambda_2, \lambda_3) \in Q$, the master cube. Define the spectral element function u_l^r on Ω_l^r by

$$u_l^r(\lambda) = \sum_{i=0}^W \sum_{j=0}^W \sum_{k=0}^W \alpha_{i,j,k} \lambda_1^i \lambda_2^j \lambda_3^k.$$

Now the spectral element functions are nonconforming in the general case. Let $[u]_{\Gamma_{l,i}^r}$ denote the jump in u across the face $\Gamma_{l,i}^r$. Let the face $\Gamma_{l,i}^r = \Gamma_{m,j}^r$ where $\Gamma_{m,j}^r$ is a face of the element Ω_m^r . We may assume the face $\Gamma_{l,i}^r$ corresponds to $\lambda_3 = 1$ and $\Gamma_{m,j}^r$ corresponds to $\lambda_3 = -1$. Then $[u]_{\Gamma_{l,i}^r}$ is a function of only λ_1 and λ_2 .

We now define

$$\begin{aligned}
\mathcal{V}_{regular}^{N,W}(\{\mathcal{F}_u\}) &= \sum_{l=1}^{N_r} \int_{\Omega_l^r} |Lu_l^r(x)|^2 dx \\
&+ \sum_{\Gamma_{l,i}^r \subseteq \bar{\Omega}^r \setminus \partial\Omega} \left(\| [u] \|_{0,\Gamma_{l,i}^r}^2 + \sum_{k=1}^3 \| [u_{x_k}] \|_{1/2,\Gamma_{l,i}^r}^2 \right) \\
&+ \sum_{\Gamma_{l,i}^r \subseteq \Gamma^{[0]}} \|u_l^r\|_{3/2,\Gamma_{l,i}^r}^2 + \sum_{\Gamma_{l,i}^r \subseteq \Gamma^{[1]}} \left\| \left(\frac{\partial u_l^r}{\partial \nu} \right)_A \right\|_{1/2,\Gamma_{l,i}^r}^2. \tag{2.16}
\end{aligned}$$

The fractional Sobolev norms used above are as defined in [46].

Since $\Gamma_{l,i}^r$, corresponding to $\lambda_3 = 1$, is the image of $S = (-1, 1)^2$, or T the master triangle, in λ_1, λ_2 coordinates

$$\|w\|_{\sigma,\Gamma_{l,i}^r}^2 = \|w\|_{0,E}^2 + \int_E \int_E \frac{(w(\lambda_1, \lambda_2) - w(\lambda'_1, \lambda'_2))^2}{((\lambda_1 - \lambda'_1)^2 + (\lambda_2 - \lambda'_2)^2)^{1+\sigma}} d\lambda_1 d\lambda_2 d\lambda'_1 d\lambda'_2 \tag{2.17a}$$

for $0 < \sigma < 1$. Here E denote either S or T .

However, if E is S then we prefer to use the equivalent norm

$$\begin{aligned}
\|w\|_{\sigma,\Gamma_{l,i}^r}^2 &= \|w\|_{0,E}^2 + \int_{-1}^1 \int_{-1}^1 \int_{-1}^1 \frac{(w(\lambda_1, \lambda_2) - w(\lambda'_1, \lambda_2))^2}{(\lambda_1 - \lambda'_1)^{1+2\sigma}} d\lambda_1 d\lambda'_1 d\lambda_2 \\
&+ \int_{-1}^1 \int_{-1}^1 \int_{-1}^1 \frac{(w(\lambda_1, \lambda_2) - w(\lambda_1, \lambda'_2))^2}{(\lambda_2 - \lambda'_2)^{1+2\sigma}} d\lambda_2 d\lambda'_2 d\lambda_1. \tag{2.17b}
\end{aligned}$$

Moreover

$$\|w\|_{1+\sigma,\Gamma_{l,i}^r}^2 = \|w\|_{0,E}^2 + \sum_{i=1}^2 \left\| \frac{\partial w}{\partial \lambda_i} \right\|_{\sigma,E}^2. \tag{2.18}$$

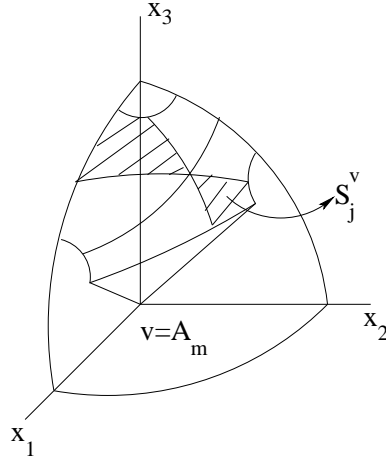
Next, we define

$$\mathcal{U}_{regular}^{N,W}(\{\mathcal{F}_u\}) = \sum_{l=1}^{N_r} \int_{Q=(M_l^r)^{-1}(\Omega_l^r)} \sum_{|\alpha| \leq 2} |D_\lambda^\alpha u_l^r|^2 d\lambda. \tag{2.19}$$

Let v be one of the vertices of Ω . In Figure 2.7 the vertex neighbourhood, described in Section 2.1, is shown. Let S^v denote the intersection of the surface of the sphere $B_{\rho_v}(v)$ with $\bar{\Omega}^v$, i.e.

$$S^v = \{x \in \bar{\Omega}^v : \text{dist}(x, v) = \rho_v\}.$$

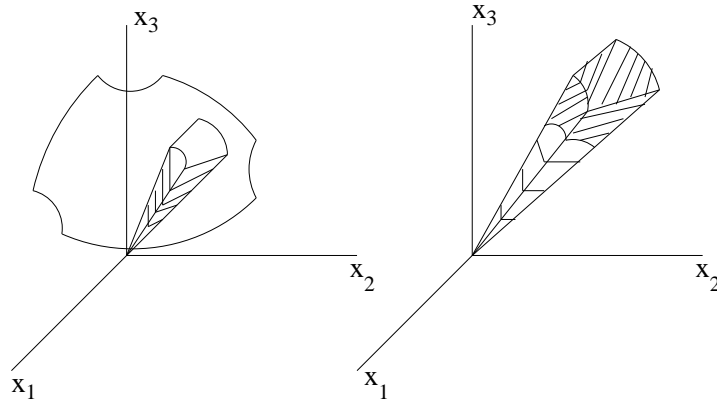
We divide the surface S^v into a set of triangular and quadrilateral elements as shown in Figure 2.8. Let S_j^v denote these elements where $1 \leq j \leq I_v$. Here I_v denotes a fixed

Figure 2.7: Mesh imposed on the spherical boundary S^v .

constant. Let μ_v be a positive constant less than one which shall be used to define a geometric mesh in the vertex neighbourhood Ω^v of the vertex v . We now divide Ω^v into $N_v = I_v(N + 1)$ curvilinear hexahedrons and prisms $\{\Omega_l^v\}_{1 \leq l \leq N_v}$, where Ω_l^v is of the form

$$\Omega_l^v = \{x : (\phi, \theta) \in S_j^v, \rho_k^v < \rho < \rho_{k+1}^v\}$$

for $1 \leq j \leq I_v$ and $0 \leq k \leq N$. Here $\rho_k^v = \rho_v(\mu_v)^{N+1-k}$ and $0 < \mu_v < 1$ for

Figure 2.8: Geometrical mesh imposed on Ω^v .

$1 \leq k \leq N + 1$. Moreover $\rho_0^v = 0$. We introduce the vertex coordinates x^v ,

$$x_1^v = \phi$$

$$x_2^v = \theta$$

$$x_3^v = \chi = \ln \rho .$$

Let $\tilde{\Omega}^v$ denote the image of Ω^v in x^v coordinates and $\tilde{\Omega}_l^v$ denote the image of the element Ω_l^v . Then the geometric mesh $\{\Omega_l^v\}_{1 \leq l \leq N_v}$ which has been defined on Ω^v , is mapped to a quasi-uniform mesh $\{\tilde{\Omega}_l^v\}_{1 \leq l \leq N_v}$ on $\tilde{\Omega}^v$, except that the corner elements

$$\Omega_l^v = \{x : (\phi, \theta) \in S_j^v, 0 < \rho < \rho_1^v\}$$

are mapped to the semi-infinite elements

$$\tilde{\Omega}_l^v = \{x^v : (\phi, \theta) \in S_j^v, -\infty < \chi < \ln \rho_1^v\} .$$

We now specify the form of the spectral element functions $u_l^v(x^v)$ on the elements. Consider first the case when $\tilde{\Omega}_l^v$ is a corner element of the form

$$\tilde{\Omega}_l^v = \{x^v : (\phi, \theta) \in S_j^v, -\infty < \chi < \ln \rho_1^v\} .$$

In this case we define $u_l^v(x^v) = h^v$, where h^v is a constant. Thus at all corner elements the spectral element functions assume the same constant value for that corner.

Now there is an analytic map M_l^v from Q , the master cube to $\tilde{\Omega}_l^v$, which has an analytic inverse. Here the map M_l^v is of the form

$$x^v = X_l^v(\lambda_1, \lambda_2, \lambda_3).$$

We define the spectral element function u_l^v on $\tilde{\Omega}_l^v$ by

$$u_l^v(\lambda) = \sum_{t=0}^{W_l} \sum_{s=0}^{W_l} \sum_{r=0}^{W_l} \beta_{r,s,t} \lambda_1^r \lambda_2^s \lambda_3^t .$$

Here $1 \leq W_l \leq W$. Moreover as in [51], $W_l = [\mu_1 i]$ for $1 \leq i \leq N$, where $\mu_1 > 0$ is a degree factor. Hereafter $[a]$ denotes the greatest positive integer $\leq a$.

Let $v \in \mathcal{V}$ denote the vertices of Ω . Define

$$\mathcal{V}_{vertices}^{N,W}(\{\mathcal{F}_u\}) = \sum_{v \in \mathcal{V}} \mathcal{V}_v^{N,W}(\{\mathcal{F}_u\}) \quad (2.20)$$

and

$$\mathcal{U}_{vertices}^{N,W}(\{\mathcal{F}_u\}) = \sum_{v \in \mathcal{V}} \mathcal{U}_v^{N,W}(\{\mathcal{F}_u\}) . \quad (2.21)$$

We now fix a vertex v and define the quadratic forms $\mathcal{V}_v^{N,W}(\{\mathcal{F}_u\})$ and $\mathcal{U}_v^{N,W}(\{\mathcal{F}_u\})$. Consider the vertex neighbourhood Ω^v and let Ω_l^v be one of the elements into which it is divided. Now Ω_l^v has n_l^v faces $\{\Gamma_{l,i}^v\}_{1 \leq i \leq n_l^v}$. Let $\tilde{\Omega}_l^v$ be the image of Ω_l^v and $\tilde{\Gamma}_{l,i}^v$ be the image of $\Gamma_{l,i}^v$ in x^v coordinates.

Define $L^v u(x^v)$ so that

$$\int_{\tilde{\Omega}_l^v} |L^v u(x^v)|^2 dx^v = \int_{\Omega_l^v} \rho^2 |Lu(x)|^2 dx. \quad (2.22)$$

Here dx^v denotes a volume element in x^v coordinates and dx a volume element in x coordinates. In Chapter 3 it will be shown that

$$L^v u(x^v) = -\text{div}_{x^v} \left(e^{x/2} \sqrt{\sin \phi} A^v \nabla_{x^v} u \right) + \sum_{i=1}^3 \hat{b}_i^v u_{x_i^v} + \hat{c}^v u. \quad (2.23)$$

In the above A^v is a symmetric, positive definite matrix.

Let $\Gamma_{l,i}^v$ be one of the faces of Ω_l^v and $\tilde{\Gamma}_{l,i}^v$ denote its image in x^v coordinates. Let \tilde{P} be a point belonging to $\tilde{\Gamma}_{l,i}^v$ and $\boldsymbol{\nu}^v$ be the unit normal to $\tilde{\Gamma}_{l,i}^v$ at the point \tilde{P} . Then define

$$\left(\frac{\partial u}{\partial \boldsymbol{\nu}^v} \right)_{A^v}(\tilde{P}) = (\boldsymbol{\nu}^v)^T A^v \nabla_{x^v} u. \quad (2.24)$$

Here the matrix A^v is as in (2.21).

Let

$$R_{l,i}^v = \sup_{x^v \in \tilde{\Gamma}_{l,i}^v} (e^{x^v}).$$

We now define

$$\begin{aligned} \mathcal{V}_v^{N,W}(\{\mathcal{F}_u\}) &= \sum_{l=1, \mu(\tilde{\Omega}_l^v) < \infty}^{N_v} \int_{\tilde{\Omega}_l^v} |L^v u_l^v(x^v)|^2 dx^v \\ &+ \sum_{\substack{\Gamma_{l,i}^v \subseteq \Omega^v \setminus \partial\Omega, \\ \mu(\tilde{\Gamma}_{l,i}^v) < \infty}} \left(\left\| \sqrt{R_{l,i}^v} [u] \right\|_{0, \tilde{\Gamma}_{l,i}^v}^2 + \sum_{k=1}^3 \left\| \sqrt{R_{l,i}^v} [u_{x_k^v}] \right\|_{1/2, \tilde{\Gamma}_{l,i}^v}^2 \right) \\ &+ \sum_{\substack{\Gamma_{l,i}^v \subseteq \Gamma^{[0]}, \\ \mu(\tilde{\Gamma}_{l,i}^v) < \infty}} \left\| \sqrt{R_{l,i}^v} u_l^v \right\|_{3/2, \tilde{\Gamma}_{l,i}^v}^2 + \sum_{\substack{\Gamma_{l,i}^v \subseteq \Gamma^{[1]}, \\ \mu(\tilde{\Gamma}_{l,i}^v) < \infty}} \left\| \sqrt{R_{l,i}^v} \left(\frac{\partial u_l^v}{\partial \boldsymbol{\nu}^v} \right)_{A^v} \right\|_{1/2, \tilde{\Gamma}_{l,i}^v}^2. \end{aligned} \quad (2.25)$$

The fractional Sobolev norms used above are as in (2.17) and (2.18). Moreover μ denotes measure.

Finally, the quadratic form $\mathcal{U}_v^{N,W}(\{\mathcal{F}_u\})$ is given by

$$\mathcal{U}_v^{N,W}(\{\mathcal{F}_u\}) = \sum_{l=1}^{N_v} \int_{\tilde{\Omega}_l^v} e^{x_3^v} \sum_{|\alpha| \leq 2} |D_{x^v}^\alpha u_l^v(x^v)|^2 dx^v. \quad (2.26)$$

We now define $\mathcal{V}_{vertex-edges}^{N,W}(\{\mathcal{F}_u\})$ and $\mathcal{U}_{vertex-edges}^{N,W}(\{\mathcal{F}_u\})$. Let $v - e$ denote one of the vertex-edges of Ω . Here $v - e \in \mathcal{V} - \mathcal{E}$, the set of vertex-edges of Ω . Let Ω^{v-e} denote the vertex-edge neighbourhood corresponding to the vertex-edge $v - e$. We divide Ω^{v-e} into N_{v-e} elements Ω_l^{v-e} , $l = 1, 2, \dots, N_{v-e}$, using a geometric mesh.

Figure 2.9 shows the vertex-edge neighbourhood Ω^{v-e} of the vertex v and the edge e . Now

$$\Omega^{v-e} = \{x \in \Omega : 0 < x_3 < \delta_v, 0 < \phi < \phi_v\}.$$

Here $\delta_v = \rho_v \cos \phi_v$. We impose a geometrical mesh on Ω^{v-e} as shown in Figure 2.9 by defining

$$(x_3)_0 = 0 \text{ and } (x_3)_i = \delta_v (\mu_v)^{N+1-i}$$

for $1 \leq i \leq N+1$. Let

$$\zeta_i^{v-e} = \ln((x_3)_i)$$

for $0 \leq i \leq N+1$.

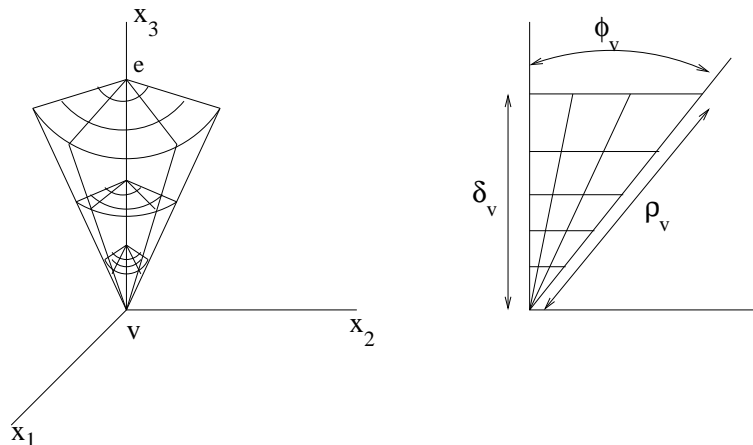


Figure 2.9: Geometrical mesh imposed on Ω^{v-e} .

Let us introduce points $\phi_0^{v-e}, \dots, \phi_{N+1}^{v-e}$ such that $\phi_0^{v-e} = 0$ and $\tan \phi_i^{v-e} = \mu_e^{N+1-i} \tan(\phi_v)$, for $1 \leq i \leq N+1$. Here μ_e is a positive constant less than one. Thus we impose a geometrical mesh on ϕ with mesh ratio μ_e . Finally, $\theta_{v-e}^l < \theta < \theta_{v-e}^u$. A quasi-uniform mesh

$$\theta_{v-e}^l = \theta_0^{v-e} < \theta_1^{v-e} < \dots < \theta_{I_{v-e}}^{v-e} = \theta_{v-e}^u$$

is imposed in θ . We introduce new coordinates in Ω^{v-e} by

$$x_1^{v-e} = \psi = \ln(\tan \phi)$$

$$x_2^{v-e} = \theta$$

$$x_3^{v-e} = \zeta = \ln x_3.$$

Let $\tilde{\Omega}^{v-e}$ be the image of Ω^{v-e} in x^{v-e} coordinates. Thus $\tilde{\Omega}^{v-e}$ is divided into $N_{v-e} = I_{v-e}(N+1)^2$ hexahedrons $\{\tilde{\Omega}_n^{v-e}\}_{n=1, \dots, N_{v-e}}$, where

$$\tilde{\Omega}_n^{v-e} = \{x^{v-e} : \psi_i^{v-e} < \psi < \psi_{i+1}^{v-e}, \theta_j^{v-e} < \theta < \theta_{j+1}^{v-e}, \zeta_k^{v-e} < \zeta < \zeta_{k+1}^{v-e}\}.$$

We now define the spectral element functions on the elements in $\tilde{\Omega}^{v-e}$. Consider an element

$$\tilde{\Omega}_n^{v-e} = \{x^{v-e} : \psi_i^{v-e} < \psi < \psi_{i+1}^{v-e}, \theta_j^{v-e} < \theta < \theta_{j+1}^{v-e}, -\infty < \zeta < \zeta_1^{v-e}\}.$$

Then on $\tilde{\Omega}_n^{v-e}$

$$u_n^{v-e} = h_{v-e} = h_v$$

where h_v is the same constant as for the spectral element function u_m^v defined on the corner element

$$\tilde{\Omega}_m^v = \{x^v : (\phi, \theta) \in S_j^v, -\infty < \chi < \ln(\rho_1^v)\}.$$

Next, we consider the element

$$\tilde{\Omega}_p^{v-e} = \{x^{v-e} : -\infty < \psi < \psi_1^{v-e}, \theta_j^{v-e} < \theta < \theta_{j+1}^{v-e}, \zeta_k^{v-e} < \zeta < \zeta_{k+1}^{v-e}\}.$$

Here $k \geq 1$.

Then on $\tilde{\Omega}_p^{v-e}$ we define

$$u_p^{v-e}(x^{v-e}) = \sum_{l=0}^{W_p} \beta_l \zeta^l.$$

Here $1 \leq W_p \leq W$. Moreover $W_p = [\mu_2 k]$ for $1 \leq k \leq N$, where $\mu_2 > 0$ is a degree factor.

Now consider

$$\tilde{\Omega}_q^{v-e} = \{x^{v-e} : \psi_i^{v-e} < \psi < \psi_{i+1}^{v-e}, \theta_j^{v-e} < \theta < \theta_{j+1}^{v-e}, \zeta_k^{v-e} < \zeta < \zeta_{k+1}^{v-e}\}$$

for $1 \leq i \leq N$, $1 \leq k \leq N$. Then on $\tilde{\Omega}_q^{v-e}$ we define

$$u_q^{v-e}(x^{v-e}) = \sum_{r=0}^{W_q} \sum_{s=0}^{W_q} \sum_{t=0}^{V_q} \gamma_{r,s,t} \psi^r \theta^s \zeta^t.$$

Here $1 \leq W_q \leq W$ and $1 \leq V_q \leq W$. Moreover $W_q = [\mu_1 i]$, $V_q = [\mu_2 k]$ for $1 \leq i, k \leq N$, where $\mu_1, \mu_2 > 0$ are degree factors [51].

Let $\tilde{\Gamma}_{n,i}^{v-e}$ be one of the faces of $\tilde{\Omega}_n^{v-e}$ such that $\mu(\tilde{\Gamma}_{n,i}^{v-e}) < \infty$, where μ denotes measure.

We introduce a norm $||| u |||_{\tilde{\Gamma}_{n,i}^{v-e}}^2$ as follows:

Let $E_{n,i}^{v-e} = \sup_{x^{v-e} \in \tilde{\Gamma}_{n,i}^{v-e}} (\sin \phi)$ and $F_{n,i}^{v-e} = \sup_{x^{v-e} \in \tilde{\Gamma}_{n,i}^{v-e}} (e^{x_3^{v-e}})$. We also define $G_{n,i}^{v-e}$ which is used in (2.29).

1) If $\tilde{\Gamma}_{n,i}^{v-e} = \{x^{v-e} : \alpha_0 < x_1^{v-e} < \alpha_1, \beta_0 < x_2^{v-e} < \beta_1, x_3^{v-e} = \gamma_0\}$ then define $G_{n,i}^{v-e} = E_{n,i}^{v-e}$ and

$$\begin{aligned} ||| u |||_{\tilde{\Gamma}_{n,i}^{v-e}}^2 &= E_{n,i}^{v-e} F_{n,i}^{v-e} \left(\int_{\beta_0}^{\beta_1} \int_{\alpha_0}^{\alpha_1} u^2(\psi, \theta, \gamma_0) d\psi d\theta \right. \\ &\quad + \int_{\beta_0}^{\beta_1} d\theta \int_{\alpha_0}^{\alpha_1} \int_{\alpha_0}^{\alpha_1} \frac{(u(\psi, \theta, \gamma_0) - u(\psi', \theta, \gamma_0))^2}{(\psi - \psi')^2} d\psi d\psi' \\ &\quad \left. + \int_{\alpha_0}^{\alpha_1} d\psi \int_{\beta_0}^{\beta_1} \int_{\beta_0}^{\beta_1} \frac{(u(\psi, \theta, \gamma_0) - u(\psi, \theta', \gamma_0))^2}{(\theta - \theta')^2} d\theta d\theta' \right). \end{aligned} \quad (2.27a)$$

2) If $\tilde{\Gamma}_{n,i}^{v-e} = \{x^{v-e} : x_1^{v-e} = \alpha_0, \beta_0 < x_2^{v-e} < \beta_1, \gamma_0 < x_3^{v-e} < \gamma_1\}$ then define $G_{n,i}^{v-e} = 1$ and

$$\begin{aligned} ||| u |||_{\tilde{\Gamma}_{n,i}^{v-e}}^2 &= F_{n,i}^{v-e} \left(\int_{\gamma_0}^{\gamma_1} \int_{\beta_0}^{\beta_1} u^2(\alpha_0, \theta, \zeta) d\theta d\zeta \right. \\ &\quad + \int_{\gamma_0}^{\gamma_1} d\zeta \int_{\beta_0}^{\beta_1} \int_{\beta_0}^{\beta_1} \frac{(u(\alpha_0, \theta, \zeta) - u(\alpha_0, \theta', \zeta))^2}{(\theta - \theta')^2} d\theta d\theta' \\ &\quad \left. + E_{n,i}^{v-e} \int_{\beta_0}^{\beta_1} d\theta \int_{\gamma_0}^{\gamma_1} \int_{\gamma_0}^{\gamma_1} \frac{(u(\alpha_0, \theta, \zeta) - u(\alpha_0, \theta, \zeta'))^2}{(\zeta - \zeta')^2} d\zeta d\zeta' \right). \end{aligned} \quad (2.27b)$$

3) If $\tilde{\Gamma}_{n,i}^{v-e} = \{x^{v-e} : \alpha_0 < x_1^{v-e} < \alpha_1, x_2^{v-e} = \beta_0, \gamma_0 < x_3^{v-e} < \gamma_1\}$ then define $G_{n,i}^{v-e} = 1$

and

$$\begin{aligned}
||| u |||_{\tilde{\Gamma}_{n,i}^{v-e}}^2 &= F_{n,i}^{v-e} \left(\int_{\gamma_0}^{\gamma_1} \int_{\alpha_0}^{\alpha_1} u^2(\psi, \beta_0, \zeta) d\psi d\zeta \right. \\
&\quad + \int_{\gamma_0}^{\gamma_1} d\zeta \int_{\alpha_0}^{\alpha_1} \int_{\alpha_0}^{\alpha_1} \frac{(u(\psi, \beta_0, \zeta) - u(\psi', \beta_0, \zeta))^2}{(\psi - \psi')^2} d\psi d\psi' \\
&\quad \left. + E_{n,i}^{v-e} \int_{\alpha_0}^{\alpha_1} d\psi \int_{\gamma_0}^{\gamma_1} \int_{\gamma_0}^{\gamma_1} \frac{(u(\psi, \beta_0, \zeta) - u(\psi, \beta_0, \zeta'))^2}{(\zeta - \zeta')^2} d\zeta d\zeta' \right). \quad (2.27c)
\end{aligned}$$

Let L^{v-e} be a differential operator such that

$$\int_{\tilde{\Omega}_n^{v-e}} |L^{v-e} u(x^{v-e})|^2 dx^{v-e} = \int_{\Omega_l^v} \rho^2 \sin^2 \phi |Lu(x)|^2 dx.$$

Here dx^{v-e} denotes a volume element in x^{v-e} coordinates and dx a volume element in x coordinates. In Chapter 3 it will be shown that

$$L^{v-e} u(x^{v-e}) = -\text{div}_{x^{v-e}} (e^{\zeta/2} A^{v-e} \nabla_{x^{v-e}} u) + \sum_{i=1}^3 \hat{b}_i^{v-e} u_{x_i^{v-e}} + \hat{c}^{v-e} u. \quad (2.28)$$

Here A^{v-e} is a symmetric, positive definite matrix.

We now define the quadratic form

$$\begin{aligned}
\mathcal{V}_{v-e}^{N,W}(\{\mathcal{F}_u\}) &= \sum_{l=1, \mu(\tilde{\Omega}_l^{v-e}) < \infty}^{N_{v-e}} \int_{\tilde{\Omega}_l^{v-e}} |L^{v-e} u_l^{v-e}(x^{v-e})|^2 dx^{v-e} \\
&\quad + \sum_{\substack{\Gamma_{n,i}^{v-e} \subseteq \tilde{\Omega}^{v-e} \setminus \partial\Omega, \\ \mu(\tilde{\Gamma}_{n,i}^{v-e}) < \infty}} \left(\left\| \sqrt{F_{n,i}^{v-e} G_{n,i}^{v-e}} [u] \right\|_{0, \tilde{\Gamma}_{n,i}^{v-e}}^2 + ||| [u_{x_1^{v-e}}] |||_{\tilde{\Gamma}_{n,i}^{v-e}}^2 \right. \\
&\quad \left. + ||| [u_{x_2^{v-e}}] |||_{\tilde{\Gamma}_{n,i}^{v-e}}^2 + ||| E_{n,i}^{v-e} [u_{x_3^{v-e}}] |||_{\tilde{\Gamma}_{n,i}^{v-e}}^2 \right) \\
&\quad + \sum_{\substack{\Gamma_{n,i}^{v-e} \subseteq \Gamma^{[0]}, \\ \mu(\tilde{\Gamma}_{n,i}^{v-e}) < \infty}} \left(\left\| \sqrt{F_{n,i}^{v-e}} u_n^{v-e} \right\|_{0, \tilde{\Gamma}_{n,i}^{v-e}}^2 + ||| u_{x_1^{v-e}} |||_{\tilde{\Gamma}_{n,i}^{v-e}}^2 \right. \\
&\quad \left. + ||| E_{n,i}^{v-e} u_{x_3^{v-e}} |||_{\tilde{\Gamma}_{n,i}^{v-e}}^2 \right) + \sum_{\substack{\Gamma_{n,i}^{v-e} \subseteq \Gamma^{[1]}, \\ \mu(\tilde{\Gamma}_{n,i}^{v-e}) < \infty}} ||| \left(\frac{\partial u}{\partial \boldsymbol{\nu}^{v-e}} \right)_{A^{v-e}} |||_{\tilde{\Gamma}_{n,i}^{v-e}}^2. \quad (2.29)
\end{aligned}$$

Once more μ denotes measure.

Here the term $\left(\frac{\partial u}{\partial \boldsymbol{\nu}^{v-e}} \right)_{A^{v-e}}$ is defined as follows. Let $\tilde{\Gamma}_{n,i}^{v-e}$ be a face of $\tilde{\Omega}_{n,i}^{v-e}$, \tilde{P} be a point

belonging to $\tilde{\Gamma}_{n,i}^{v-e}$ and $\boldsymbol{\nu}^{v-e}$ denote the unit normal to $\tilde{\Gamma}_{n,i}^{v-e}$ at the point \tilde{P} . Then

$$\left(\frac{\partial u}{\partial \boldsymbol{\nu}^{v-e}} \right)_{A^{v-e}}(\tilde{P}) = (\boldsymbol{\nu}^{v-e})^T A^{v-e} \nabla_{x^{v-e}} u. \quad (2.30)$$

Now the quadratic form $\mathcal{V}_{vertex-edges}^{N,W}(\{\mathcal{F}_u\})$ is given by

$$\mathcal{V}_{vertex-edges}^{N,W}(\{\mathcal{F}_u\}) = \sum_{v-e \in \mathcal{V}-\mathcal{E}} \mathcal{V}_{v-e}^{N,W}(\{\mathcal{F}_u\}). \quad (2.31)$$

Next, we define the quadratic form $\mathcal{U}_{v-e}^{N,W}(\{\mathcal{F}_u\})$. Let $w^{v-e}(x_1^{v-e})$ be a positive, smooth weight function such that

$$w^{v-e}(x_1^{v-e}) = 1 \quad \text{for} \quad x_1^{v-e} \geq \zeta_1^{v-e} = \ln(\tan \phi_1^{v-e})$$

and which satisfies

$$\int_{-\infty}^{\zeta_1^{v-e}} w^{v-e}(x_1^{v-e}) dx_1^{v-e} = 1.$$

We shall choose

$$w^{v-e}(x_1^{v-e}) = 1 \quad \text{for} \quad x_1^{v-e} \geq \zeta_1^{v-e} - 1$$

and

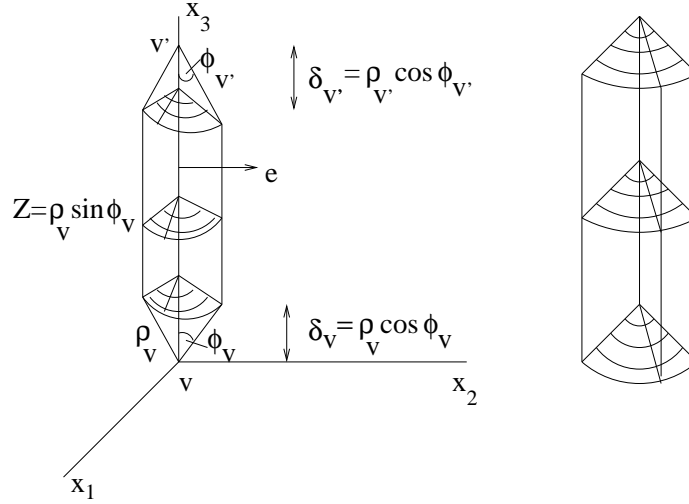
$$w^{v-e}(x_1^{v-e}) = 0 \quad \text{for} \quad x_1^{v-e} < \zeta_1^{v-e} - 1.$$

Then

$$\begin{aligned} \mathcal{U}_{v-e}^{N,W}(\{\mathcal{F}_u\}) &= \sum_{l=1, \mu(\tilde{\Omega}_l^{v-e}) < \infty}^{N_{v-e}} \int_{\tilde{\Omega}_l^{v-e}} e^{x_3^{v-e}} \left(\sum_{i,j=1,2} \left(\frac{\partial^2 u_l^{v-e}}{\partial x_i^{v-e} \partial x_j^{v-e}} \right)^2 \right. \\ &\quad + \sum_{i=1}^2 \sin^2 \phi \left(\frac{\partial^2 u_l^{v-e}}{\partial x_i^{v-e} \partial x_3^{v-e}} \right)^2 + \sin^4 \phi \left(\frac{\partial^2 u_l^{v-e}}{(\partial x_3^{v-e})^2} \right)^2 + \sum_{i=1}^2 \left(\frac{\partial u_l^{v-e}}{\partial x_i^{v-e}} \right)^2 \\ &\quad \left. + \sin^2 \phi \left(\frac{\partial u_l^{v-e}}{\partial x_3^{v-e}} \right)^2 + (u_l^{v-e})^2 \right) dx^{v-e} \\ &\quad + \sum_{l=1, \mu(\tilde{\Omega}_l^{v-e}) = \infty}^{N_{v-e}} \int_{\tilde{\Omega}_l^{v-e}} (u_l^{v-e})^2 e^{x_3^{v-e}} w^{v-e}(x_1^{v-e}) dx^{v-e}. \end{aligned} \quad (2.32)$$

The quadratic form $\mathcal{U}_{vertex-edges}^{N,W}(\{\mathcal{F}_u\})$ is then given by

$$\mathcal{U}_{vertex-edges}^{N,W}(\{\mathcal{F}_u\}) = \sum_{v-e \in \mathcal{V}-\mathcal{E}} \mathcal{U}_{v-e}^{N,W}(\{\mathcal{F}_u\}). \quad (2.33)$$

Figure 2.10: Geometrical mesh imposed on Ω^e .

Finally, we define the quadratic forms $\mathcal{V}_{edges}^{N,W}(\{\mathcal{F}_u\})$ and $\mathcal{U}_{edges}^{N,W}(\{\mathcal{F}_u\})$. Consider the edge e whose end points are v and v' . The edge e coincides with the x_3 axis and the vertex v with the origin. Let the length of the edge e be l_e . Now the edge neighbourhood Ω^e is defined as

$$\Omega^e = \{x \in \Omega : 0 < r < Z = \rho_v \sin \phi_v, \theta_{v-e}^l < \theta < \theta_{v-e}^u, \delta_v < x_3 < l_e - \delta'_v\}.$$

Here (r, θ, x_3) denote cylindrical coordinates with origin at v , $\delta_v = \rho_v \cos \phi_v$ and $\delta'_v = \rho'_v \cos \phi'_v$ are as shown in Figure 2.10.

A geometrical mesh in r is imposed by defining $r_0^e = 0$ and $r_j^e = Z(\mu_e)^{N+1-j}$ for $j = 1, 2, \dots, N+1$. We impose the same quasi-uniform mesh on θ as we did in the vertex-edge neighbourhood, viz.

$$\theta_{v-e}^l = \theta_0^{v-e} < \theta_1^{v-e} < \dots < \theta_{I_e}^{v-e} = \theta_{v-e}^u.$$

Here $I_e = I_{v-e}$ and $\theta_k^e = \theta_k^{v-e}$ for $0 \leq k \leq I_e$. A quasi-uniform mesh is defined in x_3 , by choosing

$$\delta_v = Z_0^e < Z_1^e < \dots < Z_{J_e}^e = l_e - \delta'_v.$$

Thus Ω^e is divided into $N_e = I_e J_e (N+1)$ elements. We introduce new coordinates in Ω^e

by

$$\begin{aligned} x_1^e &= \tau = \ln r \\ x_2^e &= \theta \\ x_3^e &= x_3. \end{aligned}$$

Let $\tilde{\Omega}^e$ be the image of Ω^e in x^e coordinates. Thus $\tilde{\Omega}^e$ is divided into N_e hexahedrons $\{\tilde{\Omega}_m^e\}_{m=1,\dots,N_e}$ where

$$\tilde{\Omega}_m^e = \{x^e : \ln(r_i^e) < x_1^e < \ln(r_{i+1}^e), \theta_j^e < x_2^e < \theta_{j+1}^e, Z_k^e < x_3^e < Z_{k+1}^e\}.$$

We now define the spectral element functions on the elements in $\tilde{\Omega}^e$. Consider an element

$$\tilde{\Omega}_p^e = \{x^e : -\infty < x_1^e < \ln(r_1^e), \theta_j^e < x_2^e < \theta_{j+1}^e, Z_n^e < x_3^e < Z_{n+1}^e\}.$$

Then

$$u_p^e(x^e) = \sum_{t=0}^W \alpha_r(x_3^e)^t.$$

This representation is valid for all j for fixed n .

Next, consider the element

$$\tilde{\Omega}_q^e = \{x^e : \ln(r_i^e) < x_1^e < \ln(r_{i+1}^e), \theta_j^e < x_2^e < \theta_{j+1}^e, Z_n^e < x_3^e < Z_{n+1}^e\}$$

for $1 \leq i \leq N$.

Then we define

$$u_q^e(x^e) = \sum_{r=0}^{W_q} \sum_{s=0}^{W_q} \sum_{t=0}^W \alpha_{r,s,t}(x_1^e)^r (x_2^e)^s (x_3^e)^t.$$

Here $1 \leq W_q \leq W$. Moreover $W_q = [\mu_1 i]$ for all $1 \leq i \leq N$, where $\mu_1 > 0$ is a degree factor [51].

Let $\tilde{\Gamma}_{m,i}^e$ be one of the faces of $\tilde{\Omega}_m^e$ such that $\mu(\tilde{\Gamma}_{m,i}^e) < \infty$, where μ denotes measure. We define a norm $|||u|||_{\tilde{\Gamma}_{m,i}^e}^2$ as follows:

Let $G_{m,i}^e = \sup_{x^e \in \tilde{\Gamma}_{m,i}^e} (e^\tau)$. We also define $H_{m,i}^e$ which is needed in (2.38).

1) If $\tilde{\Gamma}_{m,i}^e = \{x^e : \alpha_0 < x_1^e < \alpha_1, \beta_0 < x_2^e < \beta_1, x_3^e = \gamma_0\}$ then define $H_{m,i}^e = G_{m,i}^e$ and

$$\begin{aligned} ||| u |||_{\tilde{\Gamma}_{m,i}^e}^2 &= G_{m,i}^e \left(\int_{\beta_0}^{\beta_1} \int_{\alpha_0}^{\alpha_1} u^2(\tau, \theta, \gamma_0) d\tau d\theta \right. \\ &\quad + \int_{\beta_0}^{\beta_1} d\theta \int_{\alpha_0}^{\alpha_1} \int_{\alpha_0}^{\alpha_1} \frac{(u(\tau, \theta, \gamma_0) - u(\tau', \theta, \gamma_0))^2}{(\tau - \tau')^2} d\tau d\tau' \\ &\quad \left. + \int_{\alpha_0}^{\alpha_1} d\tau \int_{\beta_0}^{\beta_1} \int_{\beta_0}^{\beta_1} \frac{(u(\tau, \theta, \gamma_0) - u(\tau, \theta', \gamma_0))^2}{(\theta - \theta')^2} d\theta d\theta' \right). \end{aligned} \quad (2.34a)$$

2) If $\tilde{\Gamma}_{m,i}^e = \{x^e : x_1^e = \alpha_0, \beta_0 < x_2^e < \beta_1, \gamma_0 < x_3^e < \gamma_1\}$ then define $H_{m,i}^e = 1$ and

$$\begin{aligned} ||| u |||_{\tilde{\Gamma}_{m,i}^e}^2 &= \left(\int_{\gamma_0}^{\gamma_1} \int_{\beta_0}^{\beta_1} u^2(\alpha_0, \theta, x_3) d\theta dx_3 \right. \\ &\quad + \int_{\gamma_0}^{\gamma_1} dx_3 \int_{\beta_0}^{\beta_1} \int_{\beta_0}^{\beta_1} \frac{(u(\alpha_0, \theta, x_3) - u(\alpha_0, \theta', x_3))^2}{(\theta - \theta')^2} d\theta d\theta' \\ &\quad \left. + G_{m,i}^e \int_{\beta_0}^{\beta_1} d\theta \int_{\gamma_0}^{\gamma_1} \int_{\gamma_0}^{\gamma_1} \frac{(u(\alpha_0, \theta, x_3) - u(\alpha_0, \theta, x'_3))^2}{(x_3 - x'_3)^2} dx_3 dx'_3 \right). \end{aligned} \quad (2.34b)$$

3) If $\tilde{\Gamma}_{m,i}^e = \{x^e : \alpha_0 < x_1^e < \alpha_1, x_2^e = \beta_0, \gamma_0 < x_3^e < \gamma_1\}$ then define $H_{m,i}^e = 1$ and

$$\begin{aligned} ||| u |||_{\tilde{\Gamma}_{m,i}^e}^2 &= \left(\int_{\gamma_0}^{\gamma_1} \int_{\alpha_0}^{\alpha_1} u^2(\tau, \beta_0, x_3) d\tau dx_3 \right. \\ &\quad + \int_{\gamma_0}^{\gamma_1} dx_3 \int_{\alpha_0}^{\alpha_1} \int_{\alpha_0}^{\alpha_1} \frac{(u(\tau, \beta_0, x_3) - u(\tau', \beta_0, x_3))^2}{(\tau - \tau')^2} d\tau d\tau' \\ &\quad \left. + G_{m,i}^e \int_{\alpha_0}^{\alpha_1} d\tau \int_{\gamma_0}^{\gamma_1} \int_{\gamma_0}^{\gamma_1} \frac{(u(\tau, \beta_0, x_3) - u(\tau, \beta_0, x'_3))^2}{(x_3 - x'_3)^2} dx_3 dx'_3 \right). \end{aligned} \quad (2.34c)$$

Let L^e be a differential operator such that

$$\int_{\tilde{\Omega}_m^e} |L^e u(x^e)|^2 dx^e = \int_{\Omega_m^e} r^2 |Lu(x)|^2 dx. \quad (2.35)$$

Here dx^e denotes a volume element in x^e coordinates and dx a volume element in x coordinates.

In Chapter 3 it will be shown that

$$L^e u(x^e) = -\operatorname{div}_{x^e} (A^e \nabla_{x^e} u) + \sum_{i=1}^3 \hat{b}_i^e u_{x_i^e} + \hat{c}^e u \quad (2.36)$$

where A^e is a symmetric, positive definite matrix.

Let $\tilde{\Gamma}_{m,i}^e$ be one of the sides of $\tilde{\Omega}_m^e$ and \tilde{P} a point belonging to $\tilde{\Gamma}_{m,i}^e$. Let ν^e be the normal to $\tilde{\Gamma}_{m,i}^e$ at \tilde{P} . Then

$$\left(\frac{\partial u}{\partial \nu^e} \right)_{A^e} (\tilde{P}) = (\nu^e)^T A^e \nabla_{x^e} u(\tilde{P}). \quad (2.37)$$

We now define the quadratic form

$$\begin{aligned}
\mathcal{V}_e^{N,W}(\{\mathcal{F}_u\}) = & \sum_{l=1, \mu(\tilde{\Omega}_l^e) < \infty}^{N_e} \int_{\tilde{\Omega}_l^e} |L^e u_l^e(x^e)|^2 dx^e \\
& + \sum_{\substack{\Gamma_{l,i}^e \subseteq \tilde{\Omega}^e \setminus \partial\Omega, \\ \mu(\tilde{\Gamma}_{l,i}^e) < \infty}} \left(\left\| \sqrt{H_{l,i}^e} [u] \right\|_{0, \tilde{\Gamma}_{l,i}^e}^2 + \left\| [u_{x_1^e}] \right\|_{\tilde{\Gamma}_{l,i}^e}^2 \right. \\
& \left. + \left\| [u_{x_2^e}] \right\|_{\tilde{\Gamma}_{l,i}^e}^2 + \left\| G_{l,i}^e [u_{x_3^e}] \right\|_{\tilde{\Gamma}_{l,i}^e}^2 \right) \\
& + \sum_{\substack{\Gamma_{l,i}^e \subseteq \Gamma^{[0]}, \\ \mu(\tilde{\Gamma}_{l,i}^e) < \infty}} \left(\|u_l^e\|_{0, \tilde{\Gamma}_{l,i}^e}^2 + \left\| u_{x_1^e} \right\|_{\tilde{\Gamma}_{l,i}^e}^2 + \left\| G_{l,i}^e u_{x_3^e} \right\|_{\tilde{\Gamma}_{l,i}^e}^2 \right) \\
& + \sum_{\substack{\Gamma_{l,i}^e \subseteq \Gamma^{[1]}, \\ \mu(\tilde{\Gamma}_{l,i}^e) < \infty}} \left\| \left(\frac{\partial u}{\partial \nu^e} \right)_{A^e} \right\|_{\tilde{\Gamma}_{l,i}^e}^2. \tag{2.38}
\end{aligned}$$

The quadratic form $\mathcal{V}_{edges}^{N,W}(\{\mathcal{F}_u\})$ is given by

$$\mathcal{V}_{edges}^{N,W}(\{\mathcal{F}_u\}) = \sum_{e \in \mathcal{E}} \mathcal{V}_e^{N,W}(\{\mathcal{F}_u\}). \tag{2.39}$$

Next, let us define the quadratic form $\mathcal{U}_e^{N,W}(\{\mathcal{F}_u\})$. Let $w^e(x_1^e)$ be a positive, smooth weight function such that

$$w^e(x_1^e) = 1 \quad \text{for} \quad x_1^e \geq \ln(r_1^e)$$

and

$$\int_{-\infty}^{\ln(r_1^e)} w^e(x_1^e) dx_1^e = 1.$$

We shall choose

$$w^e(x_1^e) = 1 \quad \text{for} \quad x_1^e \geq \ln(r_1^e) - 1$$

and

$$w^e(x_1^e) = 0 \quad \text{for} \quad x_1^e < \ln(r_1^e) - 1.$$

Then

$$\begin{aligned}
\mathcal{U}_e^{N,W}(\{\mathcal{F}_u\}) = & \sum_{l=1, \mu(\tilde{\Omega}_l^e) < \infty}^{N_e} \int_{\tilde{\Omega}_l^e} \left(\sum_{i,j=1,2} \left(\frac{\partial^2 u_l^e}{\partial x_i^e \partial x_j^e} \right)^2 + e^{2\tau} \sum_{i=1}^2 \left(\frac{\partial^2 u_l^e}{\partial x_i^e \partial x_3^e} \right)^2 \right. \\
& + e^{4\tau} \left(\frac{\partial^2 u_l^e}{(\partial x_3^e)^2} \right)^2 + \sum_{i=1}^2 \left(\frac{\partial u_l^e}{\partial x_i^e} \right)^2 + e^{2\tau} \left(\frac{\partial u_l^e}{\partial x_3^e} \right)^2 + (u_l^e)^2 \Big) dx^e \\
& + \sum_{l=1, \mu(\tilde{\Omega}_l^e) = \infty}^{N_e} \int_{\tilde{\Omega}_l^e} (u_l^e)^2 w^e(x_1^e) dx^e.
\end{aligned} \tag{2.40}$$

Here μ denotes measure.

We define

$$\mathcal{U}_{edges}^{N,W}(\{\mathcal{F}_u\}) = \sum_{e \in \mathcal{E}} \mathcal{U}_e^{N,W}(\{\mathcal{F}_u\}). \tag{2.41}$$

Finally, using (2.14) and (2.15) we can define the quadratic forms $\mathcal{V}^{N,W}(\{\mathcal{F}_u\})$ and $\mathcal{U}^{N,W}(\{\mathcal{F}_u\})$.

We now state the main result of this chapter. It is assumed that N is proportional to W .

Theorem 2.3.1. *Consider the elliptic boundary value problem (2.1). Suppose the boundary conditions are Dirichlet. Then*

$$\mathcal{U}^{N,W}(\{\mathcal{F}_u\}) \leq C(\ln W)^2 \mathcal{V}^{N,W}(\{\mathcal{F}_u\}). \tag{2.42}$$

Next, we state the corresponding result for general boundary conditions.

Theorem 2.3.2. *If the boundary conditions for the elliptic boundary value problem (2.1) are mixed then*

$$\mathcal{U}^{N,W}(\{\mathcal{F}_u\}) \leq CN^4 \mathcal{V}^{N,W}(\{\mathcal{F}_u\}) \tag{2.43}$$

provided $W = O(e^{N^\alpha})$ for $\alpha < 1/2$.

The rapid growth of the factor CN^4 with N creates difficulties in parallelizing the numerical scheme. To overcome this problem we state a version of Theorem 2.3.2 when the spectral element functions vanish on the wirebasket. Let WB denotes the wirebasket along which the spectral element functions need to be conforming. Here the wirebasket denotes the union of the vertices and edges of the elements.

Theorem 2.3.3. *If the spectral element functions $(\{\mathcal{F}_u\})$ are conforming on the wire basket WB and vanish on WB then*

$$\mathcal{U}^{N,W}(\{\mathcal{F}_u\}) \leq C(\ln W)^2 \mathcal{V}^{N,W}(\{\mathcal{F}_u\}) \quad (2.44)$$

provided $W = O(e^{N^\alpha})$ for $\alpha < 1/2$.

Chapter 3

Proof of the Stability Theorem

3.1 Introduction

In this chapter we prove the stability estimate, which we use to formulate our numerical scheme.

In Chapter 2 we have introduced a set of local coordinate systems in various neighbourhoods of the polyhedron Ω , which we referred to as *modified coordinates*, in the vertex, vertex-edge and edge neighbourhoods. These local coordinates are modified versions of the spherical and cylindrical co-ordinate systems in vertex and edge neighbourhoods respectively. In vertex-edge neighbourhoods modified coordinates are a combination of spherical and cylindrical coordinates. Away from the corners and edges in the regular region of the domain we use standard Cartesian coordinates. The *differentiability estimates* for the solution of the elliptic boundary value problem in a polyhedral domain in terms of these new local coordinates were obtained. We also stated a *stability estimate* for a *non-conforming* spectral element representation of the solution. For problems with mixed Neumann and Dirichlet boundary conditions the spectral element functions may be chosen to be continuous on the wirebasket of the elements.

We now briefly describe the contents of this chapter. In Sections 3.2 and 3.3, we derive estimates for the second order derivatives and the lower order derivatives of the solution respectively. Estimates for terms in the interior and on the boundary of the polyhedron Ω

are obtained in Sections 3.4 and 3.5. In Section 3.6, we combine all the results of sections 3.2, 3.3, 3.4 and 3.5 to complete the proof of the stability estimate which has been stated in Chapter 2.

In Chapter 4 we shall give the numerical scheme and error estimates. It will be shown that the error between the exact and the approximate solution is exponentially small in N , the number of layers in the geometrical mesh. Optimal rate of convergence with respect to the number of degrees of freedom is also provided.

3.2 Estimates for the Second Derivatives of Spectral Element Functions

3.2.1 Estimates for the second derivatives in the interior

We first obtain estimates for elements in the regular region Ω^r of Ω . Divide Ω^r into N_r elements, which may consist of curvilinear cubes, prisms and tetrahedrons, Ω_l^r for $1 \leq l \leq N_r$.

Let

$$Lu = \sum_{i,j=1}^3 - (a_{i,j} u_{x_j})_{x_i} + \sum_{i=1}^3 b_i u_{x_i} + cu \quad (3.1)$$

be a strongly elliptic operator that satisfies the Lax-Milgram conditions. Hence there exists a positive constant μ_0 such that

$$\sum_{i,j=1}^3 a_{i,j} \zeta_i \zeta_j \geq \mu_0 |\zeta|^2.$$

We consider the mixed boundary value problem

$$Lw = f \quad \text{in } \Omega, \quad (3.2a)$$

$$\gamma_0 w = w|_{\Gamma^{[0]}} = g^{[0]}, \quad (3.2b)$$

$$\gamma_1 w = \left(\frac{\partial w}{\partial \nu} \right) \Big|_A \Big|_{\Gamma^{[1]}} = g^{[1]}. \quad (3.2c)$$

Let

$$Mu = \sum_{i,j=1}^3 (a_{i,j} u_{x_j})_{x_i}. \quad (3.3)$$

Consider an element Ω_l^r . Then Ω_l^r has n_l faces $\{\Gamma_{l,i}^r\}_{1 \leq i \leq n_l}$. Let $\partial\Gamma_{l,i}^r$ denote the boundary of the face $\Gamma_{l,i}^r$.

To proceed we need to review some material in [46]. Let O be a bounded open subset of R^3 with a Lipschitz boundary ∂O . Assume in addition that ∂O is piecewise C^2 . Let P be a point on ∂O in a neighbourhood of which ∂O is C^2 . It is possible to find two curves of class C^2 in a neighbourhood of P , passing through P and being orthogonal there. Let us denote these curves by $\mathcal{C}_1, \mathcal{C}_2$ and by $\boldsymbol{\tau}_1, \boldsymbol{\tau}_2$ the unit tangent vectors to $\mathcal{C}_1, \mathcal{C}_2$ respectively and by s_1, s_2 the arc lengths along these curves. We assume that $\boldsymbol{\tau}_1, \boldsymbol{\tau}_2$ has the direct orientation at P . Let $\boldsymbol{\nu}$ be the unit normal at P defined as $\boldsymbol{\nu} = \boldsymbol{\tau}_1 \times \boldsymbol{\tau}_2$. Then at P , \mathcal{B}_P , the second fundamental form at P is the bilinear form

$$(\boldsymbol{\zeta}, \boldsymbol{\eta}) \mapsto - \sum_{j,k=1}^2 \frac{\partial \boldsymbol{\nu}}{\partial s_j} \cdot \boldsymbol{\tau}_k \zeta_j \eta_k \quad (3.4)$$

where $\boldsymbol{\zeta}, \boldsymbol{\eta}$ are the tangent vectors to ∂O at P and $\boldsymbol{\zeta} = (\zeta_1, \zeta_2)$ and $\boldsymbol{\eta} = (\eta_1, \eta_2)$ in the basis $\{\boldsymbol{\tau}_1, \boldsymbol{\tau}_2\}$. In other words,

$$\mathcal{B}(\boldsymbol{\zeta}, \boldsymbol{\eta}) = - \frac{\partial \boldsymbol{\nu}}{\partial \boldsymbol{\zeta}} \cdot \boldsymbol{\eta} \quad (3.5)$$

where $\frac{\partial}{\partial \boldsymbol{\zeta}}$ denotes differentiation in the $\boldsymbol{\zeta}$ direction.

Let \boldsymbol{w} be a vector field defined in a neighbourhood of O . If P is a point on ∂O then by \boldsymbol{w}_ν we shall denote the component of \boldsymbol{w} in the direction of $\boldsymbol{\nu}$, while we shall denote by \boldsymbol{w}_T , the projection of \boldsymbol{w} on the tangent hyperplane to ∂O , i.e.

$$\boldsymbol{w}_\nu = \boldsymbol{w} \cdot \boldsymbol{\nu}, \quad (3.6)$$

$$\boldsymbol{w}_T = \boldsymbol{w} - \boldsymbol{w}_\nu \boldsymbol{\nu} = \boldsymbol{w}_{\tau_1} \boldsymbol{\tau}_1 + \boldsymbol{w}_{\tau_2} \boldsymbol{\tau}_2. \quad (3.7)$$

Here $\boldsymbol{w}_{\tau_i} = \boldsymbol{w} \cdot \boldsymbol{\tau}_i$ for $i = 1, 2$.

We shall denote by ∇_T the projection of the gradient vector on the tangent hyperplane

$$\nabla_T u = \nabla u - \frac{\partial u}{\partial \boldsymbol{\nu}} \boldsymbol{\nu} = \sum_{j=1}^2 \frac{\partial u}{\partial s_j} \boldsymbol{\tau}_j. \quad (3.8)$$

Let \boldsymbol{h} be a vector field defined on ∂O such that \boldsymbol{h} is tangent to O except on a set of zero measure. Then

$$\operatorname{div}_T(\boldsymbol{h}) = \sum_{j=1}^2 \left(\frac{\partial \boldsymbol{h}}{\partial s_j} \right) \cdot \boldsymbol{\tau}_j. \quad (3.9)$$

We now cite Theorem 3.1.1.2 of [46].

Theorem 3.2.1. *Let O be a bounded open subset of R^3 with a Lipschitz boundary ∂O . Assume, in addition that ∂O is piecewise C^2 . Then for all $\mathbf{w} \in (H^2(O))^3$ we have*

$$\begin{aligned} \int_O (\operatorname{div}(\mathbf{w}))^2 dx - \sum_{i,j=1}^3 \int_O \frac{\partial w_i}{\partial x_j} \frac{\partial w_j}{\partial x_i} dx &= \int_{\partial O} \{ \operatorname{div}_T(\mathbf{w}_\nu \mathbf{w}_T) - 2\mathbf{w}_T \cdot \nabla_T \mathbf{w}_\nu \} d\sigma \\ &\quad - \int_{\partial O} \{ (\operatorname{tr} \mathcal{B}) \mathbf{w}_\nu^2 + \mathcal{B}(\mathbf{w}_T, \mathbf{w}_T) \} d\sigma. \end{aligned} \quad (3.10)$$

Here dx denotes a volume element and $d\sigma$ an element of surface area.

Consider an element Ω_l^r which is assumed to be a curvilinear cube as shown in Figure 3.1. Let $\Gamma_{l,i}^r$ denote one of the faces of Ω_l^r . Let Q be a point inside $\Gamma_{l,i}^r$. The unit tangent vectors $\boldsymbol{\tau}_1, \boldsymbol{\tau}_2$ and the unit normal vector $\boldsymbol{\nu}$ at Q are shown in Figure 3.1. Consider a point $P \in \partial \Gamma_{l,i}^r$ and assume that P is not a vertex of Ω_l^r . Then we can define the vector \mathbf{n} at P as the vector belonging to the tangent hyperplane which is orthogonal to the tangent vector to the curve $\partial \Gamma_{l,i}^r$ at P . Moreover \mathbf{n} is chosen to point out of $\Gamma_{l,i}^r$. Recall A is the

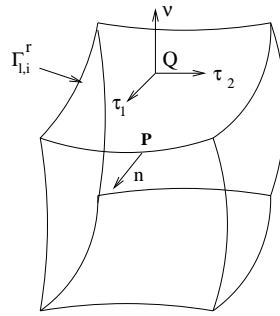


Figure 3.1: The element Ω_l^r .

matrix $(a_{i,j})$. Define

$$\begin{aligned} \left(\frac{\partial u}{\partial \mathbf{n}} \right)_A (P) &= (\mathbf{n} \cdot A \nabla u)(P), \\ \left(\frac{\partial u}{\partial \boldsymbol{\tau}_1} \right)_A (P) &= (\boldsymbol{\tau}_1 \cdot A \nabla u)(P), \\ \left(\frac{\partial u}{\partial \boldsymbol{\tau}_2} \right)_A (P) &= (\boldsymbol{\tau}_2 \cdot A \nabla u)(P), \\ \left(\frac{\partial u}{\partial \boldsymbol{\nu}} \right)_A (P) &= (\boldsymbol{\nu} \cdot A \nabla u)(P). \end{aligned} \quad (3.11)$$

Let s_1, s_2 denote arc lengths along $\boldsymbol{\tau}_1$ and $\boldsymbol{\tau}_2$ and s denote arc length measured along $\partial\Gamma_{l,i}^r$.

We can now prove the following result.

Lemma 3.2.1. *Let $u \in H^3(\Omega_l^r)$. Then*

$$\begin{aligned} & \frac{\mu_0^2}{2} \rho_v^2 \sin^2(\phi_v) \int_{\Omega_l^r} \sum_{i,j=1}^3 \left| \frac{\partial^2 u}{\partial x_i \partial x_j} \right|^2 dx \\ & \leq \rho_v^2 \sin^2(\phi_v) \int_{\Omega_l^r} |Lu|^2 dx - \rho_v^2 \sin^2(\phi_v) \left\{ \sum_i \oint_{\partial\Gamma_{l,i}^r} \left(\frac{\partial u}{\partial \mathbf{n}} \right)_A \left(\frac{\partial u}{\partial \boldsymbol{\nu}} \right)_A ds \right. \\ & \quad \left. - 2 \sum_i \int_{\Gamma_{l,i}^r} \sum_{j=1}^2 \left(\frac{\partial u}{\partial \boldsymbol{\tau}_j} \right)_A \frac{\partial}{\partial s_j} \left(\left(\frac{\partial u}{\partial \boldsymbol{\nu}} \right)_A \right) d\sigma \right\} \\ & \quad + C \int_{\Omega_l^r} \sum_{|\alpha| \leq 1} |D_x^\alpha u|^2 dx. \end{aligned} \quad (3.12)$$

Here C denotes a constant. Moreover dx denotes a volume element, $d\sigma$ an element of surface area and ds an element of arc length.

Proof. The proof is similar to the proof of Lemma 3.1 in [38]. We define the vector field \mathbf{w} by $\mathbf{w} = A \nabla_x u$. Then

$$Mu = \sum_{i,j=1}^3 \frac{\partial}{\partial x_i} \left(a_{i,j} \frac{\partial u}{\partial x_j} \right) = \text{div}(\mathbf{w}), \quad (3.13a)$$

$$\left(\frac{\partial u}{\partial \boldsymbol{\nu}} \right)_A = \sum_{i,j=1}^3 \nu_i a_{i,j} \frac{\partial u}{\partial x_j} = \mathbf{w}_\nu \text{ and} \quad (3.13b)$$

$$\left(\frac{\partial u}{\partial \boldsymbol{\tau}_j} \right)_A = \sum_{i,k=1}^3 (\boldsymbol{\tau}_j)_i a_{i,k} \frac{\partial u}{\partial x_k} = \mathbf{w}_{\tau_j}. \quad (3.13c)$$

Applying Theorem 3.2.1

$$\begin{aligned} & \int_{\Omega_l^r} |Mu|^2 dx - \sum_{i,j=1}^3 \int_{\Omega_l^r} \frac{\partial w_i}{\partial x_j} \frac{\partial w_j}{\partial x_i} dx = \left\{ \sum_i \int_{\Gamma_{l,i}^r} \text{div}_T(\mathbf{w}_\nu \mathbf{w}_T) d\sigma \right. \\ & \quad \left. - 2 \sum_i \int_{\Gamma_{l,i}^r} \sum_{j=1}^2 \left(\frac{\partial u}{\partial \boldsymbol{\tau}_j} \right)_A \frac{\partial}{\partial s_j} \left(\left(\frac{\partial u}{\partial \boldsymbol{\nu}} \right)_A \right) d\sigma \right\} - \sum_i \int_{\Gamma_{l,i}^r} \left\{ (\text{tr} \mathcal{B}) \left(\frac{\partial u}{\partial \boldsymbol{\nu}} \right)_A^2 \right. \\ & \quad \left. + \mathcal{B} \left(\sum_{j=1}^2 \left(\frac{\partial u}{\partial \boldsymbol{\tau}_j} \right)_A \boldsymbol{\tau}_j, \sum_{j=1}^2 \left(\frac{\partial u}{\partial \boldsymbol{\tau}_j} \right)_A \boldsymbol{\tau}_j \right) \right\} d\sigma. \end{aligned} \quad (3.14)$$

Now by Lemma 3.1.3.4 of [46] the following inequality holds for all $u \in H^2(\Omega)$:

$$\mu_0^2 \sum_{i,j=1}^3 \left| \frac{\partial^2 u}{\partial x_i \partial x_j} \right|^2 \leq \sum_{i,j=1}^3 \frac{\partial w_i}{\partial x_j} \frac{\partial w_j}{\partial x_i} + 2 \sum_{i,j,k,l=1}^3 \left| a_{i,k} \frac{\partial^2 u}{\partial x_j \partial x_k} \frac{\partial a_{j,l}}{\partial x_i} \frac{\partial u}{\partial x_l} \right| dx .$$

a.e. in Ω . Integrating we have

$$\begin{aligned} \mu_0^2 \sum_{i,j=1}^3 \int_{\Omega_l^r} \left| \frac{\partial^2 u}{\partial x_i \partial x_j} \right|^2 dx &\leq \sum_{i,j=1}^3 \int_{\Omega_l^r} \frac{\partial w_i}{\partial x_j} \frac{\partial w_j}{\partial x_i} dx \\ &+ C \int_{\Omega_l^r} \sum_{i=1}^3 \left| \frac{\partial u}{\partial x_i} \right| \sum_{i,j=1}^3 \left| \frac{\partial^2 u}{\partial x_i \partial x_j} \right| dx . \end{aligned}$$

The constant C in the above inequality depends on M where M is a common bound for all C^1 norms of the $a_{i,j}$. Hence

$$\begin{aligned} \frac{\mu_0^2}{2} \sum_{i,j=1}^3 \int_{\Omega_l^r} \left| \frac{\partial^2 u}{\partial x_i \partial x_j} \right|^2 dx &\leq \sum_{i,j=1}^3 \int_{\Omega_l^r} \frac{\partial w_i}{\partial x_j} \frac{\partial w_j}{\partial x_i} dx \\ &+ C \int_{\Omega_l^r} \sum_{|\alpha|=1} |D_x^\alpha u|^2 dx . \end{aligned} \quad (3.15)$$

Here C denotes a generic constant. Now from Lemma 3.2.2 we have

$$\sum_i \int_{\Gamma_{l,i}^r} \text{div}_T(\mathbf{w}_\nu \mathbf{w}_T) d\sigma = \sum_i \int_{\partial \Gamma_{l,i}^r} \mathbf{w}_\nu \mathbf{w}_n ds .$$

Here $\mathbf{w}_n = \mathbf{w} \cdot \mathbf{n}$ and \mathbf{n} is the vector depicted in Figure 3.1 lying on the tangent hyperplane at the point P and orthogonal to the tangent vector to the curve $\partial \Gamma_{l,i}^r$. Now

$$Mu = Lu - \sum_{i=1}^3 b_i u_{x_i} - cu .$$

Combining (3.14) and (3.15) and proceeding as in Lemma 3.4 in [38] we obtain

$$\begin{aligned} &\frac{\mu_0^2}{2} \rho_v^2 \sin^2(\phi_v) \int_{\Omega_l^r} \sum_{i,j=1}^3 \left| \frac{\partial^2 u}{\partial x_i \partial x_j} \right|^2 dx \\ &\leq \rho_v^2 \sin^2(\phi_v) \int_{\Omega_l^r} |Lu|^2 dx - \rho_v^2 \sin^2(\phi_v) \left\{ \sum_i \oint_{\partial \Gamma_{l,i}^r} \left(\frac{\partial u}{\partial \mathbf{n}} \right)_A \left(\frac{\partial u}{\partial \boldsymbol{\nu}} \right)_A ds \right. \\ &\quad \left. - 2 \sum_i \int_{\Gamma_{l,i}^r} \sum_{j=1}^2 \left(\frac{\partial u}{\partial \boldsymbol{\tau}_j} \right)_A \frac{\partial}{\partial s_j} \left(\left(\frac{\partial u}{\partial \boldsymbol{\nu}} \right)_A \right) d\sigma \right\} \\ &+ C \int_{\Omega_l^r} \sum_{|\alpha| \leq 1} |D_x^\alpha u|^2 dx + D \sum_i \int_{\Gamma_{l,i}^r} \sum_{|\alpha|=1} |D_x^\alpha u|^2 d\sigma . \end{aligned} \quad (3.16)$$

Now for any $\epsilon > 0$ there exists a constant K_ϵ such that

$$\int_{\Gamma_{l,i}^r} \sum_{|\alpha|=1} |D_x^\alpha u|^2 d\sigma \leq \epsilon \int_{\Omega_l^r} \sum_{|\alpha|=2} |D_x^\alpha u|^2 dx + K_\epsilon \int_{\Omega_l^r} \sum_{|\alpha|=1} |D_x^\alpha u|^2 dx.$$

Using above in (3.16) and choosing ϵ small enough (3.12) follows. \square

We now prove the following result which we have used in the proof of Lemma 3.2.1.

Lemma 3.2.2. *Let $w \in H^2(\Omega_l^r)$ and $\Gamma_{l,k}^r$ denote one of the faces of Ω_l^r . Then*

$$\int_{\Gamma_{l,k}^r} \text{div}_T(\mathbf{w}_\nu \mathbf{w}_T) d\sigma = \int_{\partial\Gamma_{l,k}^r} \mathbf{w}_\nu \mathbf{w}_n ds. \quad (3.17)$$

Here $d\sigma$ denotes an element of surface area and ds an element of arc length.

Proof. We shall use geodesic coordinates to prove the result. For any point $P \in \text{closure}(\Gamma_{l,k}^r)$ there is an open subset U of R^2 containing $(0,0)$ such that $\pi : U \rightarrow R^3$ is an allowable surface patch for $\Gamma_{l,k}^r$ in a neighbourhood of P . Moreover the first fundamental form of π is $d\zeta^2 + G(\zeta, \eta)d\eta^2$ where G is a smooth function on U such that $G(0, \eta) = 1$ and $G_\zeta(0, \eta) = 0$ whenever $(0, \eta) \in U$. Hence for any $\epsilon > 0$ we can choose a fine enough triangulation of $\Gamma_{l,k}^r$ so that on each triangle there is a set of geodesic coordinates such that $|G_\zeta/G| \leq \epsilon$ for all $(\zeta, \eta) \in U_i$ for all i . Here the curve corresponding to $\zeta = 0$ is chosen to be a geodesic. All the curves $\eta = \text{constant}$ are geodesics orthogonal to the curve $\zeta = 0$. This can always be done if the surface patch is small enough. Such a system of coordinates is called *Fermi coordinates* [89].

Now integrating over one such triangle we obtain

$$\begin{aligned} \int_{\pi_i(U_i)} \text{div}_T(\mathbf{w}_\nu \mathbf{w}_T) d\sigma &= \int_{\pi_i(U_i)} \sum_{j=1}^2 \frac{\partial}{\partial s_j} (\mathbf{w}_\nu (\mathbf{w}_T \cdot \boldsymbol{\tau}_j)) d\sigma \\ &\quad - \int_{\pi_i(U_i)} \sum_{j=1}^2 \mathbf{w}_\nu \left(\mathbf{w}_T \cdot \frac{\partial \boldsymbol{\tau}_j}{\partial s_j} \right) d\sigma. \end{aligned} \quad (3.18)$$

Clearly

$$\begin{aligned}
\int_{\pi_i(U_i)} \sum_{j=1}^2 \frac{\partial}{\partial s_j} (\mathbf{w}_\nu(\mathbf{w}_T \cdot \boldsymbol{\tau}_j)) d\sigma &= \int_{U_i} \left\{ \frac{\partial}{\partial \zeta} (\mathbf{w}_\nu(\mathbf{w}_T \cdot \boldsymbol{\tau}_1)) \sqrt{G} \right. \\
&\quad \left. + \frac{\partial}{\partial \eta} (\mathbf{w}_\nu(\mathbf{w}_T \cdot \boldsymbol{\tau}_2)) \right\} d\zeta d\eta \\
&= \int_{U_i} \left\{ \frac{\partial}{\partial \zeta} (\mathbf{w}_\nu(\mathbf{w}_T \cdot \boldsymbol{\tau}_1) \sqrt{G}) \right. \\
&\quad \left. + \frac{\partial}{\partial \eta} (\mathbf{w}_\nu(\mathbf{w}_T \cdot \boldsymbol{\tau}_2)) \right\} d\zeta d\eta \\
&\quad - \int_{U_i} \left\{ \mathbf{w}_\nu(\mathbf{w}_T \cdot \boldsymbol{\tau}_1) \frac{\partial \sqrt{G}}{\partial \zeta} / \sqrt{G} \right\} \sqrt{G} d\zeta d\eta.
\end{aligned}$$

Hence

$$\begin{aligned}
\int_{\pi_i(U_i)} \sum_{j=1}^2 \frac{\partial}{\partial s_j} (\mathbf{w}_\nu(\mathbf{w}_T \cdot \boldsymbol{\tau}_j)) d\sigma &= \int_{\partial U_i} (\mathbf{w}_\nu(\mathbf{w}_T \cdot \boldsymbol{\tau}_1) \sqrt{G} d\eta - \mathbf{w}_\nu(\mathbf{w}_T \cdot \boldsymbol{\tau}_2) d\zeta) \\
&\quad - \int_{\pi_i(U_i)} \mathbf{w}_\nu(\mathbf{w}_T \cdot \boldsymbol{\tau}_1) \left(\frac{\partial \sqrt{G}}{\partial \zeta} / \sqrt{G} \right) d\sigma.
\end{aligned}$$

Now

$$\frac{dx}{ds} = x_\zeta \frac{d\zeta}{ds} + x_\eta \frac{d\eta}{ds} = \boldsymbol{\tau}_1 \frac{d\zeta}{ds} + \boldsymbol{\tau}_2 \sqrt{G} \frac{d\eta}{ds}.$$

Hence $\mathbf{n} = \boldsymbol{\tau}_1 \sqrt{G} \frac{d\eta}{ds} - \boldsymbol{\tau}_2 \frac{d\zeta}{ds}$ is the unit outward normal to $\partial\pi_i(U_i)$. And so

$$\begin{aligned}
&\int_{\pi_i(U_i)} \sum_{j=1}^2 \frac{\partial}{\partial s_j} (\mathbf{w}_\nu(\mathbf{w}_T \cdot \boldsymbol{\tau}_j)) d\sigma \\
&= \int_{\partial\pi_i(U_i)} \mathbf{w}_\nu \mathbf{w}_n ds - \int_{\pi_i(U_i)} \mathbf{w}_\nu(\mathbf{w}_T \cdot \boldsymbol{\tau}_1) \left(\frac{\partial \sqrt{G}}{\partial \zeta} / \sqrt{G} \right) d\sigma.
\end{aligned}$$

Summing over all triangular elements of the form $\pi_i(U_i)$ we obtain using (3.18)

$$\begin{aligned}
\int_{\Gamma_{l,k}^r} \operatorname{div}_T(\mathbf{w}_\nu \mathbf{w}_T) d\sigma &= \int_{\partial\Gamma_{l,k}^r} \mathbf{w}_\nu \mathbf{w}_n ds - \sum_i \int_{\pi_i(U_i)} \mathbf{w}_\nu(\mathbf{w}_T \cdot \boldsymbol{\tau}_1) \left(\frac{\partial \sqrt{G}}{\partial \zeta} / \sqrt{G} \right) d\sigma \\
&\quad - \sum_i \int_{\pi_i(U_i)} \sum_{j=1}^2 \mathbf{w}_\nu \left(\mathbf{w}_T \cdot \frac{\partial \boldsymbol{\tau}_j}{\partial s_j} \right) d\sigma. \tag{3.19}
\end{aligned}$$

Now

$$\left| \sum_i \int_{\pi_i(U_i)} \mathbf{w}_\nu(\mathbf{w}_T \cdot \boldsymbol{\tau}_1) \left(\frac{\partial \sqrt{G}}{\partial \zeta} / \sqrt{G} \right) d\sigma \right| \leq \epsilon \int_{\Gamma_{l,k}^r} |\mathbf{w}|^2 d\sigma \tag{3.20a}$$

Next at the point P the the ζ parameter curves and the η parameter curves are geodesics. Hence at P , $\frac{\partial \tau_j}{\partial s_j} \cdot T' = 0$ for any vector T' which lies on the tangent plane at P . Thus for any $\epsilon > 0$ we can choose a fine enough triangulation so that

$$\begin{aligned} \left| \sum_i \int_{\pi_i(U_i)} \mathbf{w}_\nu(\mathbf{w}_T \cdot \frac{\partial \tau_j}{\partial s_j}) d\sigma \right| &\leq \epsilon \int_{\Gamma_{l,i}^r} (\mathbf{w}_\nu^2 + |\mathbf{w}_T|^2) d\sigma \\ &\leq \epsilon \int_{\Gamma_{l,i}^r} |\mathbf{w}|^2 d\sigma. \end{aligned} \quad (3.20b)$$

Now from (3.19) and (3.20) we obtain the result since ϵ is arbitrary. \square

3.2.2 Estimates for second derivatives in vertex neighbourhoods

In Figure 2.2 the intersection of Ω with a sphere of radius ρ_v with center at the vertex v is shown. On removing the vertex-edge neighbourhoods, which are shaded, we obtain the vertex neighbourhood Ω^v where $v \in \mathcal{V}$ and \mathcal{V} denotes the set of vertices. Choose ρ_v and ϕ_v so that $\rho_v \sin(\phi_v) = Z$, a constant, for all $v \in V$. Let S^v denote the intersection of the closure of Ω^v with $B_{\rho_v}(v) = \{x : |x - v| \leq \rho_v\}$. S^v is divided into triangular and quadrilateral elements S_j^v for $1 \leq j \leq I_v$, where I_v is a fixed constant. We define a geometric mesh in the vertex neighbourhood Ω^v of the vertex v as shown in Figure 2.8. Thus Ω^v is divided into N_v curvilinear cubes and prisms $\{\Omega_l^v\}_{1 \leq l \leq N_v}$. Let us introduce the new coordinate system

$$\begin{aligned} x_1^v &= \phi \\ x_2^v &= \theta \\ x_3^v &= \ln \rho = \mathcal{X}. \end{aligned} \quad (3.21)$$

Let $\tilde{\Omega}_l^v$ be the image of Ω_l^v in (x_1^v, x_2^v, x_3^v) coordinates. Now

$$\int_{\Omega_l^v} \rho^2 |Lu|^2 dx = \int_{\tilde{\Omega}_l^v} e^{\mathcal{X}} \sin \phi |e^{2\mathcal{X}} Lu|^2 d\phi d\theta d\mathcal{X}. \quad (3.22)$$

Define

$$L^v u(x^v) = e^{\frac{\mathcal{X}}{2}} \sqrt{\sin \phi} (e^{2\mathcal{X}} Lu). \quad (3.23)$$

We have the relation

$$\rho \nabla_x u = Q^v \nabla_{x^v} u. \quad (3.24)$$

Here

$$Q^v = O^v P^v \quad (3.25a)$$

where O^v is the orthogonal matrix

$$O^v = \begin{bmatrix} \cos \phi \cos \theta & -\sin \theta & \sin \phi \cos \theta \\ \cos \phi \sin \theta & \cos \theta & \sin \phi \sin \theta \\ -\sin \phi & 0 & \cos \phi \end{bmatrix} \quad (3.25b)$$

and

$$P^v = \begin{bmatrix} 1 & 0 & 0 \\ 0 & 1/\sin \phi & 0 \\ 0 & 0 & 1 \end{bmatrix}. \quad (3.25c)$$

Define

$$A^v = (Q^v)^T A Q^v. \quad (3.25d)$$

Since $\phi_0 < \phi < \pi - \phi_0$ where ϕ_0 denotes a positive constant, $\mu_0 I \leq A^v \leq \mu_1 I$ for some positive constants μ_0 and μ_1 . Let $\tilde{\Omega}_l^v$ be a curvilinear cube and let its faces be denoted by $\{\tilde{\Gamma}_{l,i}^v\}$. We now prove the following result.

Lemma 3.2.3. *There exist positive constants C_v such that*

$$\begin{aligned} & \frac{\mu_0^2}{2} \sin^2(\phi_v) \int_{\tilde{\Omega}_l^v} e^{x_3^v} \sum_{r,s=1}^3 \left| \frac{\partial^2 u}{\partial x_r^v \partial x_s^v} \right|^2 dx^v \\ & \leq \sin^2(\phi_v) \int_{\tilde{\Omega}_l^v} |L^v u(x^v)|^2 dx^v \\ & - \sin^2(\phi_v) \left\{ \sum_i \oint_{\partial \tilde{\Gamma}_{l,i}^v} e^{x_3^v} \sin(x_1^v) \left(\frac{\partial u}{\partial \mathbf{n}^v} \right)_{A^v} \left(\frac{\partial u}{\partial \boldsymbol{\nu}^v} \right)_{A^v} ds^v \right. \\ & - 2 \sum_i \int_{\tilde{\Gamma}_{l,i}^v} e^{x_3^v} \sin(x_1^v) \sum_{j=1}^2 \left(\frac{\partial u}{\partial \boldsymbol{\tau}_j^v} \right)_{A^v} \frac{\partial}{\partial s_j^v} \left(\left(\frac{\partial u}{\partial \boldsymbol{\nu}^v} \right)_{A^v} \right) d\sigma^v \Big\} \\ & + C_v \int_{\tilde{\Omega}_l^v} \sum_{|\alpha| \leq 1} e^{x_3^v} |D_{x^v}^\alpha u|^2 dx^v \end{aligned} \quad (3.26)$$

for $u \in H^3(\tilde{\Omega}_l^v)$. Here dx^v denotes a volume element in x^v coordinates, $d\sigma^v$ an element of surface area and ds^v an element of arc length in x^v coordinates.

Proof. We let \mathbf{f} denote a vector field. Then

$$\rho \operatorname{div}_x(\mathbf{f}) = \frac{e^{-2\mathcal{X}}}{\sin \phi} \operatorname{div}_{x^v} (e^{2\mathcal{X}} \sin \phi (Q^v)^T \mathbf{f}).$$

Take $\mathbf{f} = A \nabla_x u$. Hence

$$\int_{\Omega_l^v} |\rho \operatorname{div}_x(A \nabla_x u)|^2 dx = \int_{\tilde{\Omega}_l^v} \frac{e^{-\mathcal{X}}}{\sin \phi} |\operatorname{div}_{x^v}(e^{\mathcal{X}} \sin \phi (Q^v)^T A Q^v \nabla_{x^v} u)|^2 dx^v.$$

Define

$$M^v u(x^v) = \operatorname{div}_{x^v} \left(e^{\mathcal{X}/2} \sqrt{\sin \phi} A^v \nabla_{x^v} u \right). \quad (3.27)$$

Then

$$\begin{aligned} \frac{e^{-\mathcal{X}/2}}{\sqrt{\sin \phi}} \operatorname{div}_{x^v} (e^{\mathcal{X}} \sin \phi A^v \nabla_{x^v} u) &= M^v u(x^v) + \frac{1}{2} e^{\mathcal{X}/2} \sqrt{\sin \phi} \sum_{j=1}^3 a_{3,j}^v \frac{\partial u}{\partial x_j^v} \\ &+ \frac{1}{2} e^{\mathcal{X}/2} \frac{\cos \phi}{\sqrt{\sin \phi}} \sum_{j=1}^3 a_{1,j}^v \frac{\partial u}{\partial x_j^v}. \end{aligned}$$

Here A^v is as defined in (3.25d).

Define the vector field \mathbf{w} by

$$\mathbf{w} = e^{\mathcal{X}/2} \sqrt{\sin \phi} A^v \nabla_{x^v} u. \quad (3.28a)$$

Then

$$L^v u(x^v) = \operatorname{div}_{x^v}(\mathbf{w}) + \eta^v u(x^v)$$

where

$$\begin{aligned} \eta^v u(x^v) &= -\frac{1}{2} e^{\mathcal{X}/2} \sqrt{\sin \phi} \sum_{j=1}^3 a_{3,j}^v \frac{\partial u}{\partial x_j^v} - \frac{1}{2} e^{\mathcal{X}/2} \frac{\cos \phi}{\sqrt{\sin \phi}} \sum_{j=1}^3 a_{1,j}^v \frac{\partial u}{\partial x_j^v} \\ &+ \sum_{i=1}^3 b_i^v \frac{\partial u}{\partial x_i^v} + c^v u. \end{aligned} \quad (3.28b)$$

Here

$$\|b_i^v\|_{0,\infty,\tilde{\Omega}_l^v} = O(e^{3\mathcal{X}/2}), \quad (3.29a)$$

$$\|c^v\|_{0,\infty,\tilde{\Omega}_l^v} = O(e^{5\mathcal{X}/2}), \quad (3.29b)$$

and

$$\left\| (e^{\mathcal{X}/2} \sqrt{\sin \phi} A^v) \right\|_{1, \infty, \tilde{\Omega}_l^v} = O(e^{\mathcal{X}/2}). \quad (3.29c)$$

To obtain (3.26) we shall use Theorem 3.2.1 applied to the vector field \mathbf{w} along with Lemma 3.2.2. Now

$$\begin{aligned} & 2 \int_{\tilde{\Gamma}_{l,i}^v} \mathbf{w}_T \cdot \nabla_T \mathbf{w}_\nu \, d\sigma^v \\ &= 2 \int_{\tilde{\Gamma}_{l,i}^v} \sum_{j=1}^2 e^{\mathcal{X}/2} \sqrt{\sin \phi} \left(\frac{\partial u}{\partial \tau_j^v} \right)_{A^v} \frac{\partial}{\partial s_j^v} \left(e^{\mathcal{X}/2} \sqrt{\sin \phi} \left(\frac{\partial u}{\partial \nu^v} \right)_{A^v} \right) d\sigma^v \\ &= 2 \int_{\tilde{\Gamma}_{l,i}^v} \sum_{j=1}^2 e^{\mathcal{X}} \sin \phi \left(\frac{\partial u}{\partial \tau_j^v} \right)_{A^v} \frac{\partial}{\partial s_j^v} \left(\left(\frac{\partial u}{\partial \nu^v} \right)_{A^v} \right) d\sigma^v \\ &+ 2 \int_{\tilde{\Gamma}_{l,i}^v} \sum_{j=1}^2 e^{\mathcal{X}/2} \sqrt{\sin \phi} \left(\frac{\partial u}{\partial \tau_j^v} \right)_{A^v} \left(\frac{\partial u}{\partial \nu^v} \right)_{A^v} \frac{\partial}{\partial s_j^v} (e^{\mathcal{X}/2} \sqrt{\sin \phi}) d\sigma^v. \end{aligned} \quad (3.30)$$

And so using (3.27), (3.28) and (3.30) we obtain

$$\begin{aligned} & \frac{\mu_0^2}{2} \sin^2(\phi_v) \int_{\tilde{\Omega}_l^v} e^{x_3^v} \sum_{r,s=1}^3 \left| \frac{\partial^2 u}{\partial x_r^v \partial x_s^v} \right|^2 dx^v \\ & \leq \sin^2(\phi_v) \int_{\tilde{\Omega}_l^v} |L^v u(x^v)|^2 dx^v \\ & - \sin^2(\phi_v) \left\{ \sum_i \oint_{\partial \tilde{\Gamma}_{l,i}^v} e^{x_3^v} \sin(x_1^v) \left(\frac{\partial u}{\partial \mathbf{n}^v} \right)_{A^v} \left(\frac{\partial u}{\partial \nu^v} \right)_{A^v} ds^v \right. \\ & \left. - 2 \sum_i \int_{\tilde{\Gamma}_{l,i}^v} e^{x_3^v} \sin(x_1^v) \sum_{j=1}^2 \left(\frac{\partial u}{\partial \tau_j^v} \right)_{A^v} \frac{\partial}{\partial s_j^v} \left(\left(\frac{\partial u}{\partial \nu^v} \right)_{A^v} \right) d\sigma^v \right\} \\ & + C_v \int_{\tilde{\Omega}_l^v} \sum_{|\alpha| \leq 1} e^{x_3^v} |D_x^\alpha u|^2 dx^v + D_v \sum_i \int_{\tilde{\Gamma}_{l,i}^v} \sum_{|\alpha|=1} e^{x_3^v} |D_x^\alpha u|^2 d\sigma^v. \end{aligned}$$

Now for any $\epsilon > 0$ there exists a constant K_ϵ such that

$$\begin{aligned} \int_{\tilde{\Gamma}_{l,i}^v} \sum_{|\alpha|=1} e^{x_3^v} |D_x^\alpha u|^2 d\sigma^v & \leq \epsilon \int_{\tilde{\Omega}_l^v} \sum_{|\alpha|=2} e^{x_3^v} |D_x^\alpha u|^2 dx^v \\ & + K_\epsilon \int_{\tilde{\Omega}_l^v} \sum_{|\alpha|=1} e^{x_3^v} |D_x^\alpha u|^2 dx^v. \end{aligned}$$

Choosing ϵ small enough (3.26) follows from the above equation. \square

We now show that the boundary integrals in Lemma 3.2.1 and Lemma 3.2.3 coincide when $\Gamma_{k,i}^v = \Gamma_{l,m}^r$ is a portion of the sphere $B_{\rho_v}(v) = \{x : |x - v| = \rho_v\}$, except that they have opposite signs. Let Q^v be the matrix defined in (3.25a). Then by (3.24)

$$\rho \nabla_x u = Q^v \nabla_{x^v} u .$$

Now if \mathbf{dx} is a tangent vector to a curve in x coordinates then its image in x^v coordinates is given by \mathbf{dx}^v where

$$\mathbf{dx}^v = \frac{(Q^v)^T}{\rho} \mathbf{dx} . \quad (3.31)$$

Clearly the first fundamental form ds^2 in x coordinates is

$$\begin{aligned} ds^2 &= \mathbf{dx}^T \mathbf{dx} \\ &= \rho^2 (\mathbf{dx}^v)^T [(Q^v)^{-1} (Q^v)^{-T}] \mathbf{dx}^v \\ &= e^{2\mathcal{X}} (d\phi^2 + \sin^2 \phi d\theta^2 + d\mathcal{X}^2) . \end{aligned} \quad (3.32)$$

Moreover on $\Gamma_{l,m}^r$

$$d\sigma = \rho_v^2 \sin \phi d\phi d\theta . \quad (3.33)$$

Choose $\boldsymbol{\tau}_1^v = (1, 0, 0)^T$ and $\boldsymbol{\tau}_2^v = (0, 1, 0)^T$. These are then orthogonal unit tangent vectors on $\tilde{\Gamma}_{k,i}^v$ since $(ds^v)^2 = d\phi^2 + d\theta^2 + d\mathcal{X}^2$. Define

$$\begin{aligned} \boldsymbol{\tau}_1 &= -(Q^v)^{-T} \boldsymbol{\tau}_1^v = -e_\phi , \\ \boldsymbol{\tau}_2 &= \frac{(Q^v)^{-T}}{\sin \phi} \boldsymbol{\tau}_2^v = e_\theta . \end{aligned} \quad (3.34)$$

Let $\boldsymbol{\nu}^v = (0, 0, 1)^T$ denote the unit normal vector on $\tilde{\Gamma}_{k,i}^v$. Then

$$\boldsymbol{\nu} = -(Q^v)^{-T} \boldsymbol{\nu}^v \quad (3.35)$$

denotes the unit normal to $\Gamma_{l,m}^r$. Finally let $\mathbf{ds}^v = (d\phi, d\theta, 0)^T$ denote a tangent vector field on $\tilde{\Gamma}_{k,i}^v$. Define

$$\begin{aligned} ds^v &= \sqrt{d\phi^2 + d\theta^2} , \\ \mathbf{ds} &= \rho_v (Q^v)^{-T} \mathbf{ds}^v \end{aligned} \quad (3.36)$$

and

$$ds = \rho_v \sqrt{d\phi^2 + \sin^2(\phi)d\theta^2}.$$

Let

$$\mathbf{n}^v = \frac{(-d\theta, d\phi, 0)^T}{\sqrt{d\theta^2 + d\phi^2}} \quad (3.37)$$

be the unit outward normal to $\partial\tilde{\Gamma}_{k,i}^v$. Define

$$\mathbf{m}^v = \left(-\sin\phi d\theta, \frac{d\phi}{\sin\phi}, 0 \right)^T / \sqrt{d\phi^2 + \sin^2\phi d\theta^2}. \quad (3.38a)$$

Then

$$\mathbf{n} = (Q^v)^{-T} \mathbf{m}^v \quad (3.38b)$$

is the unit normal vector to $\partial\Gamma_{l,m}^r$. We now prove the following result.

Lemma 3.2.4. *Let $\Gamma_{k,i}^v = \Gamma_{l,m}^r$. Then the following identities hold.*

$$\begin{aligned} & \rho_v^2 \sin^2(\phi_v) \oint_{\partial\Gamma_{l,m}^r} \left(\frac{\partial u}{\partial \mathbf{n}} \right)_A \left(\frac{\partial u}{\partial \boldsymbol{\nu}} \right)_A ds \\ &= -\sin^2(\phi_v) \oint_{\partial\tilde{\Gamma}_{k,i}^v} e^{x_3^v} \sin(x_1^v) \left(\frac{\partial u}{\partial \mathbf{n}^v} \right)_{A^v} \left(\frac{\partial u}{\partial \boldsymbol{\nu}^v} \right)_{A^v} ds^v \end{aligned} \quad (3.39)$$

and

$$\begin{aligned} & \rho_v^2 \sin^2(\phi_v) \int_{\Gamma_{l,m}^r} \sum_{j=1}^2 \left(\frac{\partial u}{\partial \boldsymbol{\tau}_j} \right)_A \frac{\partial}{\partial s_j} \left(\left(\frac{\partial u}{\partial \boldsymbol{\nu}} \right)_A \right) d\sigma \\ &= -\sin^2(\phi_v) \int_{\tilde{\Gamma}_{k,i}^v} e^{x_3^v} \sin(x_1^v) \sum_{j=1}^2 \left(\frac{\partial u}{\partial \boldsymbol{\tau}_j^v} \right)_{A^v} \frac{\partial}{\partial s_j^v} \left(\left(\frac{\partial u}{\partial \boldsymbol{\nu}^v} \right)_{A^v} \right) d\sigma^v. \end{aligned} \quad (3.40)$$

Proof. We first evaluate $\rho_v^2 \sin^2(\phi_v) \oint_{\partial\Gamma_{l,m}^r} \left(\frac{\partial u}{\partial \mathbf{n}} \right)_A \left(\frac{\partial u}{\partial \boldsymbol{\nu}} \right)_A ds$. By (3.24) and (3.35)

$$\begin{aligned} \left(\frac{\partial u}{\partial \boldsymbol{\nu}} \right)_A &= \boldsymbol{\nu}^T A \nabla_x u = -\frac{(\boldsymbol{\nu}^v)^T}{\rho_v} ((Q^v)^{-1} A Q^v) \nabla_{x^v} u \\ &= \frac{-(\boldsymbol{\nu}^v)^T (Q^v)^{-1} (Q^v)^{-T}}{\rho_v} A^v \nabla_{x^v} u. \end{aligned}$$

Now by (3.32) and (3.35)

$$(\boldsymbol{\nu}^v)^T (Q^v)^{-1} (Q^v)^{-T} = (\boldsymbol{\nu}^v)^T.$$

Hence we can conclude that

$$\left(\frac{\partial u}{\partial \boldsymbol{\nu}} \right)_A = \frac{-1}{\rho_v} \left(\frac{\partial u}{\partial \boldsymbol{\nu}^v} \right)_{A^v}. \quad (3.41)$$

Now by (3.38b)

$$\left(\frac{\partial u}{\partial \mathbf{n}} \right)_A = n^T A \nabla_x u = \frac{1}{\rho_v} ((\mathbf{m}^v)^T (Q^v)^{-1} (Q^v)^{-T} A^v \nabla_{x^v} u) .$$

Clearly

$$((\mathbf{m}^v)^T (Q^v)^{-1} (Q^v)^{-T}) = \frac{\sin \phi(-d\theta, d\phi, 0)}{\sqrt{d\phi^2 + \sin^2 \phi d\theta^2}} .$$

Using (3.35), (3.36) and (3.37) gives

$$\frac{1}{\rho_v} ((\mathbf{m}^v)^T (Q^v)^{-1} (Q^v)^{-T}) = \sin \phi \frac{ds^v}{ds} (\mathbf{n}^v)^T .$$

Hence

$$\left(\frac{\partial u}{\partial \mathbf{n}} \right)_A ds = \sin \phi \left(\frac{\partial u}{\partial \mathbf{n}^v} \right)_{A^v} ds^v . \quad (3.42)$$

Thus from (3.41) and (3.42) we obtain (3.39). Finally we evaluate the term

$$\rho_v^2 \sin^2(\phi_v) \int_{\Gamma_{l,m}^r} \sum_{j=1}^2 \left(\frac{\partial u}{\partial \boldsymbol{\tau}_j} \right)_A \frac{\partial}{\partial s_j} \left(\left(\frac{\partial u}{\partial \boldsymbol{\nu}} \right)_A \right) d\sigma .$$

Using (3.34) it is easy to show that

$$\begin{aligned} \left(\frac{\partial u}{\partial \boldsymbol{\tau}_1} \right)_A &= \frac{-1}{\rho_v} \left(\frac{\partial u}{\partial \boldsymbol{\tau}_1^v} \right)_{A^v} , \text{ and} \\ \left(\frac{\partial u}{\partial \boldsymbol{\tau}_2} \right)_A &= \frac{\sin \phi}{\rho_v} \left(\frac{\partial u}{\partial \boldsymbol{\tau}_2^v} \right)_{A^v} . \end{aligned} \quad (3.43)$$

Moreover by (3.41)

$$\left(\frac{\partial u}{\partial \boldsymbol{\nu}} \right)_A = \frac{-1}{\rho_v} \left(\frac{\partial u}{\partial \boldsymbol{\nu}^v} \right)_{A^v} .$$

Hence

$$\begin{aligned} \frac{\partial}{\partial s_1} \left(\left(\frac{\partial u}{\partial \boldsymbol{\nu}} \right)_A \right) &= \frac{1}{\rho_v^2} \frac{\partial}{\partial s_1^v} \left(\left(\frac{\partial u}{\partial \boldsymbol{\nu}^v} \right)_{A^v} \right) , \text{ and} \\ \frac{\partial}{\partial s_2} \left(\left(\frac{\partial u}{\partial \boldsymbol{\nu}} \right)_A \right) &= -\frac{1}{\rho_v^2 \sin \phi} \frac{\partial}{\partial s_2^v} \left(\left(\frac{\partial u}{\partial \boldsymbol{\nu}^v} \right)_{A^v} \right) . \end{aligned} \quad (3.44)$$

Moreover from (3.32)

$$d\sigma = \rho_v^2 \sin \phi d\sigma^v . \quad (3.45)$$

Combining (3.43), (3.44) and (3.45) we obtain (3.40). \square

3.2.3 Estimates for second derivatives in vertex-edge neighbourhoods

Figure 2.4 shows the vertex-edge neighbourhood Ω^{v-e} of the vertex v and the edge e . As before we have $\rho_v \sin \phi_v = Z$. Now

$$\Omega^{v-e} = \{x \in \Omega : 0 < x_3 < \delta_v, 0 < \phi < \phi_v\}.$$

A geometric mesh is imposed on Ω^{v-e} as shown in Figure 2.9. To proceed further we introduce new coordinates in Ω^{v-e} by

$$\begin{aligned} x_1^{v-e} &= \psi = \ln(\tan \phi) \\ x_2^{v-e} &= \theta \\ x_3^{v-e} &= \zeta = \ln x_3 = \mathcal{X} + \ln(\cos \phi). \end{aligned} \tag{3.46}$$

Here

$$\begin{aligned} x_1^v &= \phi \\ x_2^v &= \theta \\ x_3^v &= \mathcal{X} = \ln \rho \end{aligned} \tag{3.47}$$

are the coordinates which have been introduced in the vertex neighbourhood Ω^v , adjoining Ω^{v-e} . Let $\tilde{\Omega}^{v-e}$ be the image of Ω^{v-e} in x^{v-e} coordinates. Thus $\tilde{\Omega}^{v-e}$ is divided into $N^{v-e} = I^{v-e}(N+1)^2$ hexahedrons $\tilde{\Omega}_n^{v-e}$. Now

$$\nabla_{x^v} u = J^{v-e} \nabla_{x^{v-e}} u \tag{3.48}$$

where

$$J^{v-e} = \begin{bmatrix} \sec^2 \phi \cot \phi & 0 & -\tan \phi \\ 0 & 1 & 0 \\ 0 & 0 & 1 \end{bmatrix}. \tag{3.49}$$

We now need to evaluate

$$\int_{\Omega_n^{v-e}} \rho^2 \sin^2 \phi |Lu(x)|^2 dx.$$

Let $\hat{\Omega}_n^{v-e}$ denote the image of Ω_n^{v-e} in x^v coordinates. Then

$$\int_{\Omega_n^{v-e}} \rho^2 \sin^2 \phi |Lu(x)|^2 dx = \int_{\hat{\Omega}_n^{v-e}} \sin^2 \phi |L^v u(x^v)|^2 dx^v.$$

Now

$$dx^v = \sin \phi \cos \phi dx^{v-e}. \quad (3.50)$$

Let \mathbf{f} denote a vector field. Then

$$\operatorname{div}_{x^v}(\mathbf{f}) = \frac{1}{\sin \phi \cos \phi} \operatorname{div}_{x^{v-e}} (\sin \phi \cos \phi (J^{v-e})^T \mathbf{f}). \quad (3.51)$$

Using (3.50) we obtain

$$\int_{\Omega_n^{v-e}} \rho^2 \sin^2 \phi |Lu(x)|^2 dx = \int_{\hat{\Omega}_n^{v-e}} \sin^3 \phi \cos \phi |L^v u(x^v)|^2 dx^{v-e}.$$

Define

$$L^{v-e} u(x^{v-e}) = (\sin \phi)^{3/2} (\cos \phi)^{1/2} L^v u(x^v). \quad (3.52)$$

Then using (3.27), (3.48) and (3.51)

$$\begin{aligned} L^{v-e} u(x^{v-e}) &= (\sin \phi)^{1/2} (\cos \phi)^{-1/2} \operatorname{div}_{x^{v-e}} (e^{\mathcal{X}/2} (\sin \phi)^{3/2} \cos \phi \\ &\quad (J^{v-e})^T A^v J^{v-e} \nabla_{x^{v-e}} u) + \sum_{i=1}^2 b_i^{v-e} u_{x_i^{v-e}} + c^{v-e} u. \end{aligned} \quad (3.53)$$

Define

$$M^{v-e} u(x^{v-e}) = \operatorname{div}_{x^{v-e}} (e^{\mathcal{X}/2} (\cos \phi)^{1/2} \sin^2 \phi (J^{v-e})^T A^v J^{v-e} \nabla_{x^{v-e}} u).$$

Or

$$M^{v-e} u(x^{v-e}) = \operatorname{div}_{x^{v-e}} (e^{\zeta/2} A^{v-e} \nabla_{x^{v-e}} u). \quad (3.54)$$

Here

$$A^{v-e} = \sin^2 \phi (J^{v-e})^T A^v J^{v-e}.$$

Or using (3.25)

$$A^{v-e} = (K^{v-e})^T A K^{v-e} \quad (3.55)$$

where

$$K^{v-e} = O^v R^{v-e}$$

and

$$R^{v-e} = \begin{bmatrix} \frac{1}{\cos \phi} & 0 & \frac{-\sin^2 \phi}{\cos \phi} \\ 0 & 1 & 0 \\ 0 & 0 & \sin \phi \end{bmatrix}.$$

Now

$$\begin{aligned} (\tan \phi)^{1/2} \operatorname{div}_{x^{v-e}} (e^{\chi/2} (\sin \phi)^{3/2} \cos \phi (J^{v-e})^T A^v J^{v-e} \nabla_{x^{v-e}} u) \\ = M^{v-e} u(x^{v-e}) - \frac{1}{2} e^{\zeta/2} \sum_{j=1}^3 \hat{a}_{1,j}^{v-e} \frac{\partial u}{\partial x_j^{v-e}}. \end{aligned}$$

Hence using (3.53)

$$L^{v-e} u(x^{v-e}) = M^{v-e} u(x^{v-e}) + \eta^{v-e} u(x^{v-e}). \quad (3.56)$$

Here

$$\begin{aligned} \eta^{v-e} u(x^{v-e}) &= \frac{-1}{2} e^{\zeta/2} \sum_{j=1}^3 \hat{a}_{1,j}^{v-e} \frac{\partial u}{\partial x_j^{v-e}} + (\sin \phi)^{3/2} (\cos \phi)^{1/2} \eta^v u(x^v) \\ &= e^{\zeta/2} \sum_{j=1}^3 \hat{a}_{1,j}^{v-e} \frac{\partial u}{\partial x_j^{v-e}} + \sum_{i=1}^3 \hat{b}_i^{v-e} \frac{\partial u}{\partial x_i^{v-e}} + \hat{c}^{v-e} u. \end{aligned}$$

Moreover using (3.28), (3.29) and (3.48), it can be shown that

$$\begin{aligned} \|\hat{b}_i^{v-e}\|_{0,\infty,\tilde{\Omega}_n^{v-e}} &= O(e^{\zeta/2}) \text{ for } i = 1, 2, \\ \|\hat{b}_3^{v-e}\|_{0,\infty,\tilde{\Omega}_n^{v-e}} &= O(e^{\zeta/2} \sin \phi), \text{ and} \\ \|\hat{c}^{v-e}\|_{0,\infty,\tilde{\Omega}_n^{v-e}} &= O(e^{3\zeta/2} \sin^{\frac{3}{2}} \phi). \end{aligned} \quad (3.57)$$

Now consider the matrix A^{v-e} defined in (3.55). We note that the matrix A^{v-e} becomes singular as $\phi \rightarrow 0$. To overcome this problem we introduce a new set of local variables $y = (y_1, y_2, y_3)$ in

$$\Omega_n^{v-e} = \{x : \phi_l^{v-e} < \phi < \phi_{l+1}^{v-e}, \theta_j^{v-e} < \theta < \theta_{j+1}^{v-e}, \delta_v(\mu_v)^k < x_3 < \delta_v(\mu_v)^{k-1}\}$$

by

$$\begin{aligned} y_1 &= x_1^{v-e} \\ y_2 &= x_2^{v-e} \\ y_3 &= \frac{x_3^{v-e}}{\sin(\phi_{l+1}^{v-e})}. \end{aligned} \quad (3.58)$$

In making this transformation $\tilde{\Omega}_n^{v-e}$ is mapped to a hexahedron $\hat{\Omega}_n^{v-e}$ such that the length of the y_3 side becomes large as Ω_n^{v-e} approaches the edge of the domain Ω . It is important to note that the trace and embedding theorems in the theory of Sobolev spaces remain valid with a uniform constant for all the domains $\hat{\Omega}_n^{v-e}$. Now

$$\nabla_{x^{v-e}} u = \begin{bmatrix} 1 & 0 & 0 \\ 0 & 1 & 0 \\ 0 & 0 & \frac{1}{\sin(\phi_{l+1}^{v-e})} \end{bmatrix} \nabla_y u, \quad (3.59)$$

$$dx^{v-e} = \sin(\phi_{l+1}^{v-e}) dy, \quad (3.60)$$

and

$$\operatorname{div}_{x^{v-e}}(f) = \operatorname{div}_y \left(\begin{bmatrix} 1 & 0 & 0 \\ 0 & 1 & 0 \\ 0 & 0 & \frac{1}{\sin(\phi_{l+1}^{v-e})} \end{bmatrix} f \right). \quad (3.61)$$

Hence

$$M^{v-e} u(x^{v-e}) = \operatorname{div}_y (e^{\zeta/2} A^y \nabla_y u) \quad (3.62a)$$

where

$$A^y = (N^y)^T A N^y. \quad (3.62b)$$

Here by (3.54) and (3.55)

$$N^y = O^v Q^y \quad (3.63)$$

where

$$Q^y = \begin{bmatrix} \frac{1}{\cos(\phi)} & 0 & \frac{-\sin^2 \phi}{\sin(\phi_{l+1}^{v-e}) \cos(\phi)} \\ 0 & 1 & 0 \\ 0 & 0 & \frac{\sin(\phi)}{\sin(\phi_{l+1}^{v-e})} \end{bmatrix}.$$

Clearly, there exist positive constants μ_0 and μ_1 such that

$$\mu_0 I \leq A^y \leq \mu_1 I \quad (3.64)$$

for all elements Ω_n^{v-e} . Moreover there exists a constant C such that $a_{i,j}^y$ and its derivatives with respect to y are uniformly bounded in $\hat{\Omega}_n^{v-e}$. Hence we obtain the following result.

Lemma 3.2.5. *Let $w^{v-e}(x_1^{v-e})$ be a smooth, positive weight function such that $w^{v-e}(x_1^{v-e}) = 1$ for all x_1^{v-e} such that*

$$x_1^{v-e} \geq \psi_1^{v-e} = \ln(\tan(\phi_1^{v-e})) \text{ and } \int_{-\infty}^{\psi_1^{v-e}} w^{v-e}(x_1^{v-e}) = 1.$$

Then there exists a positive constant C_{v-e} such that the estimate

$$\begin{aligned} & \frac{\mu_0^2}{2} \int_{\tilde{\Omega}_n^{v-e}} e^{x_3^{v-e}} \left(\sum_{i,j=1}^2 \left(\frac{\partial^2 u}{\partial x_i^{v-e} \partial x_j^{v-e}} \right)^2 + \sum_{i=1}^2 \sin^2(\phi) \left(\frac{\partial^2 u}{\partial x_i^{v-e} \partial x_3^{v-e}} \right)^2 \right. \\ & \quad \left. + \sin^4(\phi) \left(\frac{\partial^2 u}{\partial (x_3^{v-e})^2} \right)^2 \right) dx^{v-e} \leq \int_{\tilde{\Omega}_n^{v-e}} |L^{v-e} u(x^{v-e})|^2 dx^{v-e} \\ & \quad - \left\{ \sum_k \oint_{\tilde{\Gamma}_{n,k}^{v-e}} e^{x_3^{v-e}} \left(\frac{\partial u}{\partial \mathbf{n}^{v-e}} \right)_{A^{v-e}} \left(\frac{\partial u}{\partial \boldsymbol{\nu}^{v-e}} \right)_{A^{v-e}} ds^{v-e} \right. \\ & \quad \left. - 2 \sum_k \int_{\tilde{\Gamma}_{n,k}^{v-e}} e^{x_3^{v-e}} \sum_{l=1}^2 \left(\frac{\partial u}{\partial \boldsymbol{\tau}_l^{v-e}} \right)_{A^{v-e}} \frac{\partial}{\partial s_l^{v-e}} \left(\frac{\partial u}{\partial \boldsymbol{\nu}^{v-e}} \right)_{A^{v-e}} d\sigma^{v-e} \right\} \\ & \quad + C_{v-e} \left(\int_{\tilde{\Omega}_n^{v-e}} e^{x_3^{v-e}} \left(\sum_{i=1}^2 \left(\frac{\partial u}{\partial x_i^{v-e}} \right)^2 + \sin^2(\phi) \left(\frac{\partial u}{\partial x_3^{v-e}} \right)^2 \right) dx^{v-e} \right. \\ & \quad \left. + \int_{\tilde{\Omega}_n^{v-e}} e^{x_3^{v-e}} u^2 w^{v-e}(x_1^{v-e}) dx^{v-e} \right) \end{aligned} \quad (3.65)$$

holds for all $\Omega_n^{v-e} \subseteq \Omega^{v-e}$.

Proof. Since the spectral element function $u(x^{v-e})$ is a function of only x_3^{v-e} if $\Omega_n^{v-e} \subseteq \{x : 0 < \phi < \phi_1^{v-e}\}$ the result follows. Here we have used the fact that the second fundamental form is identically zero. \square

Now we can prove the following result.

Lemma 3.2.6. *Let $\Gamma_{k,i}^v = \Gamma_{q,r}^{v-e}$. Then the following identity holds.*

$$\begin{aligned} & \sin^2(\phi_v) \oint_{\tilde{\Gamma}_{k,i}^v} e^{x_3^v} \sin(x_1^v) \left(\frac{\partial u}{\partial \mathbf{n}^v} \right)_{A^v} \left(\frac{\partial u}{\partial \boldsymbol{\nu}^v} \right)_{A^v} ds^v \\ & \quad - 2 \sin^2(\phi_v) \int_{\tilde{\Gamma}_{k,i}^v} e^{x_3^v} \sin(x_1^v) \sum_{j=1}^2 \left(\frac{\partial u}{\partial \boldsymbol{\tau}_j^v} \right)_{A^v} \frac{\partial}{\partial s_j^v} \left(\left(\frac{\partial u}{\partial \boldsymbol{\nu}^v} \right)_{A^v} \right) d\sigma^v \\ & = - \oint_{\tilde{\Gamma}_{q,r}^{v-e}} e^{x_3^{v-e}} \left(\frac{\partial u}{\partial \mathbf{n}^{v-e}} \right)_{A^{v-e}} \left(\frac{\partial u}{\partial \boldsymbol{\nu}^{v-e}} \right)_{A^{v-e}} ds^{v-e} \\ & \quad + 2 \int_{\tilde{\Gamma}_{q,r}^{v-e}} e^{x_3^{v-e}} \sum_{j=1}^2 \left(\frac{\partial u}{\partial \boldsymbol{\tau}_j^{v-e}} \right)_{A^{v-e}} \frac{\partial}{\partial s_j^{v-e}} \left(\left(\frac{\partial u}{\partial \boldsymbol{\nu}^{v-e}} \right)_{A^{v-e}} \right) d\sigma^{v-e}. \end{aligned} \quad (3.66)$$

Proof. The proof is provided in Appendix B.1. \square

3.2.4 Estimates for second derivatives in edge neighbourhoods

Consider the edge e whose end points are v and v' . Let the length of e be l_e . We define the edge neighbourhood (Figure 2.3)

$$\Omega^e = \{x \in \Omega : 0 < r < \rho_v \sin \phi_v = Z, \theta_{v-e}^l < \theta < \theta_{v-e}^u, \delta_v < x_3 < l_e - \delta_{v'}\}.$$

Here (r, θ, x_3) are polar coordinates with origin at v . We define a geometrical mesh on Ω^e as in Figure 2.10.

Let Ω_u^e denote an element

$$\Omega_u^e = \{x : r_j^e < r < r_{j+1}^e, \theta_k^e < \theta < \theta_{k+1}^e, Z_m^e < x_3 < Z_{m+1}^e\} \quad (3.67)$$

of the geometrical mesh imposed on the edge neighbourhood Ω^e . We now introduce a new set of coordinates in the edge neighbourhood

$$\begin{aligned} x_1^e &= \tau = \ln r \\ x_2^e &= \theta \\ x_3^e &= x_3. \end{aligned} \quad (3.68)$$

Let $\tilde{\Omega}_u^e$ denote the image of Ω_u^e in x^e coordinate. Now

$$\nabla_x u = R^e \nabla_{x^e} u \quad (3.69)$$

where

$$R^e = \begin{bmatrix} e^{-\tau} \cos \theta & -e^{-\tau} \sin \theta & 0 \\ e^{-\tau} \sin \theta & e^{-\tau} \cos \theta & 0 \\ 0 & 0 & 1 \end{bmatrix}. \quad (3.70)$$

Hence

$$dx = e^{2\tau} dx^e. \quad (3.71)$$

Moreover

$$\operatorname{div}_x(\mathbf{f}) = e^{-2\tau} \operatorname{div}_{x^e}(e^{2\tau} (R^e)^T \mathbf{f}). \quad (3.72)$$

Here \mathbf{f} denotes a vector field.

We need to evaluate

$$\int_{\Omega_u^e} (\rho^2 \sin^2 \phi) |Lu(x)|^2 dx = \int_{\Omega_u^e} r^2 |Lu(x)|^2 dx .$$

Clearly

$$\int_{\Omega_u^e} r^2 |Lu(x)|^2 dx = \int_{\tilde{\Omega}_u^e} |e^{2\tau} Lu(x)|^2 dx^e . \quad (3.73)$$

Let

$$Mu(x) = \operatorname{div}(A \nabla_x u)$$

Now

$$e^{2\tau} Mu(x) = \operatorname{div}_{x^e} (e^{2\tau} (R^e)^T A R^e \nabla_{x^e} u) .$$

Or

$$e^{2\tau} Mu(x) = \operatorname{div}_{x^e} (A^e \nabla_{x^e} u) . \quad (3.74)$$

Here

$$A^e = (S^e)^T A S^e \quad (3.75)$$

and

$$S^e = \begin{bmatrix} \cos \theta & -\sin \theta & 0 \\ \sin \theta & \cos \theta & 0 \\ 0 & 0 & e^\tau \end{bmatrix} . \quad (3.76)$$

Hence

$$e^{2\tau} Lu(x) = \operatorname{div}_{x^e} (A^e \nabla_{x^e} u) + \sum_{i=1}^3 \hat{b}_i^e u_{x_i^e} + \hat{c}^e u . \quad (3.77)$$

Now the matrix A^e becomes singular as the element Ω_u^e approaches the edge e . We note that

$$\begin{aligned} \|\hat{b}^e\|_{0,\infty,\tilde{\Omega}^e} &= O(e^\tau) \text{ and} \\ \|\hat{c}^e\|_{0,\infty,\tilde{\Omega}^e} &= O(e^{2\tau}) . \end{aligned} \quad (3.78)$$

Now

$$\Omega_u^e = \{x : r_j^e < r < r_{j+1}^e, \theta_k^e < \theta < \theta_{k+1}^e, \delta_v < x_3 < l_e - \delta_{v'}\} .$$

To overcome the singular nature of A^e as $j \rightarrow 0$ we once again introduce a set of local coordinates z in $\tilde{\Omega}_u^e$ defined as

$$\begin{aligned} z_1 &= x_1^e \\ z_2 &= x_2^e \\ z_3 &= \frac{x_3^e}{r_{j+1}^e}. \end{aligned} \quad (3.79)$$

Then $\tilde{\Omega}_u^e$ is mapped onto the hexahedron $\hat{\Omega}_u^e$ such that the length of the z_3 side becomes large as Ω_u^e approaches the edge of the domain Ω .

Define

$$M^e u(x^e) = e^{2\tau} M u(x) = \text{div}_{x^e} (A^e \nabla_{x^e} u). \quad (3.80)$$

Then

$$M^e u(x^e) = M^z u(z) = \text{div}_z (A^z \nabla_z u). \quad (3.81)$$

Here

$$A^z = (T^z)^T A T^z \quad (3.82)$$

where

$$T^z = \begin{bmatrix} \cos \theta & \sin \theta & 0 \\ -\sin \theta & \cos \theta & 0 \\ 0 & 0 & \frac{e^\tau}{r_{j+1}^e} \end{bmatrix}. \quad (3.83)$$

Clearly there exist positive constants μ_0 and μ_1 such that

$$\mu_0 I \leq A^z \leq \mu_1 I. \quad (3.84)$$

Moreover there exists a constant C such that $a_{i,j}^z$ and its derivatives with respect to z are uniformly bounded in $\hat{\Omega}_u^e$. Here $a_{i,j}^z$ denotes the elements of the matrix A^z . Hence we obtain the following result.

Lemma 3.2.7. *Let $w^e(x_1^e)$ be a smooth, positive weight function such that $w^e(x_1^e) = 1$ for all $x_1^e \geq \tau_1^e = \ln(r_1^e)$ and $\int_{-\infty}^{\tau_1^e} w^e(x_1^e) dx_1^e = 1$. Then there exists a positive constant C_e*

such that

$$\begin{aligned}
& \frac{\mu_0^2}{2} \int_{\tilde{\Omega}_u^e} \left(\sum_{i,j=1}^2 \left(\frac{\partial^2 u}{\partial x_i^e \partial x_j^e} \right)^2 + e^{2\tau} \sum_{i=1}^2 \left(\frac{\partial^2 u}{\partial x_i^e \partial x_3^e} \right)^2 + e^{4\tau} \left(\frac{\partial^2 u}{\partial x_3^{e2}} \right)^2 \right) dx^e \\
& \leq \int_{\tilde{\Omega}_u^e} |L^e u(x^e)|^2 dx^e - \left(\sum_k \oint_{\partial \tilde{\Gamma}_{u,k}^e} \left(\frac{\partial u}{\partial \mathbf{n}^e} \right)_{A^e} \left(\frac{\partial u}{\partial \boldsymbol{\nu}^e} \right)_{A^e} ds^e \right. \\
& \quad \left. - 2 \sum_k \int_{\tilde{\Gamma}_{u,k}^e} \sum_{l=1}^2 \left(\frac{\partial u}{\partial \boldsymbol{\tau}_l^e} \right)_{A^e} \frac{\partial}{\partial s_l^e} \left(\left(\frac{\partial u}{\partial \boldsymbol{\nu}^e} \right)_{A^e} \right) d\sigma^e \right) \\
& \quad + C_e \left(\int_{\tilde{\Omega}_u^e} \left(\sum_{i=1}^2 \left(\frac{\partial u}{\partial x_i^e} \right)^2 + e^{2\tau} \left(\frac{\partial u}{\partial x_3^e} \right)^2 \right) dx^e + \int_{\tilde{\Omega}_u^e} u^2 w^e(x_1^e) dx^e \right) \quad (3.85)
\end{aligned}$$

holds for all $\Omega_u^e \subseteq \Omega^e$.

Proof. Since the spectral element function $u(x^e)$ is only a function of x_3^e if $\Omega_u^e \subseteq \{x : r < r_1^e\}$ the result follows. Here we have used the fact that the second fundamental form is zero. \square

Finally we state the following results.

Lemma 3.2.8. *Let $\Gamma_{u,k}^e = \Gamma_{n,l}^{v-e}$. Then*

$$\begin{aligned}
& \oint_{\partial \tilde{\Gamma}_{n,l}^{v-e}} e^{x_3^{v-e}} \left(\frac{\partial u}{\partial \mathbf{n}^{v-e}} \right)_{A^{v-e}} \left(\frac{\partial u}{\partial \boldsymbol{\nu}^{v-e}} \right)_{A^{v-e}} ds^{v-e} \\
& - 2 \sum_{j=1}^2 \int_{\tilde{\Gamma}_{n,l}^{v-e}} e^{x_3^{v-e}} \left(\frac{\partial u}{\partial \boldsymbol{\tau}_j^{v-e}} \right)_{A^{v-e}} \frac{\partial}{\partial s_j^{v-e}} \left(\left(\frac{\partial u}{\partial \boldsymbol{\nu}^{v-e}} \right)_{A^{v-e}} \right) d\sigma^{v-e} \\
& = - \oint_{\partial \tilde{\Gamma}_{u,k}^e} \left(\frac{\partial u}{\partial \mathbf{n}^e} \right)_{A^e} \left(\frac{\partial u}{\partial \boldsymbol{\nu}^e} \right)_{A^e} ds^e \\
& + 2 \sum_{j=1}^2 \int_{\tilde{\Gamma}_{u,k}^e} \left(\frac{\partial u}{\partial \boldsymbol{\tau}_j^e} \right)_{A^e} \frac{\partial}{\partial s_j^e} \left(\left(\frac{\partial u}{\partial \boldsymbol{\nu}^e} \right)_{A^e} \right) d\sigma^e. \quad (3.86)
\end{aligned}$$

Proof. The proof is provided in Appendix B.2. \square

Lemma 3.2.9. *Let $\Gamma_{u,k}^e = \Gamma_{l,j}^r$. Then*

$$\oint_{\partial \tilde{\Gamma}_{u,k}^e} \left(\frac{\partial u}{\partial \boldsymbol{\nu}^e} \right)_{A^e} \left(\frac{\partial u}{\partial \mathbf{n}^e} \right)_{A^e} ds^e = -\rho_v^2 \sin^2(\phi_v) \oint_{\partial \Gamma_{l,j}^r} \left(\frac{\partial u}{\partial \mathbf{n}} \right)_A \left(\frac{\partial u}{\partial \boldsymbol{\nu}} \right)_A ds, \quad (3.87)$$

and

$$\begin{aligned} & \sum_{m=1}^2 \int_{\tilde{\Gamma}_{u,k}^e} \left(\frac{\partial u}{\partial \tau_m^e} \right)_{A^e} \frac{\partial}{\partial s_m^e} \left(\frac{\partial u}{\partial \nu^e} \right)_{A^e} d\sigma^e \\ &= -\rho_v^2 \sin^2(\phi_v) \left(\sum_{m=1}^2 \int_{\Gamma_{l,j}^r} \left(\frac{\partial u}{\partial \tau_m} \right)_A \frac{\partial}{\partial s_m} \left(\frac{\partial u}{\partial \nu} \right)_A d\sigma \right). \end{aligned} \quad (3.88)$$

Proof. The proof is provided in Appendix B.3. \square

3.3 Estimates for Lower Order Derivatives

Lemma 3.3.1. *We can define a set of corrections $\{\eta_l^r\}_{l=1,\dots,N_r}$, $\{\eta_l^v\}_{l=1,\dots,N_v}$ for $v \in \mathcal{V}$, $\{\eta_l^{v-e}\}_{l=1,\dots,N_{v-e}}$ for $v-e \in \mathcal{V} - \mathcal{E}$ and $\{\eta_l^e\}_{l=1,\dots,N_e}$ for $e \in \mathcal{E}$ such that the corrected spectral element function p defined as*

$$\begin{aligned} p_l^r &= u_l^r + \eta_l^r && \text{for } l = 1, \dots, N_r, \\ p_l^v &= u_l^v + \eta_l^v && \text{for } l = 1, \dots, N_v \text{ and } v \in \mathcal{V}, \\ p_l^{v-e} &= u_l^{v-e} + \eta_l^{v-e} && \text{for } l = 1, \dots, N_{v-e} \text{ and } v-e \in \mathcal{V} - \mathcal{E}, \\ p_l^e &= u_l^e + \eta_l^e && \text{for } l = 1, \dots, N_e \text{ and } e \in \mathcal{E}, \end{aligned} \quad (3.89)$$

is conforming and $p \in H_0^1(\Omega)$ i.e. $p \in H^1(\Omega)$ and p vanishes on $\Gamma^{[0]}$. Define

$$\begin{aligned} \mathcal{U}_{(1)}^{N,W}(\{\mathcal{F}_s\}) &= \sum_{l=1}^{N_r} \|s_l^r(x_1, x_2, x_3)\|_{1,\Omega_l^r}^2 + \sum_{v \in \mathcal{V}} \sum_{l=1}^{N_v} \|s_l^v(x_1^v, x_2^v, x_3^v) e^{x_3^v/2}\|_{1,\tilde{\Omega}_l^v}^2 \\ &+ \sum_{v-e \in \mathcal{V}-\mathcal{E}} \left(\sum_{l=1}^{N_{v-e}} \int_{\tilde{\Omega}_l^{v-e}} e^{x_3^{v-e}} \left(\sum_{i=1}^2 \left(\frac{\partial s_l^{v-e}}{\partial x_i^{v-e}} \right)^2 + \sin^2 \phi \left(\frac{\partial s_l^{v-e}}{\partial x_3^{v-e}} \right)^2 \right. \right. \\ &\quad \left. \left. + (s_l^{v-e})^2 \right) dx^{v-e} + \sum_{l=1}^{N_{v-e}} \int_{\tilde{\Omega}_l^{v-e}} e^{x_3^{v-e}} (s_l^{v-e})^2 w^{v-e}(x_1^{v-e}) dx^{v-e} \right) \\ &+ \sum_{e \in \mathcal{E}} \left(\sum_{l=1}^{N_e} \int_{\tilde{\Omega}_l^e} \left(\sum_{i=1}^2 \left(\frac{\partial s_l^e}{\partial x_i^e} \right)^2 + e^{2\tau} \left(\frac{\partial s_l^e}{\partial x_3^e} \right)^2 + (s_l^e)^2 \right) dx^e \right. \\ &\quad \left. + \sum_{l=1}^{N_e} \int_{\tilde{\Omega}_l^e} (s_l^e)^2 w^e(x_1^e) dx^e \right) \end{aligned} \quad (3.90)$$

Then the estimate

$$\mathcal{U}_{(1)}^{N,W}(\{\mathcal{F}_\eta\}) \leq C_W \mathcal{V}^{N,W}(\{\mathcal{F}_u\}) \quad (3.91)$$

holds. Here C_W is a constant, if the spectral element functions are conforming on the wirebasket WB of the elements, otherwise $C_W = C(\ln W)$, where C is a constant.

Proof. The proof is provided in Appendix C.1. \square

Theorem 3.3.1. *The following estimate for the spectral element functions holds*

$$\mathcal{U}_{(1)}^{N,W}(\{\mathcal{F}_u\}) \leq K_{N,W} \mathcal{V}^{N,W}(\{\mathcal{F}_u\}) \quad (3.92)$$

Here $K_{N,W} = CN^4$, when the boundary conditions are mixed and $K_{N,W} = C(\ln W)^2$ when the boundary conditions are Dirichlet.

If the spectral element functions vanish on the wirebasket WB of the elements then $K_{N,W} = C(\ln W)^2$, where C is a constant.

Proof. The proof is similar to the proof of Theorem 3.1 in [38] and is provided in Appendix C.2. \square

3.4 Estimates for Terms in the Interior

3.4.1 Estimates for terms in the interior of Ω^r

Lemma 3.4.1. *Let Ω_m^r and Ω_p^r be elements in the regular region Ω^r of Ω and $\Gamma_{m,i}^r$ be a face of Ω_m^r and $\Gamma_{p,j}^r$ be a face of Ω_p^r such that $\Gamma_{m,i}^r = \Gamma_{p,j}^r$. Then for any $\epsilon > 0$ there exists a constant C_ϵ such that for W large enough*

$$\begin{aligned} & \left| \int_{\partial\Gamma_{m,i}^r} \left(\left(\frac{\partial u_m^r}{\partial \boldsymbol{\nu}} \right)_A \left(\frac{\partial u_m^r}{\partial \mathbf{n}} \right)_A - \left(\frac{\partial u_p^r}{\partial \boldsymbol{\nu}} \right)_A \left(\frac{\partial u_p^r}{\partial \mathbf{n}} \right)_A \right) ds \right| \\ & \leq C_\epsilon (\ln W)^2 \sum_{k=1}^3 \| [u_{x_k}] \|_{1/2, \Gamma_{m,i}^r}^2 + \epsilon \sum_{1 \leq |\alpha| \leq 2} \left(\| D_x^\alpha u_m^r \|_{0, \Omega_m^r}^2 + \| D_x^\alpha u_p^r \|_{0, \Omega_p^r}^2 \right). \end{aligned} \quad (3.93)$$

Proof. The proof is similar to the proof of Lemma 3.1 in [37] and is provided in Appendix D.1. \square

Lemma 3.4.2. *Let Ω_m^r and Ω_p^r be elements in the regular region Ω^r of Ω and $\Gamma_{m,i}^r$ be a face of Ω_m^r and $\Gamma_{p,j}^r$ be a face of Ω_p^r such that $\Gamma_{m,i}^r = \Gamma_{p,j}^r$. Then for any $\epsilon > 0$ there exists a constant C_ϵ such that for W large enough*

$$\begin{aligned} & \left| \sum_{j=1}^2 \left(\int_{\Gamma_{m,i}^r} \left(\frac{\partial u_m^r}{\partial \boldsymbol{\tau}_j} \right)_A \frac{\partial}{\partial s_j} \left(\frac{\partial u_m^r}{\partial \boldsymbol{\nu}} \right)_A d\sigma - \int_{\Gamma_{p,j}^r} \left(\frac{\partial u_p^r}{\partial \boldsymbol{\tau}_j} \right)_A \frac{\partial}{\partial s_j} \left(\frac{\partial u_p^r}{\partial \boldsymbol{\nu}} \right)_A d\sigma \right) \right| \\ & \leq C_\epsilon (\ln W)^2 \sum_{k=1}^3 \| [u_{x_k}] \|_{1/2, \Gamma_{p,j}^r}^2 + \epsilon \sum_{1 \leq |\alpha| \leq 2} \left(\| D_x^\alpha u_m^r \|_{0, \Omega_m^r}^2 + \| D_x^\alpha u_p^r \|_{0, \Omega_p^r}^2 \right). \end{aligned} \quad (3.94)$$

Proof. The proof is similar to the proof of Lemma 3.3 in [37] and is provided in Appendix D.2. \square

3.4.2 Estimates for terms in the interior of Ω^e

Lemma 3.4.3. *Let Ω_m^e and Ω_p^e be elements in the edge neighbourhood Ω^e of Ω and $\Gamma_{m,i}^e$ be a face of Ω_m^e and $\Gamma_{p,j}^e$ be a face of Ω_p^e such that $\Gamma_{m,i}^e = \Gamma_{p,j}^e$ and $\mu(\tilde{\Gamma}_{m,i}^e) < \infty$. Then for any $\epsilon > 0$ there exists a constant C_ϵ such that for W large enough*

$$\begin{aligned} & \left| \oint_{\partial \tilde{\Gamma}_{m,i}^e} \left(\left(\frac{\partial u_m^e}{\partial \mathbf{n}^e} \right)_{A^e} \left(\frac{\partial u_m^e}{\partial \boldsymbol{\nu}^e} \right)_{A^e} - \left(\frac{\partial u_p^e}{\partial \mathbf{n}^e} \right)_{A^e} \left(\frac{\partial u_p^e}{\partial \boldsymbol{\nu}^e} \right)_{A^e} \right) ds^e \right| \\ & \leq C_\epsilon (\ln W)^2 \left(\| [u_{x_1}^e] \|_{\tilde{\Gamma}_{m,i}^e}^2 + \| [u_{x_2}^e] \|_{\tilde{\Gamma}_{m,i}^e}^2 + \| G_{m,i}^e [u_{x_3}^e] \|_{\tilde{\Gamma}_{m,i}^e}^2 \right) \\ & + \epsilon \sum_{k=m,p} \left(\int_{\tilde{\Omega}_k^e} \left(\sum_{i,j=1,2} \left(\frac{\partial^2 u_k^e}{\partial x_i^e \partial x_j^e} \right)^2 + e^{2\tau} \sum_{i=1}^2 \left(\frac{\partial^2 u_k^e}{\partial x_i^e \partial x_3^e} \right)^2 + e^{4\tau} \left(\frac{\partial^2 u_k^e}{(\partial x_3^e)^2} \right)^2 \right. \right. \\ & \left. \left. + \sum_{i=1}^2 \left(\frac{\partial u_k^e}{\partial x_i^e} \right)^2 + e^{2\tau} \left(\frac{\partial u_k^e}{\partial x_3^e} \right)^2 \right) dx^e \right). \end{aligned} \quad (3.95a)$$

Here C_ϵ is a constant which depends on ϵ but is uniform for all $\tilde{\Gamma}_{m,i}^e \subseteq \tilde{\Omega}^e$, and $G_{m,i}^e = \sup_{x^e \in \tilde{\Gamma}_{m,i}^e} (e^\tau)$.

If $\mu(\tilde{\Gamma}_{m,i}^e) = \infty$ then for any $\epsilon > 0$

$$\begin{aligned} & \left| \oint_{\partial \tilde{\Gamma}_{m,i}^e} \left(\left(\frac{\partial u_m^e}{\partial \mathbf{n}^e} \right)_{A^e} \left(\frac{\partial u_m^e}{\partial \boldsymbol{\nu}^e} \right)_{A^e} - \left(\frac{\partial u_p^e}{\partial \mathbf{n}^e} \right)_{A^e} \left(\frac{\partial u_p^e}{\partial \boldsymbol{\nu}^e} \right)_{A^e} \right) ds^e \right| \\ & \leq \epsilon \left(\int_{\tilde{\Omega}_m^e} (u_m^e)^2 w^e(x_1^e) dx^e + \int_{\tilde{\Omega}_p^e} (u_p^e)^2 w^e(x_1^e) dx^e \right) \end{aligned} \quad (3.95b)$$

provided $W = O(e^{N^\alpha})$ with $\alpha < 1/2$.

Proof. The proof is provided in Appendix D.3. \square

Lemma 3.4.4. *Let Ω_m^e and Ω_p^e be elements in the edge neighbourhood Ω^e of Ω and $\Gamma_{m,i}^e$ be a face of Ω_m^e and $\Gamma_{p,j}^e$ be a face of Ω_p^e such that $\Gamma_{m,i}^e = \Gamma_{p,j}^e$ and $\mu(\tilde{\Gamma}_{m,i}^e) < \infty$. Then for any $\epsilon > 0$ there exists a constant C_ϵ such that for W large enough*

$$\begin{aligned} & \left| \int_{\tilde{\Gamma}_{m,i}^e} \sum_{l=1}^2 \left(\left(\frac{\partial u_m^e}{\partial \tau_l^e} \right)_{A^e} \frac{\partial}{\partial s_l^e} \left(\left(\frac{\partial u_m^e}{\partial \nu^e} \right)_{A^e} \right) - \left(\frac{\partial u_p^e}{\partial \tau_l^e} \right)_{A^e} \frac{\partial}{\partial s_l^e} \left(\left(\frac{\partial u_p^e}{\partial \nu^e} \right)_{A^e} \right) \right) d\sigma^e \right| \\ & \leq C_\epsilon (\ln W)^2 \left(||| [u_{x_1}^e] |||_{\tilde{\Gamma}_{m,i}^e}^2 + ||| [u_{x_2}^e] |||_{\tilde{\Gamma}_{m,i}^e}^2 + ||| G_{m,i}^e [u_{x_3}^e] |||_{\tilde{\Gamma}_{m,i}^e}^2 \right) \\ & + \epsilon \sum_{k=m,p} \left(\int_{\tilde{\Omega}_k^e} \left(\sum_{i,j=1,2} \left(\frac{\partial^2 u_k^e}{\partial x_i^e \partial x_j^e} \right)^2 + e^{2\tau} \sum_{i=1}^2 \left(\frac{\partial^2 u_k^e}{\partial x_i^e \partial x_3^e} \right)^2 + e^{4\tau} \left(\frac{\partial^2 u_k^e}{(\partial x_3^e)^2} \right)^2 \right. \right. \\ & \left. \left. + \sum_{i=1}^2 \left(\frac{\partial u_k^e}{\partial x_i^e} \right)^2 + e^{2\tau} \left(\frac{\partial u_k^e}{\partial x_3^e} \right)^2 \right) dx^e \right). \end{aligned} \quad (3.96a)$$

If $\mu(\tilde{\Gamma}_{m,i}^e) = \infty$ then for any $\epsilon > 0$

$$\begin{aligned} & \left| \int_{\tilde{\Gamma}_{m,i}^e} \sum_{l=1}^2 \left(\left(\frac{\partial u_m^e}{\partial \tau_l^e} \right)_{A^e} \frac{\partial}{\partial s_l^e} \left(\left(\frac{\partial u_m^e}{\partial \nu^e} \right)_{A^e} \right) - \left(\frac{\partial u_p^e}{\partial \tau_l^e} \right)_{A^e} \frac{\partial}{\partial s_l^e} \left(\left(\frac{\partial u_p^e}{\partial \nu^e} \right)_{A^e} \right) \right) d\sigma^e \right| \\ & \leq \epsilon \left(\int_{\tilde{\Omega}_m^e} (u_m^e)^2 w^e(x_1^e) dx^e + \int_{\tilde{\Omega}_p^e} (u_p^e)^2 w^e(x_1^e) dx^e \right) \end{aligned} \quad (3.96b)$$

provided $W = O(e^{N^\alpha})$ with $\alpha < 1/2$.

Proof. The proof is provided in Appendix D.4. \square

We now state estimates for terms in the interior of vertex neighbourhoods and vertex-edge neighbourhoods the proofs of which are similar to those for Lemma 3.4.1 to Lemma 3.4.4.

3.4.3 Estimates for terms in the interior of Ω^v

Lemma 3.4.5. *Let Ω_m^v and Ω_p^v be elements in the vertex neighbourhood Ω^v of Ω and $\Gamma_{m,i}^v$ be a face of Ω_m^v and $\Gamma_{p,j}^v$ be a face of Ω_p^v such that $\Gamma_{m,i}^v = \Gamma_{p,j}^v$. Then for any $\epsilon > 0$ there*

exists a constant C_ϵ such that for W large enough

$$\begin{aligned}
& \left| \oint_{\partial \tilde{\Gamma}_{m,i}^v} e^{x_3^v} \sin(x_1^v) \left(\left(\frac{\partial u_m^v}{\partial \mathbf{n}^v} \right)_{A^v} \left(\frac{\partial u_m^v}{\partial \boldsymbol{\nu}^v} \right)_{A^v} - \left(\frac{\partial u_p^v}{\partial \mathbf{n}^v} \right)_{A^v} \left(\frac{\partial u_p^v}{\partial \boldsymbol{\nu}^v} \right)_{A^v} \right) ds^v \right| \\
& \leq C_\epsilon (\ln W)^2 \sum_{k=1}^3 R_{m,i}^v \| [u_{x_k}] \|_{1/2, \tilde{\Gamma}_{m,i}^v}^2 \\
& + \epsilon \sum_{1 \leq |\alpha| \leq 2} \left(\| e^{x_3^v/2} D_{x^v}^\alpha u_m^v \|_{0, \tilde{\Omega}_m^v}^2 + \| e^{x_3^v/2} D_{x^v}^\alpha u_p^v \|_{0, \tilde{\Omega}_p^v}^2 \right). \tag{3.97}
\end{aligned}$$

Here $R_{m,i}^v = \sup_{x^v \in \tilde{\Gamma}_{m,i}^v} (e^{x_3^v})$.

If $\mu(\tilde{\Gamma}_{m,i}^v) = \infty$ then the integral in left hand side of (3.97) is zero.

Lemma 3.4.6. *Let Ω_m^v and Ω_p^v be elements in the vertex neighbourhood Ω^v of Ω and $\Gamma_{m,i}^v$ be a face of Ω_m^v and $\Gamma_{p,j}^v$ be a face of Ω_p^v such that $\Gamma_{m,i}^v = \Gamma_{p,j}^v$. Then for any $\epsilon > 0$ there exists a constant C_ϵ such that for W large enough*

$$\begin{aligned}
& \left| \sum_{l=1}^2 \left(\int_{\Gamma_{m,i}^v} e^{x_3^v} \sin(x_1^v) \left(\left(\frac{\partial u_m^v}{\partial \boldsymbol{\tau}_l^v} \right)_{A^v} \frac{\partial}{\partial s_l^v} \left(\left(\frac{\partial u_m^v}{\partial \boldsymbol{\nu}^v} \right)_{A^v} \right) d\sigma^v \right. \right. \right. \\
& \quad \left. \left. - \int_{\Gamma_{p,j}^v} \left(\frac{\partial u_p^v}{\partial \boldsymbol{\tau}_l^v} \right)_{A^v} \frac{\partial}{\partial s_l^v} \left(\left(\frac{\partial u_p^v}{\partial \boldsymbol{\nu}^v} \right)_{A^v} \right) d\sigma^v \right) \right| \\
& \leq C_\epsilon (\ln W)^2 \sum_{k=1}^3 R_{m,i}^v \| [u_{x_k}] \|_{1/2, \tilde{\Gamma}_{m,i}^v}^2 \\
& + \epsilon \sum_{1 \leq |\alpha| \leq 2} \left(\| e^{x_3^v/2} D_{x^v}^\alpha u_m^v \|_{0, \tilde{\Omega}_m^v}^2 + \| e^{x_3^v/2} D_{x^v}^\alpha u_p^v \|_{0, \tilde{\Omega}_p^v}^2 \right). \tag{3.98}
\end{aligned}$$

If $\mu(\tilde{\Gamma}_{m,i}^v) = \infty$ then the integral in left hand side of (3.98) is zero.

3.4.4 Estimates for terms in the interior of Ω^{v-e}

Lemma 3.4.7. *Let Ω_m^{v-e} and Ω_p^{v-e} be elements in the vertex-edge neighbourhood Ω^{v-e} of Ω and $\Gamma_{m,i}^{v-e}$ be a face of Ω_m^{v-e} and $\Gamma_{p,j}^{v-e}$ be a face of Ω_p^{v-e} such that $\Gamma_{m,i}^{v-e} = \Gamma_{p,j}^{v-e}$. Then for*

any $\epsilon > 0$ there exists a constant C_ϵ such that for W large enough

$$\begin{aligned}
& \left| \oint_{\partial \tilde{\Gamma}_{m,i}^{v-e}} e^{x_3^{v-e}} \left(\left(\frac{\partial u_m^{v-e}}{\partial \mathbf{n}^{v-e}} \right)_{A^{v-e}} \left(\frac{\partial u_m^{v-e}}{\partial \boldsymbol{\nu}^{v-e}} \right)_{A^{v-e}} \right. \right. \\
& \quad \left. \left. - \left(\frac{\partial u_p^{v-e}}{\partial \mathbf{n}^{v-e}} \right)_{A^{v-e}} \left(\frac{\partial u_p^{v-e}}{\partial \boldsymbol{\nu}^{v-e}} \right)_{A^{v-e}} \right) ds^{v-e} \right| \\
& \leq C_\epsilon (\ln W)^2 \left(||| [u_{x_1}^{v-e}] |||_{\tilde{\Gamma}_{m,i}^{v-e}}^2 + ||| [u_{x_2}^{v-e}] |||_{\tilde{\Gamma}_{m,i}^{v-e}}^2 \right. \\
& \quad \left. + ||| E_{m,i}^{v-e}[u_{x_3}^{v-e}] |||_{\tilde{\Gamma}_{m,i}^{v-e}}^2 \right) + \epsilon \sum_{k=m,p} \left(\int_{\tilde{\Omega}_k^{v-e}} \left(\sum_{i,j=1,2} \left(\frac{\partial^2 u_k^{v-e}}{\partial x_i^{v-e} \partial x_j^{v-e}} \right)^2 \right. \right. \\
& \quad \left. \left. + \sin^2 \phi \sum_{i=1}^2 \left(\frac{\partial^2 u_k^{v-e}}{\partial x_i^{v-e} \partial x_3^{v-e}} \right)^2 + \sin^4 \phi \left(\frac{\partial^2 u_k^{v-e}}{(\partial x_3^{v-e})^2} \right)^2 + \sum_{i=1}^2 \left(\frac{\partial u_k^{v-e}}{\partial x_i^{v-e}} \right)^2 \right. \right. \\
& \quad \left. \left. + \sin^2 \phi \left(\frac{\partial u_k^{v-e}}{\partial x_3^{v-e}} \right)^2 \right) e^{x_3^{v-e}} dx^{v-e} \right). \tag{3.99a}
\end{aligned}$$

Here C_ϵ is a constant which depend on ϵ but is uniform for all $\tilde{\Gamma}_{m,i}^{v-e} \subseteq \tilde{\Omega}^{v-e}$, and $E_{m,i}^{v-e} =$

$$\sup_{x^{v-e} \in \tilde{\Gamma}_{m,i}^{v-e}} (\sin \phi).$$

If $\mu(\tilde{\Gamma}_{m,i}^{v-e}) = \infty$ then for any $\epsilon > 0$

$$\begin{aligned}
& \left| \oint_{\partial \tilde{\Gamma}_{m,i}^{v-e}} e^{x_3^{v-e}} \left(\left(\frac{\partial u_m^{v-e}}{\partial \mathbf{n}^{v-e}} \right)_{A^{v-e}} \left(\frac{\partial u_m^{v-e}}{\partial \boldsymbol{\nu}^{v-e}} \right)_{A^{v-e}} \right. \right. \\
& \quad \left. \left. - \left(\frac{\partial u_p^{v-e}}{\partial \mathbf{n}^{v-e}} \right)_{A^{v-e}} \left(\frac{\partial u_p^{v-e}}{\partial \boldsymbol{\nu}^{v-e}} \right)_{A^{v-e}} \right) ds^{v-e} \right| \\
& \leq \epsilon \left(\sum_{k=m,p} \int_{\tilde{\Omega}_k^{v-e}} (u_k^{v-e})^2 e^{x_3^{v-e}} w^{v-e}(x_1^{v-e}) dx^{v-e} \right) \tag{3.99b}
\end{aligned}$$

provided $W = O(e^{N^\alpha})$ with $\alpha < 1/2$.

Lemma 3.4.8. Let Ω_m^{v-e} and Ω_p^{v-e} be elements in the edge neighbourhood Ω^{v-e} of Ω and $\Gamma_{m,i}^{v-e}$ be a face of Ω_m^{v-e} and $\Gamma_{p,j}^{v-e}$ be a face of Ω_p^{v-e} such that $\Gamma_{m,i}^{v-e} = \Gamma_{p,j}^{v-e}$. Then for any

$\epsilon > 0$ there exists a constant C_ϵ such that for W large enough

$$\begin{aligned}
& \left| \int_{\tilde{\Gamma}_{m,i}^{v-e}} e^{x_3^{v-e}} \left(\sum_{l=1}^2 \left(\left(\frac{\partial u_m^{v-e}}{\partial \tau_l^{v-e}} \right)_{A^{v-e}} \frac{\partial}{\partial s_l^{v-e}} \left(\left(\frac{\partial u_m^{v-e}}{\partial \nu^{v-e}} \right)_{A^{v-e}} \right) \right. \right. \right. \\
& \quad \left. \left. \left. - \left(\frac{\partial u_p^{v-e}}{\partial \tau_l^{v-e}} \right)_{A^{v-e}} \frac{\partial}{\partial s_l^{v-e}} \left(\left(\frac{\partial u_p^{v-e}}{\partial \nu^{v-e}} \right)_{A^{v-e}} \right) \right) \right) d\sigma^{v-e} \right| \\
& \leq C_\epsilon (\ln W)^2 \left(||| [u_{x_1}^{v-e}] |||_{\tilde{\Gamma}_{m,i}^{v-e}}^2 + ||| [u_{x_2}^{v-e}] |||_{\tilde{\Gamma}_{m,i}^{v-e}}^2 \right. \\
& \quad \left. + ||| E_{m,i}^{v-e}[u_{x_3}^{v-e}] |||_{\tilde{\Gamma}_{m,i}^{v-e}}^2 \right) + \epsilon \sum_{k=m,p} \left(\int_{\tilde{\Omega}_k^{v-e}} \left(\sum_{i,j=1,2} \left(\frac{\partial^2 u_k^{v-e}}{\partial x_i^{v-e} \partial x_j^{v-e}} \right)^2 \right. \right. \\
& \quad \left. \left. + \sin^2 \phi \sum_{i=1}^2 \left(\frac{\partial^2 u_k^{v-e}}{\partial x_i^{v-e} \partial x_3^{v-e}} \right)^2 + \sin^4 \phi \left(\frac{\partial^2 u_k^{v-e}}{(\partial x_3^{v-e})^2} \right)^2 + \sum_{i=1}^2 \left(\frac{\partial u_k^{v-e}}{\partial x_i^{v-e}} \right)^2 \right. \right. \\
& \quad \left. \left. + \sin^2 \phi \left(\frac{\partial u_k^{v-e}}{\partial x_3^{v-e}} \right)^2 \right) e^{x_3^{v-e}} dx^{v-e} \right). \tag{3.100a}
\end{aligned}$$

If $\mu(\tilde{\Gamma}_{m,i}^{v-e}) = \infty$ then for any $\epsilon > 0$

$$\begin{aligned}
& \left| \int_{\tilde{\Gamma}_{m,i}^{v-e}} e^{x_3^{v-e}} \left(\sum_{l=1}^2 \left(\left(\frac{\partial u_m^{v-e}}{\partial \tau_l^{v-e}} \right)_{A^{v-e}} \frac{\partial}{\partial s_l^{v-e}} \left(\left(\frac{\partial u_m^{v-e}}{\partial \nu^{v-e}} \right)_{A^{v-e}} \right) \right. \right. \right. \\
& \quad \left. \left. \left. - \left(\frac{\partial u_p^{v-e}}{\partial \tau_l^{v-e}} \right)_{A^{v-e}} \frac{\partial}{\partial s_l^{v-e}} \left(\left(\frac{\partial u_p^{v-e}}{\partial \nu^{v-e}} \right)_{A^{v-e}} \right) \right) \right) d\sigma^{v-e} \right| \\
& \leq \epsilon \left(\sum_{k=m,p} \int_{\tilde{\Omega}_k^{v-e}} (u_k^{v-e})^2 e^{x_3^{v-e}} w^{v-e}(x_1^{v-e}) dx^{v-e} \right) \tag{3.100b}
\end{aligned}$$

provided $W = O(e^{N^\alpha})$ with $\alpha < 1/2$.

3.5 Estimates for Terms on the Boundary

3.5.1 Estimates for terms on the boundary of Ω^r

To simplify the presentation we assume the face constituting part of the boundary of Ω lies on the $x_2 - x_3$ plane. The contributions from the boundary which have to be estimated will then consist of terms from the regular region, the vertex region, the vertex-edge region and the edge region as shown in Figure 3.2. We first examine how to estimate the terms on the boundary of Ω for the regular region, terms from the other regions can be estimated similarly.

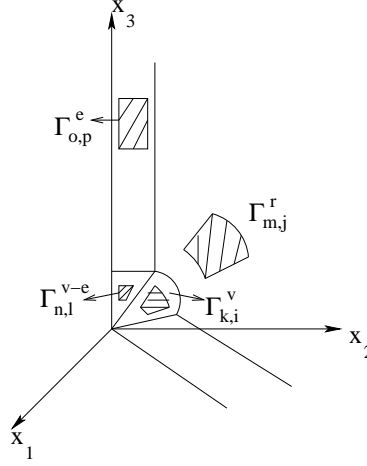


Figure 3.2: Boundary terms.

Lemma 3.5.1. *Let $\Gamma_{m,j}^r$ be part of the boundary of the element Ω_m^r which lies on the $x_2 - x_3$ axis. Define the contributions from $\Gamma_{m,j}^r$ by*

$$\begin{aligned} (BT)_{m,j}^r &= \rho_v^2 \sin^2(\phi_v) \left(- \oint_{\partial \Gamma_{m,j}^r} \left(\frac{\partial u}{\partial \mathbf{n}} \right)_A \left(\frac{\partial u}{\partial \boldsymbol{\nu}} \right)_A ds \right. \\ &\quad \left. + 2 \int_{\Gamma_{m,j}^r} \sum_{j=1}^2 \left(\frac{\partial u}{\partial \boldsymbol{\tau}_j} \right)_A \frac{\partial}{\partial s_j} \left(\left(\frac{\partial u}{\partial \boldsymbol{\nu}} \right)_A \right) d\sigma \right). \end{aligned} \quad (3.101)$$

If Dirichlet boundary conditions are imposed on $\Gamma_{m,j}^r$ then for any $\epsilon > 0$ there exist constants C_ϵ and K_ϵ such that

$$\begin{aligned} |(BT)_{m,j}^r| &\leq C_\epsilon (\ln W)^2 \|u_m^r\|_{3/2, \Gamma_{m,j}^r}^2 + K_\epsilon \sum_{|\alpha|=1} \|D_x^\alpha u_m^r\|_{0, \Omega_m^r}^2 \\ &\quad + \epsilon \sum_{|\alpha|=2} \|D_x^\alpha u_m^r\|_{0, \Omega_m^r}^2. \end{aligned} \quad (3.102)$$

If Neumann boundary conditions are imposed on $\Gamma_{m,j}^r$ then for any $\epsilon > 0$ there exists a constant C_ϵ such that

$$|(BT)_{m,j}^r| \leq C_\epsilon (\ln W)^2 \left\| \left(\frac{\partial u_m^r}{\partial \boldsymbol{\nu}} \right)_A \right\|_{1/2, \Gamma_{m,j}^r}^2 + \epsilon \sum_{1 \leq |\alpha| \leq 2} \|D_x^\alpha u_m^r\|_{2, \Omega_m^r}^2. \quad (3.103)$$

Proof. The proof is provided in Appendix D.5. □

3.5.2 Estimates for terms on the boundary of Ω^e

Lemma 3.5.2. *Let $\Gamma_{m,j}^e$ be part of the boundary of the element Ω_m^e which lies on the $x_2 - x_3$ axis. Define the contributions from $\Gamma_{m,j}^e$ by*

$$\begin{aligned} (BT)_{m,j}^e = & - \oint_{\partial \tilde{\Gamma}_{m,j}^e} \left(\frac{\partial u}{\partial \mathbf{n}^e} \right)_{A^e} \left(\frac{\partial u}{\partial \boldsymbol{\nu}^e} \right)_{A^e} ds^e \\ & - 2 \int_{\tilde{\Gamma}_{m,j}^e} \sum_{l=1}^2 \left(\frac{\partial u}{\partial \boldsymbol{\tau}_l^e} \right)_{A^e} \frac{\partial}{\partial s_l^e} \left(\left(\frac{\partial u}{\partial \boldsymbol{\nu}^e} \right)_{A^e} \right) d\sigma^e. \end{aligned} \quad (3.104)$$

If Dirichlet boundary conditions are imposed on $\Gamma_{m,j}^e$ and $\mu(\tilde{\Gamma}_{m,j}^e) < \infty$ then for any $\epsilon > 0$ there exists constants C_ϵ, K_ϵ such that for W large enough

$$\begin{aligned} |(BT)_{m,j}^e| \leq & C_\epsilon (\ln W)^2 \left(\|u_m^e\|_{0,\tilde{\Gamma}_{m,j}^e}^2 + \left\| \left(\frac{\partial u_m^e}{\partial x_1^e} \right) \right\|_{\tilde{\Gamma}_{m,j}^e}^2 + \left\| G_{m,j}^e \left(\frac{\partial u_m^e}{\partial x_3^e} \right) \right\|_{\tilde{\Gamma}_{m,j}^e}^2 \right) \\ & + K_\epsilon \int_{\tilde{\Omega}_m^e} \left(\sum_{i=1}^2 \left(\frac{\partial u_m^e}{\partial x_i^e} \right)^2 + e^{2\tau} \left(\frac{\partial u_m^e}{\partial x_3^e} \right)^2 \right) dx^e \\ & + \epsilon \int_{\tilde{\Omega}_m^e} \left(\sum_{i,j=1,2} \left(\frac{\partial^2 u_m^e}{\partial x_i^e \partial x_j^e} \right)^2 + e^{2\tau} \sum_{i=1}^2 \left(\frac{\partial^2 u_m^e}{\partial x_i^e \partial x_3^e} \right)^2 + e^{4\tau} \left(\frac{\partial^2 u_m^e}{(\partial x_3^e)^2} \right)^2 \right) dx^e \end{aligned} \quad (3.105)$$

If Neumann boundary conditions are imposed on $\Gamma_{m,j}^e$ and $\mu(\tilde{\Gamma}_{m,j}^e) < \infty$ then for any $\epsilon > 0$ there exists a constant C_ϵ such that

$$\begin{aligned} |(BT)_{m,j}^e| \leq & C_\epsilon (\ln W)^2 \left\| \left(\frac{\partial u}{\partial \boldsymbol{\nu}^e} \right)_{A^e} \right\|_{\tilde{\Gamma}_{m,j}^e}^2 + \epsilon \left(\int_{\tilde{\Omega}_m^e} \left(\sum_{i,j=1}^2 \left(\frac{\partial^2 u_m^e}{\partial x_i^e \partial x_j^e} \right)^2 \right. \right. \\ & + e^{2\tau} \sum_{i=1}^2 \left(\frac{\partial^2 u_m^e}{\partial x_i^e \partial x_3^e} \right)^2 + e^{4\tau} \left(\frac{\partial^2 u_m^e}{(\partial x_3^e)^2} \right)^2 + \sum_{i=1}^2 \left(\frac{\partial u_m^e}{\partial x_i^e} \right)^2 \\ & \left. \left. + e^{2\tau} \left(\frac{\partial u_m^e}{\partial x_3^e} \right)^2 \right) dx^e \right). \end{aligned} \quad (3.106)$$

If $\mu(\tilde{\Gamma}_{m,j}^e) = \infty$ then for any $\epsilon > 0$ for N, W large enough

$$|(BT)_{m,j}^e| \leq \epsilon \int_{\tilde{\Omega}_m^e} (u_m^e)^2 w^e(x_1^e) dx^e \quad (3.107)$$

provided $W = O(e^{N^\alpha})$ for $\alpha < 1/2$.

Proof. The proof is provided in Appendix D.6. □

We now state estimates for terms on the boundary of vertex neighbourhoods and vertex-edge neighbourhoods.

3.5.3 Estimates for terms on the boundary of Ω^v

Lemma 3.5.3. *Let $\Gamma_{m,j}^v$ be part of the boundary of the element Ω_m^v which lies on the $x_2 - x_3$ axis. Define the contributions from $\Gamma_{m,j}^v$ by*

$$\begin{aligned} (BT)_{m,j}^v &= \sin^2(\phi_v) \left(- \oint_{\partial \tilde{\Gamma}_{m,j}^v} e^{x_3^v} \sin(x_1^v) \left(\frac{\partial u}{\partial \mathbf{n}^v} \right)_{A^v} \left(\frac{\partial u}{\partial \boldsymbol{\nu}^v} \right)_{A^v} ds^v \right. \\ &\quad \left. - 2 \int_{\tilde{\Gamma}_{m,j}^v} e^{x_3^v} \sin(x_1^v) \sum_{l=1}^2 \left(\frac{\partial u}{\partial \boldsymbol{\tau}_l^v} \right)_{A^v} \frac{\partial}{\partial s_l^v} \left(\left(\frac{\partial u}{\partial \boldsymbol{\nu}^v} \right)_{A^v} \right) d\sigma^v \right). \end{aligned} \quad (3.108)$$

If Dirichlet boundary conditions are imposed on $\Gamma_{m,j}^v$ and $\mu(\tilde{\Gamma}_{m,j}^v) < \infty$ then for any $\epsilon > 0$ there exists constants C_ϵ and K_ϵ such that

$$\begin{aligned} |(BT)_{m,j}^v| &\leq C_\epsilon (\ln W)^2 R_{m,j}^v \|u_m^v\|_{3/2, \tilde{\Gamma}_{m,j}^v}^2 + K_\epsilon \sum_{|\alpha|=1} \|e^{x_3^v/2} D_{x^v}^\alpha u_m^v\|_{0, \tilde{\Omega}_m^v}^2 \\ &\quad + \epsilon \sum_{|\alpha|=2} \|e^{x_3^v/2} D_{x^v}^\alpha u_m^v\|_{0, \tilde{\Omega}_m^v}^2. \end{aligned} \quad (3.109)$$

If Neumann boundary conditions are imposed on $\Gamma_{m,j}^v$ then

$$\begin{aligned} |(BT)_{m,j}^v| &\leq C_\epsilon (\ln W)^2 R_{m,j}^v \left\| \left(\frac{\partial u_m^v}{\partial \boldsymbol{\nu}^v} \right)_{A^v} \right\|_{1/2, \tilde{\Gamma}_{m,j}^v}^2 \\ &\quad + \epsilon \sum_{1 \leq |\alpha| \leq 2} \|e^{x_3^v/2} D_{x^v}^\alpha u_m^v\|_{0, \tilde{\Omega}_m^v}^2. \end{aligned} \quad (3.110)$$

If $\mu(\tilde{\Gamma}_{m,j}^v) = \infty$ then $(BT)_{m,j}^v = 0$.

3.5.4 Estimates for terms on the boundary of Ω^{v-e}

Lemma 3.5.4. *Let $\Gamma_{m,j}^{v-e}$ be part of the boundary of the element Ω_m^{v-e} which lies on the $x_2 - x_3$ axis. Define the contributions from $\Gamma_{m,j}^{v-e}$ by*

$$\begin{aligned} (BT)_{m,j}^{v-e} &= - \oint_{\partial \tilde{\Gamma}_{m,j}^{v-e}} e^{x_3^{v-e}} \left(\frac{\partial u}{\partial \mathbf{n}^{v-e}} \right)_{A^{v-e}} \left(\frac{\partial u}{\partial \boldsymbol{\nu}^{v-e}} \right)_{A^{v-e}} ds^{v-e} \\ &\quad - 2 \int_{\tilde{\Gamma}_{m,j}^{v-e}} e^{x_3^{v-e}} \sum_{l=1}^2 \left(\frac{\partial u}{\partial \boldsymbol{\tau}_l^{v-e}} \right)_{A^{v-e}} \frac{\partial}{\partial s_l^{v-e}} \left(\left(\frac{\partial u}{\partial \boldsymbol{\nu}^{v-e}} \right)_{A^{v-e}} \right) d\sigma^{v-e}. \end{aligned} \quad (3.111)$$

If Dirichlet boundary conditions are imposed on $\Gamma_{m,j}^{v-e}$ and $\mu(\tilde{\Gamma}_{m,j}^{v-e}) < \infty$ then for any $\epsilon > 0$ there exists constants C_ϵ and K_ϵ such that

$$\begin{aligned}
|(BT)_{m,j}^{v-e}| &\leq C_\epsilon (\ln W)^2 \left(\|u_m^{v-e}\|_{0,\tilde{\Gamma}_{m,i}^{v-e}}^2 + \left\| \left(\frac{\partial u_m^{v-e}}{\partial x_1^{v-e}} \right) \right\|_{\tilde{\Gamma}_{m,j}^{v-e}}^2 + \left\| E_{m,j}^{v-e} \left(\frac{\partial u_m^{v-e}}{\partial x_3^{v-e}} \right) \right\|_{\tilde{\Gamma}_{m,j}^{v-e}}^2 \right) \\
&\quad + K_\epsilon \int_{\tilde{\Omega}_m^{v-e}} \left(\sum_{i=1}^2 \left(\frac{\partial u_m^{v-e}}{\partial x_i^{v-e}} \right)^2 + \sin^2 \phi \left(\frac{\partial u_m^{v-e}}{\partial x_3^{v-e}} \right)^2 \right) e^{x_3^{v-e}} dx^{v-e} \\
&\quad + \epsilon \int_{\tilde{\Omega}_m^{v-e}} \left(\sum_{i,j=1,2} \left(\frac{\partial^2 u_m^{v-e}}{\partial x_i^{v-e} \partial x_j^{v-e}} \right)^2 + \sin^2 \phi \sum_{i=1}^2 \left(\frac{\partial^2 u_m^{v-e}}{\partial x_i^{v-e} \partial x_3^{v-e}} \right)^2 \right. \\
&\quad \left. + \sin^4 \phi \left(\frac{\partial^2 u_m^{v-e}}{(\partial x_3^{v-e})^2} \right)^2 \right) e^{x_3^{v-e}} dx^{v-e}. \tag{3.112}
\end{aligned}$$

If Neumann boundary conditions are imposed on $\Gamma_{m,j}^{v-e}$ and $\mu(\tilde{\Gamma}_{m,j}^{v-e}) < \infty$ then for any $\epsilon > 0$ there exists a constant C_ϵ such that

$$\begin{aligned}
|(BT)_{m,j}^{v-e}| &\leq C_\epsilon (\ln W)^2 \left\| \left(\frac{\partial u}{\partial \nu^{v-e}} \right)_{A^{v-e}} \right\|_{\tilde{\Gamma}_{m,j}^{v-e}}^2 + \epsilon \left(\int_{\tilde{\Omega}_m^{v-e}} \left(\sum_{i,j=1}^2 \left(\frac{\partial^2 u_m^{v-e}}{\partial x_i^{v-e} \partial x_j^{v-e}} \right)^2 \right. \right. \\
&\quad \left. \left. + \sin^2 \phi \sum_{i=1}^2 \left(\frac{\partial^2 u_m^{v-e}}{\partial x_i^{v-e} \partial x_3^{v-e}} \right)^2 + \sin^4 \phi \left(\frac{\partial^2 u_m^{v-e}}{(\partial x_3^{v-e})^2} \right)^2 + \sum_{i=1}^2 \left(\frac{\partial u_m^{v-e}}{\partial x_i^{v-e}} \right)^2 \right. \right. \\
&\quad \left. \left. + \sin^2 \phi \left(\frac{\partial u_m^{v-e}}{\partial x_3^{v-e}} \right)^2 \right) e^{x_3^{v-e}} dx^{v-e} \right). \tag{3.113}
\end{aligned}$$

If $\mu(\tilde{\Gamma}_{m,j}^{v-e}) = \infty$ then for any $\epsilon > 0$ for N, W large enough

$$|(BT)_{m,j}^{v-e}| \leq \epsilon \int_{\tilde{\Omega}_m^{v-e}} (u_m^{v-e})^2 e^{x_3^{v-e}} w^{v-e}(x_1^{v-e}) dx^{v-e}$$

provided $W = O(e^{N^\alpha})$ for $\alpha < 1/2$.

3.6 Proof of the Stability Theorem

We are now in a position to prove the stability estimates stated in Theorems 2.3.1, 2.3.2 and 2.3.3. We recall them again.

Theorem 2.3.1. *Consider the elliptic boundary value problem (2.1). Suppose the boundary conditions are Dirichlet. Then*

$$\mathcal{U}^{N,W}(\{\mathcal{F}_u\}) \leq C(\ln W)^2 \mathcal{V}^{N,W}(\{\mathcal{F}_u\}).$$

Theorem 2.3.2. *If the boundary conditions for the elliptic boundary value problem (2.1) are mixed then*

$$\mathcal{U}^{N,W}(\{\mathcal{F}_u\}) \leq CN^4 \mathcal{V}^{N,W}(\{\mathcal{F}_u\})$$

provided $W = O(e^{N^\alpha})$ for $\alpha < 1/2$.

Theorem 2.3.3. *If the boundary conditions are mixed and the spectral element functions $(\{\mathcal{F}_u\})$ are conforming on the wirebasket WB and vanish on WB then*

$$\mathcal{U}^{N,W}(\{\mathcal{F}_u\}) \leq C(\ln W)^2 \mathcal{V}^{N,W}(\{\mathcal{F}_u\})$$

provided $W = O(e^{N^\alpha})$ for $\alpha < 1/2$.

Proof. Define

$$\begin{aligned} \mathcal{U}_{(2)}^{N,W}(\{\mathcal{F}_u\}) &= \sum_{l=1}^{N_r} \int_{\Omega_l^r} \sum_{i,j=1}^3 \left(\frac{\partial^2 u_l^r}{\partial x_i \partial x_j} \right)^2 dx \\ &+ \sum_{v \in \mathcal{V}} \left(\sum_{l=1, \mu(\tilde{\Omega}_l^v) < \infty}^{N_v} \int_{\tilde{\Omega}_l^v} e^{x_3^v} \sum_{i,j=1}^3 \left(\frac{\partial^2 u_l^v}{\partial x_i^v \partial x_j^v} \right)^2 dx^v \right) \\ &+ \sum_{v-e \in \mathcal{V}-E} \left(\sum_{l=1, \mu(\tilde{\Omega}_l^{v-e}) < \infty}^{N_{v-e}} \int_{\tilde{\Omega}_l^{v-e}} e^{x_3^{v-e}} \left(\sum_{i,j=1,2} \left(\frac{\partial^2 u_l^{v-e}}{\partial x_i^{v-e} \partial x_j^{v-e}} \right)^2 \right. \right. \\ &+ \sin^2 \phi \sum_{i=1}^2 \left(\frac{\partial^2 u_l^{v-e}}{\partial x_i^{v-e} \partial x_3^{v-e}} \right)^2 + \sin^4 \phi \left(\frac{\partial^2 u_l^{v-e}}{(\partial x_3^{v-e})^2} \right)^2 \left. \right) dx^{v-e} \\ &+ \sum_{e \in \mathcal{E}} \left(\int_{\tilde{\Omega}_l^e} \left(\sum_{i,j=1,2} \left(\frac{\partial^2 u_l^e}{\partial x_i^e \partial x_j^e} \right)^2 + e^{2\tau} \sum_{i=1}^2 \left(\frac{\partial^2 u_l^e}{\partial x_i^e \partial x_3^e} \right)^2 \right. \right. \\ &\left. \left. + e^{4\tau} \left(\frac{\partial^2 u_l^e}{(\partial x_3^e)^2} \right)^2 \right) dx^e \right). \end{aligned}$$

Then combining the results in Sections 3.1, 3.2, 3.3 and 3.4 we obtain that for any $\epsilon > 0$ there exist constants C_ϵ and K_ϵ such that

$$\begin{aligned} \mathcal{U}_{(2)}^{N,W}(\{\mathcal{F}_u\}) &\leq C_\epsilon (\ln W)^2 \mathcal{V}^{N,W}(\{\mathcal{F}_u\}) + \epsilon \mathcal{U}_{(2)}^{N,W}(\{\mathcal{F}_u\}) \\ &+ K_\epsilon \mathcal{U}_{(1)}^{N,W}(\{\mathcal{F}_u\}). \end{aligned} \tag{3.114}$$

Here $\mathcal{U}_{(1)}^{N,W}(\{\mathcal{F}_u\})$ is as defined in (3.90). Hence choosing ϵ small enough we obtain

$$\mathcal{U}_{(2)}^{N,W}(\{\mathcal{F}_u\}) \leq 2 \left(C_\epsilon (\ln W)^2 \mathcal{V}^{N,W}(\{\mathcal{F}_u\}) + K_\epsilon \mathcal{U}_{(1)}^{N,W}(\{\mathcal{F}_u\}) \right). \tag{3.115}$$

At the same time using Theorem 3.3.1 we have

$$\mathcal{U}_{(1)}^{N,W}(\{\mathcal{F}_u\}) \leq K_{N,W} \mathcal{V}^{N,W}(\{\mathcal{F}_u\}) . \quad (3.116)$$

Now

$$\mathcal{U}^{N,W}(\{\mathcal{F}_u\}) = \mathcal{U}_{(1)}^{N,W}(\{\mathcal{F}_u\}) + \mathcal{U}_{(2)}^{N,W}(\{\mathcal{F}_u\}) . \quad (3.117)$$

Combining (3.115), (3.116) and (3.117) the result follows. \square

Chapter 4

The Numerical Scheme and Error Estimates

4.1 Introduction

In Chapters 2 and 3 we have described a method for solving three dimensional elliptic boundary value problems on non-smooth domains using $h - p$ spectral element methods.

In this chapter we provide the numerical scheme based on the stability estimates of Chapters 2 and 3. We shall define a functional which is closely related to the quadratic forms defined in Chapter 2 in the regular region and in the various neighbourhoods of vertices, edges and vertex-edges. We seek a solution which minimizes this functional.

The functional which we minimize is the sum of a weighted squared norm of the residuals in the partial differential equations and the squared norm of the residuals in the boundary conditions in fractional Sobolev spaces and the sum of the squares of the jumps in the function and its derivatives across inter-element boundaries in fractional Sobolev norms. The Sobolev spaces in vertex-edge and edge neighbourhoods are anisotropic and become singular at the corners and edges.

In section 4.3 we obtain error estimates and show that the error is exponentially small in terms of the number of degrees of freedom and number of layers in the geometric mesh.

4.2 The Numerical Scheme

In Chapter 2, we had divided the polyhedral domain Ω into a regular region Ω^r , a set of vertex neighborhoods Ω^v , a set of edge neighborhoods Ω^e and a set of vertex-edge neighborhoods Ω^{v-e} . We had further divided each of these sub domains into still smaller elements as curvilinear hexahedrons, tetrahedrons and prisms and by virtue of the fact that a tetrahedron can be split into four hexahedrons and a prism can be split into three hexahedrons we can assume that all our elements are hexahedrons to keep the exposition simple (and to keep the programming simple).

In Chapter 2, we had introduced a spectral element representation of the function u on each of these elements in various parts of the domain Ω . To formulate the numerical scheme we will define a functional $\mathcal{R}^{N,W}(\{\mathcal{F}_u\})$, closely related to the quadratic form $\mathcal{V}^{N,W}(\{\mathcal{F}_u\})$ as follows:

$$\begin{aligned} \mathcal{R}^{N,W}(\{\mathcal{F}_u\}) &= \mathcal{R}_{regular}^{N,W}(\{\mathcal{F}_u\}) + \mathcal{R}_{vertices}^{N,W}(\{\mathcal{F}_u\}) + \mathcal{R}_{vertex-edges}^{N,W}(\{\mathcal{F}_u\}) \\ &\quad + \mathcal{R}_{edges}^{N,W}(\{\mathcal{F}_u\}). \end{aligned} \quad (4.1)$$

Let us first consider the regular region Ω^r of Ω and define the functional $\mathcal{R}_{regular}^{N,W}(\{\mathcal{F}_u\})$. Ω^r is divided into N_r curvilinear hexahedrons $\Omega_l^r, l = 1, 2, \dots, N_r$ and we map each of these Ω_l^r onto the master cube

$$Q = (-1, 1)^3 = \{\lambda = (\lambda_1, \lambda_2, \lambda_3) \mid -1 \leq \lambda_i \leq 1, 1 \leq i \leq 3\}$$

using an analytic map M_l^r having an analytic inverse.

We now define a non-conforming spectral element representation on each of these elements as follows:

$$u_l^r(\lambda) = \sum_{i=0}^W \sum_{j=0}^W \sum_{k=0}^W \alpha_{i,j,k} \lambda_1^i \lambda_2^j \lambda_3^k.$$

Let $\lambda = (\lambda_1, \lambda_2, \lambda_3)$ and let $f_l^r(\lambda) = f(M_l^r(\lambda_1, \lambda_2, \lambda_3))$ where $\lambda \in Q$ for $l = 1, 2, \dots, N_r$ and let $J_l^r(\lambda)$ denote the Jacobian of the mapping M_l^r . Define

$$F_l^r(\lambda) = f_l^r(\lambda) \sqrt{J_l^r(\lambda)},$$

and

$$L_l^r u_l^r(\lambda) = L u_l^r(M_l^r(\lambda)) \sqrt{J_l^r(\lambda)}.$$

Now consider the boundary conditions $w = g_k$ on Γ_k for $k \in \mathcal{D} = \Gamma^{[0]}$ and $(\frac{\partial w}{\partial \nu})_A = h_k$ on Γ_k for $k \in \mathcal{N} = \Gamma^{[1]}$. Let $\Gamma_{i,k}^r = \Gamma_k \cap \partial\Omega_i^r$ be the image of the mapping M_i^r corresponding to $\lambda_1 = -1$. Let $g_{i,k}^r = g_k(M_i^r(-1, \lambda_2, \lambda_3))$ and $h_{i,k}^r = h_k(M_i^r(-1, \lambda_2, \lambda_3))$ where $-1 \leq \lambda_2, \lambda_3 \leq 1$.

We now define

$$\begin{aligned} \mathcal{R}_{regular}^{N,W}(\{\mathcal{F}_u\}) &= \sum_{l=1}^{N_r} \int_{Q=(M_l^r)^{-1}(\Omega_l^r)} |L_l^r u_l^r(\lambda) - F_l^r(\lambda)|^2 d\lambda \\ &+ \sum_{\Gamma_{l,i}^r \subseteq \bar{\Omega}^r \setminus \partial\Omega} \left(\| [u] \|_{0,\Gamma_{l,i}^r}^2 + \sum_{k=1}^3 \| [u_{x_k}] \|_{1/2,\Gamma_{l,i}^r}^2 \right) \\ &+ \sum_{\Gamma_{l,i}^r \subseteq \Gamma^{[0]}} \| u_l^r - g_{l,i}^r \|_{3/2,\Gamma_{l,i}^r}^2 \\ &+ \sum_{\Gamma_{l,i}^r \subseteq \Gamma^{[1]}} \left\| \left(\frac{\partial u_l^r}{\partial \nu} \right)_A - h_{l,i}^r \right\|_{1/2,\Gamma_{l,i}^r}^2. \end{aligned} \quad (4.2)$$

Let v be one of the vertices of Ω . Consider the vertex neighborhood Ω^v of the vertex $v \in \mathcal{V}$, the set of vertices (defined in Chapter 2). Ω^v is divided into N_v curvilinear hexahedrons $\Omega_l^v, l = 1, 2, \dots, N_v$. We define a non-conforming spectral element representation as follows: Let $\tilde{\Omega}_l^v$ be the image of Ω_l^v in x^v coordinates. Then there is an analytic map $M_l^v : Q \rightarrow \tilde{\Omega}_l^v$ having an analytic inverse. If $\tilde{\Omega}_l^v$ is a corner element of the form

$$\tilde{\Omega}_l^v = \{x^v : (\phi, \theta) \in S_j^v, -\infty < \chi < \ln(\rho_1^v)\}$$

then we define $u_l^v = h_v$, where h_v is a constant.

If $\tilde{\Omega}_l^v$ is of the form

$$\tilde{\Omega}_l^v = \{x^v : (\phi, \theta) \in S_j^v, \ln(\rho_i^v) < \chi < \ln(\rho_{i+1}^v)\}$$

we define

$$u_l^v(x^v) = \sum_{t=0}^{W_l} \sum_{s=0}^{W_l} \sum_{r=0}^{W_l} \beta_{r,s,t} \phi^r \theta^s \chi^t.$$

Here $1 \leq W_l \leq W$. Moreover as in [51], $W_l = [\mu_1 i]$ for all $1 \leq i \leq N$, where $\mu_1 > 0$ is a degree factor. Hereafter $[a]$ denotes the greatest positive integer $\leq a$.

Let $A_v = (x_1^v, x_2^v, x_3^v)$ denote one of the vertices of Ω . Let $F_l^v(x^v) = e^{5/2\chi} \sqrt{\sin \phi} f(x(x^v))$ for $x_l^v \in \tilde{\Omega}_l^v$, $1 \leq l \leq N_v$.

We now consider the boundary conditions $w = g_i$ on Γ_i for $i \in \mathcal{D} = \Gamma^{[0]}$ and $(\frac{\partial w}{\partial \boldsymbol{\nu}})_A = h_i$ on Γ_i for $i \in \mathcal{N} = \Gamma^{[1]}$. Let $\Gamma_{l,i}^v = \Gamma_i \cap \partial\Omega_l^v$ and suppose Ω_l^v is not a corner element. Moreover it is assumed that $\Gamma_{l,i}^v$ lies on the $x_2 - x_3$ plane for simplicity. Define

$$\begin{aligned} g_{l,i}^v(x^v) &= w = g_i(x(x^v)) \text{ for } \Gamma_{l,i}^v \subseteq \Gamma^{[0]}, \\ h_{l,i}^v(x^v) &= \left(\frac{\partial w}{\partial \boldsymbol{\nu}^v} \right)_{A^v} = \frac{e^\chi}{\sin \phi} h_i(x(x^v)) \text{ for } \Gamma_{l,i}^v \subseteq \Gamma^{[1]}. \end{aligned}$$

Let

$$R_{l,i}^v = \sup_{x^v \in \tilde{\Gamma}_{l,i}^v} (e^{x_3^v}).$$

We now define the functional

$$\begin{aligned} \mathcal{R}_v^{N,W}(\{\mathcal{F}_u\}) &= \sum_{l=1, \mu(\tilde{\Omega}_l^v) < \infty}^{N_v} \int_{\tilde{\Omega}_l^v} |L^v u_l^v(x^v) - F_l^v(x^v)|^2 dx^v \\ &+ \sum_{\substack{\Gamma_{l,i}^v \subseteq \partial\Omega^v \setminus \partial\Omega \\ \mu(\tilde{\Gamma}_{l,i}^v) < \infty}} \left(\left\| \sqrt{R_{l,i}^v} [u] \right\|_{0, \tilde{\Gamma}_{l,i}^v}^2 + \sum_{k=1}^3 \left\| \sqrt{R_{l,i}^v} [u_{x_k^v}] \right\|_{1/2, \tilde{\Gamma}_{l,i}^v}^2 \right) \\ &+ \sum_{\substack{\Gamma_{l,i}^v \subseteq \Gamma^{[0]}, \\ \mu(\tilde{\Gamma}_{l,i}^v) < \infty}} \left\| \sqrt{R_{l,i}^v} (u_l^v - g_{l,i}^v) \right\|_{3/2, \tilde{\Gamma}_{l,i}^v}^2 \\ &+ \sum_{\substack{\Gamma_{l,i}^v \subseteq \Gamma^{[1]}, \\ \mu(\tilde{\Gamma}_{l,i}^v) < \infty}} \left\| \sqrt{R_{l,i}^v} \left(\left(\frac{\partial u_l^v}{\partial \boldsymbol{\nu}^v} \right)_{A^v} - h_{l,i}^v \right) \right\|_{1/2, \tilde{\Gamma}_{l,i}^v}^2. \end{aligned} \quad (4.3)$$

The functional $\mathcal{R}_{vertices}^{N,W}(\{\mathcal{F}_u\})$ is then given by

$$\mathcal{R}_{vertices}^{N,W}(\{\mathcal{F}_u\}) = \sum_{v \in \mathcal{V}} \mathcal{R}_v^{N,W}(\{\mathcal{F}_u\}). \quad (4.4)$$

Next, we define $\mathcal{R}_{vertex-edges}^{N,W}(\{\mathcal{F}_u\})$. Let Ω^{v-e} denote the vertex-edge neighborhood of the vertex-edge $v-e \in \mathcal{V} - \mathcal{E}$. Ω^{v-e} is divided into N_{v-e} elements Ω_l^{v-e} , $l = 1, 2, \dots, N_{v-e}$. As in Chapter 2, let us define a non-conforming spectral element representation on each of these sub-domains as follows:

Let $\tilde{\Omega}_l^{v-e}$ be the image of Ω_l^{v-e} in x^{v-e} coordinates. If $\tilde{\Omega}_n^{v-e}$ is a corner element of the form

$$\tilde{\Omega}_n^{v-e} = \{x^{v-e} : \psi_i^{v-e} < \psi < \psi_{i+1}^{v-e}, \theta_j^{v-e} < \theta < \theta_{j+1}^{v-e}, -\infty < \zeta < \zeta_1^{v-e}\}$$

then on $\tilde{\Omega}_n^{v-e}$ we define

$$u_n^{v-e} = h_{v-e} = h_v.$$

Next, suppose $\tilde{\Omega}_p^{v-e}$ is a corner element of the form

$$\tilde{\Omega}_p^{v-e} = \{x^{v-e} : -\infty < \psi < \psi_1^{v-e}, \theta_j^{v-e} < \theta < \theta_{j+1}^{v-e}, \zeta_n^{v-e} < \zeta < \zeta_{n+1}^{v-e}\}$$

with $k \geq 1$. Then on $\tilde{\Omega}_p^{v-e}$ we define

$$u_p^{v-e}(x^{v-e}) = \sum_{l=0}^{W_p} \beta_l \zeta^l.$$

Here $1 \leq W_p \leq W$. Moreover $W_p = [\mu_2 n]$ for $1 \leq n \leq N$, where $\mu_2 > 0$ is a degree factor.

Finally, suppose $\tilde{\Omega}_q^{v-e}$ is of the form

$$\tilde{\Omega}_q^{v-e} = \{x^{v-e} : \psi_i^{v-e} < \psi < \psi_{i+1}^{v-e}, \theta_j^{v-e} < \theta < \theta_{j+1}^{v-e}, \zeta_n^{v-e} < \zeta < \zeta_{n+1}^{v-e}\}$$

with $i \geq 1, n \geq 1$. Then on $\tilde{\Omega}_q^{v-e}$ we define

$$u_q^{v-e}(x^{v-e}) = \sum_{r=0}^{W_q} \sum_{s=0}^{W_q} \sum_{t=0}^{V_q} \gamma_{r,s,t} \psi^r \theta^s \zeta^t.$$

Here $1 \leq W_q \leq W$ and $1 \leq V_q \leq W$. Moreover $W_q = [\mu_1 i], V_q = [\mu_2 n]$ for $1 \leq i, n \leq N$, where $\mu_1, \mu_2 > 0$ are degree factors [51].

Let $F_l^{v-e}(x^{v-e}) = e^{2x_1^{v-e}} e^{\frac{5}{2}x_3^{v-e}} f(x(x^{v-e}))$ for $x^{v-e} \in \tilde{\Omega}_l^{v-e}, 1 \leq l \leq N_{v-e}$.

We now consider the boundary conditions $w = g_k$ on Γ_k for $k \in \mathcal{D} = \Gamma^{[0]}$ and $(\frac{\partial w}{\partial \mathbf{v}})_A = h_k$ on Γ_k for $k \in \mathcal{N} = \Gamma^{[1]}$. Then $(\frac{\partial w}{\partial \mathbf{v}^{v-e}})_{A^{v-e}} = e^{x_3^{v-e}} e^{x_1^{v-e}} h_k(x(x^{v-e}))$. Let $\Gamma_{l,k}^{v-e} = \Gamma_k \cap \partial \Omega_l^{v-e}$ and suppose Ω_l^{v-e} is not a corner element. Moreover it is assumed that $\Gamma_{l,k}^{v-e}$ lies on the $x_2 - x_3$ plane for simplicity and $\mu(\tilde{\Gamma}_{l,k}^{v-e}) < \infty$. Define

$$\begin{aligned} g_{l,k}^{v-e}(x^{v-e}) &= w = g_k(x(x^{v-e})) \text{ for } \Gamma_{l,k}^{v-e} \subseteq \Gamma^{[0]}, \\ h_{l,k}^{v-e}(x^{v-e}) &= \left(\frac{\partial w}{\partial \mathbf{v}^{v-e}} \right)_{A^{v-e}} = e^{x_3^{v-e}} e^{x_1^{v-e}} h_k(x(x^{v-e})) \text{ for } \Gamma_{l,k}^{v-e} \subseteq \Gamma^{[1]}. \end{aligned}$$

We define the functional

$$\begin{aligned}
\mathcal{R}_{v-e}^{N,W}(\{\mathcal{F}_u\}) = & \sum_{l=1, \mu(\tilde{\Omega}_l^{v-e}) < \infty}^{N_{v-e}} \int_{\tilde{\Omega}_l^{v-e}} |L^{v-e} u_l^{v-e}(x^{v-e}) - F_l^{v-e}(x^{v-e})|^2 dx^{v-e} \\
& + \sum_{\substack{\Gamma_{l,k}^{v-e} \subseteq \tilde{\Omega}^{v-e} \setminus \partial\Omega, \\ \mu(\tilde{\Gamma}_{l,k}^{v-e}) < \infty}} \left(\left\| \sqrt{F_{l,k}^{v-e} G_{l,k}^{v-e}} [u] \right\|_{0, \tilde{\Gamma}_{l,k}^{v-e}}^2 + \left\| [u_{x_1^{v-e}}] \right\|_{\tilde{\Gamma}_{l,k}^{v-e}}^2 \right. \\
& \left. + \left\| [u_{x_2^{v-e}}] \right\|_{\tilde{\Gamma}_{l,k}^{v-e}}^2 + \left\| E_{l,k}^{v-e} [u_{x_3^{v-e}}] \right\|_{\tilde{\Gamma}_{l,k}^{v-e}}^2 \right) \\
& + \sum_{\substack{\Gamma_{l,k}^{v-e} \subseteq \Gamma^{[0]}, \\ \mu(\tilde{\Gamma}_{l,k}^{v-e}) < \infty}} \left(\left\| \sqrt{F_{l,k}^{v-e}} (u_l^{v-e} - g_{l,k}^{v-e}) \right\|_{0, \tilde{\Gamma}_{l,k}^{v-e}}^2 \right. \\
& \left. + \left\| \left(u_{x_1^{v-e}} - (g_{l,k}^{v-e})_{x_1^{v-e}} \right) \right\|_{\tilde{\Gamma}_{l,k}^{v-e}}^2 \right. \\
& \left. + \left\| E_{l,k}^{v-e} \left(u_{x_3^{v-e}} - (g_{l,k}^{v-e})_{x_3^{v-e}} \right) \right\|_{\tilde{\Gamma}_{l,k}^{v-e}}^2 \right) \\
& + \sum_{\substack{\Gamma_{l,k}^{v-e} \subseteq \Gamma^{[1]}, \\ \mu(\tilde{\Gamma}_{l,k}^{v-e}) < \infty}} \left\| \left(\frac{\partial u}{\partial \nu^{v-e}} \right)_{A^{v-e}} - h_{l,k}^{v-e} \right\|_{\tilde{\Gamma}_{l,k}^{v-e}}^2. \tag{4.5}
\end{aligned}$$

Here $E_{l,k}^{v-e} = \sup_{x^{v-e} \in \tilde{\Gamma}_{l,k}^{v-e}} (\sin \phi)$ and $G_{l,k}^{v-e} = \sup_{x^{v-e} \in \tilde{\Gamma}_{l,k}^{v-e}} (e^{x_3^{v-e}})$. Moreover, $G_{l,k}^{v-e}$ is defined in (2.27).

Then the functional $\mathcal{R}_{vertex-edges}^{N,W}(\{\mathcal{F}_u\})$ is defined as follows:

$$\mathcal{R}_{vertex-edges}^{N,W}(\{\mathcal{F}_u\}) = \sum_{v-e \in \mathcal{V}-E} \mathcal{R}_{v-e}^{N,W}(\{\mathcal{F}_u\}). \tag{4.6}$$

Finally, we define the functional $\mathcal{R}_{edges}^{N,W}(\{\mathcal{F}_u\})$. Let Ω^e denote the edge neighborhood of the edge $e \in \mathcal{E}$. Ω^e is divided into N_e elements $\Omega_l^e, l = 1, 2, \dots, N_e$. Once again we define a non-conforming spectral element representation on each of these sub-domains as follows:

Let $\tilde{\Omega}_m^e$ be the image of Ω_m^e in x^e coordinates. If $\tilde{\Omega}_p^e$ is a corner element of the form

$$\tilde{\Omega}_p^e = \{x^e : -\infty < x_1^e < \ln(r_1^e), \theta_j^e < x_2^e < \theta_{j+1}^e, Z_n^e < x_3^e < Z_{n+1}^e\}$$

then we define

$$u_p^e(x^e) = \sum_{t=0}^W \alpha_t (x_3^e)^t.$$

Next, let $\tilde{\Omega}_q^e$ be of the form

$$\tilde{\Omega}_q^e = \{x^e : \ln(r_i^e) < x_1^e < \ln(r_{i+1}^e), \theta_j^e < x_2^e < \theta_{j+1}^e, Z_n^e < x_3^e < Z_{n+1}^e\}$$

with $1 \leq i \leq N$, $0 \leq j \leq I_e$, $0 \leq n \leq J_e$.

Then we define

$$u_q^e(x^e) = \sum_{r=0}^{W_q} \sum_{s=0}^{W_q} \sum_{t=0}^W \alpha_{r,s,t} (x_1^e)^r (x_2^e)^s (x_3^e)^t.$$

Here $1 \leq W_q \leq W$. Moreover $W_q = [\mu_1 i]$ for $1 \leq i \leq N$, $\mu_1 > 0$ is a degree factor.

Let $F_l^e(x^e) = e^{2x_1^e} f(x(x^e))$ for $x^e \in \tilde{\Omega}_l^e$, $1 \leq l \leq N_e$.

We now consider the boundary conditions $w = g_k$ on Γ_k for $k \in \mathcal{D} = \Gamma^{[0]}$ and $(\frac{\partial w}{\partial \nu})_A = h_k$ on Γ_k for $k \in \mathcal{N} = \Gamma^{[1]}$. Then $(\frac{\partial w}{\partial \nu})_{A^e} = e^{x_1^e} h_k(x(x^e))$. Let $\Gamma_{m,k}^e = \Gamma_k \cap \partial\Omega_m^e$ and suppose Ω_m^e is not a corner element. Moreover it is assumed that $\Gamma_{m,k}^e$ lies on the $x_2 - x_3$ plane for simplicity and $\mu(\tilde{\Gamma}_{m,k}^e) < \infty$. Define

$$\begin{aligned} g_{m,k}^e(x^e) &= w = g_k(x(x^e)) \text{ for } \Gamma_{m,k}^e \subseteq \Gamma^{[0]}, \\ h_{m,k}^e(x^e) &= \left(\frac{\partial w}{\partial \nu} \right)_{A^e} = e^{x_1^e} h_k(x(x^e)) \text{ for } \Gamma_{m,k}^e \subseteq \Gamma^{[1]}. \end{aligned}$$

We define

$$\begin{aligned} \mathcal{R}_e^{N,W}(\{\mathcal{F}_u\}) &= \sum_{l=1, \mu(\tilde{\Omega}_l^e) < \infty}^{N_e} \int_{\tilde{\Omega}_l^e} |L^e u_l^e(x^e) - F_l^e(x^e)|^2 dx^e \\ &+ \sum_{\substack{\Gamma_{m,k}^e \subseteq \tilde{\Omega}^e \setminus \partial\Omega, \\ \mu(\tilde{\Gamma}_{m,k}^e) < \infty}} \left(\left\| \sqrt{H_{m,k}^e} [u] \right\|_{0, \tilde{\Gamma}_{m,k}^e}^2 + \left\| [u_{x_1^e}] \right\|_{\tilde{\Gamma}_{m,k}^e}^2 \right. \\ &\left. + \left\| [u_{x_2^e}] \right\|_{\tilde{\Gamma}_{m,k}^e}^2 + \left\| G_{m,k}^e [u_{x_3^e}] \right\|_{\tilde{\Gamma}_{m,k}^e}^2 \right) \\ &+ \sum_{\substack{\Gamma_{m,k}^e \subseteq \Gamma^{[0]}, \\ \mu(\tilde{\Gamma}_{m,k}^e) < \infty}} \left(\left\| (u_m^e - g_{m,k}^e) \right\|_{0, \tilde{\Gamma}_{m,k}^e}^2 + \left\| (u_{x_1^e} - (g_{m,k}^e)_{x_1^e}) \right\|_{\tilde{\Gamma}_{m,k}^e}^2 \right) \\ &+ \left\| G_{m,k}^e (u_{x_3^e} - (g_{m,k}^e)_{x_3^e}) \right\|_{\tilde{\Gamma}_{m,k}^e}^2 \\ &+ \sum_{\substack{\Gamma_{m,k}^e \subseteq \Gamma^{[1]}, \\ \mu(\tilde{\Gamma}_{m,k}^e) < \infty}} \left\| \left(\frac{\partial u}{\partial \nu} \right)_{A^e} - h_{m,k}^e \right\|_{\tilde{\Gamma}_{m,k}^e}^2. \end{aligned} \tag{4.7}$$

Here $G_{m,k}^e = \sup_{x^e \in \tilde{\Gamma}_{m,k}^e} (e^\tau)$ and $H_{m,k}^e$ is as defined in (2.34).

The functional $\mathcal{R}_{edges}^{N,W}(\{\mathcal{F}_u\})$ can now be defined as:

$$\mathcal{R}_{edges}^{N,W}(\{\mathcal{F}_u\}) = \sum_{e \in \mathcal{E}} \mathcal{R}_e^{N,W}(\{\mathcal{F}_u\}). \quad (4.8)$$

Finally using (4.2), (4.4), (4.6) and (4.8) in (4.1) we can define $\mathcal{R}^{N,W}(\{\mathcal{F}_u\})$.

Our numerical scheme may now be formulated as follows:

Find $\mathcal{F}_s \in \mathcal{S}^{N,W}$ which minimizes the functional $\mathcal{R}^{N,W}(\{\mathcal{F}_u\})$ over all $\mathcal{F}_u \in \mathcal{S}^{N,W}$.

Here $\mathcal{S}^{N,W}$ denotes the space of spectral element functions \mathcal{F}_u .

4.3 Error Estimates

It is well known that for three dimensional elliptic problems containing singularities in the form of vertices and edges, the geometric mesh and a proper choice of element degree distribution leads to exponential convergence and efficiency of computations (see [12, 13, 49, 51] and references therein).

Let N denote the number of refinements in the geometrical mesh and W denote an upper bound on the degree of the polynomial representation of the spectral element functions. We assume that N is proportional to W .

In this Section we show that the error obtained from the proposed method is exponentially small in N . The optimal rate of convergence with respect to N_{dof} , the number of degrees of freedom is also provided.

Our analysis of error estimates is similar to that in two dimensions (see [8, 11, 60, 86] and references therein). Here, we briefly describe the main steps of the proof, for details one may refer to [60].

Let $\mathcal{S}^{N,W}(\Omega^v)$, $\mathcal{S}^{N,W}(\Omega^{v-e})$, $\mathcal{S}^{N,W}(\Omega^e)$, and $\mathcal{S}^{N,W}(\Omega^r)$ denote the space of spectral element functions (SEF) over the set of vertex neighbourhoods Ω^v , vertex-edge neighbourhoods Ω^{v-e} , edge neighbourhoods Ω^e and regular region Ω^r respectively. Let us denote by $\mathcal{S}^{N,W}(\Omega)$ the space of SEF over the whole domain Ω whose restrictions to Ω^v , Ω^{v-e} , Ω^e and Ω^r belong to $\mathcal{S}^{N,W}(\Omega^v)$, $\mathcal{S}^{N,W}(\Omega^{v-e})$, $\mathcal{S}^{N,W}(\Omega^e)$, and $\mathcal{S}^{N,W}(\Omega^r)$ respectively.

Let $\{\mathcal{F}_z\}$ minimize $\mathcal{R}^{N,W}(\{\mathcal{F}_u\})$ over all $\{\mathcal{F}_u\} \in \mathcal{S}^{N,W}(\Omega)$, the space of spectral element functions. We write one more representation for $\{\mathcal{F}_z\}$ as follows:-

$$\{\mathcal{F}_z\} = \left\{ \{z_l^r(\lambda_1, \lambda_2, \lambda_3)\}_{l=1}^{N_r}, \{z_l^v(\phi, \theta, \chi)\}_{l=1}^{N_v}, \{z_l^{v-e}(\psi, \theta, \zeta)\}_{l=1}^{N_{v-e}}, \{z_l^e(\tau, \theta, x_3)\}_{l=1}^{N_e} \right\}.$$

Here $z_l^r(\lambda_1, \lambda_2, \lambda_3)$ is a polynomial of degree W in each of its variables.

$z_l^v = a_v$, where a_v is a constant, on corner elements $\tilde{\Omega}_l^v$ with $\mu(\tilde{\Omega}_l^v) = \infty$. In all other elements in the vertex neighbourhoods, $z_l^v(\phi, \theta, \chi)$ is a polynomial of degree W_l , $1 \leq W_l \leq W$, $W_l = [\mu_1 i]$ for all $1 \leq i \leq N+1$, in ϕ, θ and χ variables separately, where $\mu_1 > 0$ is a degree factor.

$z_l^{v-e} = a_{v-e} = a_v$, on corner elements $\tilde{\Omega}_l^{v-e}$ of the form

$$\tilde{\Omega}_l^{v-e} = \{x^{v-e} : \psi_i^{v-e} < \psi < \psi_{i+1}^{v-e}, \theta_j^{v-e} < \theta < \theta_{j+1}^{v-e}, -\infty < \zeta < \zeta_1^{v-e}\}$$

and z_l^{v-e} is a polynomial of degree V_l in ζ , $1 \leq V_l \leq W$, $V_l = [\mu_2 n]$ for all $1 \leq n \leq N$, $\mu_2 > 0$, on corner elements $\tilde{\Omega}_l^{v-e}$ of the form

$$\tilde{\Omega}_l^{v-e} = \{x^{v-e} : -\infty < \psi < \psi_1^{v-e}, \theta_j^{v-e} < \theta < \theta_{j+1}^{v-e}, \zeta_n^{v-e} < \zeta < \zeta_{n+1}^{v-e}\}$$

with $n \geq 1$.

On the remaining elements in the vertex-edge neighbourhoods, $z_l^{v-e}(\psi, \theta, \zeta)$ is a polynomial of degree W_l , $1 \leq W_l \leq W$, $W_l = [\mu_1 i]$ for all $1 \leq i \leq N$, in ψ, θ variables and of degree V_l , $1 \leq V_l \leq W$, $V_l = [\mu_2 n]$ for all $1 \leq n \leq N$, in ζ variable with $\mu_1 > 0, \mu_2 > 0$.

Finally, on corner elements $\tilde{\Omega}_l^e$ with $\mu(\tilde{\Omega}_l^e) = \infty$, z_l^e is a polynomial of degree W in x_3 and on the remaining elements $\tilde{\Omega}_l^e$ away from edges $z_l^e(\tau, \theta, x_3)$ is a polynomial of degree W_l , $1 \leq W_l \leq W$, $W_l = [\mu_1 i]$, $1 \leq i \leq N$, $\mu_1 > 0$ in τ, θ variables and of degree W in the x_3 variable.

Approximation in the regular region:

Let us first consider the regular region Ω^r of Ω . In Chapter 2, Ω^r has been divided into Ω_l^r , $l = 1, \dots, N_r$ curvilinear hexahedrons, tetrahedrons and prisms. Let M_l^r be the analytic map from Q to Ω_l^r .

Let $\Pi^{W,W,W}(w(M_l^r(\lambda)))$ denote the projection of the solution w into the space of polynomials of degree N in each of its variables with respect to the usual inner product in

$H^2(Q)$. Then on Ω_l^r we define

$$s_l^r(\lambda) = \Pi^{W,W,W}(w(M_l^r(\lambda))) = \Pi^{W,W,W}(w(\lambda)), \text{ for } \lambda \in Q.$$

Approximation in vertex neighbourhoods:

Let us now consider the vertex neighbourhood Ω^v of the vertex $v \in \mathcal{V}$, where \mathcal{V} denotes the set of vertices of Ω (see Figure 2.8). We had divided Ω^v into $\Omega_l^v, l = 1, \dots, N_v$ elements (Chapter 2). If $\tilde{\Omega}_l^v$ is a corner element of the form

$$\tilde{\Omega}_l^v = \{x^v : (\phi, \theta) \in S_j^v, -\infty < \chi < \ln(\rho_1^v)\}$$

then on $\tilde{\Omega}_l^v$ we define

$$s_l^v = w_v,$$

where $w_v = w(v)$ denotes the value of w at the vertex v defined as in our differentiability estimates of Chapter 2.

If $\tilde{\Omega}_l^v$ is of the form

$$\tilde{\Omega}_l^v = \{x^v : (\phi, \theta) \in S_j^v, \ln(\rho_i^v) < \chi < \ln(\rho_{i+1}^v)\}$$

then on $\tilde{\Omega}_l^v$ we approximate $(w(x^v) - w_v)$ by its projection, denoted by Π^{W_l, W_l, W_l} , into the space of polynomials of degree N in each of its variables separately with respect to the usual inner product in $H^2(\tilde{\Omega}_l^v)$ and define

$$s_l^v(x^v) = \Pi^{W_l, W_l, W_l}(w(x^v) - w_v) + w_v.$$

Here $1 \leq W_l \leq W$, $W_l = [\mu_1 i]$ for all $1 \leq i \leq N$, where $\mu_1 > 0$ is a degree factor [51].

Approximation in vertex-edge neighbourhoods:

We now consider the vertex-edge neighborhood Ω^{v-e} of the vertex-edge $v - e \in \mathcal{V} - \mathcal{E}$ (see Figure 2.9). Here, as earlier, $\mathcal{V} - \mathcal{E}$ denotes the set of vertex-edges of the domain Ω . Ω^{v-e} is divided into $\Omega_q^{v-e}, q = 1, \dots, N_{v-e}$ elements using a geometric mesh in ϕ, x_3 variables and a quasi-uniform mesh in θ variable.

Let $\tilde{\Omega}_q^{v-e}$ be the image of Ω_q^{v-e} in x^{v-e} coordinates. If $\tilde{\Omega}_q^{v-e}$ is a corner element of the form

$$\tilde{\Omega}_q^{v-e} = \{x^{v-e} : \psi_i^{v-e} < \psi < \psi_{i+1}^{v-e}, \theta_j^{v-e} < \theta < \theta_{j+1}^{v-e}, -\infty < \zeta < \zeta_1^{v-e}\}$$

then on $\tilde{\Omega}_q^{v-e}$ we define

$$s_l^{v-e} = w_{v-e} = w_v .$$

Here w_v is the value of w at the vertex v (Chapter 2).

Next, suppose $\tilde{\Omega}_q^{v-e}$ is a corner element of the form

$$\tilde{\Omega}_q^{v-e} = \{x^{v-e} : -\infty < \psi < \psi_1^{v-e}, \theta_j^{v-e} < \theta < \theta_{j+1}^{v-e}, \zeta_n^{v-e} < \zeta < \zeta_{n+1}^{v-e}\}$$

with $n \geq 1$. Let $s(x_3^{v-e}) = w(x_1, x_2, x_3)|_{(x_1=0, x_2=0)}$ be the value of w along the edge e . Define

$$\sigma(x_3^{v-e}) = s(x_3^{v-e}) - w_v.$$

Let $\Pi^{V_q}(\sigma(x_3^{v-e}))$ be the orthogonal projection of $\sigma(x_3^{v-e})$ into the space of polynomials in $H^2(I)$. Then we define

$$s_l^{v-e}(x_3^{v-e}) = \Pi^{V_q}(\sigma(x_3^{v-e})) + w_v = \Pi^{V_q}s(x_3^{v-e}).$$

Here $1 \leq V_q \leq W$. Moreover $W_q = [\mu_2 n]$ for all $1 \leq n \leq N$, where $\mu_2 > 0$ is a degree factor.

The remaining elements $\tilde{\Omega}_q^{v-e}$ in $\tilde{\Omega}^{v-e}$ are of the form

$$\tilde{\Omega}_q^{v-e} = \{x^{v-e} : \psi_i^{v-e} < \psi < \psi_{i+1}^{v-e}, \theta_j^{v-e} < \theta < \theta_{j+1}^{v-e}, \zeta_n^{v-e} < \zeta < \zeta_{n+1}^{v-e}\}$$

with $i \geq 1, k \geq 1$. Let us write $\alpha(x^{v-e}) = w(x^{v-e}) - s(x_3^{v-e})$. Then on $\tilde{\Omega}_q^{v-e}$ we approximate $\alpha(x^{v-e})$ by its projection, denoted by Π^{W_q, W_q, V_q} , into the space of polynomials with respect to the usual inner product in $H^2(\tilde{\Omega}_q^{v-e})$. We now define

$$s_l^{v-e}(x^{v-e}) = \Pi^{W_q, W_q, V_q}(\alpha(x^{v-e})) + \Pi^{V_q}(s(x_3^{v-e})).$$

Here $1 \leq W_q \leq W$ and $1 \leq V_q \leq W$. Moreover $W_q = [\mu_1 i], V_q = [\mu_2 n]$ for all $1 \leq i, n \leq N$, where $\mu_1, \mu_2 > 0$ are degree factors [51].

Finally, we discuss approximation in the edge neighbourhood elements and define comparison functions there.

Approximation in edge neighbourhoods:

Consider the edge neighborhood Ω^e of the edge $e \in \mathcal{E}$ (see Figure 2.10). Here, as before, \mathcal{E} denotes the set of edges of the domain Ω . In Chapter 2, we had divided Ω^e into $\Omega_p^e, p = 1, \dots, N_e$ elements.

Let $\tilde{\Omega}_p^e$ be the image of Ω_p^e in x^e coordinates. Let $\tilde{\Omega}_p^e$ be a corner element of the form

$$\tilde{\Omega}_p^e = \{x^e : -\infty < x_1^e < \ln(r_1^e), \theta_j^e < x_2^e < \theta_{j+1}^e, Z_n^e < x_3^e < Z_{n+1}^e\}.$$

Let $s(x_3^e) = w(x_1, x_2, x_3)|_{(x_1=0, x_2=0)}$. Then on $\tilde{\Omega}_p^e$ we approximate $s(x_3^e)$ by its projection onto the space of polynomials with respect to the usual inner product in $H^2(I)$. Let $\Pi^W(s(x_3^e))$ denote this projection, then we define

$$s_l^e(x_3^e) = \Pi^W(s(x_3^e)).$$

Next, let $\tilde{\Omega}_p^e$ be of the form

$$\tilde{\Omega}_p^e = \{x^e : \ln(r_i^e) < x_1^e < \ln(r_{i+1}^e), \theta_j^e < x_2^e < \theta_{j+1}^e, Z_n^e < x_3^e < Z_{n+1}^e\}$$

with $1 \leq i \leq N, 0 \leq j \leq I_e, 0 \leq n \leq J_e$. Let us write $\beta(x^e) = w(x^e) - s(x_3^e)$. Then on $\tilde{\Omega}_p^e$ we approximate $\beta(x^e)$ by its projection, denoted by $\Pi^{W_p, W_p, W}$, into the space of polynomials with respect to the usual inner product in $H^2(\tilde{\Omega}_p^e)$. Define

$$s_l^e(x^e) = \Pi^{W_p, W_p, W}(\beta(x^e)) + \Pi^W(s(x_3^e)).$$

Here $1 \leq W_p \leq W$. Moreover $W_p = [\mu_1 i]$ for all $1 \leq i \leq N$, where $\mu_1 > 0$ is a degree factor [51].

Now consider the set of functions $\left\{ \{s_l^r\}_{l=1}^{N_r}, \{s_l^v\}_{l=1}^{N_v}, \{s_l^{v-e}\}_{l=1}^{N_{v-e}}, \{s_l^e\}_{l=1}^{N_e} \right\}$ and denote it by $\{\mathcal{F}_s\}$.

We will show that the functional defined by

$$\begin{aligned} \mathcal{R}^{N, W}(\{\mathcal{F}_s\}) &= \mathcal{R}_{regular}^{N, W}(\{\mathcal{F}_s\}) + \mathcal{R}_{vertices}^{N, W}(\{\mathcal{F}_s\}) \\ &\quad + \mathcal{R}_{vertex-edges}^{N, W}(\{\mathcal{F}_s\}) + \mathcal{R}_{edges}^{N, W}(\{\mathcal{F}_s\}) \end{aligned} \quad (4.9)$$

is exponentially small in N . Here the functionals $\mathcal{R}_{regular}^{N, W}(\{\mathcal{F}_s\})$, $\mathcal{R}_{vertices}^{N, W}(\{\mathcal{F}_s\})$ etc. are similar to those as defined in Section 4.2.

Using results on approximation theory in [11, 12, 60] it follows that there exist constants C and $b > 0$ such that the estimate

$$\mathcal{R}^{N,W}(\{\mathcal{F}_s\}) \leq Ce^{-bN} \quad (4.10)$$

holds.

Now $\{\mathcal{F}_z\}$ minimizes $\mathcal{R}^{N,W}(\{\mathcal{F}_u\})$ over all $\{\mathcal{F}_u\} \in \mathcal{S}^{N,W}(\Omega)$, the space of spectral element functions. Then from (4.10), we have

$$\mathcal{R}^{N,W}(\{\mathcal{F}_z\}) \leq Ce^{-bN}. \quad (4.11)$$

Let $\mathcal{V}^{N,W}$ be the quadratic form as defined in Chapter 2. Then from (4.10) and (4.11) we can conclude that

$$\mathcal{V}^{N,W}(\{\mathcal{F}_{(s-z)}\}) \leq Ce^{-bN} \quad (4.12)$$

where C and b are generic constants.

Hence using the Stability Theorem 2.3.1 we obtain

$$\mathcal{U}^{N,W}(\{\mathcal{F}_{(s-z)}\}) \leq Ce^{-bN}. \quad (4.13)$$

Here the quadratic form $\mathcal{U}^{N,W}(\{\mathcal{F}_{(s-z)}\})$ is defined similar to the quadratic form $\mathcal{U}^{N,W}(\{\mathcal{F}_u\})$ as in (2.15) of Chapter 2.

Let $U_l^r(\lambda) = w(X_l^r(\lambda_1, \lambda_2, \lambda_3)) \equiv w(M_l^r(\lambda))$ for $\lambda \in Q$, $U_l^v(x^v) = w(x^v)$ for $x^v \in \tilde{\Omega}_l^v$, $U_l^{v-e}(x^{v-e}) = w(x^{v-e})$ for $x^{v-e} \in \tilde{\Omega}_l^{v-e}$ and $U_l^e(x^e) = w(x^e)$ for $x^e \in \tilde{\Omega}_l^e$. Here w is the solution of the boundary value problem (2.1).

We now define another quadratic form $\mathcal{E}^{N,W}(\{z - U\})$ as follows:-

$$\begin{aligned} \mathcal{E}^{N,W}(\{z - U\}) &= \mathcal{E}_{regular}^{N,W}(\{z_l^r - U_l^r\}) + \mathcal{E}_{vertices}^{N,W}(\{z_l^v - U_l^v\}) \\ &\quad + \mathcal{E}_{vertex-edges}^{N,W}(\{z_l^{v-e} - U_l^{v-e}\}) + \mathcal{E}_{edges}^{N,W}(\{z_l^e - U_l^e\}), \end{aligned} \quad (4.14)$$

where

$$\begin{aligned}
\mathcal{E}_{regular}^{N,W}(\{z_l^r - U_l^r\}) &= \sum_{l=1}^{N_r} \int_{Q=(M_l^r)^{-1}(\Omega_l^r)} \sum_{|\alpha| \leq 2} |D_\lambda^\alpha (z_l^r - U_l^r)(\lambda)|^2 d\lambda, \\
\mathcal{E}_{vertices}^{N,W}(\{z_l^v - U_l^v\}) &= \sum_{v \in \mathcal{V}} \mathcal{E}_v^{N,W}(z_l^v - U_l^v), \\
\mathcal{E}_v^{N,W}(\{z_l^v - U_l^v\}) &= \sum_{l=1}^{N_v} \int_{\tilde{\Omega}_l^v} e^{x_3^v} \sum_{|\alpha| \leq 2} |D_{x^v}^\alpha (z_l^v - U_l^v)(x^v)|^2 dx^v, \\
\mathcal{E}_{vertex-edges}^{N,W}(\{z_l^{v-e} - U_l^{v-e}\}) &= \sum_{v-e \in \mathcal{V}-\mathcal{E}} \mathcal{E}_{v-e}^{N,W}(z_l^{v-e} - U_l^{v-e}), \\
\mathcal{E}_{v-e}^{N,W}(\{z_l^{v-e} - U_l^{v-e}\}) &= \sum_{l=1}^{N_{v-e}} \int_{\tilde{\Omega}_l^{v-e}} e^{x_3^{v-e}} \sum_{|\alpha| \leq 2} |D_{x^{v-e}}^\alpha (z_l^{v-e} - U_l^{v-e})(x^{v-e})|^2 dx^{v-e}, \\
\mathcal{E}_{edges}^{N,W}(\{z_l^e - U_l^e\}) &= \sum_{e \in \mathcal{E}} \mathcal{E}_e^{N,W}(z_l^e - U_l^e), \\
\mathcal{E}_e^{N,W}(\{z_l^e - U_l^e\}) &= \sum_{l=1}^{N_e} \int_{\tilde{\Omega}_l^e} \sum_{|\alpha| \leq 2} |D_{x^e}^\alpha (z_l^e - U_l^e)(x^e)|^2 dx^e.
\end{aligned}$$

It is easy to show that

$$\begin{aligned}
\mathcal{E}_{regular}^{N,W}(\{s_l^r - U_l^r\}) &\leq C e^{-bN}, \\
\mathcal{E}_{vertices}^{N,W}(\{s_l^v - U_l^v\}) &\leq C e^{-bN}, \\
\mathcal{E}_{vertex-edges}^{N,W}(\{s_l^{v-e} - U_l^{v-e}\}) &\leq C e^{-bN}, \\
\mathcal{E}_{edges}^{N,W}(\{s_l^e - U_l^e\}) &\leq C e^{-bN}
\end{aligned} \tag{4.15}$$

where the quadratic forms $\mathcal{E}_{regular}^{N,W}(\{s_l^r - U_l^r\})$, $\mathcal{E}_{vertices}^{N,W}(\{s_l^v - U_l^v\})$ etc. are defined similar to those in (4.14). Now define

$$\begin{aligned}
\mathcal{E}^{N,W}(\{s - U\}) &= \mathcal{E}_{regular}^{N,W}(\{s_l^r - U_l^r\}) + \mathcal{E}_{vertices}^{N,W}(\{s_l^v - U_l^v\}) \\
&\quad + \mathcal{E}_{vertex-edges}^{N,W}(\{s_l^{v-e} - U_l^{v-e}\}) + \mathcal{E}_{edges}^{N,W}(\{s_l^e - U_l^e\}).
\end{aligned}$$

Then from (4.15) it follows that

$$\mathcal{E}^{N,W}(\{s - U\}) \leq C e^{-bN}. \tag{4.16}$$

Finally, using estimates (4.13) and (4.16), we obtain

$$\mathcal{U}^{N,W}(\{\mathcal{F}_{(z-U)}\}) \leq C e^{-bN}.$$

Our main theorem on error estimates is now stated

Theorem 4.3.1. *Let $\{\mathcal{F}_z\}$ minimize $\mathcal{R}^{N,W}(\{\mathcal{F}_u\})$ over all $\{\mathcal{F}_u\} \in \mathcal{S}^{N,W}(\Omega)$. Then there exist constants C and b (independent of N) such that*

$$\mathcal{U}^{N,W}(\{\mathcal{F}_{(z-U)}\}) \leq Ce^{-bN}. \quad (4.17)$$

Here $\mathcal{U}^{N,W}(\{\mathcal{F}_{(z-U)}\})$ is as defined in (2.15) of Chapter 2.

Remark 4.3.1. *After having obtained the non-conforming spectral element solution we can make a correction to it so that the corrected solution is conforming and the error in the H^1 norm is exponentially small in N . These corrections are similar to those described in [60, 85, 86] in two dimensions and are explained in the proof of Lemma 3.3.1 in Appendix C.1.*

To end this chapter, let us estimate the error in terms of number of degrees of freedom in various subregions of the domain Ω .

The regular region Ω^r :

The regular region Ω^r contains no vertices and edges of the domain Ω . Here the solution w has no singularity and is analytic.

There are $O(1)$ number of elements in this region and each element has $O(W^3)$ degrees of freedom. Let $N_{dof}(\Omega^r)$ denotes the number of degrees of freedom in Ω^r . Then

$$N_{dof}(\Omega^r) = O(W^3) = O(N^3).$$

The vertex neighbourhoods Ω^v :

In a vertex neighbourhood Ω^v there are $O(N)$ elements with $O(W^3)$ degrees of freedom in each element. If $N_{dof}(\Omega^v)$ denotes the number of degrees of freedom in Ω^v . Then

$$N_{dof}(\Omega^v) = O(NW^3) = O(N^4).$$

The vertex-edge neighbourhoods Ω^{v-e} :

There are $O(N^2)$ number of elements in each of the vertex-edge neighbourhoods Ω^{v-e} and each element has $O(W^3)$ degrees of freedom. Then

$$N_{dof}(\Omega^{v-e}) = O(N^2W^3) = O(N^5).$$

Here $N_{dof}(\Omega^{v-e})$ denotes the number of degrees of freedom in Ω^{v-e} .

The edge neighbourhoods Ω^e :

An edge neighbourhood Ω^e has $O(N)$ elements with $O(W^3)$ degrees of freedom within each element. Let $N_{dof}(\Omega^e)$ be the number of degrees of freedom in Ω^e . Then

$$N_{dof}(\Omega^e) = O(NW^3) = O(N^4).$$

Hence, the error estimate Theorem 4.3.1 in terms of number of degrees of freedom assumes the form

Theorem 4.3.2. *Let $\{\mathcal{F}_z\}$ minimizes $\mathcal{R}^{N,W}(\{\mathcal{F}_u\})$ over all $\{\mathcal{F}_u\} \in \mathcal{S}^{N,W}(\Omega)$. Then there exist constants C and b (independent of N) such that*

$$\mathcal{U}^{N,W}(\{\mathcal{F}_{(z-U)}\}) \leq Ce^{-bN_{dof}^{1/5}}. \quad (4.18)$$

Here $\mathcal{U}^{N,W}(\{\mathcal{F}_{(z-U)}\})$ is as defined in (2.15) and $N_{dof} = \dim(\mathcal{S}^{N,W}(\Omega))$ is the number of degrees of freedom.

Proof. Follows from Theorem 4.3.1. □

Remark 4.3.2. *From the above theorem it is clear that the exponential rate of convergence will be visible only for a large value of N_{dof} , as a result we need to sufficiently refine the geometric mesh both in the direction of edges and in the direction perpendicular to the edges.*

Remark 4.3.3. *Since the majority of degrees of freedom is present in the vertex-edge neighbourhoods the factor $N_{dof}^{1/5}$ in the theorem is due to the vertex-edge singularity in the solution. Hence the optimal convergence rate will be $e^{-bN_{dof}^{1/5}}$.*

Remark 4.3.4. *It was conjectured in [13, 51] that for $h-p$ version of the finite element method in \mathbb{R}^3 the optimal convergence rate will be $e^{-bN_{dof}^{1/5}}$, and it can not be improved further with any mesh and any anisotropic polynomial order within the elements.*

Chapter 5

Solution Techniques on Parallel Computers

5.1 Introduction

In Chapter 4 we had described the numerical scheme and the error estimates for the numerical solution were stated.

The method is essentially a *least-squares* collocation method. To solve the minimization problem we need to solve the *normal equations* arising from the minimization problem. We use *preconditioned conjugate gradient method* (PCGM) to solve the normal equations using a *block diagonal preconditioner* which is nearly optimal as the condition number of the preconditioned system is polylogarithmic in N , the number of refinements in the geometric mesh. Moreover, to compute the residuals in the normal equations we do not need to compute mass and stiffness matrices.

We use only non-conforming spectral element functions. We shall examine spectral element functions which are conforming on the wirebasket in future work.

It is shown that we can define a preconditioner for the minimization problem which allows the problem to decouple. Construction of preconditioner on each element in various regions of the polyhedron is also provided. It will be shown as in [36] that there exists a new preconditioner which can be diagonalized in a new set of basis functions using

separation of variables technique.

The coefficients in the differential operator and the data are projected into the polynomial spaces (we call them *filtered coefficients* of the differential operator and *filtered data*) so that the integrands involved in the numerical formulation are exactly evaluated using Gauss-Lobatto-Legendre (GLL) quadrature. However, in our computations we do not need to filter the coefficients of the differential operator and the data. Of course, in doing so we commit an error and it can be argued as in [86] that this error is spectrally small.

In section 5.3 we shall describe the steps involved in computing the residuals in the normal equations without computing mass and stiffness matrices on a distributed memory parallel computer. The evaluation of these residuals on each processor requires the interchange of boundary values between neighbouring processors. Hence the communication involved is quite small. Thus we can compute the residuals in the normal equations inexpensively and efficiently. Finally, we shall discuss computational complexity of our method.

5.2 Preconditioning

We now come to the aspect of preconditioning. Our construction of preconditioners is similar to that for elliptic problems in two dimensions (see [37, 38, 85, 86]).

5.2.1 Preconditioners on the regular region

In the regular region the preconditioner which needs to be examined corresponds to the quadratic form

$$\mathcal{B}(u) = \|u\|_{H^2(Q)}^2 \tag{5.1}$$

where $Q = (-1, 1)^3$ = master cube, $u = u(\lambda) = u(\lambda_1, \lambda_2, \lambda_3)$ is a polynomial of degree W in λ_1, λ_2 and λ_3 separately.

Let $u(\lambda_1, \lambda_2, \lambda_3)$ be the spectral element function, defined on $Q = (-1, 1)^3$, as

$$u(\lambda_1, \lambda_2, \lambda_3) = \sum_{i=0}^W \sum_{j=0}^W \sum_{k=0}^W a_{i,j,k} L_i(\lambda_1) L_j(\lambda_2) L_k(\lambda_3). \quad (5.2)$$

Here $L_i(\cdot)$ denotes the Legendre polynomial of degree i .

The quadratic form $\mathcal{B}(u)$ can be written as

$$\mathcal{B}(u) = \int_Q \sum_{|\alpha| \leq 2} |D_\lambda^\alpha u|^2 d\lambda. \quad (5.3)$$

We shall show that there is another quadratic form $\mathcal{C}(u)$ which is spectrally equivalent to $\mathcal{B}(u)$ and which can be easily diagonalized using separation of variables.

Let I denote the interval $(-1, 1)$ and

$$v(\lambda_1) = \sum_{i=0}^W \beta_i L_i(\lambda_1). \quad (5.4)$$

Moreover $b = (\beta_0, \beta_1, \dots, \beta_W)^T$. We now define the quadratic form

$$\mathcal{E}(v) = \int_I (v_{\lambda_1 \lambda_1}^2 + v_{\lambda_1}^2) d\lambda_1 \quad (5.5)$$

and

$$\mathcal{F}(v) = \int_I v^2 d\lambda_1. \quad (5.6)$$

Clearly there exist $(W+1) \times (W+1)$ matrices E and F such that

$$\mathcal{E}(v) = b^T E b \quad (5.7)$$

and

$$\mathcal{F}(v) = b^T F b. \quad (5.8)$$

Here the matrices E and F are symmetric and F is positive definite.

Hence there exist $W+1$ eigenvalues $0 \leq \mu_0 \leq \mu_1 \leq \dots \leq \mu_W$ and $W+1$ eigenvectors b_0, b_1, \dots, b_W of the symmetric eigenvalue problem

$$(E - \mu F)b = 0. \quad (5.9)$$

Here

$$(E - \mu_i F)b_i = 0.$$

The eigenvectors b_i are normalized so that

$$b_i^T F b_j = \delta_j^i . \quad (5.10a)$$

Moreover the relations

$$b_i^T E b_j = \mu_i \delta_j^i \quad (5.10b)$$

hold. Let $b_i = (b_{i,0}, b_{i,1}, \dots, b_{i,W})$. We now define the polynomial

$$\phi_i(\lambda_1) = \sum_{j=0}^W b_{i,j} L_j(\lambda_1) \text{ for } 0 \leq i \leq W . \quad (5.11)$$

Next, let $\psi_{i,j,k}$ denote the polynomial

$$\psi_{i,j,k}(\lambda_1, \lambda_2, \lambda_3) = \phi_i(\lambda_1) \phi_j(\lambda_2) \phi_k(\lambda_3) \quad (5.12)$$

for $0 \leq i \leq W, 0 \leq j \leq W, 0 \leq k \leq W$.

Let $u(\lambda_1, \lambda_2, \lambda_3)$ be a polynomial as in (5.2). Define the quadratic form

$$\mathcal{C}(u) = \int_Q (u_{\lambda_1 \lambda_1}^2 + u_{\lambda_2 \lambda_2}^2 + u_{\lambda_3 \lambda_3}^2 + u_{\lambda_1}^2 + u_{\lambda_2}^2 + u_{\lambda_3}^2 + u^2) d\lambda_1 d\lambda_2 d\lambda_3 . \quad (5.13)$$

Then the quadratic form $\mathcal{C}(u)$ is spectrally equivalent to the quadratic form $\mathcal{B}(u)$, defined in (5.1). Moreover, the quadratic form $\mathcal{C}(u)$ can be diagonalized in the basis $\psi_{i,j,k}(\lambda_1, \lambda_2, \lambda_3)$. Note that $\{\psi_{i,j,k}(\lambda_1, \lambda_2, \lambda_3)\}_{i,j,k}$ is the tensor product of the polynomials $\phi_i(\lambda_1)$, $\phi_j(\lambda_2)$ and $\phi_k(\lambda_3)$. The eigenvalue $\mu_{i,j,k}$ corresponding to the eigenvector $\psi_{i,j,k}$ is given by the relation

$$\mu_{i,j,k} = \mu_i + \mu_j + \mu_k + 1 . \quad (5.14)$$

Hence the matrix corresponding to the quadratic form $\mathcal{C}(u)$ is easy to invert.

Using the extension theorems in [1] and Lemma 2.1 in [36] we can extend $u(\lambda_1, \lambda_2, \lambda_3)$ defined in (5.2) to $U(\lambda_1, \lambda_2, \lambda_3)$ by the method of reflection (see Theorem 4.26 of [1]). This extension $U(\lambda_1, \lambda_2, \lambda_3)$ of $u(\lambda_1, \lambda_2, \lambda_3)$ is such that $U(\lambda_1, \lambda_2, \lambda_3) \in H^2(\mathbb{R}^3)$ and satisfies the estimate

$$\int_{\mathbb{R}^3} (U_{\lambda_1 \lambda_1}^2 + U_{\lambda_2 \lambda_2}^2 + U_{\lambda_3 \lambda_3}^2 + U^2) d\lambda \leq K \int_Q (u_{\lambda_1 \lambda_1}^2 + u_{\lambda_2 \lambda_2}^2 + u_{\lambda_3 \lambda_3}^2 + u^2) d\lambda .$$

Here K is a constant independent of W . Now making use of Theorem 2.1 of [36] and extending it to three dimensions it follows that there exists a constant L (independent of W) such that

$$\begin{aligned} \frac{1}{L} \|u\|_{H^2(Q)}^2 &\leq \int_Q (|u_{\lambda_1 \lambda_1}|^2 + |u_{\lambda_2 \lambda_2}|^2 + |u_{\lambda_3 \lambda_3}|^2 + |u_{\lambda_1}|^2 + |u_{\lambda_2}|^2 + |u_{\lambda_3}|^2 + |u|^2) d\lambda \\ &\leq \|u\|_{H^2(Q)}^2 . \end{aligned}$$

i.e. the quadratic forms $\mathcal{B}(u)$ and $\mathcal{C}(u)$ are spectrally equivalent.

Theorem 5.2.1. *The quadratic forms $\mathcal{B}(u)$ and $\mathcal{C}(u)$ are spectrally equivalent.*

We now show that the quadratic form $\mathcal{C}(u)$ defined in (5.13) as

$$\mathcal{C}(u) = \int_Q (u_{\lambda_1 \lambda_1}^2 + u_{\lambda_2 \lambda_2}^2 + u_{\lambda_3 \lambda_3}^2 + u_{\lambda_1}^2 + u_{\lambda_2}^2 + u_{\lambda_3}^2 + u^2) d\lambda_1 d\lambda_2 d\lambda_3$$

can be diagonalized in the basis $\{\psi_{i,j,k}\}_{i,j,k}$. Here u is a polynomial in λ_1 , λ_2 and λ_3 as defined in (5.2). Let $\tilde{\mathcal{C}}(f, g)$ denote the bilinear form induced by the quadratic form $\mathcal{C}(u)$. Then

$$\begin{aligned} \tilde{\mathcal{C}}(f, g) = \int_Q &(f_{\lambda_1 \lambda_1} g_{\lambda_1 \lambda_1} + f_{\lambda_2 \lambda_2} g_{\lambda_2 \lambda_2} + f_{\lambda_3 \lambda_3} g_{\lambda_3 \lambda_3} + f_{\lambda_1} g_{\lambda_1} + f_{\lambda_2} g_{\lambda_2} \\ &+ f_{\lambda_3} g_{\lambda_3} + f g) d\lambda_1 d\lambda_2 d\lambda_3 . \end{aligned} \quad (5.15)$$

Let $\mathcal{E}(v)$ and $\mathcal{F}(v)$ be the quadratic forms defined in (5.5) and (5.6) and let $\tilde{\mathcal{E}}(f, g)$ and $\tilde{\mathcal{F}}(f, g)$ denote the bilinear forms induced by $\mathcal{E}(v)$ and $\mathcal{F}(v)$ respectively. Then

$$\tilde{\mathcal{E}}(f, g) = \int_I (f_{\lambda_1 \lambda_1} g_{\lambda_1 \lambda_1} + f_{\lambda_1} g_{\lambda_1}) d\lambda_1 \quad (5.16a)$$

and

$$\tilde{\mathcal{F}}(f, g) = \int_I f g d\lambda_1 . \quad (5.16b)$$

Here I denotes the unit interval and $f(\lambda_1)$, $g(\lambda_1)$ are polynomials of degree W in λ_1 .

Finally, let $\phi_i(\lambda_1)$ be the polynomial as defined in (5.11). Then relation (5.10a) may be written as

$$\tilde{\mathcal{F}}(\phi_i, \phi_j) = \int_I \phi_i(\lambda_1) \phi_j(\lambda_1) d\lambda_1 = \delta_j^i . \quad (5.17a)$$

Moreover, relation (5.10b) may be stated as

$$\tilde{\mathcal{E}}(\phi_i, \phi_j) = \int_I ((\phi_i)_{\lambda_1 \lambda_1} (\phi_j)_{\lambda_1 \lambda_1} + (\phi_i)_{\lambda_1} (\phi_j)_{\lambda_1}) d\lambda_1 = \mu_i \delta_j^i. \quad (5.17b)$$

Recalling that $\psi_{i,j,k}(\lambda_1, \lambda_2, \lambda_3) = \phi_i(\lambda_1)\phi_j(\lambda_2)\phi_k(\lambda_3)$ and using (5.17) in (5.15) it is easy to show that

$$\begin{aligned} \tilde{\mathcal{C}}(\psi_{i,j,k}, \psi_{l,m,n}) &= (\mu_i + \mu_j + \mu_k + 1) \delta_l^i \delta_m^j \delta_n^k \\ &= \mu_{i,j,k} \delta_l^i \delta_m^j \delta_n^k. \end{aligned}$$

Hence the eigenvectors of the quadratic form $\mathcal{C}(u)$ are $\{\psi_{i,j,k}\}_{i,j,k}$ and the eigenvalues are $\{\mu_{i,j,k}\}_{i,j,k}$. Moreover the quadratic form $\mathcal{C}(u)$ can be diagonalized in the basis $\{\psi_{i,j,k}\}_{i,j,k}$ and consequently the matrix corresponding to $\mathcal{C}(u)$ is easy to invert.

Let

$$u(\lambda_1, \lambda_2, \lambda_3) = \sum_{i=0}^W \sum_{j=0}^W \sum_{k=0}^W \beta_{i,j,k} L_i(\lambda_1) L_j(\lambda_2) L_k(\lambda_3)$$

and β denotes the column vector whose components are $\beta_{i,j,k}$ arranged in lexicographic order. Then there is a $(W+1)^3 \times (W+1)^3$ matrix C such that

$$\mathcal{C}(u) = \beta^T C \beta.$$

As in [36] it can be shown that the system of equations

$$C\beta = \rho$$

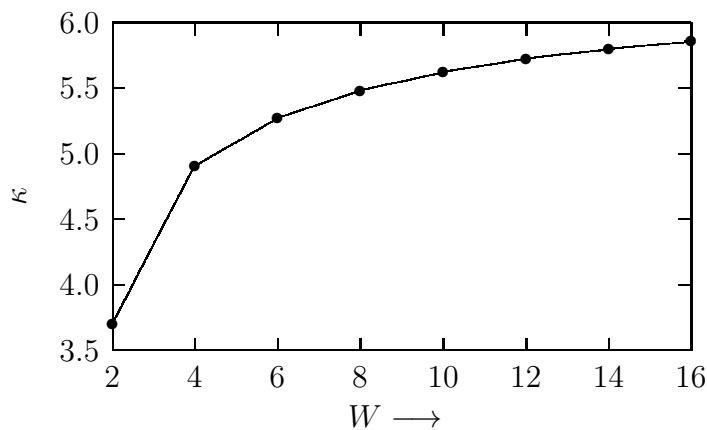
can be solved in $O(W^4)$ operations. Therefore the quadratic form $\mathcal{C}(u)$ can be inverted in $O(W^4)$ operations.

Let κ denote the condition number of the preconditioned system obtained by using the quadratic form $\mathcal{C}(u)$ as a preconditioner for the quadratic form $\mathcal{B}(u)$. Then the values of κ as a function of W are shown in Table 5.1.

Table 5.1: Condition number κ as a function of W

W	κ
2	3.699999999999999
4	4.90406593328559
6	5.27448215795748
8	5.48239323328901
10	5.62480021244268
12	5.72673215953223
14	5.80192403338903
16	5.85907843805046

In Figure 5.1, the condition number κ is plotted against the polynomial order W .

Figure 5.1: Condition number κ vs. W .

5.2.2 Preconditioners on singular regions

In Chapter 2 we had divided the polyhedral domain Ω into a regular region Ω^r , a set of vertex neighbourhoods Ω^v , a set of edge neighbourhoods Ω^e and a set of vertex-edge neighbourhoods Ω^{v-e} . Ω^r is divided into a set of curvilinear hexahedrons, tetrahedrons

and prisms and the singular regions in the neighbourhoods of vertices, edges and vertex-edges are divided into hexahedrons and prisms using a geometric mesh.

A set of spectral element functions has been defined on all elements in the regular region and various singular regions.

Let N denote the number of refinements in the geometric mesh. We shall assume that N is proportional to W . Then the proposed method gives exponentially accurate solution in N provided the data satisfy usual regularity conditions [51, 52, 86].

We choose our spectral element functions to be fully non-conforming. Let \mathcal{F}_u denote the spectral element representation of the function u . We define the quadratic form

$$\begin{aligned} \mathcal{W}^{N,W}(\{\mathcal{F}_u\}) &= \mathcal{W}_{regular}^{N,W}(\{\mathcal{F}_u\}) + \mathcal{W}_{vertices}^{N,W}(\{\mathcal{F}_u\}) + \mathcal{W}_{vertex-edges}^{N,W}(\{\mathcal{F}_u\}) \\ &\quad + \mathcal{W}_{edges}^{N,W}(\{\mathcal{F}_u\}). \end{aligned} \quad (5.18)$$

Here $\mathcal{W}_{regular}^{N,W}(\{\mathcal{F}_u\})$, $\mathcal{W}_{vertices}^{N,W}(\{\mathcal{F}_u\})$, $\mathcal{W}_{vertex-edges}^{N,W}(\{\mathcal{F}_u\})$ and $\mathcal{W}_{edges}^{N,W}(\{\mathcal{F}_u\})$ are defined similar to the quadratic forms $\mathcal{U}_{regular}^{N,W}(\{\mathcal{F}_u\})$, $\mathcal{U}_{vertices}^{N,W}(\{\mathcal{F}_u\})$, $\mathcal{U}_{vertex-edges}^{N,W}(\{\mathcal{F}_u\})$ and $\mathcal{U}_{edges}^{N,W}(\{\mathcal{F}_u\})$ as in (2.19), (2.21), (2.33) and (2.41) respectively. Then for problems with Dirichlet boundary conditions by Theorem 2.3.1 it follows that the following estimate is true

$$\mathcal{W}^{N,W}(\{\mathcal{F}_u\}) \leq C(\ln W)^2 \mathcal{V}^{N,W}(\{\mathcal{F}_u\}) \quad (5.19)$$

provided $W = O(e^{N^\alpha})$ for $\alpha < 1/2$.

At the same time using trace theorems for Sobolev spaces there exists a constant k such that

$$\frac{1}{k} \mathcal{V}^{N,W}(\{\mathcal{F}_u\}) \leq \mathcal{W}^{N,W}(\{\mathcal{F}_u\}). \quad (5.20)$$

Hence using (5.19) and (5.20) we conclude that the two quadratic forms $\mathcal{W}^{N,W}(\{\mathcal{F}_u\})$ and $\mathcal{V}^{N,W}(\{\mathcal{F}_u\})$ are spectrally equivalent and there exists a constant K such that

$$\frac{1}{K} \mathcal{V}^{N,W}(\{\mathcal{F}_u\}) \leq \mathcal{W}^{N,W}(\{\mathcal{F}_u\}) \leq K(\ln W)^2 \mathcal{V}^{N,W}(\{\mathcal{F}_u\}) \quad (5.21)$$

provided $W = O(e^{N^\alpha})$ for $\alpha < 1/2$.

We can now use the quadratic form $\mathcal{W}^{N,W}(\{\mathcal{F}_u\})$ which consists of a decoupled set of quadratic forms on each element as a preconditioner. It follows that the condition number of the preconditioned system is $O(\ln W)^2$.

The other case is when the boundary conditions are of mixed Neumann and Dirichlet type. In this case, as above, using Theorem 2.3.2 and trace theorems for Sobolev spaces it follows that for W and N large enough the following estimate holds

$$\frac{1}{K} \mathcal{V}^{N,W}(\{\mathcal{F}_u\}) \leq \mathcal{W}^{N,W}(\{\mathcal{F}_u\}) \leq KN^4 \mathcal{V}^{N,W}(\{\mathcal{F}_u\}).$$

Here K is a constant. It is clear that the quadratic form $\mathcal{W}^{N,W}(\{\mathcal{F}_u\})$ can be used as a preconditioner and the condition number of the preconditioned system is $O(N^4)$.

We will now construct preconditioners on each of the elements in the neighbourhoods of vertices, edges, vertex-edges and the regular region. Here u denotes the spectral element function which is a polynomial of degree W in each of its variables separately defined in various regions of the polyhedron.

The quadratic forms which need to be examined are

$$\mathcal{B}_{regular}(u) = \|u\|_{H^2(Q)}^2 = \int_Q \sum_{|\alpha| \leq 2} |D_{\lambda_1, \lambda_2, \lambda_3}^\alpha u|^2 d\lambda_1 d\lambda_2 d\lambda_3, \quad (5.22)$$

$$\mathcal{B}_{vertices}(u) = \|e^{\chi/2} u\|_{H^2(\tilde{\Omega}_l^v)}^2 = \int_{\tilde{\Omega}_l^v} e^\chi \sum_{|\alpha| \leq 2} |D_{\phi, \theta, \chi}^\alpha u|^2 d\phi d\theta d\chi, \quad (5.23)$$

$$\begin{aligned} \mathcal{B}_{vertex-edges}(u) = & \int_{\tilde{\Omega}_l^{v-e}} e^\zeta (u_{\psi\psi}^2 + u_{\theta\theta}^2 + u_{\psi\theta}^2 + \sin^2 \phi u_{\phi\zeta}^2 + \sin^2 \phi u_{\theta\zeta}^2 \\ & + \sin^4 \phi u_{\zeta\zeta}^2 + u_\psi^2 + u_\theta^2 + \sin^2 \phi u_\zeta^2 + u^2) d\psi d\theta d\zeta, \end{aligned} \quad (5.24)$$

$$\begin{aligned} \mathcal{B}_{edges}(u) = & \int_{\tilde{\Omega}_l^e} (u_{\tau\tau}^2 + u_{\theta\theta}^2 + u_{\tau\theta}^2 + e^{2\tau} u_{\tau x_3}^2 + e^{2\tau} u_{\theta x_3}^2 + e^{4\tau} u_{x_3 x_3}^2 \\ & + u_\tau^2 + u_\theta^2 + e^{2\tau} u_{x_3}^2 + u^2) d\tau d\theta dx_3. \end{aligned} \quad (5.25)$$

Here (ϕ, θ, χ) , (ψ, θ, ζ) and (τ, θ, x_3) denote the modified systems of coordinates introduced in Chapter 2 in vertex neighbourhoods, vertex-edge neighbourhoods and edge neighbourhoods respectively. Moreover $\tilde{\Omega}_l^v$, $\tilde{\Omega}_l^{v-e}$ and $\tilde{\Omega}_l^e$ denote elements in the vertex neighbourhood, vertex-edge neighbourhood and edge neighbourhood respectively.

The construction of preconditioners corresponding to the quadratic forms $\mathcal{B}_{regular}(u)$ and $\mathcal{B}_{vertices}(u)$ is similar to the case of a smooth domain already discussed so we omit the details. It follows that there exist quadratic forms $\mathcal{C}_{regular}(u)$ and $\mathcal{C}_{vertices}(u)$ which

are spectrally equivalent to $\mathcal{B}_{regular}(u)$ and $\mathcal{B}_{vertices}(u)$ respectively and which can be diagonalized using separation of variables technique. We will now obtain preconditioners for edge and vertex-edge neighbourhood elements. For this purpose we observe that for quadratic forms in edge and vertex-edge neighbourhoods it is enough to examine the quadratic form

$$\begin{aligned} \mathcal{B}^*(u) = \int_{-1}^1 \int_{-1}^1 \int_{-1}^1 (u_{xx}^2 + u_{yy}^2 + \eta^2 u_{xz}^2 + \eta^2 u_{yz}^2 + \eta^4 u_{zz}^2 \\ + u_x^2 + u_y^2 + \eta^2 u_z^2 + u^2) dx dy dz . \end{aligned} \quad (5.26)$$

Here $\eta = \sin \phi$ and $\eta = e^\tau$ for vertex-edge and edge neighbourhood elements respectively. We remark that the factor η becomes smaller towards the vertices and edges of the domain Ω .

Making the transformation $\tilde{z} = \frac{z}{\eta}$, so that $\frac{d}{dz} = \frac{1}{\eta} \frac{d}{d\tilde{z}}$, the quadratic form $\mathcal{B}^*(u)$ assumes the form

$$\mathcal{B}^*(u) = \int_{-\frac{1}{\eta}}^{\frac{1}{\eta}} \int_{-1}^1 \int_{-1}^1 (u_{xx}^2 + u_{yy}^2 + u_{xy}^2 + u_{x\tilde{z}}^2 + u_{y\tilde{z}}^2 + u_{\tilde{z}\tilde{z}}^2 + u_x^2 + u_y^2 + u_{\tilde{z}}^2 + u^2) dx dy d\tilde{z} .$$

Let us define the quadratic form

$$\mathcal{C}^*(u) = \int_{-1}^1 \int_{-1}^1 \int_{-1}^1 (u_{xx}^2 + u_{yy}^2 + \eta^4 u_{zz}^2 + u_x^2 + u_y^2 + \eta^2 u_z^2 + u^2) dx dy dz . \quad (5.27)$$

We now show that the quadratic form $\mathcal{C}^*(u)$ is spectrally equivalent to the quadratic form $\mathcal{B}^*(u)$, defined in (5.26). Moreover, $\mathcal{C}^*(u)$ can be diagonalized using separation of variables technique.

Let

$$v(x) = \sum_{i=0}^W \beta_i L_i(x), \quad \text{and} \quad v(z) = \sum_{i=0}^W \gamma_i L_i(z) .$$

Moreover $b = (\beta_0, \beta_1, \dots, \beta_W)^T$ and $d = (\gamma_0, \gamma_1, \dots, \gamma_W)^T$.

We now define the quadratic form

$$\mathcal{E}(v) = \int_I (v_{xx}^2 + v_x^2) dx \quad (5.28)$$

and

$$\mathcal{F}(v) = \int_I v^2 dx . \quad (5.29)$$

We also define the quadratic form

$$\mathcal{G}(v) = \int_I (\eta^4 v_{zz}^2 + \eta^2 v_z^2) dz \quad (5.30)$$

and

$$\mathcal{H}(v) = \int_I v^2 dz . \quad (5.31)$$

Here I denotes the unit interval $(-1, 1)$. Clearly there exist $(W + 1) \times (W + 1)$ matrices E, G and F, H such that

$$\mathcal{E}(v) = b^T E b , \quad \mathcal{G}(v) = d^T G d \quad (5.32)$$

and

$$\mathcal{F}(v) = b^T F b , \quad \mathcal{H}(v) = d^T H d . \quad (5.33)$$

Here the matrices E, G and F, H are symmetric and F, H are positive definite.

Hence there exist $W + 1$ eigenvalues $0 \leq \mu_0 \leq \mu_1 \leq \dots \leq \mu_W$ and $W + 1$ eigenvectors b_0, b_1, \dots, b_W of the symmetric eigenvalue problem

$$(E - \mu F)b = 0 . \quad (5.34)$$

Here

$$(E - \mu_i F)b_i = 0 .$$

Similarly, there exist $W + 1$ eigenvalues $0 \leq \nu_0 \leq \nu_1 \leq \dots \leq \nu_W$ and $W + 1$ eigenvectors d_0, d_1, \dots, d_W of the symmetric eigenvalue problem

$$(G - \nu H)d = 0 . \quad (5.35)$$

Here

$$(G - \nu_i H)d_i = 0 .$$

The eigenvectors b_i and c_i are normalized so that

$$b_i^T F b_j = \delta_j^i, \quad \text{and} \quad d_i^T H d_j = \delta_j^i . \quad (5.36a)$$

Moreover the relations

$$b_i^T E b_j = \mu_i \delta_j^i \quad \text{and} \quad d_i^T G d_j = \nu_i \delta_j^i \quad (5.36b)$$

hold. Let $b_i = (b_{i,0}, b_{i,1}, \dots, b_{i,W})$ and $d_i = (d_{i,0}, d_{i,1}, \dots, d_{i,W})$. We now define the polynomials

$$\phi_i(x) = \sum_{m=0}^W b_{i,m} L_m(x) \text{ for } 0 \leq i \leq W, \quad (5.37a)$$

$$\phi_j(y) = \sum_{m=0}^W b_{j,m} L_m(y) \text{ for } 0 \leq j \leq W, \quad (5.37b)$$

$$\theta_k(z) = \sum_{m=0}^W d_{k,m} L_m(z) \text{ for } 0 \leq k \leq W. \quad (5.37c)$$

Next, let $\chi_{i,j,k}$ denote the polynomial

$$\chi_{i,j,k}(x, y, z) = \phi_i(x) \phi_j(y) \theta_k(z) \quad (5.38)$$

for $0 \leq i \leq W, 0 \leq j \leq W, 0 \leq k \leq W$.

Note that $\{\chi_{i,j,k}(x, y, z)\}_{i,j,k}$ is the tensor product of the polynomials $\phi_i(x)$, $\phi_j(y)$ and $\theta_k(z)$. The eigenvalue $\sigma_{i,j,k}$ corresponding to the eigenvector $\chi_{i,j,k}$ is given by the relation

$$\sigma_{i,j,k} = \mu_i + \mu_j + \nu_k + 1. \quad (5.39)$$

Let $\tilde{\mathcal{C}}^*(f, g)$ be the bilinear form induced by the quadratic form $\mathcal{C}^*(u)$. Then

$$\begin{aligned} \tilde{\mathcal{C}}^*(f, g) = \int_{-1}^1 \int_{-1}^1 \int_{-1}^1 (f_{xx} f_{xx} + f_{yy} g_{yy} + \eta^4 f_{zz} g_{zz} + f_x g_x + f_y g_y \\ + \eta^2 f_z g_z + f g) dx dy dz. \end{aligned}$$

It is easy to show that

$$\begin{aligned} \tilde{\mathcal{C}}^*(\chi_{i,j,k}, \chi_{l,m,n}) &= (\mu_i + \mu_j + \nu_k + 1) \delta_l^i \delta_m^j \delta_n^k \\ &= \sigma_{i,j,k} \delta_l^i \delta_m^j \delta_n^k. \end{aligned}$$

Hence the eigenvectors of the quadratic form $\mathcal{C}^*(u)$ are $\{\chi_{i,j,k}\}_{i,j,k}$ and the eigenvalues are $\{\sigma_{i,j,k}\}_{i,j,k}$. Thus, the quadratic form $\mathcal{C}^*(u)$ can be diagonalized in the basis $\{\chi_{i,j,k}\}_{i,j,k}$. Therefore, the matrix corresponding to the quadratic form $\mathcal{C}^*(u)$ is easy to invert.

Now proceeding as earlier, it can be shown that the quadratic forms $\mathcal{B}^*(u)$ and $\mathcal{C}^*(u)$ are spectrally equivalent. Moreover, the quadratic form $\mathcal{C}^*(u)$ can be inverted in $O(W^4)$ operations.

Thus, it follows that there exist quadratic forms $\mathcal{C}_{vertex-edges}(u)$ and $\mathcal{C}_{edges}(u)$ which are spectrally equivalent to $\mathcal{B}_{vertex-edges}(u)$ and $\mathcal{B}_{edges}(u)$ respectively and which can be diagonalized using separation of variables technique.

5.3 Parallelization Techniques

In minimizing the functional $\mathcal{R}^{N,W}(\{\mathcal{F}_v\})$ we seek a solution which minimizes the sum of weighted norms of the residuals in the partial differential equation and a fractional Sobolev norm of the residuals in the boundary conditions and enforce continuity by adding a term which measures the sum of squares of the jumps in the function and its derivatives at inter-element boundaries in appropriate Sobolev norms, suitably weighted in various regions of the polyhedron.

In order to obtain a solution using PCGM we must be able to compute residuals in the normal equations inexpensively. Since we are minimizing $\mathcal{R}^{N,W}(\{\mathcal{F}_v\})$ over all $\{\mathcal{F}_v\} \in \mathcal{S}^{N,W}$ (space of spectral element functions) we have

$$\mathcal{R}^{N,W}(U + \epsilon V) = \mathcal{R}^{N,W}(U) + 2\epsilon V^t(XU - YG) + O(\epsilon^2)$$

for all V , where U is a vector assembled from the values of

$$\left\{ \{u_l^r(\lambda)\}_{l=1}^{N_r}, \{u_l^v(x^v)\}_{l=1}^{N_v}, \{u_l^{v-e}(x^{v-e})\}_{l=1}^{N_{v-e}}, \{u_l^e(x^e)\}_{l=1}^{N_e} \right\}.$$

V is a vector similarly assembled and G is assembled from the data. Here X and Y denote matrices. Thus we have to solve $XU - YG = 0$ and so we must be able to compute $XV - YG$ economically during the iterative process. We will now explain in brief how this can be done. The idea is very similar to the case of two dimensional problems so we refer the reader to [85] for details.

The above minimization amounts to an overdetermined system of equations consisting of collocating the residuals in the partial differential equation, the residuals in the boundary conditions and jumps in the function and its derivatives at inter-element boundaries at an over determined set of collocation points, weighted suitably. In fact, we collocate the partial differential equation on a finer grid of Gauss-Lobatto-Legendre (GLL) points

and then we apply the adjoint differential operator to these residuals and project these values back to the original grid. Such a treatment obviously involves integration by parts and hence leads to evaluation of terms at the boundaries. These boundary terms can be evaluated by a collocation procedure and the other boundary terms corresponding to jump terms at the inter-element boundaries can be easily calculated.

5.3.1 Integrals on the element domain

We first show how to compute the integrals on the element domain. Since each element is mapped onto the master cube $Q = (-1, 1)^3 = (-1, 1) \times (-1, 1) \times (-1, 1)$, so we consider the computations only on Q .

Consider the integral

$$\|(\mathcal{L})^a u - \hat{F}\|_Q^2. \quad (5.40)$$

Its variation is

$$\int_Q (\mathcal{L})^a v ((\mathcal{L})^a u - \hat{F}) d\xi_1 d\xi_2 d\xi_3. \quad (5.41)$$

Here

$$\begin{aligned} (\mathcal{L})^a w = & \hat{A}w_{\xi_1\xi_1} + \hat{B}w_{\xi_2\xi_2} + \hat{C}w_{\xi_3\xi_3} + \hat{D}w_{\xi_1\xi_2} + \hat{E}w_{\xi_2\xi_3} + \hat{F}w_{\xi_3\xi_1} \\ & + \hat{G}w_{\xi_1} + \hat{H}w_{\xi_2} + \hat{I}w_{\xi_3} + \hat{J}w, \end{aligned}$$

where the coefficients $\hat{A}, \hat{B}, \hat{C}$ etc. are polynomials of degree N and \hat{F} is a filtered representation of F .

Let,

$$u(\xi_1, \xi_2, \xi_3) = \sum_{i=0}^{2N} \sum_{j=0}^{2N} \sum_{k=0}^{2N} \alpha_{i,j,k} \xi_1^i \xi_2^j \xi_3^k$$

and

$$v(\xi_1, \xi_2, \xi_3) = \sum_{i=0}^{2N} \sum_{j=0}^{2N} \sum_{k=0}^{2N} \beta_{i,j,k} \xi_1^i \xi_2^j \xi_3^k.$$

The differential operator $(\mathcal{L})^a$ is obtained from the differential operator

$$\begin{aligned} Lw = & Aw_{\xi_1\xi_1} + Bw_{\xi_2\xi_2} + Cw_{\xi_3\xi_3} + Dw_{\xi_1\xi_2} + Ew_{\xi_2\xi_3} + Fw_{\xi_3\xi_1} \\ & + Gw_{\xi_1} + Hw_{\xi_2} + Iw_{\xi_3} + Jw, \end{aligned}$$

with analytic coefficients A, B, C etc. We choose the coefficients $\widehat{A}, \widehat{B}, \widehat{C}$ etc. so that they are the orthogonal projections of A, B, C etc. into the space of polynomials of degree N with respect to the usual inner product in $H^2(Q)$.

Let $(\mathcal{L}^a)^T$ denote the formal adjoint of the differential operator $(\mathcal{L})^a$.

Then

$$\begin{aligned} (\mathcal{L}^a)^T w = & \left(\widehat{A}w \right)_{\xi_1 \xi_1} + \left(\widehat{B}w \right)_{\xi_2 \xi_2} + \left(\widehat{C}w \right)_{\xi_3 \xi_3} + \left(\widehat{D}w \right)_{\xi_1 \xi_2} + \left(\widehat{E}w \right)_{\xi_2 \xi_3} \\ & + \left(\widehat{F}w \right)_{\xi_3 \xi_1} - \left(\widehat{G}w \right)_{\xi_1} - \left(\widehat{H}w \right)_{\xi_2} - \left(\widehat{I}w \right)_{\xi_3} + \widehat{J}w, \end{aligned}$$

Let \mathfrak{z} denote $(\mathcal{L})^a u - \widehat{F}$. Integrating (5.41) by parts we obtain

$$\begin{aligned} & \int_Q (\mathcal{L})^a v \mathfrak{z} \, d\xi_1 \, d\xi_2 \, d\xi_3 \\ &= \int_Q v (\mathcal{L}^a)^T \mathfrak{z} \, d\xi_1 \, d\xi_2 \, d\xi_3 \\ &+ \int_{-1}^1 \int_{-1}^1 \left((\widehat{A}v_{\xi_1} + \widehat{G}v) \mathfrak{z} - v \left((\widehat{A}\mathfrak{z})_{\xi_1} + (\widehat{F}\mathfrak{z})_{\xi_3} + (\widehat{D}\mathfrak{z})_{\xi_2} \right) \right) (1, \xi_2, \xi_3) d\xi_2 \, d\xi_3 \\ &- \int_{-1}^1 \int_{-1}^1 \left((\widehat{A}v_{\xi_1} + \widehat{D}v_{\xi_2} + \widehat{G}v) \mathfrak{z} - v \left((\widehat{A}\mathfrak{z})_{\xi_1} + (\widehat{F}\mathfrak{z})_{\xi_3} \right) \right) (-1, \xi_2, \xi_3) d\xi_2 \, d\xi_3 \\ &+ \int_{-1}^1 v(\widehat{D}\mathfrak{z})(1, 1, \xi_3) d\xi_3 - \int_{-1}^1 v(\widehat{D}\mathfrak{z})(1, -1, \xi_3) d\xi_3 \\ &+ \int_{-1}^1 \int_{-1}^1 \left((\widehat{B}v_{\xi_2} + \widehat{H}v) \mathfrak{z} - v \left((\widehat{B}\mathfrak{z})_{\xi_2} + (\widehat{D}\mathfrak{z})_{\xi_1} + (\widehat{E}\mathfrak{z})_{\xi_3} \right) \right) (\xi_1, 1, \xi_3) d\xi_1 \, d\xi_3 \\ &- \int_{-1}^1 \int_{-1}^1 \left((\widehat{B}v_{\xi_2} + \widehat{E}v_{\xi_3} + \widehat{H}v) \mathfrak{z} - v \left((\widehat{B}\mathfrak{z})_{\xi_2} + (\widehat{D}\mathfrak{z})_{\xi_1} \right) \right) (\xi_1, -1, \xi_3) d\xi_1 \, d\xi_3 \\ &+ \int_{-1}^1 v(\widehat{E}\mathfrak{z})(\xi_1, 1, 1) d\xi_1 - \int_{-1}^1 v(\widehat{E}\mathfrak{z})(\xi_1, 1, -1) d\xi_1 \\ &+ \int_{-1}^1 \int_{-1}^1 \left((\widehat{C}v_{\xi_3} + \widehat{I}v) \mathfrak{z} - v \left((\widehat{C}\mathfrak{z})_{\xi_3} + (\widehat{E}\mathfrak{z})_{\xi_2} + (\widehat{F}\mathfrak{z})_{\xi_1} \right) \right) (\xi_1, \xi_2, 1) d\xi_1 \, d\xi_2 \\ &- \int_{-1}^1 \int_{-1}^1 \left((\widehat{C}v_{\xi_3} + \widehat{F}v_{\xi_1} + \widehat{I}v) \mathfrak{z} - v \left((\widehat{C}\mathfrak{z})_{\xi_3} + (\widehat{E}\mathfrak{z})_{\xi_2} \right) \right) (\xi_1, \xi_2, -1) d\xi_1 \, d\xi_2 \\ &+ \int_{-1}^1 v(\widehat{F}\mathfrak{z})(1, \xi_2, 1) d\xi_2 - \int_{-1}^1 v(\widehat{F}\mathfrak{z})(-1, \xi_2, 1) d\xi_2 \end{aligned} \tag{5.42}$$

Now u, v and $\widehat{A}, \widehat{B}, \widehat{C}$ etc. are polynomials of degree N in each of the variables ξ_1, ξ_2 and ξ_3 . Moreover \widehat{F} is a polynomial of degree $2N$. Hence all the integrands are polynomials of degree $4N$ in each of the variables ξ_1, ξ_2 and ξ_3 and so the integral may be exactly

evaluated by the Gauss-Lobatto-Legendre (GLL) quadrature formula with $2N + 1$ points. Let $\xi_{1,0}^{2N}, \dots, \xi_{1,2N}^{2N}$, $\xi_{2,0}^{2N}, \dots, \xi_{2,2N}^{2N}$ and $\xi_{3,0}^{2N}, \dots, \xi_{3,2N}^{2N}$ represent the quadrature points in ξ_1 , ξ_2 and ξ_3 directions respectively and $w_0^{2N}, \dots, w_{2N}^{2N}$ the corresponding weights.

Proposition 5.3.1. *Let the matrix $D^{2N} = d_{i,j}^{2N}$ denote the differentiation matrix. Then*

$$\frac{dl}{d\xi}(\xi_i^{2N}) = \sum_{j=0}^{2N} d_{i,j}^{2N} l(\xi_j^{2N}) \quad (5.43)$$

if l is a polynomial of degree less than or equal to $2N$.

Using the GLL quadrature rule we obtain

$$\begin{aligned} & \int_Q (\mathcal{L})^a v ((\mathcal{L})^a u - \tilde{F}) d\xi_1 d\xi_2 d\xi_3 \\ &= \sum_{i=0}^{2N} \sum_{j=0}^{2N} \sum_{k=0}^{2N} v(\xi_{1,i}^{2N}, \xi_{2,j}^{2N}, \xi_{3,k}^{2N}) (w_i^{2N} w_j^{2N} w_k^{2N} L^T \mathfrak{z}(\xi_{1,i}^{2N}, \xi_{2,j}^{2N}, \xi_{3,k}^{2N})) \\ &+ \sum_{i=0}^{2N} \sum_{j=0}^{2N} \sum_{k=0}^{2N} v(\xi_{1,i}^{2N}, \xi_{2,j}^{2N}, \xi_{3,k}^{2N}) (w_j^{2N} w_k^{2N} d_{2N,i}^{2N} A(1, \xi_{2,j}^{2N}, \xi_{3,k}^{2N}) \mathfrak{z}(1, \xi_{2,j}^{2N}, \xi_{3,k}^{2N})) \\ &+ \sum_{j=0}^{2N} \sum_{k=0}^{2N} v(1, \xi_{2,j}^{2N}, \xi_{3,k}^{2N}) (w_j^{2N} w_k^{2N} (G\mathfrak{z} - (A\mathfrak{z})_{\xi_1} - (F\mathfrak{z})_{\xi_3} - (D\mathfrak{z})_{\xi_2})(1, \xi_{2,j}^{2N}, \xi_{3,k}^{2N})) \\ &- \sum_{i=0}^{2N} \sum_{j=0}^{2N} \sum_{k=0}^{2N} v(\xi_{1,i}^{2N}, \xi_{2,j}^{2N}, \xi_{3,k}^{2N}) (w_j^{2N} w_k^{2N} (d_{0,i}^{2N} A(-1, \xi_{2,j}^{2N}, \xi_{3,k}^{2N}) \mathfrak{z}(-1, \xi_{2,j}^{2N}, \xi_{3,k}^{2N}) \\ &\quad + d_{j,i}^{2N} D(-1, \xi_{2,j}^{2N}, \xi_{3,k}^{2N}) \mathfrak{z}(-1, \xi_{2,j}^{2N}, \xi_{3,k}^{2N}))) \\ &- \sum_{j=0}^{2N} \sum_{k=0}^{2N} v(-1, \xi_{2,j}^{2N}, \xi_{3,k}^{2N}) (w_j^{2N} w_k^{2N} (G\mathfrak{z} - (A\mathfrak{z})_{\xi_1} - (F\mathfrak{z})_{\xi_3})(-1, \xi_{2,j}^{2N}, \xi_{3,k}^{2N})) \\ &+ \sum_{i=0}^{2N} \sum_{j=0}^{2N} \sum_{k=0}^{2N} v(\xi_{1,i}^{2N}, \xi_{2,j}^{2N}, \xi_{3,k}^{2N}) (w_i^{2N} w_k^{2N} d_{2N,j}^{2N} B(\xi_{1,i}^{2N}, 1, \xi_{3,k}^{2N}) \mathfrak{z}(\xi_{1,i}^{2N}, 1, \xi_{3,k}^{2N})) \\ &+ \sum_{i=0}^{2N} \sum_{k=0}^{2N} v(\xi_{1,i}^{2N}, 1, \xi_{3,k}^{2N}) (w_i^{2N} w_k^{2N} (H\mathfrak{z} - (B\mathfrak{z})_{\xi_2} - (D\mathfrak{z})_{\xi_1} - (E\mathfrak{z})_{\xi_3})(\xi_{1,i}^{2N}, 1, \xi_{3,k}^{2N})) \\ &- \sum_{i=0}^{2N} \sum_{j=0}^{2N} \sum_{k=0}^{2N} v(\xi_{1,i}^{2N}, \xi_{2,j}^{2N}, \xi_{3,k}^{2N}) (w_i^{2N} w_k^{2N} (d_{0,j}^{2N} B(\xi_{1,i}^{2N}, -1, \xi_{3,k}^{2N}) \mathfrak{z}(\xi_{1,i}^{2N}, -1, \xi_{3,k}^{2N}) \\ &\quad + d_{k,j}^{2N} E(\xi_{1,i}^{2N}, -1, \xi_{3,k}^{2N}) \mathfrak{z}(\xi_{1,i}^{2N}, -1, \xi_{3,k}^{2N}))) \\ &- \sum_{i=0}^{2N} \sum_{k=0}^{2N} v(\xi_{1,i}^{2N}, -1, \xi_{3,k}^{2N}) (w_i^{2N} w_k^{2N} (H\mathfrak{z} - (B\mathfrak{z})_{\xi_2} - (D\mathfrak{z})_{\xi_1})(\xi_{1,i}^{2N}, -1, \xi_{3,k}^{2N})) \end{aligned}$$

$$\begin{aligned}
& + \sum_{i=0}^{2N} \sum_{j=0}^{2N} \sum_{k=0}^{2N} v(\xi_{1,i}^{2N}, \xi_{2,j}^{2N}, \xi_{3,k}^{2N}) (w_i^{2N} w_j^{2N} d_{2N,k}^{2N} C(\xi_{1,i}^{2N}, \xi_{2,j}^{2N}, 1) \mathfrak{z}(\xi_{1,i}^{2N}, \xi_{2,j}^{2N}, 1)) \\
& + \sum_{i=0}^{2N} \sum_{j=0}^{2N} v(\xi_{1,i}^{2N}, \xi_{2,j}^{2N}, 1) (w_i^{2N} w_j^{2N} (I\mathfrak{z} - (C\mathfrak{z})_{\xi_3} - (E\mathfrak{z})_{\xi_2} - (F\mathfrak{z})_{\xi_1}) (\xi_{1,i}^{2N}, \xi_{2,j}^{2N}, 1)) \\
& - \sum_{i=0}^{2N} \sum_{j=0}^{2N} \sum_{k=0}^{2N} v(\xi_{1,i}^{2N}, \xi_{2,j}^{2N}, \xi_{3,k}^{2N}) (w_i^{2N} w_j^{2N} (d_{0,k}^{2N} C(\xi_{1,i}^{2N}, \xi_{2,j}^{2N}, -1) \mathfrak{z}(\xi_{1,i}^{2N}, \xi_{2,j}^{2N}, -1) \\
& \quad + d_{i,k}^{2N} F(\xi_{1,i}^{2N}, \xi_{2,j}^{2N}, -1) \mathfrak{z}(\xi_{1,i}^{2N}, \xi_{2,j}^{2N}, -1))) \\
& - \sum_{i=0}^{2N} \sum_{j=0}^{2N} v(\xi_{1,i}^{2N}, \xi_{2,j}^{2N}, -1) (w_i^{2N} w_j^{2N} (I\mathfrak{z} - (C\mathfrak{z})_{\xi_3} - (E\mathfrak{z})_{\xi_2}) (\xi_{1,i}^{2N}, \xi_{2,j}^{2N}, -1)) \\
& + \sum_{k=0}^{2N} v(1, 1, \xi_{3,k}^{2N}) w_k^{2N} D(1, 1, \xi_{3,k}^{2N}) \mathfrak{z}(1, 1, \xi_{3,k}^{2N}) - \sum_{k=0}^{2N} v(1, -1, \xi_{3,k}^{2N}) w_k^{2N} D(1, -1, \xi_{3,k}^{2N}) \\
& \times \mathfrak{z}(1, -1, \xi_{3,k}^{2N}) + \sum_{i=0}^{2N} v(\xi_{1,i}^{2N}, 1, 1) w_i^{2N} E(\xi_{1,i}^{2N}, 1, 1) \mathfrak{z}(\xi_{1,i}^{2N}, 1, 1) \\
& - \sum_{i=0}^{2N} v(\xi_{1,i}^{2N}, 1, -1) w_i^{2N} E(\xi_{1,i}^{2N}, 1, -1) \mathfrak{z}(\xi_{1,i}^{2N}, 1, -1) \\
& + \sum_{j=0}^{2N} v(1, \xi_{2,j}^{2N}, 1) w_j^{2N} F(1, \xi_{2,j}^{2N}, 1) \mathfrak{z}(1, \xi_{2,j}^{2N}, 1) - \sum_{j=0}^{2N} v(-1, \xi_{2,j}^{2N}, 1) w_j^{2N} F(-1, \xi_{2,j}^{2N}, 1) \\
& \times \mathfrak{z}(-1, \xi_{2,j}^{2N}, 1)
\end{aligned} \tag{5.44}$$

Note that we have used unfiltered coefficients A, B, C etc. in the right hand side.

Remark 5.3.1. *The stability estimate is stated in terms of unfiltered coefficients of the differential operator, and we use unfiltered coefficients in our computations. Of course, in writing the above we commit an error. It can be argued as in [37, 38, 85, 86] that this error is spectrally small. In fact, if we assume that the boundary of the domain Ω is analytic, the coefficients of the differential operator are analytic and the data is analytic then the error committed is exponentially small in N . Hence we do not need to filter the coefficients of the differential and boundary operators or the data in any of our computations.*

Rewrite $u(\xi_{1,i}^N, \xi_{2,j}^N, \xi_{3,k}^N)$ by arranging them in lexicographic order and denote

$$U_{(N+1)^2k+(N+1)j+i}^N = u(\xi_{1,i}^N, \xi_{2,j}^N, \xi_{3,k}^N) \quad \text{for } 0 \leq i, j, k \leq N,$$

and let

$$U_{(2N+1)^2k+(2N+1)j+i}^{2N} = u(\xi_{1,i}^{2N}, \xi_{2,j}^{2N}, \xi_{3,k}^{2N}) \quad \text{for } 0 \leq i, j, k \leq 2N.$$

Similarly

$$Z_{(2N+1)^2k+(2N+1)j+i}^{2N} = (Lu - F)(\xi_{1,i}^{2N}, \xi_{2,j}^{2N}, \xi_{3,k}^{2N}),$$

for $0 \leq i, j, k \leq 2N$, are arranged in lexicographic order.

Then we may write

$$\int_Q (\mathcal{L})^a v ((\mathcal{L})^a u - \widehat{F}) d\xi_1 d\xi_2 d\xi_3 = (V^{2N})^T R Z^{2N},$$

where R is a matrix such that RZ^{2N} is easily computed.

5.3.2 Integrals on the boundary of the elements

We now show how to evaluate the boundary terms. For this we have to examine the norm $H^{1/2}(E)$, here E denote either S or T . Now

$$\|l\|_{1/2,E}^2 = \|l\|_{0,E}^2 + \int_E \int_E \frac{(l(\xi_1, \xi_2) - l(\xi'_1, \xi'_2))^2}{((\xi_1 - \xi'_1)^2 + (\xi_2 - \xi'_2)^2)^{3/2}} d\xi_1 d\xi_2 d\xi'_1 d\xi'_2.$$

However if E is S , which is always the case, then we prefer to use the equivalent norm [64]

$$\begin{aligned} \|l\|_{1/2,S}^2 &= \|l\|_{0,S}^2 + \int_{-1}^1 \int_{-1}^1 \int_{-1}^1 \frac{(l(\xi_1, \xi_2) - l(\xi'_1, \xi'_2))^2}{(\xi_1 - \xi'_1)^2} d\xi_1 d\xi'_1 d\xi_2 \\ &\quad + \int_{-1}^1 \int_{-1}^1 \int_{-1}^1 \frac{(l(\xi_1, \xi_2) - l(\xi_1, \xi'_2))^2}{(\xi_2 - \xi'_2)^2} d\xi_2 d\xi'_2 d\xi_1. \end{aligned}$$

Let $l(\xi_1, \xi_2)$ be a polynomial of degree less than or equal to $2N$. Then $\frac{l(\xi_1, \xi_2) - l(\xi'_1, \xi'_2)}{(\xi_1 - \xi'_1)}$ is a polynomial of degree less than or equal to $2N$ in ξ_1 and ξ'_1 . Now using the GLL quadrature

rule we can write

$$\begin{aligned}
\|l\|_{1/2,S}^2 &= \sum_{i=0}^{2N} \sum_{j=0}^{2N} w_i^{2N} w_j^{2N} l^2(\xi_{1,i}^{2N}, \xi_{2,j}^{2N}) \\
&+ \sum_{j=0}^{2N} \sum_{i=0, i' \neq i}^{2N} \sum_{i'=0}^{2N} w_j^{2N} w_i^{2N} w_{i'}^{2N} \left(\frac{l(\xi_{1,i}^{2N}, \xi_{2,j}^{2N}) - l(\xi_{1,i'}^{2N}, \xi_{2,j}^{2N})}{(\xi_{1,i}^{2N} - \xi_{1,i'}^{2N})} \right)^2 \\
&+ \sum_{i=0}^{2N} \sum_{j=0, j' \neq j}^{2N} \sum_{j'=0}^{2N} w_i^{2N} w_j^{2N} w_{j'}^{2N} \left(\frac{l(\xi_{1,i}^{2N}, \xi_{2,j}^{2N}) - l(\xi_{1,i}^{2N}, \xi_{2,j'}^{2N})}{(\xi_{2,j}^{2N} - \xi_{2,j'}^{2N})} \right)^2 \\
&+ \sum_{i=0}^{2N} \sum_{j=0}^{2N} (w_i^{2N})^2 w_j^{2N} \left(\sum_{k=0}^{2N} d_{i,k} l(\xi_{1,k}^{2N}, \xi_{2,j}^{2N}) \right)^2 \\
&+ \sum_{j=0}^{2N} \sum_{i=0}^{2N} (w_j^{2N})^2 w_i^{2N} \left(\sum_{k=0}^{2N} d_{j,k} l(\xi_{1,i}^{2N}, \xi_{2,k}^{2N}) \right)^2
\end{aligned}$$

Thus there is a symmetric positive definite matrix H^{2N} such that

$$\|l\|_{1/2,S}^2 = \sum_{i=0}^{2N} \sum_{j=0}^{2N} \sum_{i'=0}^{2N} \sum_{j'=0}^{2N} l(\xi_i^{2N}, \eta_j^{2N}) H_{i,j,i',j'}^{2N} l(\xi_{i'}^{2N}, \eta_{j'}^{2N}) \quad (5.45)$$

A typical boundary term will be of the form

$$\|(\hat{P}u_{\xi_1} + \hat{Q}u_{\xi_2} + \hat{R}u_{\xi_3})(\xi_1, \xi_2, 1) - \hat{g}(\xi_1, \xi_2)\|_{1/2,S}$$

and its variation is given by

$$\begin{aligned}
&\sum_{i=0}^{2N} \sum_{j=0}^{2N} \sum_{i'=0}^{2N} \sum_{j'=0}^{2N} (\hat{P}v_{\xi_1} + \hat{Q}v_{\xi_2} + \hat{R}v_{\xi_3})(\xi_{1,i}^{2N}, \xi_{2,j}^{2N}, 1) H_{i,j,i',j'}^{2N} \\
&\times ((\hat{P}u_{\xi_1} + \hat{Q}u_{\xi_2} + \hat{R}u_{\xi_3})(\xi_{1,i'}^{2N}, \xi_{2,j'}^{2N}, 1) - \hat{g}(\xi_{1,i'}^{2N}, \xi_{2,j'}^{2N})). \quad (5.46)
\end{aligned}$$

Let

$$\sigma_{i,j}^{2N} = \sum_{i'=0}^{2N} \sum_{j'=0}^{2N} H_{i,j,i',j'}^{2N} ((\hat{P}u_{\xi_1} + \hat{Q}u_{\xi_2} + \hat{R}u_{\xi_3})(\xi_{1,i'}^{2N}, \xi_{2,j'}^{2N}, 1) - \hat{g}(\xi_{1,i'}^{2N}, \xi_{2,j'}^{2N})).$$

Then

$$\begin{aligned}
& \sum_{i=0}^{2N} \sum_{j=0}^{2N} (\hat{P}v_{\xi_1} + \hat{Q}v_{\xi_2} + \hat{R}v_{\xi_3})(\xi_{1,i}^{2N}, \xi_{2,j}^{2N}, 1) \sigma_{i,j}^{2N} \\
&= \sum_{i=0}^{2N} \sum_{i'=0}^{2N} \sum_{j=0}^{2N} v(\xi_{1,i'}^{2N}, \xi_{2,j}^{2N}, 1) d_{i,i'}^{2N} \left(\hat{P}(\xi_{1,i}^{2N}, \xi_{2,j}^{2N}, 1) \sigma_{i,j}^{2N} \right) \\
&+ \sum_{i=0}^{2N} \sum_{j=0}^{2N} \sum_{j'=0}^{2N} v(\xi_{1,i}^{2N}, \xi_{2,j'}^{2N}, 1) d_{j,j'}^{2N} \left(\hat{Q}(\xi_{1,i}^{2N}, \xi_{2,j}^{2N}, 1) \sigma_{i,j}^{2N} \right) \\
&+ \sum_{i=0}^{2N} \sum_{j=0}^{2N} \sum_{k=0}^{2N} v(\xi_{1,i}^{2N}, \xi_{2,j}^{2N}, \xi_{3,k}^{2N}) d_{2N,k}^{2N} \left(\hat{R}(\xi_{1,i}^{2N}, \xi_{2,j}^{2N}, 1) \sigma_{i,j}^{2N} \right).
\end{aligned}$$

Proposition 5.3.2. *Let*

$$Y_{i,j}^{2N} = (Pu_{\xi_1} + Qu_{\xi_2} + Ru_{\xi_3} - g)(\xi_{1,i}^{2N}, \xi_{2,j}^{2N}, 1), \quad X^{2N} = H^{2N} Y^{2N},$$

and let \hat{P} , \hat{Q} and \hat{R} be filtered representations of P , Q and R . Similarly \hat{g} is a filtered representation of the actual boundary data g .

Then we may write

$$\begin{aligned}
& \sum_{i=0}^{2N} \sum_{j=0}^{2N} \sum_{i'=0}^{2N} \sum_{j'=0}^{2N} (\hat{P}v_{\xi_1} + \hat{Q}v_{\xi_2} + \hat{R}v_{\xi_3})(\xi_{1,i}^{2N}, \xi_{2,j}^{2N}, 1) H_{i,j,i',j'}^{2N} \\
& \times ((\hat{P}u_{\xi_1} + \hat{Q}u_{\xi_2} + \hat{R}u_{\xi_3})(\xi_{1,i'}^{2N}, \xi_{2,j'}^{2N}, 1) - \hat{g}(\xi_{1,i'}^{2N}, \xi_{2,j'}^{2N})) \\
&= \sum_{i=0}^{2N} \sum_{i'=0}^{2N} \sum_{j=0}^{2N} v(\xi_{1,i'}^{2N}, \xi_{2,j}^{2N}, 1) d_{i,i'}^{2N} (P(\xi_{1,i}^{2N}, \xi_{2,j}^{2N}, 1) X_{i,j}^{2N}) \\
&+ \sum_{i=0}^{2N} \sum_{j=0}^{2N} \sum_{j'=0}^{2N} v(\xi_{1,i}^{2N}, \xi_{2,j'}^{2N}, 1) d_{j,j'}^{2N} (Q(\xi_{1,i}^{2N}, \xi_{2,j}^{2N}, 1) X_{i,j}^{2N}) \\
&+ \sum_{i=0}^{2N} \sum_{j=0}^{2N} \sum_{k=0}^{2N} v(\xi_{1,i}^{2N}, \xi_{2,j}^{2N}, \xi_{3,k}^{2N}) d_{2N,k}^{2N} (R(\xi_{1,i}^{2N}, \xi_{2,j}^{2N}, 1) X_{i,j}^{2N}) \\
&= (V^{2N})^t T X^{2N}.
\end{aligned}$$

Here T is a $(2N+1)^3 \times (2N+1)^2$ matrix and $T X^{2N}$ can be easily computed. In writing the above we are again committing an error and this error can be shown to be exponentially small in N once more. Hence there is no need to filter the coefficients of the boundary operators or the data.

Adding all the terms we obtain

$$\begin{aligned}
& \int_Q (\mathcal{L})^a v ((\mathcal{L})^a u - \widehat{F}) d\xi_1 d\xi_2 d\xi_3 \\
& + \sum_{i=0}^{2N} \sum_{j=0}^{2N} \sum_{i'=0}^{2N} \sum_{j'=0}^{2N} (\widehat{P}v_{\xi_1} + \widehat{Q}v_{\xi_2} + \widehat{R}v_{\xi_3})(\xi_{1,i}^{2N}, \xi_{2,j}^{2N}, 1) H_{i,j,i',j'}^{2N} \\
& \times ((\widehat{P}u_{\xi_1} + \widehat{Q}u_{\xi_2} + \widehat{R}u_{\xi_3})(\xi_{1,i'}^{2N}, \xi_{2,j'}^{2N}, 1) - \widehat{g}(\xi_{1,i'}^{2N}, \xi_{2,j'}^{2N})) + \dots \\
& = (V^{2N})^t (RZ^{2N} + TX^{2N} + \dots) = (V^{2N})^t O^{2N}
\end{aligned}$$

where $O^{2N} = RZ^{2N} + TX^{2N} + \dots$ is a $(2N+1)^3$ vector which can be easily computed.

Now there exists a matrix G^N such that $V^{2N} = G^N V^N$. Hence

$$(V^{2N})^t O^{2N} = (V^N)^T \left((G^N)^T O^{2N} \right).$$

In [85, 86] it has been shown how $(G^N)^T O^{2N}$ can be computed for two dimensional problems without having to compute and store any mass and stiffness matrices. Same idea extends here and so we just describe the steps involved in brief and refer the reader to [85, 86] for details.

Let γ_m^N be the normalizing factors used in computing the *discrete Legendre transform* as

$$\gamma_m^N = \begin{cases} (m+1/2)^{-1} & \text{if } m < N, \\ 2/N & \text{if } m = N \end{cases}.$$

Let $\{O_{i,j,k}\}_{0 \leq i,j,k \leq 2N}$ be defined as $O_{i,j,k} = O_{k(2N+1)^2 + j(2N+1) + i}^{2N}$. Now we perform the following set of operations.

1. Define $O_{i,j,k} \leftarrow O_{i,j,k} / w_i^{2N} w_j^{2N} w_k^{2N}$.
2. Calculate $\{\Delta_{i,j,k}\}_{0 \leq i,j,k \leq 2N}$ the Legendre transform of $\{O_{i,j,k}\}_{0 \leq i,j,k \leq 2N}$. Define

$$\Delta_{i,j,k} \leftarrow \gamma_i^{2N} \gamma_j^{2N} \gamma_k^{2N} \Delta_{i,j,k}.$$

3. Calculate $\mu_{i,j,k} \leftarrow \Delta_{i,j,k} / \gamma_i^N \gamma_j^N \gamma_k^N$, $0 \leq i, j, k \leq N$.

4. Compute ε , the *inverse Legendre transform* of μ . Define

$$\varepsilon_{i,j,k} \leftarrow w_i^N w_j^N w_k^N \varepsilon_{i,j,k}, \quad 0 \leq i, j, k \leq N.$$

5. Define a vector J of dimension $(N+1)^3$ as

$$J_{k(N+1)^2+j(N+1)+i} = \varepsilon_{i,j,k} \text{ for } 0 \leq i, j, k \leq N.$$

Then $J = (G^N)^t O^{2N}$. Thus we see to compute J we do not need to compute and store any matrices such as the mass and stiffness matrices.

Clearly, $O(N^4)$ operations are required to compute the residual vector on a parallel computer. In order to compute the residual vector we need to communicate the values of the function and its derivatives on the boundary of the element between neighbouring elements. Moreover, when computing the two global scalars, needed to update the approximate solution and the search direction during each step of PCGM, some scalars have to be exchanged among all the processors. Thus we see that inter processor communication is small.

Chapter 6

Numerical Results

6.1 Introduction

In this chapter we present the results of the numerical simulations which have been performed to validate the asymptotic error estimates and estimates of computational complexity that we have obtained. First, we consider test problems on non-smooth domains with smooth solutions (i.e. solutions without singularities) which include Laplace, Poisson and Helmholtz problems with different types of homogeneous and non-homogeneous boundary conditions (e.g. Dirichlet, mixed, Neumann and Robin). Next, we consider a general elliptic equation with mixed boundary conditions. Numerical results for a variable coefficient problem on L -shaped domain are also presented which confirm the theoretical estimates obtained.

The method works for non self-adjoint problems too. Computational results for a non self-adjoint problem with variable coefficients are provided.

In order to show the effectiveness of the method in dealing with elliptic problems on non-smooth domains containing singularities we shall consider various examples of Laplace and Poisson equations on a number of polyhedral domains containing all three types of singularities namely, vertex, edge and vertex-edge singularities with Dirichlet and mixed type of boundary conditions to include all possible cases of singularities that may arise due to the presence of corners and edges. We show that the error between the exact

and the approximate solution is exponentially small.

The spectral element functions are nonconforming. The method we have described is a least-squares collocation method and to obtain our approximate solution we solve the normal equations using Preconditioned Conjugate Gradient Method (PCGM). The residuals in the normal equations can be obtained without computing and storing mass and stiffness matrices. A preconditioner is defined for the method which is a block diagonal matrix, where each diagonal block corresponds to an element. It is also shown in Chapter 5 that there exists a new preconditioner which is a diagonal preconditioner on each element. Let N denote the number of refinements in the geometrical mesh and W denote an upper bound on the polynomial degree. We shall assume that N is proportional to W . Then the condition number of the preconditioned system is $K_{N,W}$, where $K_{N,W} = O((\ln W)^2)$ for Dirichlet problems and $K_{N,W} = O(N^4)$ for mixed problems with Neumann and Dirichlet boundary conditions, provided $W = O(e^{N^\alpha})$ for $\alpha < 1/2$.

As stated in previous chapters after obtaining our approximate solution consisting of non-conforming spectral element functions we can make a correction to it so that the corrected solution is conforming and is an exponentially accurate approximation to the true solution in the H^1 norm over the whole domain. These corrections are explained in the proof of Lemma 3.3.1 in Appendix C.1.

We perform the PCGM until a stopping criterion on the relative norm of the residual vector for the normal equations becoming less than ϵ , a specified number, is satisfied. Since we would need to perform $O\left(\frac{\sqrt{\kappa}}{2} \left|\log\left(\frac{2}{\epsilon}\right)\right|\right)$ iterations of the PCGM to satisfy the stopping criterion, we would need to perform $O(N(\ln(N)))$ and $O(N^3)$ iterations of the PCGM for Dirichlet and mixed problems respectively to obtain the approximate solution. Here κ denotes condition number of the preconditioner.

We shall denote by $\Omega, \Omega^{(v)}, \Omega^{(e)}, \Omega^{(v-e)}$ etc. polyhedral domains in R^3 . Throughout this chapter, (x_1, x_2, x_3) , (ϕ, θ, ρ) and (r, θ, x_3) will denote the Cartesian, the spherical and the cylindrical coordinates, respectively of points in these domains. In case the solution is smooth we shall denote the Cartesian coordinates by (x, y, z) .

Let $u_{appx.}$ be the spectral element solution obtained from the minimization problem

and $u_{ex.}$ be the exact solution. Then the relative error is defined as

$$||E||_{rel} = \frac{||u_{approx.} - u_{ex.}||_{H^1}}{||u_{ex.}||_{H^1}}.$$

The computations are carried out on a distributed memory parallel computer which consists of V20Z and V40Z Sun Fire Servers. Each of the Sun Fire Servers is a 2 CPU 64 bit 2.4 GHZ Oepron AMD machine with 4GB RAM. The library used for inter processor communication is Message Passing Interface (MPI).

6.2 Test Problems in Regular Regions

We start with the numerical results for various test problems on polyhedral domains on which the solution is analytic. Let $\Omega = Q = (-1, 1)^3$ denote the standard cube in \mathbb{R}^3 with boundary $\partial\Omega$. Let N denote the number of refinements in each direction and W denote the degree of the polynomials used for approximation. In each of the examples that will follow we have used three different meshes with uniform mesh size $h = 2.0, 1.0$ and 0.67 in each direction which corresponds to $N = 1, 2$ and 3 respectively (Figure 6.1).

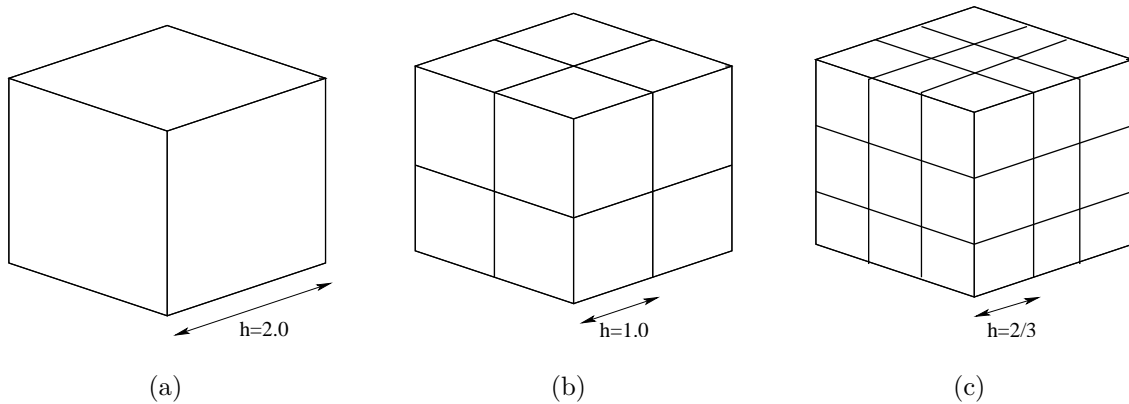


Figure 6.1: The domain $\Omega = Q = (-1, 1)^3$ = standard cube with uniform mesh refinements. (a) Mesh 1, (b) Mesh 2 and (c) Mesh 3.

It is known from Chapter 4 that the error in the regular (smooth) region obeys

$$||u_{approx.} - u_{ex.}||_{H^1} \leq C e^{-b N_{dof}^{1/3}}. \quad (6.1)$$

Here N_{dof} denotes the number of degrees of freedom (DOF).

Thus, in case the solution is analytic on $\bar{\Omega}$, exponential convergence can be achieved by increasing the polynomial order and keeping the number of elements fixed. Hence, for practical implementation it is enough to compute the error for p -version of the method. In what follows by iterations we always mean the total number of iterations required to compute the solution upto desired accuracy by PCGM.

Remark 6.2.1. *For computational simplicity, in all our computations we assume that the degrees of the approximating polynomials are uniform within each element.*

Example 6.2.1. (Laplace equation with Dirichlet boundary conditions):

Our first example is the Laplace equation in the unit cube $\Omega = (0, 1)^3$ shown in Figure 6.2, with Dirichlet boundary conditions:

$$\begin{aligned}\Delta u &= u_{xx} + u_{yy} + u_{zz} = 0 & \text{in } \Omega, \\ u &= g & \text{on } \partial\Omega\end{aligned}$$

where the data g is chosen so that the exact solution is

$$u(x, y, z) = \frac{1}{\pi^2 \sinh \sqrt{2}\pi} \sin(\pi x) \sin(\pi y) \sinh(\sqrt{2}\pi z).$$

The results are given in Table 6.1. The relative error (in %) against polynomial order

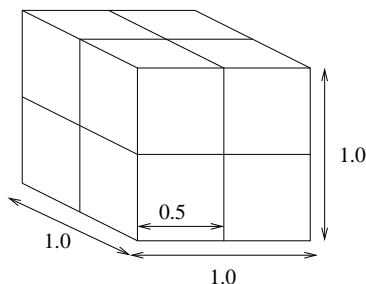


Figure 6.2: Mesh imposed on $\Omega = (0, 1)^3$ with mesh size $h = 0.5$.

p and iterations against p are plotted in Figure 6.3(a) and 6.3(b) respectively. The error curve is a straight line and this shows the exponential rate of convergence. The relative error is plotted on a log-scale in each case.

Table 6.1: Performance of the p -version for **Laplace** equation with Dirichlet boundary conditions

$p = W$	DOF	Iterations	$\ E\ _{rel}(\%)$
2	64	51	0.380275E+02
4	512	213	0.204875E+01
6	1728	303	0.269917E-01
8	4096	380	0.221613E-03
10	8000	456	0.106885E-05
12	13824	523	0.452056E-08

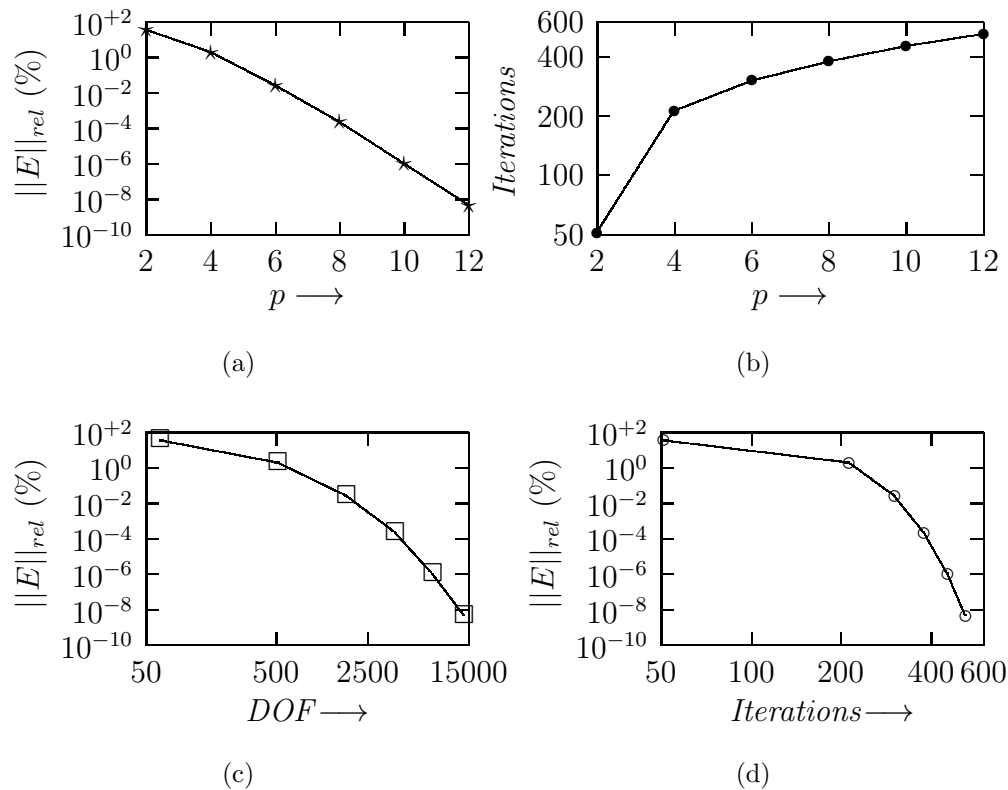


Figure 6.3: (a) Error, (b) Iterations vs. p , (c) Error vs. DOF and (d) Error vs. Iterations for Laplace equation with Dirichlet boundary conditions.

In Figure 6.3(c) a graph is drawn for $\|E\|_{rel}$ against degrees of freedom on a log – log scale. It is clear that the error obeys (6.1).

Example 6.2.2. (Poisson equation with homogeneous boundary conditions):

We now consider the Poisson equation posed on $\Omega = Q = (-1, 1)^3$ with homogeneous Dirichlet boundary conditions as follows:

$$\begin{aligned} Lu = -\Delta u &= f && \text{in } \Omega, \\ u &= 0 && \text{on } \partial\Omega \end{aligned}$$

where the right hand side function f is chosen so that the exact solution is

$$u(x, y, z) = \sin(\pi x) \sin(\pi y) \sin(\pi z).$$

The performance of the p –version on Mesh 2 of Figure 6.1(b) is given in Table 6.2 for

Table 6.2: Performance of the p –version for **Poisson** equation with homogeneous boundary conditions

$p = W$	DOF	Iterations	$\ E\ _{rel}(\%)$
2	64	10	0.131056E+02
4	512	56	0.178835E+01
6	1728	87	0.607343E-01
8	4096	100	0.872751E-03
10	8000	109	0.717092E-05
12	13824	116	0.384300E-07

different values of the polynomial order W . In Figure 6.4(a), the relative error (in %) is plotted against p . The error decays to $\approx 10^{-8}\%$ with $p = 12$. Figure 6.4(b) depicts iterations against p . The relative error is plotted on a log-scale. The relative error against degrees of freedom and iterations is plotted on a log – log scale in Figure 6.4(c) and Figure 6.4(d) respectively.

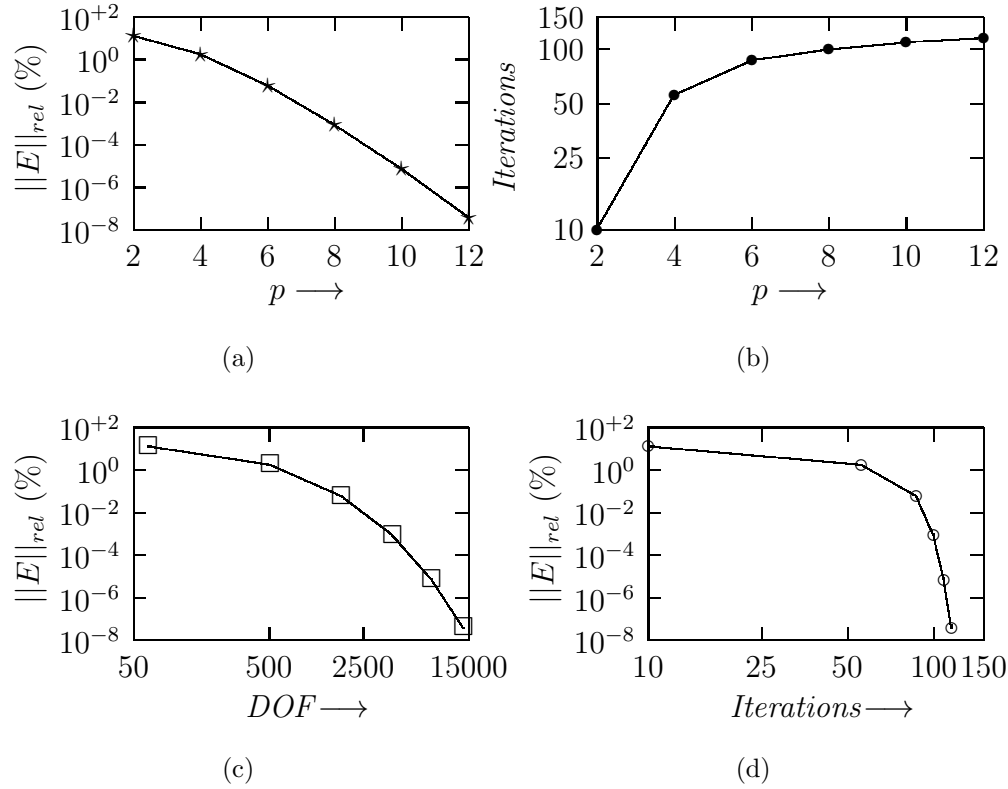


Figure 6.4: (a) Error, (b) Iterations as a function of p , (c) Error vs. DOF and (d) Error vs. Iterations for Poisson equation with homogeneous boundary conditions.

Example 6.2.3. (Poisson equation with mixed boundary conditions):

Now, let us consider the Poisson equation posed on $\Omega = (-1, 1)^3$ with mixed Dirichlet and Neumann boundary conditions as follows:

$$\begin{aligned}
 Lu &= -\Delta u = f && \text{in } \Omega, \\
 u &= g && \text{on } \mathcal{D} \subset \partial\Omega \\
 \frac{\partial u}{\partial \nu} &= h && \text{on } \mathcal{N} = \partial\Omega \setminus \mathcal{D}.
 \end{aligned}$$

Here $\mathcal{D} = \Gamma_1 \cup \Gamma_2 \cup \Gamma_3$, where Γ_1, Γ_2 and Γ_3 are the faces corresponding to $x = -1, x = 1$ and $y = -1$ respectively. $\mathcal{N} = \Gamma_4 \cup \Gamma_5 \cup \Gamma_6$, where Γ_4, Γ_5 and Γ_6 are the faces corresponding to $y = 1, z = -1$ and $z = 1$ respectively. Moreover, ν denotes the outer unit normal to the faces where Neumann boundary conditions are imposed.

Table 6.3: Performance of the p -version for **Poisson** equation with mixed boundary conditions

$p = W$	DOF	Iterations	$\ E\ _{rel}(\%)$
2	64	97	0.103976E+02
4	512	159	0.540972E+00
6	1728	183	0.614615E-02
8	4096	201	0.284761E-04
10	8000	217	0.716345E-07
12	13824	232	0.876167E-09

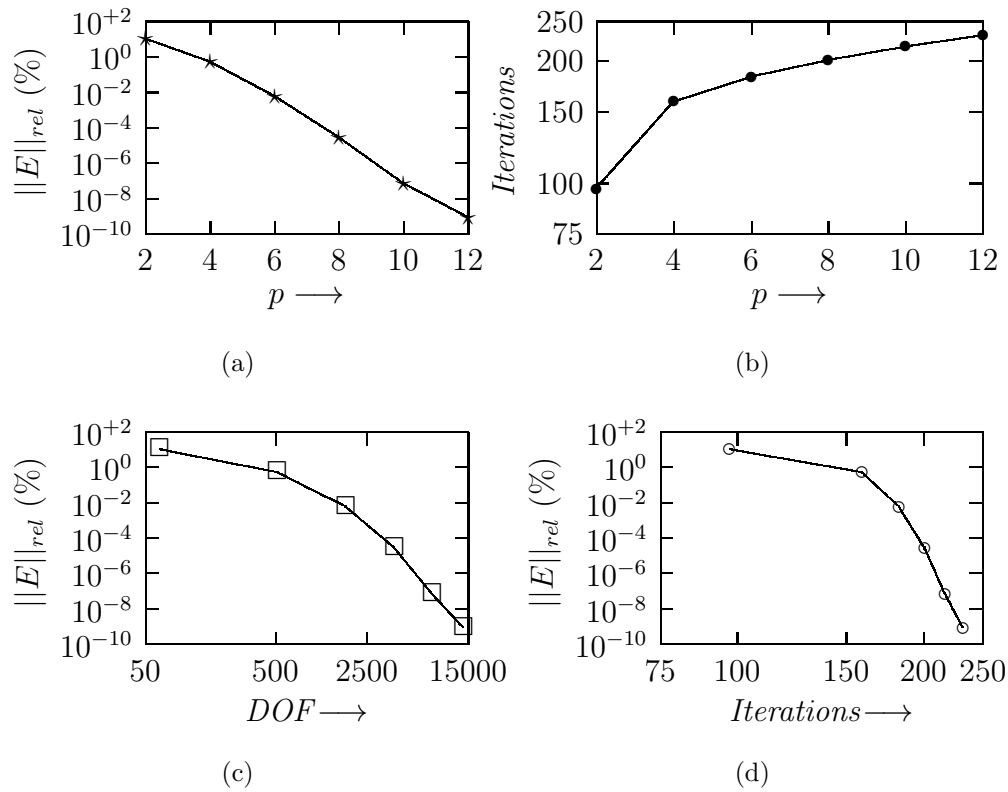


Figure 6.5: (a) Error vs. p , (b) Iterations vs. p , (c) Error vs. DOF and (d) Error vs. Iterations for Poisson equation with mixed boundary conditions.

The right hand side function f and the data g, h are chosen so that the true solution is

$$u(x, y, z) = \frac{2}{\pi^2} \sin\left(\frac{\pi x}{2}\right) \left(\cos\left(\frac{\pi y}{2}\right) - \sin\left(\frac{\pi z}{2}\right) \right).$$

Results for p -version of the method for the mesh in Figure 6.1(b) are provided in Table 6.3. The relevant curves are given in Figure 6.5. In Figure 6.5(a), $\log ||E||_{rel}$ is plotted against W and the graph is almost linear.

In our next example, we consider a constant coefficient elliptic problem of Helmholtz type with mixed boundary conditions and examine the performance of the h -version for the three meshes shown in Figure 6.1 i.e. for $h = 2, 1$ and 0.67 . Polynomials with a uniform degree $W = 4$ are used. Comparison with p -version of the spectral element method is provided to show its effectiveness over h -version.

Example 6.2.4. (Helmholtz equation with constant coefficients):

Consider the elliptic boundary value problem

$$\begin{aligned} Lu &= -\Delta u + u = f & \text{in } \Omega, \\ Bu &= g & \text{on } \partial\Omega \end{aligned}$$

where $\Omega = (-1, 1)^3$ and let us choose the data f and g so that the exact solution is

$$u(x, y, z) = e^x \cos y \sin z.$$

Different choices of the operator B , give rise to different boundary conditions. For our analysis we impose mixed Dirichlet and Neumann boundary conditions on $\partial\Omega$ by choosing B as follows:

$$\begin{aligned} B_1(u) &= u(-1, y, z), B_2(u) = u(1, y, z), B_3(u) = u(x, -1, z), \\ B_4(u) &= \frac{\partial u}{\partial y}(x, 1, z), B_5(u) = -\frac{\partial u}{\partial z}(x, y, -1) \text{ and } B_6(u) = \frac{\partial u}{\partial z}(x, y, 1). \end{aligned}$$

The h -version:

Table 6.4 shows relative errors (%) against different mesh sizes h for $W = 4$. The relative error decays to $\approx 0.05\%$ when $h = 2/3$ and $N_{dof} \approx 1800$.

The p -version:

Performance of the p -version is given in Table 6.5. A uniform mesh of size $h = 1$ is used which corresponds to the Mesh 2 (Figure 6.1).

In Figure 6.6(a), the relative error is plotted against p . Figure 6.6(b), contains iterations vs. p . The relative error (%) is plotted on a log-scale.

Table 6.4: Performance of the h -version for **Helmholtz** problem

h	N_{dof}	Iterations	$ E _{rel}(\%)$
2	64	54	0.839583E+00
1	512	76	0.114335E+00
2/3	1728	216	0.377972E-01

Table 6.5: Performance of the p -version for **Helmholtz** problem on Mesh 2

$p=N$	N_{dof}	Iterations	$ E _{rel}(\%)$
2	64	25	0.696654E+01
4	512	76	0.114335E+00
6	1728	135	0.521586E-03
8	4096	222	0.993449E-06
10	8000	294	0.109613E-08
12	13824	302	0.149336E-08

Comparison between the h and p versions are shown in Figure 6.7, where the relative errors are plotted against the number of degrees of freedom on a $\log - \log$ scale. It is clear that the p -version is superior to the h -version as expected.

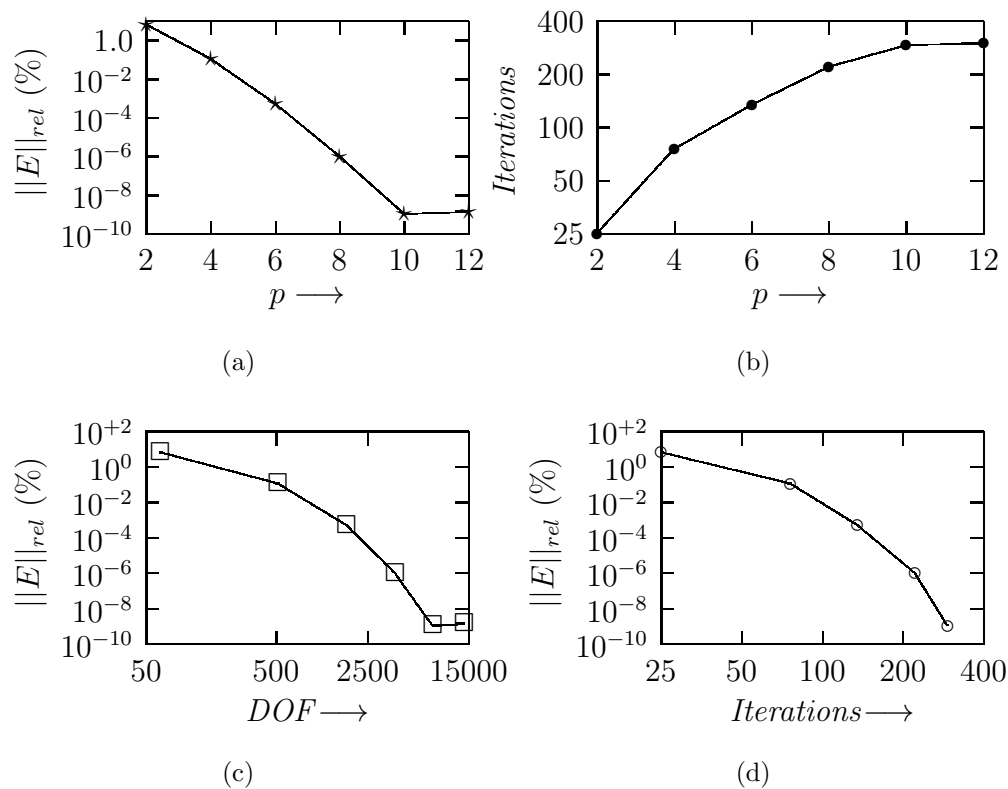


Figure 6.6: (a) Error vs. p , (b) Iterations vs. p , (c) Error vs. DOF and (d) Error vs. Iterations for Helmholtz problem with mixed boundary conditions.

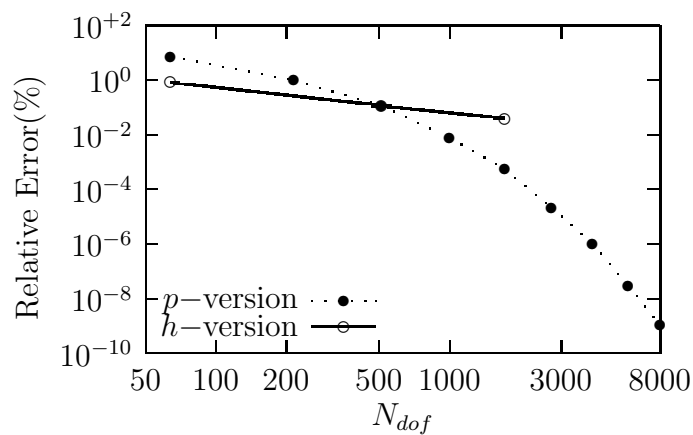


Figure 6.7: Comparison between h and p versions: Error vs. Degrees of Freedom.

The examples presented so far deal with constant coefficient differential operators. However, the method is equally efficient for a general elliptic problem too. To illustrate this we now give more examples which include problems with variable coefficients, non

self-adjoint problems and a general elliptic problem on L -shaped domain.

Example 6.2.5. (Elliptic equation with variable coefficients):

Let us consider the following variable coefficient boundary value problem with Robin boundary conditions:

$$\begin{aligned} a(x, y, z)u_{xx} + b(x, y, z)u_{yy} + c(x, y, z)u_{zz} + d(x, y, z)u &= f \quad \text{in } \Omega = (-1, 1)^3, \\ \frac{\partial u}{\partial \nu} + u &= g \quad \text{on } \partial\Omega \end{aligned}$$

where ν denotes the outward unit normal to the boundary $\partial\Omega$. We choose the coefficients as:

$$\begin{aligned} a(x, y, z) &= -(1.00 + 0.01y \sin x), \quad b(x, y, z) = -(2.50 + 0.02 \cos(x^2 + z)), \\ c(x, y, z) &= -(3.00 + 0.03ye^z) \quad \text{and} \quad d(x, y, z) = 0.15 \sin(2\pi(y + z)). \end{aligned}$$

Moreover, the right hand side function f and the data g are chosen such that the exact solution is

$$u(x, y, z) = \cos(\pi(x + y)) \exp(z).$$

We examine the p -version of the spectral element method with fixed mesh size $h = 2/3$

Table 6.6: Performance of the p -version for elliptic problem with **variable** coefficients

$p = W$	DOF	Iterations	Relative Error(%)
2	216	231	0.284009E+02
3	729	332	0.737578E+01
4	1728	369	0.203203E+01
5	3375	397	0.318021E+00
6	5832	414	0.352678E-01
7	9216	428	0.337654E-02
8	13824	437	0.263263E-03
9	19683	445	0.185170E-04

that corresponds to the Mesh 3 in Figure 6.1. Results are given in Table 6.6.

Figure 6.8(a) shows a graph between $\log \|E\|_{rel}$ against polynomial degree p . The relationship is almost linear demonstrating that the error decays exponentially. In Figure 6.8(b), $\log(\text{iterations})$ is drawn against p while in Figure 6.8(c) error against degrees of freedom is plotted on a $\log - \log$ scale.

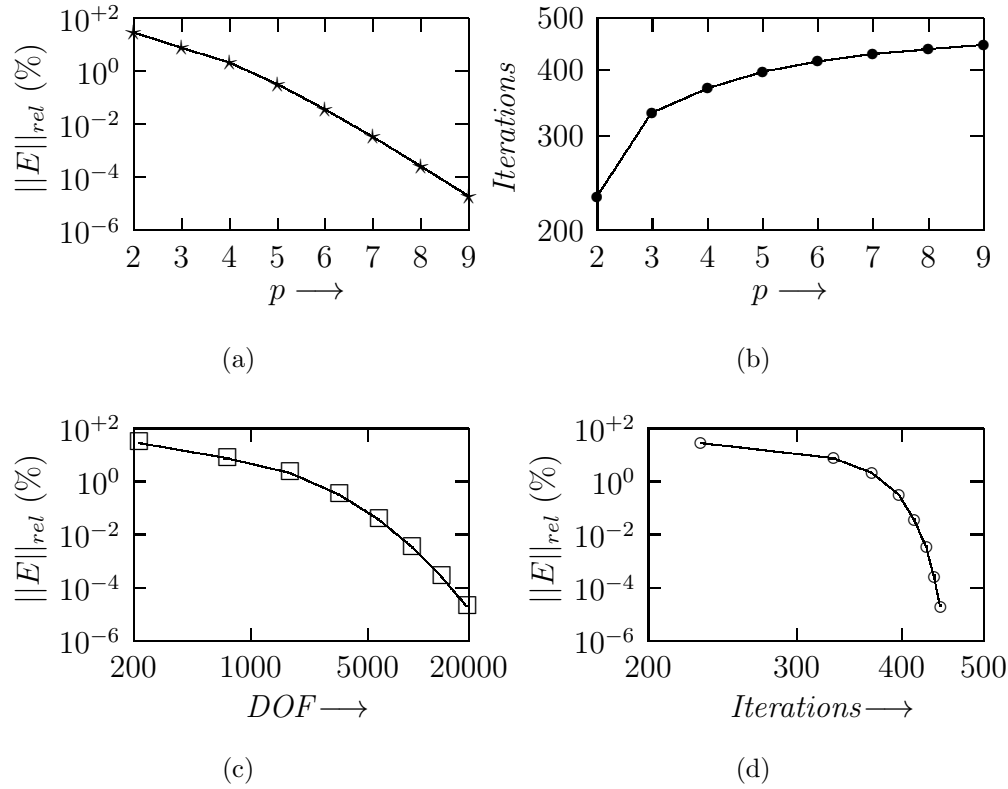


Figure 6.8: (a) Error vs. p , (b) Iterations vs. p , (c) Error vs. DOF and (d) Error vs. Iterations for elliptic problem with variable coefficients.

Example 6.2.6. (Variable coefficient problem on L shaped domain):

In our next example we consider the following variable coefficients problem with Dirichlet boundary conditions on the solution domain Ω shown in Figure 6.9:

$$\begin{aligned}
 &a(x, y, z)u_{xx} + b(x, y, z)u_{yy} + c(x, y, z)u_{zz} + d(x, y, z)u_x \\
 &\quad + e(x, y, z)u_y + h(x, y, z)u_z + l(x, y, z)u = f \quad \text{in } \Omega, \\
 &\quad u = g \quad \text{on } \mathcal{D} = \partial\Omega
 \end{aligned}$$

where the choice of the coefficients is as follows:

$$\begin{aligned} a(x, y, z) &= -(0.50 + 0.01y \sin x), \quad b(x, y, z) = -(1.50 + 0.02 \cos(x^2 + z)), \\ c(x, y, z) &= -(2.00 + 0.03ye^z), \quad d(x, y, z) = 0.25 \sin(2\pi(y + z)), \\ e(x, y, z) &= 0.25 \sin(2\pi(z + x)), \quad h(x, y, z) = 0.25 \sin(2\pi(x + y)), \\ \text{and } l(x, y, z) &= 2.50 - 0.025 \exp\left(\frac{\pi(x+y+z)}{2}\right). \end{aligned}$$

Moreover, the right hand side function f and the data g are chosen such that the exact solution is

$$u(x, y, z) = \sin\left(\frac{\pi(x + y + z)}{2}\right) \exp\left(\frac{\pi z}{2}\right).$$

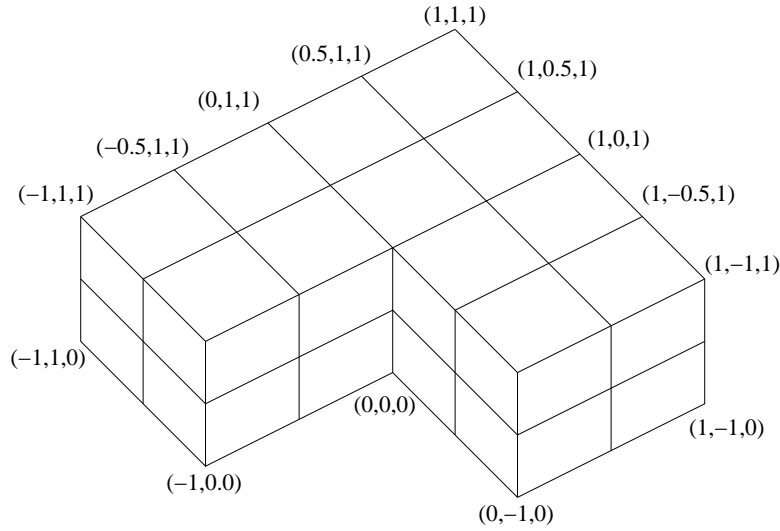


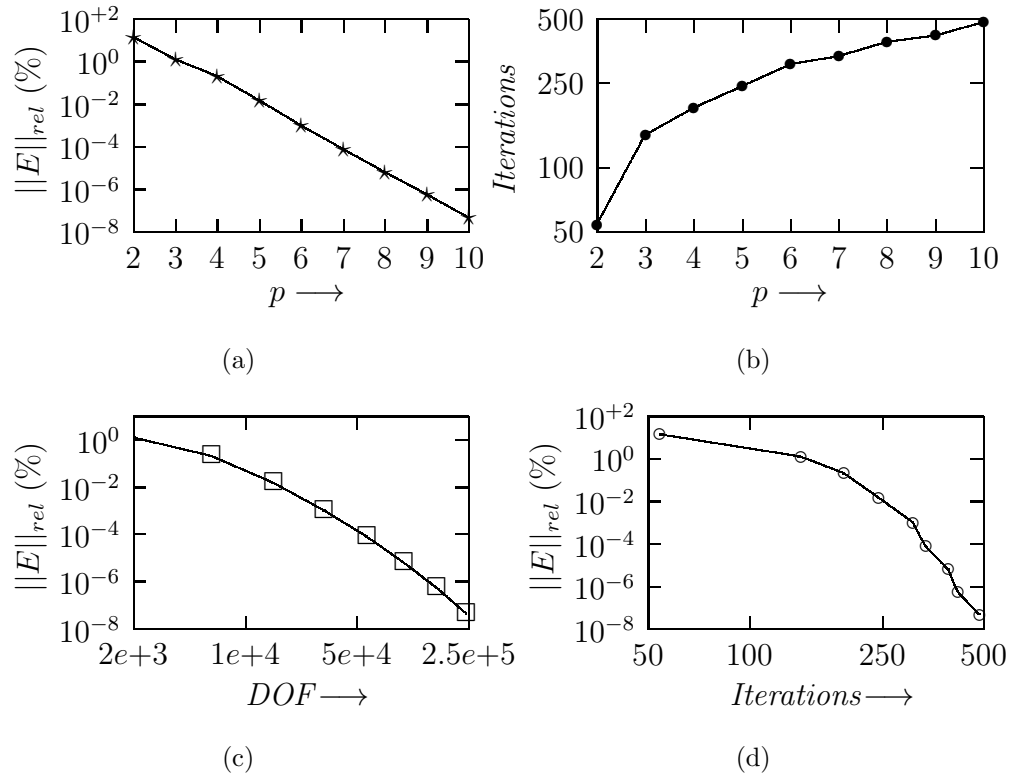
Figure 6.9: Mesh imposed on domain Ω containing 24 brick elements

Performance of the p -version on mesh (containing brick elements) shown in Figure 6.9 is provided in Table 6.7. The relative error decays to $\approx 10^{-8}$ when $p = 10$ and $N_{dof} = 240000$.

Relative error and iterations are plotted against polynomial degree p in Figure 6.10(a) and 6.10(b) respectively. In Figure 6.10(c) we plot the relative error as a function of degrees of freedom. The graph would be a straight line if the error obeys (6.1) exactly.

Table 6.7: Performance of the p -version for elliptic problem on **L-shaped** domain

$p = W$	DOF	Iterations	Relative Error(%)
2	384	54	0.143522E+02
3	1944	143	0.131046E+01
4	6144	192	0.209803E+00
5	15000	243	0.149981E-01
6	31104	308	0.101674E-02
7	57624	336	0.785544E-04
8	98304	393	0.611724E-05
9	157464	420	0.549101E-06
10	240000	488	0.447650E-07

Figure 6.10: (a) Error vs. p , (b) Iterations vs. p , (c) Error vs. DOF and (d) Error vs. Iterations for elliptic problem on L-shaped domain.

Example 6.2.7. (General elliptic equation with variable coefficients: A non self-adjoint problem):

The method works for non self-adjoint problems too. To verify this, let us consider the following non self-adjoint general elliptic problem with mixed boundary conditions.

$$\begin{aligned}
 & a(x, y, z)u_{xx} + b(x, y, z)u_{yy} + c(x, y, z)u_{zz} \\
 & + d(x, y, z)(u_{xy} + u_{yz} + u_{zx}) + e(x, y, z)u = f \quad \text{in } \Omega = (-1, 1)^3, \\
 & u = g \quad \text{on } \mathcal{D} \subset \partial\Omega \\
 & \frac{\partial u}{\partial \nu} = h \quad \text{on } \mathcal{N} = \partial\Omega \setminus \mathcal{D}.
 \end{aligned}$$

Here \mathcal{D} and \mathcal{N} denote the Dirichlet and Neumann boundary part of $\partial\Omega$ respectively and are chosen similar to those in example 6.2.3. Further, we choose the coefficients of the problem as follows:

$$\begin{aligned}
 & a(x, y, z) = -(0.50 + 0.05 \exp(xyz)), \quad b(x, y, z) = -(1.00 + 0.015 \cos(x + y)), \\
 & c(x, y, z) = -(2.50 + 0.02 \exp(y + z)), \quad d(x, y, z) = -0.001 \sin(\pi(x + y + z)) \\
 & \text{and } e(x, y, z) = \left(4.05 + 0.045 \cos\left(\frac{\pi(x+y+z)}{2}\right) \right).
 \end{aligned}$$

Moreover, the right hand side function f and the data g and h are chosen such that the true solution is

$$u(x, y, z) = \left(\sin(\pi x) + \sin\left(\frac{\pi y}{2}\right) \right) \cos(\pi z).$$

We examine the p -version of the method on different meshes in Table 6.8 for polynomial degree $p = 2, \dots, 10$. It is clear that the method performs best on Mesh 3 and the error reduces to approximately $10^{-6}\%$. However, on Mesh 1 the relative error decays slowly. Figure 6.11 shows $\log \|E\|_{rel}$ plotted against p for different meshes.

In Figure 6.12(a) we plot error against polynomial order p . Error as a function of degrees of freedom is plotted in Figure 6.12(c) on a $\log - \log$ scale.

Table 6.8: Performance of the p -version on different meshes for general elliptic (non self-adjoint) problem with **variable** coefficients

$p = W$	Mesh 1	Mesh 2	Mesh 3
2	0.498666E+02	0.485737E+02	0.291328E+02
3	0.507328E+02	0.107829E+02	0.586317E+01
4	0.227058E+02	0.517751E+01	0.149092E+01
5	0.143968E+02	0.814482E+00	0.237686E+00
6	0.408230E+01	0.234810E+00	0.292025E-01
7	0.184822E+01	0.279261E-01	0.289156E-02
8	0.311612E+00	0.430208E-02	0.236661E-03
9	0.104765E+00	0.377498E-03	0.168223E-04
10	0.136308E-01	0.431639E-04	0.352480E-05

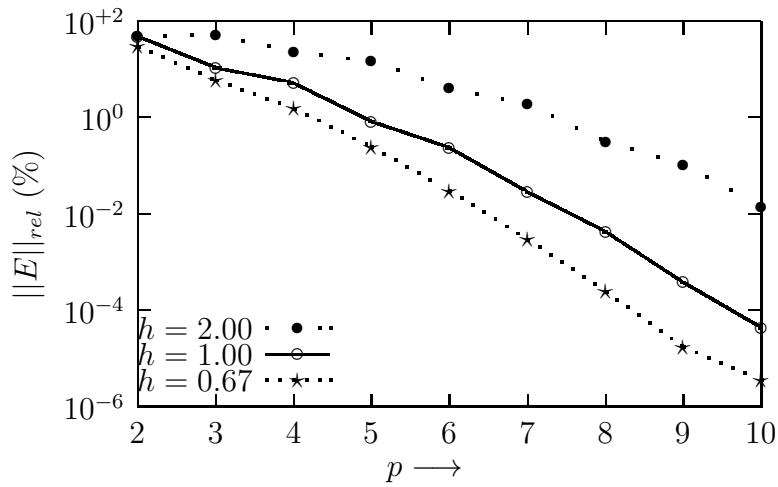
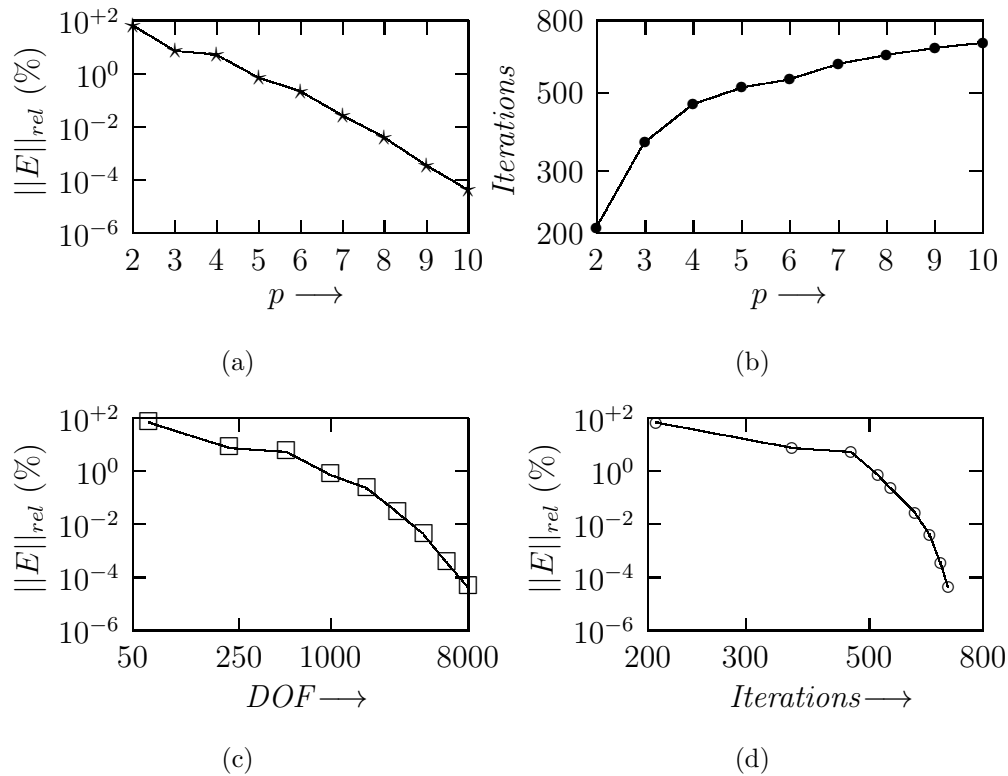


Figure 6.11: Error as a function of W for different values of h for general elliptic (non self-adjoint) problem.

Table 6.9: Performance of the p -version for **non self-adjoint** problem.

$p = W$	DOF	Iterations	Relative Error(%)
2	64	207	0.670184E+02
3	216	364	0.741499E+01
4	512	464	0.536971E+01
5	1000	519	0.725120E+00
6	1728	547	0.228276E+00
7	2744	605	0.267290E-01
8	4096	642	0.420000E-02
9	5832	671	0.364194E-03
10	8000	694	0.424524E-04

Figure 6.12: (a) Error vs. p , (b) Iterations vs. p , (c) Error vs. DOF and (d) Error vs. Iterations for general elliptic (non self-adjoint) equation with variable coefficients.

6.3 Test Problems in Singular Regions

In order to show the effectiveness of the proposed method in dealing with three dimensional elliptic boundary value problems containing singularities we now present results of numerical simulations for model problems on various polyhedral domains containing different types of singularities discussed in the previous chapters which aim to verify the validity of the asymptotic error estimates and estimates of computational complexity that have been obtained.

Hereafter N will always denote the number of layers in the geometric mesh and W , the polynomial order used. It is assumed that N is proportional to W . In case of examples with vertex and edge singularities all our calculations are based on a parallel computer with $O(N)$ processors and each element is being mapped onto a separate processor. However, in case of examples with vertex-edge singularities we have used a parallel computer with $O(N^2)$ processors. The geometric mesh factors in the neighbourhoods of vertices and edges are chosen as $\mu_v = 0.15$ and $\mu_e = 0.15$ which give optimal results.

The examples reported here will include all three types of singularities. In addition, to compare our results with those existing in the literature we shall consider a few examples similar to those of Guo and Oh [52] as well.

Our first example is the Poisson equation containing only a vertex singularity with Dirichlet boundary conditions. For computational simplicity we shall assume that the singularity arises only at one vertex of the domain under consideration. However, in general, a typical domain may contain singularities at more than one corner in which case the same technique can be applied to each vertex containing a singularity.

Example 6.3.1. (Poisson equation with vertex singularity)

Consider the domain $\Omega^{(v)}$ shown in Figure 6.13 defined by

$$\Omega^{(v)} = \{(\phi, \theta, \rho) \mid \pi/6 \leq \phi \leq \pi/3, 0 \leq \theta \leq 3\pi/2, \rho \leq 1\}.$$

We consider the following model problem:

$$\begin{aligned} -\Delta u &= f \quad \text{in } \Omega^{(v)}, \\ u &= g \quad \text{on } \partial\Omega^{(v)}. \end{aligned} \quad (6.2)$$

Let $w(\phi, \theta, \rho) = \rho^{1/2} \sin(\frac{\phi}{2})$. Then this axially symmetric function w is the true solution

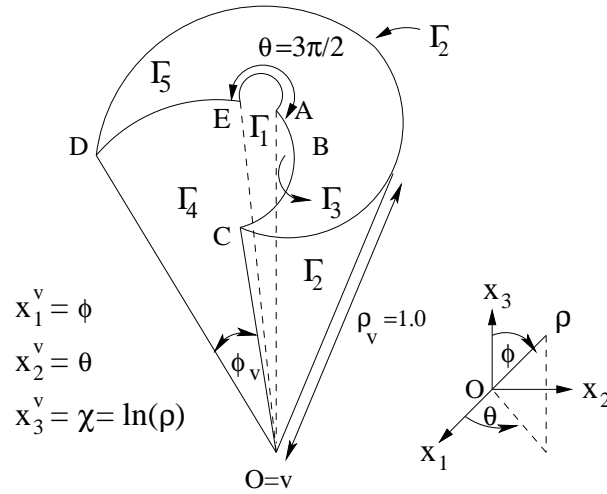


Figure 6.13: The domain $\Omega^{(v)}$ containing a vertex singularity.

of the model problem 6.2. Note that w has a vertex singularity at the origin and none other. Let x_1^v, x_2^v and x_3^v denote the modified coordinates in the vertex neighbourhood introduced in Chapter 2.

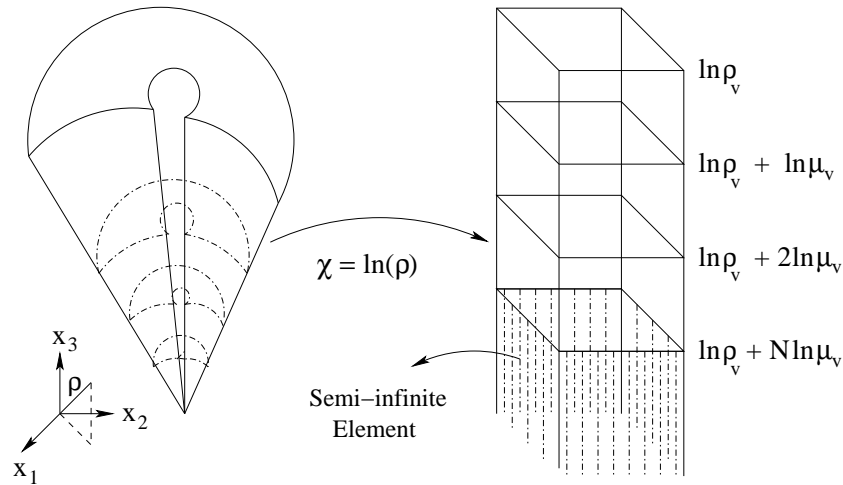


Figure 6.14: Geometric mesh imposed on $\Omega^{(v)}$ (front view) and elements after mapping.

Performance of the $h - p$ version of the spectral element method is analyzed on geometrically refined meshes shown in Figure 6.14 with mesh ratio $\mu_v = 0.15$ (optimal for geometric mesh refinement [9, 13, 18, 51, 52] for the $h - p$ version of the finite element method). Results are given in Table 6.10.

Table 6.10: Performance of the $h - p$ version for Dirichlet problem on domain $\Omega^{(v)}$ containing a vertex singularity

$p = W$	DOF(N_{dof})	Iterations	Relative Error(%)
2	9	46	0.100821E+01
3	55	56	0.841462E-01
4	193	86	0.309263E-02
5	501	109	0.273612E-03
6	1081	123	0.733920E-04
7	2059	143	0.180276E-04
8	3585	158	0.503131E-05
9	5833	179	0.984438E-06
10	9001	191	0.480789E-06

We know that the error in the neighbourhoods of vertices satisfies

$$\|u_{approx.} - u_{ex.}\|_{H^1} \leq C e^{-bN_{dof}^{1/4}}. \quad (6.3)$$

Here N_{dof} denotes the number of degrees of freedom.

In figure 6.15(a) the relative error versus polynomial degree p is drawn. Iterations as a function of N , the number of layers are given in Figure 6.15(b). Relative error against degrees of freedom is depicted on a log – log scale in Figure 6.15(c), the curve is a straight line which confirms the estimate (6.3). The error decays to $\approx 10^{-7}$ when $p = 10$. Further, the number of iterations required to obtain the solution to the desired accuracy is nearly 200 which is fairly low.

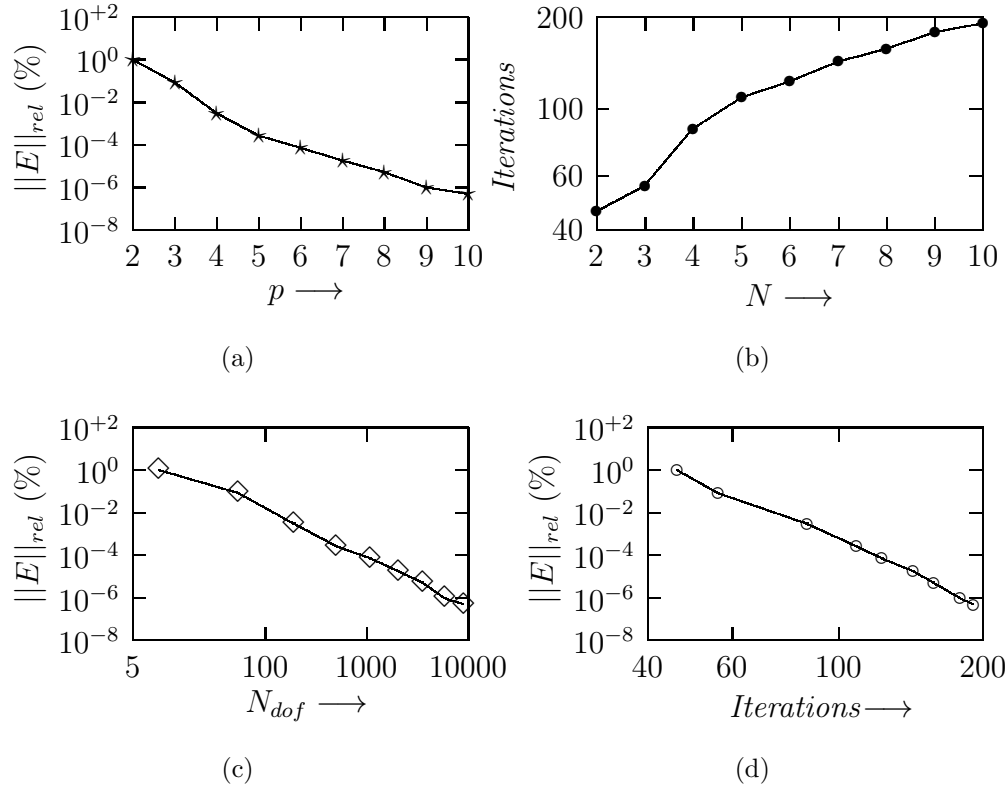


Figure 6.15: (a) Error vs. p , (b) Iterations vs. N , (c) Error vs. N_{dof} and (d) Error vs. Iterations for Poisson equation containing a vertex singularity.

The second example illustrates the effectiveness of the method for problems with mixed boundary conditions containing a vertex singularity and is similar to that of Guo and Oh reported in [52].

Example 6.3.2. (Mixed problem containing vertex singularity):

Consider the axisymmetric Poisson equation with mixed boundary conditions:

$$\begin{aligned}
 -\Delta u &= f \quad \text{in } \Omega^{(v)}, \\
 u &= g \quad \text{on } \mathcal{D} \subset \partial\Omega^{(v)}, \\
 \frac{\partial u}{\partial \nu} &= h \quad \text{on } \mathcal{N} = \partial\Omega^{(v)} \setminus \mathcal{D},
 \end{aligned} \tag{6.4}$$

where the domain $\Omega^{(v)}$ is shown in Figure 6.13 and

$$\begin{aligned}\mathcal{D} &= \Gamma_1 \cup \Gamma_2 \cup \Gamma_3 \cup \Gamma_4 = \Gamma_{\mathcal{D}}^1 \cup \Gamma_{\mathcal{D}}^2, \\ \Gamma_{\mathcal{D}}^1 &= \{(\phi, \theta, \rho) : \phi = \pi/6, \pi/3, 0 \leq \theta \leq 3\pi/2, 0 \leq \rho \leq 1\}, \\ \Gamma_{\mathcal{D}}^2 &= \{(\phi, \theta, \rho) : \pi/6 \leq \phi \leq \pi/3, \theta = 0, 3\pi/2, 0 \leq \rho \leq 1\}, \\ \mathcal{N} &= \Gamma_5 = \{(\phi, \theta, \rho) : \pi/6 \leq \phi \leq \pi/3, 0 \leq \theta \leq 3\pi/2, \rho = 1\}.\end{aligned}$$

We choose data f , g and h such that the function $w = \rho^{0.1}(1 - \rho)\sin 2\phi$ is the true solution of (6.4) satisfying prescribed boundary conditions. Here ν denotes the exterior unit normal to the part of the boundary where we impose Neumann boundary conditions.

Table 6.11: Performance of the $h - p$ version for mixed problem on polyhedral domain $\Omega^{(v)}$ containing a vertex singularity

$p = W$	DOF(N_{dof})	Iterations	Relative Error(%)
2	9	16	0.962637E+01
3	55	39	0.252012E+01
4	193	128	0.191490E+00
5	501	176	0.212320E-01
6	1081	314	0.192391E-02
7	2059	409	0.884830E-03
8	3585	743	0.412629E-03
9	5833	814	0.470681E-04

Table 6.11 contains the relative error obtained by applying the method on geometrically refined mesh in ρ . The relative error versus degrees of freedom is depicted in Figure 6.15. It is clear that the method gives exponential accuracy.

Next, we apply our method to an elliptic problem containing an edge singularity.

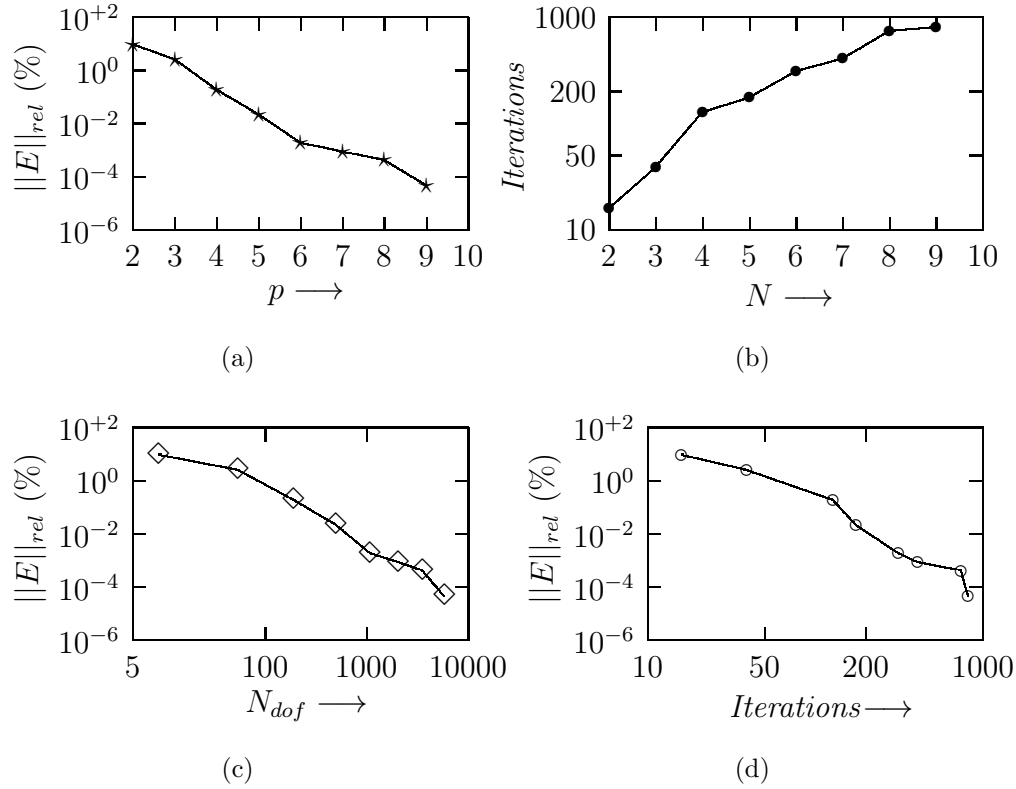


Figure 6.16: (a) Error vs. p , (b) Iterations vs. N , (c) Error vs. N_{dof} and (d) Error vs. Iterations for mixed problem containing a vertex singularity.

Example 6.3.3. (Elliptic equation containing edge singularity)

Consider the following Laplace equation:

$$\begin{aligned} -\Delta u &= 0 \quad \text{in } \Omega_1^{(e)}, \\ u &= g \quad \text{on } \partial\Omega_1^{(e)}. \end{aligned} \tag{6.5}$$

where the domain $\Omega_1^{(e)}$ is shown in Figure 6.17 and is given by

$$\Omega_1^{(e)} = \{(r, \theta, x_3) : 0 \leq r \leq 1, 0 \leq \theta \leq \pi/2, 0 \leq x_3 \leq 1\}.$$

We impose Dirichlet boundary conditions on all the faces marked as $\Gamma_i, i = 1, \dots, 5$.

Let $w(r, \theta, x_3) = r^{\frac{1}{3}} \sin(\frac{\theta}{3}) x_3$. Then w is the exact solution of (6.5) satisfying the Dirichlet boundary conditions $u|_{\partial\Omega_1^{(e)}} = w$. Note that w has an edge singularity. Let x_1^e, x_2^e and x_3^e denote the modified coordinates in the edge neighbourhood introduced in Chapter 2.

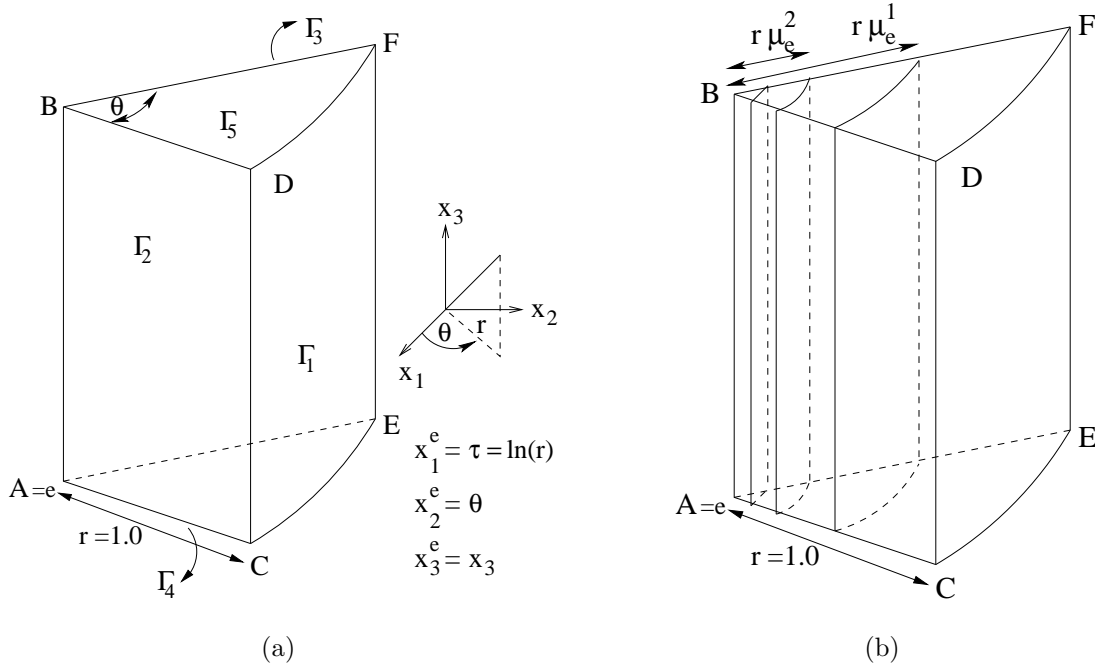


Figure 6.17: (a) The domain $\Omega_1^{(e)}$ containing an edge singularity, (b) Geometrical mesh imposed on $\Omega_1^{(e)}$.

Table 6.12 contains the numerical results and it shows that $\approx 10^{-4}(\%)$ of relative error in the H^1 -norm is achieved with $p = 8$ and $N_{dof} \approx 4000$.

Table 6.12: Performance of the $h - p$ version for Laplace equation on $\Omega_1^{(e)}$

$p = W$	DOF(N_{dof})	Iterations	Relative Error(%)
2	10	24	0.464542E+00
3	57	34	0.131359E+00
4	196	38	0.402204E-01
5	504	49	0.123974E-01
6	1085	58	0.364617E-02
7	2064	68	0.107525E-02
8	3592	75	0.315249E-03
9	5840	85	0.920349E-04
10	9001	98	0.279848E-04

The relative error against polynomial degree p for $p = 2, \dots, 10$ is drawn in Figure 6.18(a). It follows that the error decays exponentially. In Figures 6.18(c) and 6.18(d) error as a function of degrees of freedom and iterations is plotted on a log – log scale.

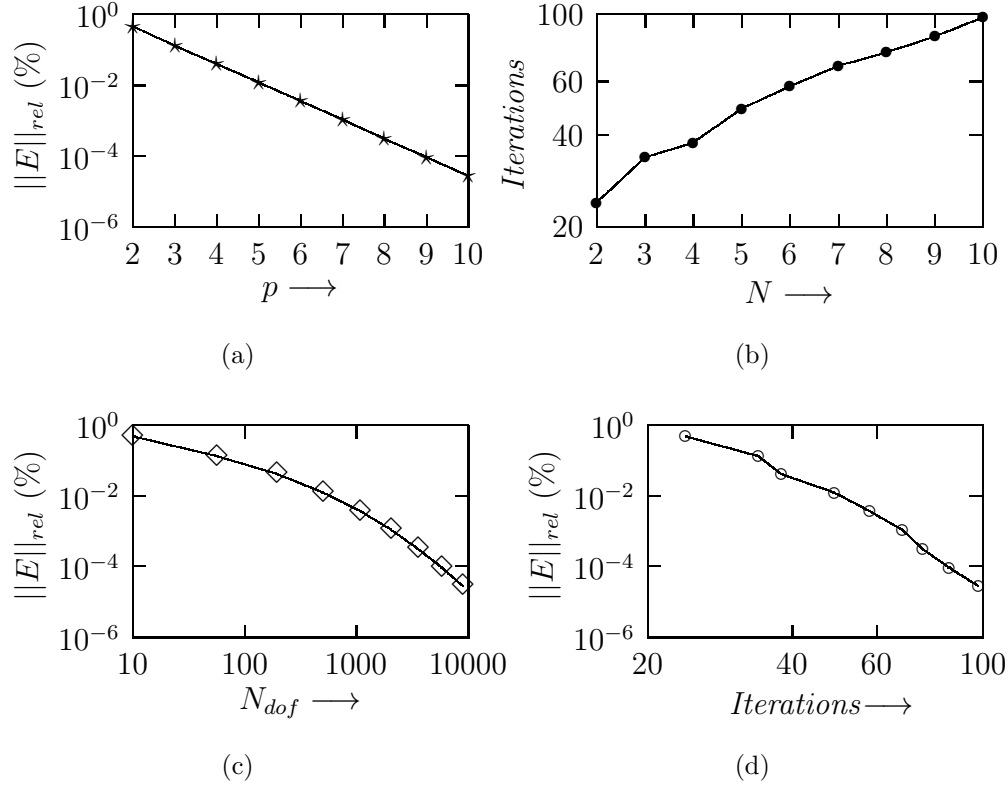


Figure 6.18: (a) Error vs. p , (b) Iterations vs. N , (c) Error vs. N_{dof} and (d) Error vs. Iterations for Laplace equation containing an edge singularity.

In the following example, we consider Laplace equation containing an edge singularity with mixed boundary conditions which is similar to that examined by Guo [52].

Example 6.3.4. (Laplace equation with mixed boundary conditions containing edge singularity: A crack problem)

Let us consider the Laplace equation:

$$\begin{aligned}
 -\Delta u &= 0 \quad \text{in } \Omega_2^{(e)}, \\
 u &= 0 \quad \text{on } \Gamma^{[0]} \subset \partial\Omega_2^{(e)}, \\
 \frac{\partial u}{\partial \nu} &= h \quad \text{on } \Gamma^{[1]} = \partial\Omega_2^{(e)} \setminus \Gamma^{[0]},
 \end{aligned} \tag{6.6}$$

where

$$\begin{aligned}
\Omega_2^{(e)} &= \{(r, \theta, x_3) : 0 \leq r \leq 1, 0 < \theta < 2\pi, 0 \leq x_3 \leq 1\}, \\
\Gamma^{[0]} &= \{(r, \theta, x_3) : 0 \leq r \leq 1, \theta = 0, 2\pi, 0 \leq x_3 \leq 1\}, \\
\Gamma^{[1]} &= \Gamma_1^{[1]} \cup \Gamma_2^{[1]} = \Gamma_2 \cup \Gamma_5 \cup \Gamma_6, \\
\Gamma_1^{[1]} &= \{(r, \theta, x_3) : r = 1, 0 < \theta < 2\pi, 0 < x_3 < 1\}, \\
\Gamma_2^{[1]} &= \{(r, \theta, x_3) : 0 < r < 1, 0 < \theta < 2\pi, x_3 = 0, 1\}, \\
h &= \begin{cases} \frac{1}{2}r^{\frac{1}{2}} \sin(\frac{\theta}{2}) & \text{on } \Gamma_1^{[1]} \\ 0 & \text{on } \Gamma_2^{[1]}. \end{cases} \tag{6.7}
\end{aligned}$$

Then the function $w(r, \theta, x_3) = r^{\frac{1}{2}} \sin(\frac{\theta}{2})$ is the exact solution of (6.6) satisfying the given boundary conditions $w|_{\Gamma^{[0]}} = 0$ and $w|_{\Gamma^{[1]}} = h$. Note that w has an edge singularity along x_3 -axis. The domain $\Omega_2^{(e)}$ and its plane section are shown in Figure 6.19.

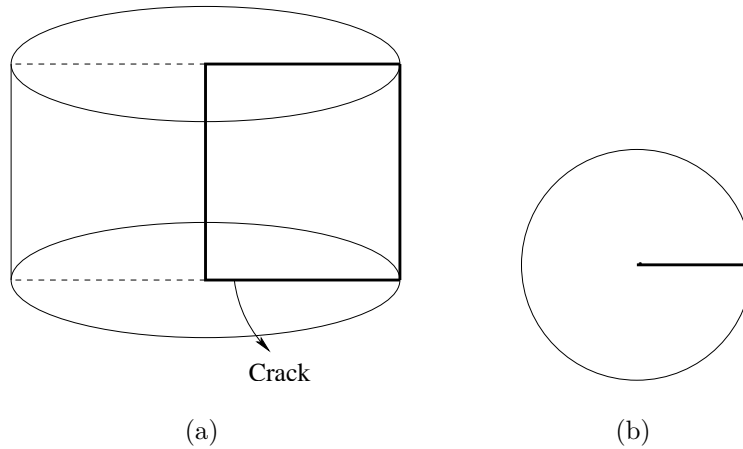


Figure 6.19: (a) The domain $\Omega_2^{(e)}$ with a crack, (b) Plane section of the domain $\Omega_2^{(e)}$.

Note that the domain $\Omega_2^{(e)}$ is obtained by removing a vertical slit of unit height from $r = 0$ to $r = 1$ i.e. a crack along $\theta = 0$, from a cylinder of unit height and radius 1 with centre at the origin.

We impose a geometric mesh on $\Omega_2^{(e)}$ as shown in Figure 6.20(a) which is refined geometrically in r with mesh ratio $\mu_e = 0.15$. All the elements in the geometric mesh are of unit height. Cross section of the mesh on $\Omega_2^{(e)}$ is shown in Figure 6.20(b).

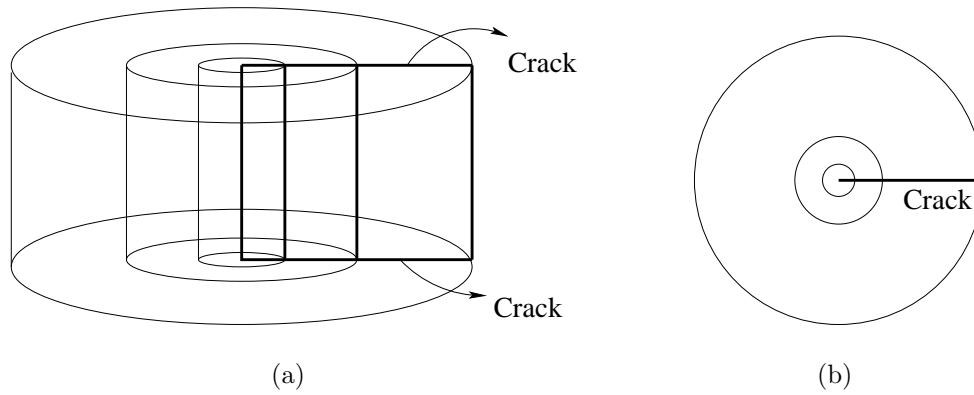


Figure 6.20: (a) Geometric mesh imposed on $\Omega_2^{(e)}$, (b) Cross section of the mesh imposed on $\Omega_2^{(e)}$.

Table 6.13 contains the relative error and iterations for different values of the polynomial order used in computations.

The relative error is plotted against polynomial degree p in Figure 6.21(a). It is clear that the error decays rapidly with increase in the polynomial order. In Figures 6.21(c) and 6.21(d) error as a function of degrees of freedom and iterations is plotted on a log – log scale.

Table 6.13: Performance of the $h - p$ version for Laplace equation with mixed boundary conditions on $\Omega_2^{(e)}$ containing an edge singularity

$p = W$	N_{dof}	Iterations	Relative Error(%)
2	26	129	0.121468E+02
3	138	167	0.979093E+01
4	452	225	0.395164E+00
5	1129	244	0.234473E+00
6	2382	400	0.571179E-02
7	4466	462	0.326770E-02
8	7688	768	0.610394E-04

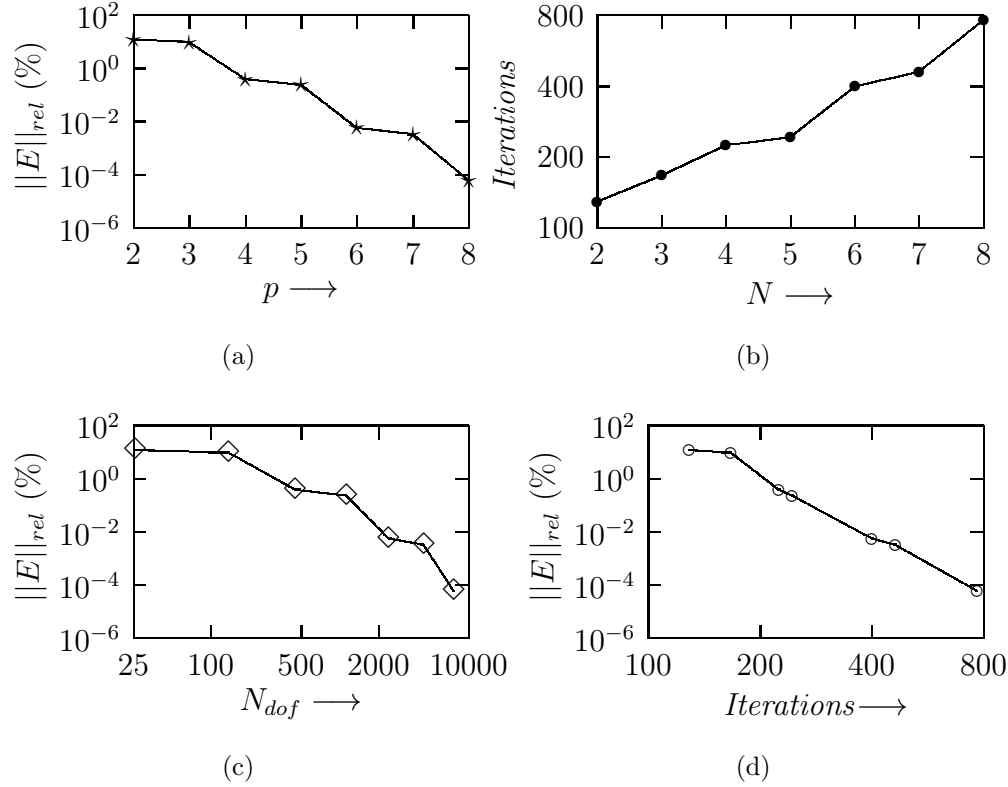


Figure 6.21: (a) Error vs. p , (b) Iterations vs. p , (c) Error vs. N_{dof} and (d) Error vs. Iterations for mixed problem containing an edge singularity.

In the next example, we consider Poisson equation on a polyhedral domain containing vertex, edge and vertex-edge singularities and analyze the performance of the method.

Example 6.3.5. (Poisson equation containing vertex-edge singularity)

Let us consider the problem:

$$\begin{aligned} -\Delta u &= f \quad \text{in } \Omega^{(v-e)}, \\ u &= g \quad \text{on } \partial\Omega^{(v-e)}. \end{aligned} \quad (6.8)$$

Let $w(\phi, \theta, \rho) = \rho^{3/4}(\sin \phi)^{1/2} \sin(\frac{\theta}{2})$ and $f = -\Delta w$. Then w is the exact solution of (6.8) in $\Omega^{(v-e)}$ satisfying the Dirichlet boundary conditions $u|_{\partial\Omega^{(v-e)}} = g$, where $\Omega^{(v-e)}$ is the domain in Figure 6.22 defined by

$$\Omega^{(v-e)} = \{(\phi, \theta, \rho) : 0 \leq \phi \leq \pi/6, 0 \leq \theta \leq 3\pi/2, \rho \leq 1\}.$$

Let us note that w has a vertex singularity at the origin, an edge singularity along the z -axis and a vertex-edge singularity. A geometrical mesh is imposed on $\Omega^{(v-e)}$ (Figure 6.23) in both ϕ (angular direction) and x_3 (radial direction) variables with geometric mesh factors μ_e and μ_v respectively.

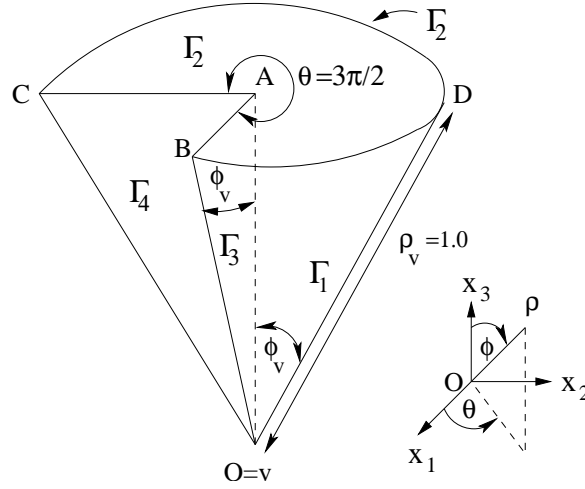


Figure 6.22: The domain $\Omega^{(v-e)}$.

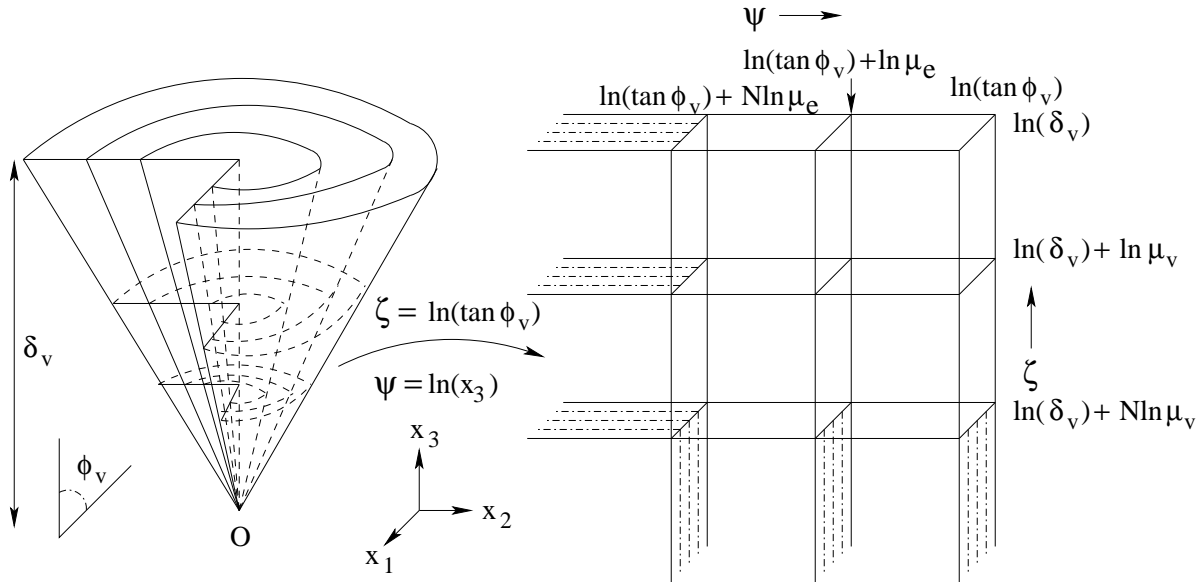


Figure 6.23: Mesh imposed on $\Omega^{(v-e)}$ and the elements after mapping.

To obtain the exponential convergence and efficiency of computations it is essential to refine the mesh geometrically in both angular and radial direction along with a proper

Table 6.14: Performance of the $h - p$ version for Poisson equation on $\Omega^{(v-e)}$ containing a vertex-edge singularity

$p = W$	N_{dof}	Iterations	Relative Error(%)
2	19	15	0.473188E+01
3	117	51	0.106067E+01
4	592	61	0.363064E+00
5	2025	69	0.165742E+00
6	5436	77	0.693299E-01

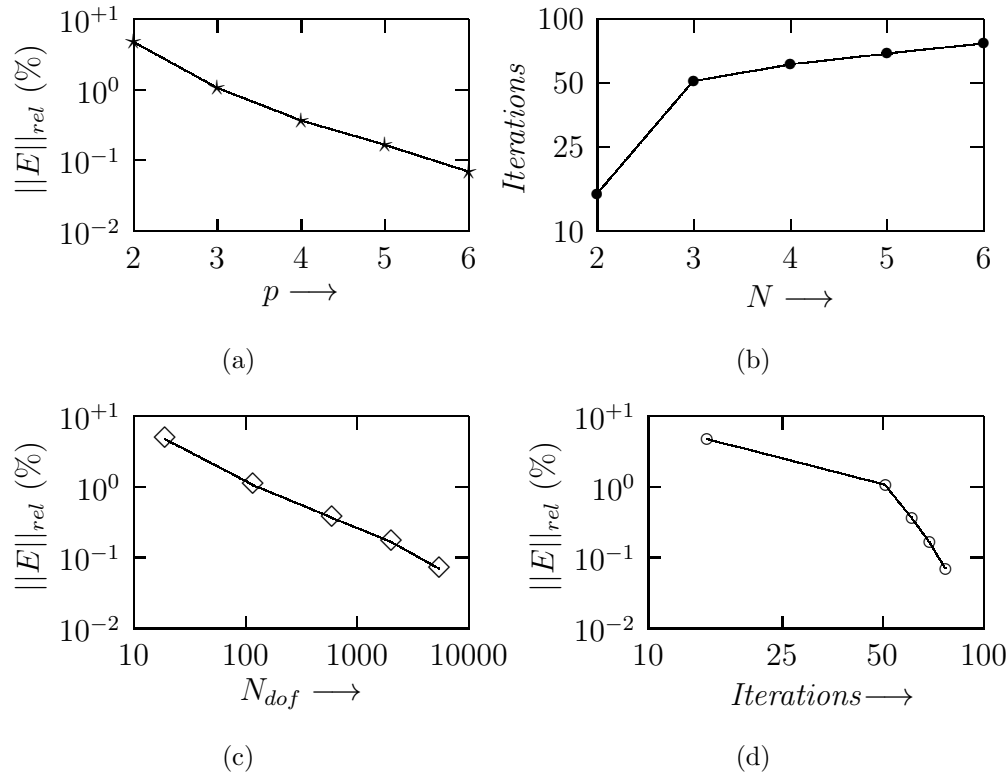


Figure 6.24: (a) Error vs. p , (b) Iterations vs. N , (c) Error vs. N_{dof} and (d) Error vs. Iterations for Poisson equation containing a vertex-edge singularity.

choice of polynomial degree distribution because the solution possesses the combined effect of a vertex singularity and an edge singularity.

The numerical results are given in Table 6.14. The relative error reduces to nearly

0.07% with $p = 6$.

Figure 6.24(a) contains the relative error versus polynomial order p . The error is plotted on a log – scale. The curve is almost a straight line and it confirms the theoretical estimates obtained. Further in Figure 6.24(b) the error is drawn as a function of N_{dof} on a log – log scale.

6.4 Conclusions and Future Work

6.4.1 Summary and conclusions

There are three different types of singularities for elliptic problems on non-smooth domains in R^3 , namely, the vertex, the edge and the vertex-edge. In addition, the solutions to these problems are anisotropic in the neighbourhoods of edges and vertex-edges.

Among many approaches that have been attempted over the past three decades to provide accurate and economical solutions to the elliptic boundary value problems containing singularities, the two principal approaches are the adaptive mesh refinement (very small elements near the singularities and large elements elsewhere) and the use of singular basis functions. In three dimensional problems, the first approach suffers the problems of limited storage capacity and high computational cost while ill-conditioning occur in the latter in presence of singularities. As an extension of the second approach, the method of auxiliary mapping (MAM) was introduced by Babuška and Oh (see [17, 65, 68, 69] and references therein). The MAM has proven to be highly successful in dealing with elliptic boundary value problems containing singularities in R^2 [17, 65, 68, 69] and R^3 [52, 63] using p -version of the finite element method. However, the success of this method depends on optimal choices of auxiliary mappings.

In the present work we have proposed an exponentially accurate $h - p$ spectral element method for three dimensional elliptic problems on non-smooth domains using parallel computers.

We choose as our solution the spectral element function which minimizes the sum of a weighted squared norm of the residuals in the partial differential equations and the

squared norm of the residuals in the boundary conditions in fractional Sobolev spaces and enforce continuity by adding a term which measures the jump in the function and its derivatives at inter-element boundaries in fractional Sobolev norms, to the functional being minimized.

The present study can be summarized as follows:-

- To resolve the singularities which arise in the neighbourhoods of vertices, edges and vertex-edges we use modified systems of coordinates that are modified versions of spherical and cylindrical coordinate systems. These modified coordinates serve as our auxiliary mappings in different neighbourhoods.
- The Sobolev spaces in vertex-edge and edge neighbourhoods are anisotropic and become singular at the corners and edges.
- We choose spectral element functions (SEF) which are fully non-conforming. i.e. there are no set of common boundary values, and hence we do not need to solve the Schur complement system.
- The method is essentially a least-squares method and to solve the minimization problem we need to solve the normal equations for the least-squares problem.
- The residuals in the normal equations can be obtained without computing and storing mass and stiffness matrices.
- We use Preconditioned Conjugate Gradient Method (PCGM) to solve normal equations using a block diagonal preconditioner. Moreover, there exists a new preconditioner which can be diagonalized in a new set of basis functions, and hence it is easily inverted on each element.
- For Dirichlet problems the condition number of the preconditioner is $O((\ln W)^2)$, provided $W = O(e^{N^\alpha})$ for $\alpha < 1/2$. However, it grows like $O(N^4)$ for mixed problems.

- For Dirichlet problems the overall complexity of the method is $O(N^5 \ln(N))$ operations on a parallel computer with $O(N^2)$ processors to compute the solution. For mixed problems it is equal to $O(N^7)$ operations on a parallel computer with $O(N^2)$ processors.
- Computational results for a number of test problems on smooth as well as non-smooth domains confirm the estimates obtained for the error and computational complexity.
- In each iteration of the PCGM we need to communicate the values of the function and its derivatives on the boundary of the element between neighbouring elements. Moreover, we need to compute two global scalars to update the approximate solution and search direction. Thus, the inter processor communication involved is small.
- Though the method is efficient and delivers exponential accuracy, more experience is needed in computations and implementation. e.g. how to implement the distribution of element degrees, what are the optimal degree factors, etc.

6.4.2 Proposed future work

Rapid growth of the factor N^4 for mixed problems creates difficulty in parallelizing the numerical scheme. To overcome this difficulty another version of the method can be defined in which we choose spectral element functions to be conforming only on the wirebasket of the elements.

The values of the spectral element functions at the wirebasket of the elements constitute the set of common boundary values and we need to solve the Schur complement matrix system corresponding to the common boundary values. We intend to consider this in future work.

Appendix A

A.1

Proof of Proposition 2.2.1

Proposition 2.2.1. *There exists a constant $\beta_v \in (0, 1/2)$ such that for all $0 < \nu \leq \rho_v$ the estimate*

$$\int_{\bar{\Omega}^v \cap \{x^v: x_3^v \leq \ln(\nu)\}} \sum_{|\alpha| \leq m} e^{x_3^v} \left| D_{x^v}^\alpha (w(x^v) - w_v) \right|^2 dx^v \leq C (d^m m!)^2 \nu^{(1-2\beta_v)} \quad (\text{A.1})$$

holds for all integers $m \geq 1$.

Proof. By Theorem 3.19 of [14] for $\beta_v \in (0, 1/2)$, $\mathbf{H}_{\beta_v}^{2,2}(\Omega^v)$ is embedded in $\mathbf{C}^0(\bar{\Omega}^v)$ and

$$\|w\|_{\mathbf{C}^0(\bar{\Omega}^v)} \leq C \|w\|_{\mathbf{H}_{\beta_v}^{2,2}(\Omega^v)} .$$

Here C denotes a constant and $\bar{\Omega}^v$ the closure of Ω^v .

Hence we can define $w_v = w(v)$, the value of w at the vertex v and

$$|w_v| \leq C \|w\|_{\mathbf{H}_{\beta_v}^{2,2}(\Omega^v)} .$$

Let $\mathcal{D}^\alpha u = u_{\phi^{\alpha_1} \theta^{\alpha_2} \rho^{\alpha_3}}$. Here $\alpha = (\alpha_1, \alpha_2, \alpha_3)$ and $\alpha' = (\alpha_1, \alpha_2)$.

Define

$$\Phi_{\beta_v}^{\alpha,2}(x) = \begin{cases} \rho^{\beta_v+|\alpha|-2} & \text{for } |\alpha| \geq 2 \\ 1 & \text{for } |\alpha| < 2 \end{cases}$$

as in (2.3) of [14]. Let

$$\mathcal{H}_{\beta_v}^{k,2}(\Omega^v) = \left\{ u \mid \|u\|_{\mathcal{H}_{\beta_v}^{k,2}(\Omega^v)}^2 = \sum_{|\alpha| \leq k} \left\| \Phi_{\beta_v}^{\alpha,2} \rho^{-|\alpha'|} \mathcal{D}^\alpha u \right\|_{L^2(\Omega^v)}^2 < \infty \right\}$$

and

$$\mathcal{B}_{\beta_v}^2(\Omega^v) = \left\{ u \mid u \in \mathcal{H}_{\beta_v}^{k,2}(\Omega^v) \text{ for all } k \geq 2, \left\| \Phi_{\beta_v}^{\alpha,2} \rho^{-|\alpha'|} \mathcal{D}^\alpha u \right\|_{L^2(\Omega^v)}^2 \leq C d^\alpha \alpha! \right\} .$$

Then from Theorem 4.13 of [14] we have that $w \in \mathcal{B}_{\beta_v}^2(\Omega^v)$ iff $w \in \mathbf{B}_{\beta_v}^2(\Omega^v)$.

Hence

$$\sum_{2 \leq |\alpha| \leq m} \int_{\Omega^v} \left| \rho^{\beta_v-2} \rho^{\alpha_3} w_{\phi^{\alpha_1} \theta^{\alpha_2} \rho^{\alpha_3}} \right|^2 \rho^2 \sin \phi \, d\rho \, d\phi \, d\theta \leq (C d^m m!)^2 . \quad (\text{A.2})$$

Define $\chi = \ln \rho$. Then

$$\frac{\partial}{\partial \chi} = \rho \frac{\partial}{\partial \rho} \text{ and } \frac{d\rho}{\rho} = d\chi.$$

Now as in [14] it can be shown using (A.2) that

$$\sum_{2 \leq |\alpha| \leq m} \int_{\tilde{\Omega}^v} e^{(2\beta_v - 1)\chi} |w_{\phi^{\alpha_1} \theta^{\alpha_2} \chi^{\alpha_3}}|^2 d\chi d\phi d\theta \leq (C d^m m!)^2.$$

Here C and d denote generic constants.

Hence

$$\sum_{2 \leq |\alpha| \leq m} \int_{\tilde{\Omega}^v \cap \{x^v: \chi \leq \ln \nu\}} |D_{x^v}^\alpha w|^2 dx^v \leq (C d^m m!)^2 \nu^{1-2\beta_v}. \quad (\text{A.3})$$

We now obtain estimates for $0 \leq |\alpha| \leq 1$. By Lemma 5.5 of [14] since $w \in \mathbf{H}_{\beta_v}^{2,2}(\Omega^v)$ the estimate

$$\int_{\Omega^v} \rho^{2(\beta_v - 2)} |w - w(v)|^2 dx \leq C \|u\|_{\mathbf{H}_{\beta_v}^{2,2}(\Omega^v)}^2$$

holds.

Hence

$$\int_{\tilde{\Omega}^v} e^{(2\beta_v - 1)\chi} |w - w_v|^2 d\chi d\phi d\theta \leq (C d^m m!)^2.$$

Thus we conclude that

$$\int_{\tilde{\Omega}^v \cap \{x^v: \chi \leq \ln \nu\}} |w - w_v|^2 dx^v \leq C (d^m m!)^2 \nu^{1-2\beta_v}. \quad (\text{A.4})$$

Finally, let $\mathbf{C}_{\beta_v}^2(\Omega^v)$ denote the set of functions $u(x) \in \mathbf{C}^0(\bar{\Omega}^v)$ such that for all $|\alpha| \geq 0$

$$|D_x^\alpha (u(x) - u(v))| \leq C d^\alpha \alpha! \rho^{-(\beta_v + |\alpha| - 1/2)}(x). \quad (\text{A.5})$$

Then by Theorem 5.6 of [14], $\mathbf{B}_{\beta_v}^2(\Omega^v) \subseteq \mathbf{C}_{\beta_v}^2(\Omega^v)$.

Now

$$\rho \nabla_x u = Q^v \nabla_{x_v} u. \quad (\text{A.6})$$

Here

$$Q^v = O^v P^v$$

where O^v is the orthogonal matrix

$$O^v = \begin{bmatrix} \cos \phi \cos \theta & -\sin \theta & \sin \phi \cos \theta \\ \cos \phi \sin \theta & \cos \theta & \sin \phi \sin \theta \\ -\sin \phi & 0 & \cos \phi \end{bmatrix}$$

and

$$P^v = \begin{bmatrix} 1 & 0 & 0 \\ 0 & \frac{1}{\sin \phi} & 0 \\ 0 & 0 & 1 \end{bmatrix}.$$

Now in Ω^v

$$\phi^v < \phi < \pi - \phi^v.$$

Hence from (A.5) and (A.6) we can conclude that

$$|\nabla_{x^v} w| \leq C \rho^{-\beta_v+1/2}. \quad (\text{A.7})$$

Using (A.7) the estimate

$$\int_{\tilde{\Omega}^v \cap \{x^v: \chi \leq \ln \nu\}} \sum_{|\alpha|=1} |D_{x^v}^\alpha w|^2 dx^v \leq C \int_{-\infty}^{\ln \nu} e^{(-2\beta_v+1)\chi} d\chi \leq C \nu^{1-2\beta_v}. \quad (\text{A.8})$$

follows.

Combining (A.3), (A.4) and (A.8) we obtain the result. \square

A.2

Proof of Proposition 2.2.2

Proposition 2.2.2. *Let $s(x_3) = w(x_1, x_2, x_3)|_{(x_1=0, x_2=0)}$. Then*

$$\int_{\delta_v}^{l_e - \delta_{v'}} \sum_{k \leq m} \left| \frac{d^k}{(dx_3^e)^k} s(x_3^e) \right|^2 dx_3^e \leq (C d^m m!)^2. \quad (\text{A.9})$$

Moreover there exists a constant $\beta_e \in (0, 1)$ such that for $\mu \leq Z$

$$\int_{\tilde{\Omega}^e \cap \{x^e: x_1^e \leq \ln \mu\}} \sum_{|\alpha| \leq m} |D_{x^e}^\alpha (w(x^e) - s(x_3^e))|^2 dx^e \leq C (d^m m!)^2 \mu^{2(1-\beta_e)} \quad (\text{A.10})$$

for all integers $m \geq 1$.

Proof. We denote by $\mathbf{C}_{\beta_e}^2(\Omega^e)$, $\beta_e \in (0, 1)$, the set of functions $u \in \mathbf{C}^0(\bar{\Omega}^e)$ such that for $|\alpha| \geq 0$

$$\left\| r^{\beta_e + \alpha_1 + \alpha_2 - 1} D_x^\alpha (u(x) - u(0, 0, x_3)) \right\|_{\mathbf{C}^0(\bar{\Omega}^e)} \leq C d^\alpha \alpha! \quad (\text{A.11})$$

and for $k \geq 0$

$$\left\| \frac{d^k}{(dx_3)^k} u(0, 0, x_3) \right\|_{\mathbf{C}^0(\bar{\Omega}^e \cap \{x: x_1=x_2=0\})} \leq C d^k k! \quad (\text{A.12})$$

as in (5.1) and (5.2) of [14]. Here $\bar{\Omega}^e$ denotes the closure of Ω^e .

Then by Theorem 5.3 of [14], $\mathbf{B}_{\beta_e}^2(\Omega^e) \subseteq \mathbf{C}_{\beta_e}^2(\Omega^e)$.

Now

$$x_1^e = \tau = \ln r$$

$$x_2^e = \theta$$

$$x_3^e = x_3.$$

Define $s(x_3) = w(x_1, x_2, x_3)|_{(x_1=0, x_2=0)}$. Then (A.9) follows immediately from (A.12) since $w \in \mathbf{B}_{\beta_e}^2(\Omega^e)$ and hence $w \in \mathbf{C}_{\beta_e}^2(\Omega^e)$.

Let

$$p(x) = w(x) - s(x_3).$$

Then by (A.11) we have that

$$\left\| r^{\beta_e + \alpha_1 + \alpha_2 - 1} D_x^\alpha p(x) \right\|_{\mathbf{C}^0(\bar{\Omega}^e)} \leq C d^\alpha \alpha! \quad (\text{A.13})$$

Now we can show just as in Theorem 4.1 of [14] that

$$\left\| r^{\beta_e - 1} D_{x^e}^\alpha p(x^e) \right\|_{\mathbf{C}^0(\bar{\Omega}^e)} \leq C d^\alpha \alpha! \quad (\text{A.14})$$

using the estimate (A.13).

Hence

$$| D_{x^e}^\alpha p(x^e) | \leq C d^\alpha \alpha! e^{(1-\beta_e)x_1^e}$$

for $x^e \in \bar{\Omega}^e$.

Using the above we conclude that

$$\int_{\bar{\Omega}^e \cap \{x^e: x_1^e \leq \ln \mu\}} \sum_{|\alpha| \leq m} | D_{x^e}^\alpha p(x^e) |^2 dx^e \leq C (d^m m!)^2 \int_{-\infty}^{\ln \mu} e^{2(1-\beta_e)\tau} d\tau$$

and this gives the required estimate (A.10). \square

A.3

Proof of Proposition 2.2.3

Proposition 2.2.3. *Let $w_v = w(v)$, the value of w evaluated at the vertex v , and $s(x_3) = w(x_1, x_2, x_3)|_{(x_1=0, x_2=0)}$. Then there exists a constant $\beta_v \in (0, 1/2)$ such that for any $0 < \nu \leq \delta_v$*

$$\int_{-\infty}^{\ln \nu} e^{x_3^{v-e}} \sum_{k \leq m} \left| D_{x_3^{v-e}}^k (s(x_3^{v-e}) - w_v) \right|^2 dx_3^{v-e} \leq C (d^m m!)^2 \nu^{(1-2\beta_v)}. \quad (\text{A.15})$$

Moreover there exists a constant $\beta_e \in (0, 1)$ such that for any $0 < \alpha \leq \tan \phi_v$ and $0 < \nu \leq \delta_v$

$$\begin{aligned} & \int_{\bar{\Omega}^{v-e} \cap \{x^{v-e}: x_1^{v-e} < \ln \alpha, x_3^{v-e} < \ln \nu\}} e^{x_3^{v-e}} \sum_{|\gamma| \leq m} \left| D_{x^{v-e}}^\gamma (w(x_3^{v-e}) - s(x_3^{v-e})) \right|^2 dx_3^{v-e} \\ & \leq C (d^m m!)^2 \alpha^{2(1-\beta_e)} \nu^{(1-2\beta_v)} \end{aligned} \quad (\text{A.16})$$

for all integers $m \geq 1$.

Proof. By $\mathbf{C}_{\beta_{v-e}}^2(\Omega^{v-e})$, where $\beta_{v-e} = (\beta_v, \beta_e)$, $\beta_v \in (0, 1/2)$ and $\beta_e \in (0, 1)$ we denote the set of functions $u(x) \in \mathbf{C}^0(\bar{\Omega}^{v-e})$ such that

$$\left\| \rho^{\beta_v + |\alpha| - 1/2} (\sin \phi)^{\beta_e + \alpha_1 + \alpha_2 - 1} D_x^\alpha (u(x) - u(0, 0, x_3)) \right\|_{\mathbf{C}^0(\bar{\Omega}^{v-e})} \leq C d^\alpha \alpha! \quad (\text{A.17})$$

and

$$\left| |x_3|^{\beta_v + k - 1/2} \frac{d^k}{dx_3^k} (u(0, 0, x_3) - u(v)) \right|_{\mathbf{C}^0(\bar{\Omega}^{v-e} \cap \{x: x_1 = x_2 = 0\})} \leq C d^k k! \quad (\text{A.18})$$

as described in (5.26) and (5.27) of [14]. Here $\bar{\Omega}^{v-e}$ denotes the closure of Ω^{v-e} .

Now by Theorem 5.9 of [14], $\mathbf{B}_{\beta_{v-e}}^2(\Omega^{v-e}) \subseteq \mathbf{C}_{\beta_{v-e}}^2(\Omega^{v-e})$. Since $w \in \mathbf{B}_{\beta_{v-e}}^2(\Omega^{v-e})$ we conclude that $w \in \mathbf{C}_{\beta_{v-e}}^2(\Omega^{v-e})$. Let $s(x_3) = w(0, 0, x_3)$ and $w_v = w(v)$. Then

$$\left| |x_3|^{\beta_v + k - 1/2} \frac{d^k}{dx_3^k} (s(x_3) - w_v) \right| \leq C d^k k!.$$

Now $x_3^{v-e} = \ln x_3$. Hence it can be shown as before that

$$\int_{-\infty}^{\ln \nu} \sum_{k \leq m} \left| D_{x_3^{v-e}}^k (s(x_3^{v-e}) - w_v) \right|^2 dx_3^{v-e} \leq C (d^m m!)^2 \nu^{(1-2\beta_v)}.$$

Let $p(x) = w(x) - s(x_3)$. Then by (A.17) we have that

$$\left\| \rho^{\beta_v + |\alpha| - 1/2} (\sin \phi)^{\beta_e + \alpha_1 + \alpha_2 - 1} D_x^\alpha p(x) \right\|_{\mathbf{C}^0(\bar{\Omega}^{v-e})} \leq C d^\alpha \alpha!.$$

It can be shown as in Theorem 4.8 of [14] that

$$\left\| \left(\rho^{\beta_v - 1/2} (\sin \phi)^{\beta_e - 1} \right) \rho^{\alpha_3} (\sin \phi)^{\alpha_1} p_{\phi^{\alpha_1} \theta^{\alpha_2} \rho^{\alpha_3}} \right\|_{\mathbf{C}^0(\check{\Omega}^{v-e})} \leq C d^\alpha \alpha!.$$

Here $\check{\Omega}^{v-e}$ is the image of $\bar{\Omega}^{v-e}$ in (ϕ, θ, ρ) coordinates.

From the above the estimate

$$\left\| e^{(\beta_v - 1/2)\chi} (\sin \phi)^{\beta_e - 1} (\sin \phi)^{\alpha_1} p_{\phi^{\alpha_1} \theta^{\alpha_2} \chi^{\alpha_3}} \right\|_{\mathbf{C}^0(\hat{\Omega}^{v-e})} \leq C d^\alpha \alpha! \quad (\text{A.19})$$

follows. Here $\hat{\Omega}^{v-e}$ is the image of $\bar{\Omega}^{v-e}$ in x^v coordinates, $x^v = (\phi, \theta, \chi)$ and $\chi = \ln \rho$.

Now the vertex-edge coordinates are defined as

$$\begin{aligned} x_1^{v-e} &= \psi = \ln(\tan \phi) \\ x_2^{v-e} &= \theta \\ x_3^{v-e} &= \zeta = \ln(x_3) = \chi + \ln(\cos \phi). \end{aligned}$$

Thus

$$\nabla_{x^v} u = J^{v-e} \nabla_{x^{v-e}} u$$

where

$$J^{v-e} = \begin{bmatrix} \sec^2 \phi \cot \phi & 0 & -\tan \phi \\ 0 & 1 & 0 \\ 0 & 0 & 1 \end{bmatrix}.$$

Hence

$$\nabla_{x^{v-e}} u = (J^{v-e})^{-1} \nabla_{x^v} u.$$

Here

$$(J^{v-e})^{-1} = \begin{bmatrix} \cos \phi \sin \phi & 0 & \sin^2 \phi \\ 0 & 1 & 0 \\ 0 & 0 & 1 \end{bmatrix}.$$

Hence

$$\begin{aligned} \frac{\partial u}{\partial \psi} &= \cos \phi \sin \phi \frac{\partial u}{\partial \phi} + \sin^2 \phi \frac{\partial u}{\partial \chi}, \\ \frac{\partial u}{\partial \zeta} &= \frac{\partial u}{\partial \chi}. \end{aligned}$$

From the above we obtain

$$\frac{\partial^m u}{\partial \psi^m} = \sum_{k=1}^m \sum_{\alpha_1 + \alpha_2 = k} \left(\sum_{j_1 + j_2 = 2m - \alpha_1} a_{\alpha_1, \alpha_2, j_1, j_2}^m (\cos \phi)^{j_1} (\sin \phi)^{j_2} ((\sin \phi)^{\alpha_1}) u_{\phi^{\alpha_1} \chi^{\alpha_2}} \right) \quad (\text{A.20})$$

It can be shown that the coefficients $a_{\alpha_1, \alpha_2, j_1, j_2}^m$ satisfy the recurrence relation

$$a_{\alpha_1, \alpha_2, j_1, j_2}^{m+1} = a_{\alpha_1 - 1, \alpha_2, j_1 - 1, j_2}^m + (\alpha_1 + j_2) a_{\alpha_1, \alpha_2, j_1 - 2, j_2}^m \quad (\text{A.21})$$

$$- j_1 a_{\alpha_1, \alpha_2, j_1, j_2 - 2}^m + a_{\alpha_1, \alpha_2 - 1, j_1, j_2 - 2}^m \quad (\text{A.22})$$

for $|\alpha| \leq m$.

For $|\alpha| = m + 1$

$$a_{\alpha_1, \alpha_2, j_1, j_2}^{m+1} = \begin{cases} 1 & \text{if } j_1 = \alpha_1, j_2 = 2m + 2 - \alpha_1 \\ 0 & \text{otherwise.} \end{cases}$$

Since $0 \leq \phi \leq \phi_v$, where $\phi_v < \pi/2$, we can conclude from (A.19) that

$$\left\| e^{(\beta_v - 1/2)\zeta} e^{(\beta_e - 1)\psi} (\sin \phi)^{\alpha_1} p_{\phi^{\alpha_1} \theta^{\alpha_2} \chi^{\alpha_3}} \right\|_{\mathbf{C}_{(\hat{\Omega}^{v-e})}^0} \leq C d^\alpha \alpha!. \quad (\text{A.23})$$

Here $\hat{\Omega}^{v-e}$ denotes the image of $\bar{\Omega}^{v-e}$ in x^{v-e} coordinates. From (A.23) the estimate

$$\left\| e^{(\beta_v - 1/2)x_3^{v-e}} e^{(\beta_e - 1)x_1^{v-e}} D_{x^{v-e}}^\alpha p \right\|_{\mathbf{C}_{(\hat{\Omega}^{v-e})}^0} \leq C d^\alpha \alpha!. \quad (\text{A.24})$$

follows.

As in [14] we show (A.24) for the cases $\alpha = (m, 0, 0)$, $\alpha = (0, m, 0)$ and $\alpha = (0, 0, m)$ since the general case can be shown in the same way. It is enough to prove (A.24) for $\alpha = (m, 0, 0)$ since the other two cases are trivial.

Let

$$A_k^m = \sum_{\alpha_1 + \alpha_2 = k} \sum_{j_1 + j_2 = 2m - \alpha_1} |a_{\alpha_1, \alpha_2, j_1, j_2}^m|. \quad (\text{A.25})$$

Then

$$A_m^m \leq 4^m. \quad (\text{A.26})$$

Moreover for $k < m$

$$A_k^m \leq 4^m \frac{m!}{k!}. \quad (\text{A.27})$$

The proof is by induction. Using the recurrence relation (A.21) we obtain

$$\begin{aligned}
A_k^{m+1} &\leq 2mA_k^m + 2A_{k-1}^m \\
&\leq 2m \left(\frac{4^m m!}{k!} \right) + 2 \left(\frac{4^m m!}{(k-1)!} \right) \\
&\leq 4^{m+1} \frac{(m+1)!}{k!} \left(\frac{2m}{4(m+1)} + \frac{2k}{4(m+1)} \right) \\
&\leq \frac{4^{m+1}}{k!} (m+1)!
\end{aligned} \tag{A.28}$$

Now using (A.19), (A.20) and (A.28) it can be shown that

$$\begin{aligned}
&\left\| e^{(\beta_v-1/2)x_3^{v-e}} e^{(\beta_e-1)x_1^{v-e}} \frac{\partial^m p}{\partial \psi^m} \right\|_{\mathbf{C}^0(\tilde{\Omega}^{v-e})} \\
&\leq \sum_{k=1}^m \sum_{\alpha_1+\alpha_2=k} \sum_{j_1+j_2=2m-\alpha_1} |d_{\alpha_1, \alpha_2, j_1, j_2}^m| C d^{\alpha_1+\alpha_2} \alpha_1! \alpha_2! \\
&\leq \sum_{k=1}^m A_k^m (C d^k k!) \\
&\leq C d^m m!
\end{aligned}$$

Here C and d denote generic constants.

The inequality (A.24) is obtained in the same way. Now the estimate (A.16) follows immediately from (A.24). \square

A.4

Proof of Proposition 2.2.4

Proposition 2.2.4. *The estimate*

$$\int_{\Omega^r} \sum_{|\alpha| \leq m} |D_x^\alpha w(x)|^2 \leq C (d^m m!)^2 \tag{A.29}$$

holds for all integers $m \geq 1$.

Proof. Now $w(x)$ is analytic in an open neighbourhood of $\bar{\Omega}^r$. Hence (A.29) follows. \square

Appendix B

B.1

Proof of Lemma 3.2.6

Lemma 3.2.6. *Let $\Gamma_{k,i}^v = \Gamma_{q,r}^{v-e}$. Then the following identity holds.*

$$\begin{aligned}
& \sin^2(\phi_v) \oint_{\partial \tilde{\Gamma}_{k,i}^v} e^{x_3^v} \sin(x_1^v) \left(\frac{\partial u}{\partial \mathbf{n}^v} \right)_{A^v} \left(\frac{\partial u}{\partial \boldsymbol{\nu}^v} \right)_{A^v} ds^v \\
& - 2 \sin^2(\phi_v) \int_{\tilde{\Gamma}_{k,i}^v} e^{x_3^v} \sin(x_1^v) \sum_{j=1}^2 \left(\frac{\partial u}{\partial \boldsymbol{\tau}_j^v} \right)_{A^v} \frac{\partial}{\partial s_j^v} \left(\left(\frac{\partial u}{\partial \boldsymbol{\nu}^v} \right)_{A^v} \right) d\sigma^v \\
& = - \oint_{\partial \tilde{\Gamma}_{q,r}^{v-e}} e^{x_3^{v-e}} \left(\frac{\partial u}{\partial \mathbf{n}^{v-e}} \right)_{A^{v-e}} \left(\frac{\partial u}{\partial \boldsymbol{\nu}^{v-e}} \right)_{A^{v-e}} ds^{v-e} \\
& + 2 \int_{\tilde{\Gamma}_{q,r}^{v-e}} e^{x_3^{v-e}} \sum_{j=1}^2 \left(\frac{\partial u}{\partial \boldsymbol{\tau}_j^{v-e}} \right)_{A^{v-e}} \frac{\partial}{\partial s_j^{v-e}} \left(\left(\frac{\partial u}{\partial \boldsymbol{\nu}^{v-e}} \right)_{A^{v-e}} \right) d\sigma^{v-e}.
\end{aligned}$$

Proof. Let

$$\begin{aligned}
x_1^v &= \phi \\
x_2^v &= \theta \\
x_3^v &= \mathcal{X} = \ln \rho.
\end{aligned} \tag{B.1}$$

and

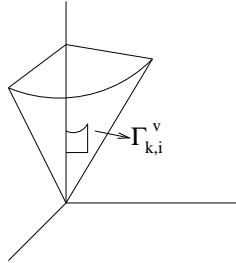


Figure B.1: Interior common boundary face $\Gamma_{k,i}^v = \Gamma_{q,r}^{v-e}$.

$$\begin{aligned}
x_1^{v-e} &= \psi = \ln(\tan x_1^v) \\
x_2^{v-e} &= \theta \\
x_3^{v-e} &= \zeta = \ln x_3 = x_3^v + \ln \cos(x_1^v).
\end{aligned} \tag{B.2}$$

Clearly

$$\nabla_{x^v} u = J^{v-e} \nabla_{x^{v-e}} u \quad (\text{B.3})$$

where

$$J^{v-e} = \begin{bmatrix} \sec^2 \phi \cot \phi & 0 & -\tan \phi \\ 0 & 1 & 0 \\ 0 & 0 & 1 \end{bmatrix}. \quad (\text{B.4})$$

Now if \mathbf{dx}^v is a tangent vector to a curve in x^v coordinates then its image in x^{v-e} coordinates is given by \mathbf{dx}^{v-e} where

$$\mathbf{dx}^{v-e} = (J^{v-e})^T \mathbf{dx}^v. \quad (\text{B.5})$$

Clearly the first fundamental form $(ds^v)^2$ in x^v coordinates is

$$(ds^v)^2 = (\mathbf{dx}^v)^T (\mathbf{dx}^v) = (\mathbf{dx}^{v-e})^T (J^{v-e})^{-1} (J^{v-e})^{-T} \mathbf{dx}^{v-e}. \quad (\text{B.6})$$

Now

$$(J^{v-e})^{-1} = \begin{bmatrix} \cos \phi \sin \phi & 0 & \sin^2 \phi \\ 0 & 1 & 0 \\ 0 & 0 & 1 \end{bmatrix}.$$

Hence

$$\begin{aligned} (ds^v)^2 &= \sin^2 \phi (dx_1^{v-e})^2 + (dx_2^{v-e})^2 + (dx_3^{v-e})^2 + 2 \sin^2 \phi dx_1^{v-e} dx_3^{v-e} \\ &= \sin^2 \phi d\psi^2 + d\theta^2 + d\zeta^2 + 2 \sin^2 \phi d\psi d\zeta. \end{aligned} \quad (\text{B.7})$$

Moreover, on $\tilde{\Gamma}_{k,i}^v$,

$$d\sigma^v = d\theta d\zeta \quad (\text{B.8})$$

since by (B.7)

$$(ds^v)^2 = d\theta^2 + d\zeta^2$$

on $\tilde{\Gamma}_{k,i}^v$. Choose $\tau_1^{v-e} = (0, 1, 0)^T$ and $\tau_2^{v-e} = -(0, 0, 1)^T$. These are orthogonal unit vectors on $\tilde{\Gamma}_{q,r}^{v-e}$ since

$$(ds^{v-e})^2 = d\psi^2 + d\theta^2 + d\zeta^2. \quad (\text{B.9})$$

Define

$$\boldsymbol{\tau}_1^v = (J^{v-e})^{-T} \boldsymbol{\tau}_1^{v-e} \quad (\text{B.10})$$

$$\boldsymbol{\tau}_2^v = -(J^{v-e})^{-T} \boldsymbol{\tau}_2^{v-e}. \quad (\text{B.11})$$

Let $\boldsymbol{\nu}^{v-e} = -(1, 0, 0)^T$ denote the unit normal vector on $\tilde{\Gamma}_{q,r}^{v-e}$ and

$$\boldsymbol{m}^{v-e} = (\sec^2 \phi \cot \phi, 0, -\tan \phi)^T. \quad (\text{B.12})$$

Then

$$\boldsymbol{\nu}^v = (1, 0, 0)^T = (J^{v-e})^{-T} \boldsymbol{m}^{v-e} \quad (\text{B.13})$$

is the unit normal to $\partial \tilde{\Gamma}_{k,i}^v$. Finally let $\mathbf{ds}^{v-e} = (0, d\theta, d\zeta)^T$ denote a tangent vector field on $\tilde{\Gamma}_{q,r}^{v-e}$. Define

$$ds^{v-e} = \sqrt{d\theta^2 + d\zeta^2} \quad (\text{B.14})$$

$$\mathbf{ds}^v = (J^{v-e})^{-T} \mathbf{ds}^{v-e} = (0, d\theta, d\mathcal{X})^T \quad (\text{B.15})$$

and

$$ds^v = \sqrt{d\theta^2 + d\mathcal{X}^2}. \quad (\text{B.16})$$

Let

$$\boldsymbol{n}^{v-e} = (0, d\zeta, -d\theta)^T / \sqrt{d\zeta^2 + d\theta^2} \quad (\text{B.17})$$

be the unit outward normal to $\partial \tilde{\Gamma}_{q,r}^{v-e}$. Then

$$\boldsymbol{n}^v = (J^{v-e})^{-T} \boldsymbol{n}^{v-e} \quad (\text{B.18})$$

is the unit outward normal to $\partial \tilde{\Gamma}_{k,i}^v$.

Now

$$\begin{aligned} \left(\frac{\partial u}{\partial \boldsymbol{n}^v} \right)_{A^v} &= (\boldsymbol{n}^v)^T (A^v) \nabla_{x^v} u \\ &= (\boldsymbol{n}^{v-e})^T (J^{v-e})^{-1} (A^v) \nabla_{x^v} u \\ &= \frac{(\boldsymbol{n}^{v-e})^T}{\sin^2 \phi} ((J^{v-e})^{-1} (J^{v-e})^{-T}) (\sin^2 \phi (J^{v-e})^T A^v J^{v-e}) \nabla_{x^{v-e}} u \\ &= \frac{(\boldsymbol{n}^{v-e})^T}{\sin^2 \phi} \begin{bmatrix} \sin^2 \phi & 0 & \sin^2 \phi \\ 0 & 1 & 0 \\ \sin^2 \phi & 0 & 1 \end{bmatrix} A^{v-e} \nabla_{x^{v-e}} u \\ &= \frac{(-d\theta \sin^2 \phi, d\zeta, -d\theta)^T}{\sin^2 \phi \sqrt{d\zeta^2 + d\theta^2}} A^{v-e} \nabla_{x^{v-e}} u. \end{aligned}$$

Hence referring to Figure B.2,

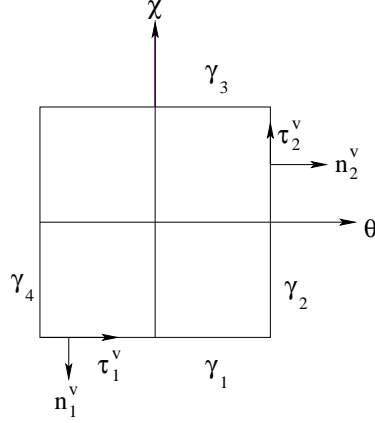


Figure B.2: The face $\tilde{\Gamma}_{k,i}^v$

$$\left(\frac{\partial u}{\partial \mathbf{n}_1^v} \right)_{A^v} = \left(\frac{\partial u}{\partial \boldsymbol{\nu}^{v-e}} \right)_{A^{v-e}} + \frac{1}{\sin^2 \phi} \left(\frac{\partial u}{\partial \boldsymbol{\tau}_2^{v-e}} \right)_{A^{v-e}} \quad (\text{B.19})$$

and

$$\left(\frac{\partial u}{\partial \mathbf{n}_2^v} \right)_{A^v} = \frac{1}{\sin^2 \phi} \left(\frac{\partial u}{\partial \boldsymbol{\tau}_1^{v-e}} \right)_{A^{v-e}}. \quad (\text{B.20})$$

Moreover

$$\left(\frac{\partial u}{\partial \boldsymbol{\nu}^v} \right)_{A^v} = \frac{(\sec^2 \phi \cot \phi, 0, -\tan \phi)}{\sin^2 \phi} \begin{bmatrix} \sin^2 \phi & 0 & \sin^2 \phi \\ 0 & 1 & 0 \\ \sin^2 \phi & 0 & 1 \end{bmatrix} A^{v-e} \nabla_{x^{v-e}} u.$$

Hence

$$\left(\frac{\partial u}{\partial \boldsymbol{\nu}^v} \right)_{A^v} = -\cot \phi \left(\frac{\partial u}{\partial \boldsymbol{\nu}^{v-e}} \right)_{A^{v-e}}. \quad (\text{B.21})$$

Finally

$$\begin{aligned} \left(\frac{\partial u}{\partial \boldsymbol{\tau}_1^v} \right)_{A^v} &= \frac{(0, 1, 0)^T}{\sin^2 \phi} \begin{bmatrix} \sin^2 \phi & 0 & \sin^2 \phi \\ 0 & 1 & 0 \\ \sin^2 \phi & 0 & 1 \end{bmatrix} A^{v-e} \nabla_{x^{v-e}} u \\ &= \frac{1}{\sin^2 \phi} \left(\frac{\partial u}{\partial \boldsymbol{\tau}_1^{v-e}} \right)_{A^{v-e}}. \end{aligned} \quad (\text{B.22})$$

And

$$\begin{aligned}
 \left(\frac{\partial u}{\partial \boldsymbol{\tau}_2^v} \right)_{A^v} &= \frac{(0, 0, 1)^T}{\sin^2 \phi} \begin{bmatrix} \sin^2 \phi & 0 & \sin^2 \phi \\ 0 & 1 & 0 \\ \sin^2 \phi & 0 & 1 \end{bmatrix} A^{v-e} \nabla_{x^{v-e}} u \\
 &= - \left(\frac{\partial u}{\partial \boldsymbol{\nu}^{v-e}} \right)_{A^{v-e}} - \frac{1}{\sin^2 \phi} \left(\frac{\partial u}{\partial \boldsymbol{\tau}_2^{v-e}} \right)_{A^{v-e}}. \tag{B.23}
 \end{aligned}$$

Now referring to Figure B.3

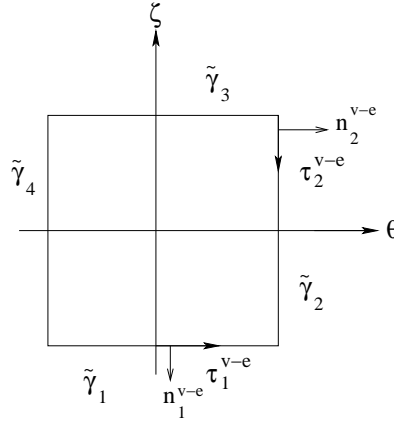


Figure B.3: The face $\tilde{\Gamma}_{q,r}^{v-e}$

$$\begin{aligned}
 &\oint_{\partial \tilde{\Gamma}_{k,i}^v} \sin^2(\phi_v) e^{x_3^v} \sin(x_1^v) \left(\frac{\partial u}{\partial \mathbf{n}^v} \right)_{A^v} \left(\frac{\partial u}{\partial \boldsymbol{\nu}^v} \right)_{A^v} ds^v \\
 &= \int_{\gamma_1} \rho \sin^3(\phi_v) \left(\frac{\partial u}{\partial \mathbf{n}_1^v} \right)_{A^v} \left(\frac{\partial u}{\partial \boldsymbol{\nu}^v} \right)_{A^v} d\theta \\
 &+ \int_{\gamma_2} \rho \sin^3(\phi_v) \left(\frac{\partial u}{\partial \mathbf{n}_2^v} \right)_{A^v} \left(\frac{\partial u}{\partial \boldsymbol{\nu}^v} \right)_{A^v} d\mathcal{X} \\
 &- \int_{\gamma_3} \rho \sin^3(\phi_v) \left(\frac{\partial u}{\partial \mathbf{n}_1^v} \right)_{A^v} \left(\frac{\partial u}{\partial \boldsymbol{\nu}^v} \right)_{A^v} d\theta \\
 &- \int_{\gamma_4} \rho \sin^3(\phi_v) \left(\frac{\partial u}{\partial \mathbf{n}_2^v} \right)_{A^v} \left(\frac{\partial u}{\partial \boldsymbol{\nu}^v} \right)_{A^v} d\mathcal{X} \\
 &= - \int_{\tilde{\gamma}_1} \rho \sin^3(\phi_v) \cot(\phi_v) \left(\frac{\partial u}{\partial \boldsymbol{\nu}^{v-e}} \right)_{A^{v-e}}^2 d\theta \\
 &- \int_{\tilde{\gamma}_1} \rho \cos(\phi_v) \left(\frac{\partial u}{\partial \boldsymbol{\tau}_2^{v-e}} \right)_{A^{v-e}} \left(\frac{\partial u}{\partial \boldsymbol{\nu}^{v-e}} \right)_{A^{v-e}} d\theta
 \end{aligned}$$

$$\begin{aligned}
& - \int_{\tilde{\gamma}_2} \rho \cos(\phi_v) \left(\frac{\partial u}{\partial \boldsymbol{\tau}_1^{v-e}} \right)_{A^{v-e}} \left(\frac{\partial u}{\partial \boldsymbol{\nu}^{v-e}} \right)_{A^{v-e}} d\zeta \\
& + \int_{\tilde{\gamma}_3} \rho \sin^3(\phi_v) \cot(\phi_v) \left(\frac{\partial u}{\partial \boldsymbol{\nu}^{v-e}} \right)_{A^{v-e}}^2 d\theta \\
& + \int_{\tilde{\gamma}_3} \rho \cos(\phi_v) \left(\frac{\partial u}{\partial \boldsymbol{\tau}_2^{v-e}} \right)_{A^{v-e}} \left(\frac{\partial u}{\partial \boldsymbol{\nu}^{v-e}} \right)_{A^{v-e}} d\theta \\
& + \int_{\tilde{\gamma}_4} \rho \cos(\phi_v) \left(\frac{\partial u}{\partial \boldsymbol{\tau}_1^{v-e}} \right)_{A^{v-e}} \left(\frac{\partial u}{\partial \boldsymbol{\nu}^{v-e}} \right)_{A^{v-e}} d\zeta .
\end{aligned} \tag{B.24}$$

Hence

$$\begin{aligned}
& \oint_{\partial \tilde{\Gamma}_{k,i}^v} \sin^2(\phi_v) e^{x_3^v} \sin(x_1^v) \left(\frac{\partial u}{\partial \boldsymbol{n}^v} \right)_{A^v} \left(\frac{\partial u}{\partial \boldsymbol{\nu}^v} \right)_{A^v} ds^v \\
& = - \oint_{\partial \tilde{\Gamma}_{q,r}^{v-e}} e^{x_3^{v-e}} \left(\frac{\partial u}{\partial \boldsymbol{n}^{v-e}} \right)_{A^{v-e}} \left(\frac{\partial u}{\partial \boldsymbol{\nu}^{v-e}} \right)_{A^{v-e}} ds^{v-e} \\
& - \int_{\tilde{\gamma}_1} \rho \sin^3(\phi_v) \cot(\phi_v) \left(\frac{\partial u}{\partial \boldsymbol{\nu}^{v-e}} \right)_{A^{v-e}}^2 d\theta \\
& + \int_{\tilde{\gamma}_3} \rho \sin^3(\phi_v) \cot(\phi_v) \left(\frac{\partial u}{\partial \boldsymbol{\nu}^{v-e}} \right)_{A^{v-e}}^2 d\theta
\end{aligned} \tag{B.25}$$

Next,

$$\begin{aligned}
& 2 \sin^2(\phi_v) \int_{\tilde{\Gamma}_{k,i}^v} e^{x_3^v} \sin(x_1^v) \left(\frac{\partial u}{\partial \boldsymbol{\tau}_1^v} \right)_{A^v} \frac{\partial}{\partial s_1^v} \left(\left(\frac{\partial u}{\partial \boldsymbol{\nu}^v} \right)_{A^v} \right) d\sigma^v \\
& = 2 \sin^2(\phi_v) \int_{\tilde{\Gamma}_{k,i}^v} \rho \sin(\phi_v) \left(\frac{\partial u}{\partial \boldsymbol{\tau}_1^v} \right)_{A^v} \frac{\partial}{\partial s_1^v} \left(\left(\frac{\partial u}{\partial \boldsymbol{\nu}^v} \right)_{A^v} \right) d\sigma^v \\
& = -2 \int_{\tilde{\Gamma}_{q,r}^{v-e}} \rho \sin^3(\phi_v) \frac{1}{\sin^2(\phi_v)} \left(\frac{\partial u}{\partial \boldsymbol{\tau}_1^{v-e}} \right)_{A^{v-e}} \\
& \quad \frac{\partial}{\partial \theta} \left(\cot(\phi_v) \left(\frac{\partial u}{\partial \boldsymbol{\nu}^{v-e}} \right)_{A^{v-e}} \right) d\theta d\zeta \\
& = -2 \int_{\tilde{\Gamma}_{q,r}^{v-e}} e^{x_3^{v-e}} \left(\frac{\partial u}{\partial \boldsymbol{\tau}_1^{v-e}} \right)_{A^{v-e}} \frac{\partial}{\partial s_1^{v-e}} \left(\left(\frac{\partial u}{\partial \boldsymbol{\nu}^{v-e}} \right)_{A^{v-e}} \right) d\sigma^{v-e}.
\end{aligned} \tag{B.26}$$

Moreover

$$\begin{aligned}
& 2 \sin^2(\phi_v) \int_{\tilde{\Gamma}_{k,i}^v} e^{x_3^v} \sin(x_1^v) \left(\frac{\partial u}{\partial \boldsymbol{\tau}_2^v} \right)_{A^v} \frac{\partial}{\partial s_2^v} \left(\left(\frac{\partial u}{\partial \boldsymbol{\nu}^v} \right)_{A^v} \right) d\sigma^v \\
& = 2 \sin^2(\phi_v) \int_{\tilde{\Gamma}_{q,r}^v} \rho \sin(\phi_v) \left(\frac{\partial u}{\partial \boldsymbol{\tau}_2^v} \right)_{A^v} \frac{\partial}{\partial s_2^v} \left(\left(\frac{\partial u}{\partial \boldsymbol{\nu}^v} \right)_{A^v} \right) d\sigma^v \\
& = 2 \int_{\tilde{\Gamma}_{q,r}^{v-e}} \left(\rho \sin^3(\phi_v) \left(\left(\frac{\partial u}{\partial \boldsymbol{\nu}^{v-e}} \right)_{A^{v-e}} \right) \right. \\
& \quad \left. + \frac{1}{\sin^2(\phi_v)} \left(\frac{\partial u}{\partial \boldsymbol{\tau}_2^{v-e}} \right)_{A^{v-e}} \right) \frac{\partial}{\partial \zeta} \left(\cot(\phi_v) \left(\frac{\partial u}{\partial \boldsymbol{\nu}^{v-e}} \right)_{A^{v-e}} \right) d\theta d\zeta
\end{aligned}$$

$$\begin{aligned}
&= \int_{\tilde{\Gamma}_{q,r}^{v-e}} \rho \sin^3(\phi_v) \cot(\phi_v) \frac{\partial}{\partial \zeta} \left(\frac{\partial u}{\partial \boldsymbol{\nu}^{v-e}} \right)_{A^{v-e}}^2 d\theta d\zeta \\
&+ 2 \int_{\tilde{\Gamma}_{q,r}^{v-e}} e^\zeta \left(\frac{\partial u}{\partial \boldsymbol{\tau}_2^{v-e}} \right)_{A^{v-e}} \frac{\partial}{\partial \zeta} \left(\frac{\partial u}{\partial \boldsymbol{\nu}^{v-e}} \right)_{A^{v-e}} d\theta d\zeta \\
&= - \int_{\tilde{\gamma}_1} \rho \sin^3(\phi_v) \cot(\phi_v) \left(\frac{\partial u}{\partial \boldsymbol{\nu}^{v-e}} \right)_{A^{v-e}}^2 d\theta \\
&+ \int_{\tilde{\gamma}_3} \rho \sin^3(\phi_v) \cot(\phi_v) \left(\frac{\partial u}{\partial \boldsymbol{\nu}^{v-e}} \right)_{A^{v-e}}^2 d\theta \\
&- 2 \int_{\tilde{\Gamma}_{q,r}^{v-e}} e^{x_3^{v-e}} \left(\frac{\partial u}{\partial \boldsymbol{\tau}_2^{v-e}} \right)_{A^{v-e}} \frac{\partial}{\partial s_2^{v-e}} \left(\frac{\partial u}{\partial \boldsymbol{\nu}^{v-e}} \right)_{A^{v-e}} d\sigma^{v-e}. \tag{B.27}
\end{aligned}$$

Combining (B.24)-(B.27) we obtain the result. \square

B.2

Proof of Lemma 3.2.8

Lemma 3.2.8. *Let $\Gamma_{u,k}^e = \Gamma_{n,l}^{v-e}$. Then*

$$\begin{aligned}
&\oint_{\partial \tilde{\Gamma}_{n,l}^{v-e}} e^{x_3^{v-e}} \left(\frac{\partial u}{\partial \boldsymbol{n}^{v-e}} \right)_{A^{v-e}} \left(\frac{\partial u}{\partial \boldsymbol{\nu}^{v-e}} \right)_{A^{v-e}} w^{v-e}(x_1^{v-e}) ds^{v-e} \\
&- 2 \sum_{j=1}^2 \int_{\tilde{\Gamma}_{n,l}^{v-e}} e^{x_3^{v-e}} \left(\frac{\partial u}{\partial \boldsymbol{\tau}_j^{v-e}} \right)_{A^{v-e}} \frac{\partial}{\partial s_j^{v-e}} \left(\left(\frac{\partial u}{\partial \boldsymbol{\nu}^{v-e}} \right)_{A^{v-e}} \right) w^{v-e}(x_1^{v-e}) d\sigma^{v-e} \\
&= - \oint_{\partial \tilde{\Gamma}_{u,k}^e} \left(\frac{\partial u}{\partial \boldsymbol{n}^e} \right)_{A^e} \left(\frac{\partial u}{\partial \boldsymbol{\nu}^e} \right)_{A^e} w^e(x_1^e) ds^e \\
&+ 2 \sum_{j=1}^2 \int_{\tilde{\Gamma}_{u,k}^e} \left(\frac{\partial u}{\partial \boldsymbol{\tau}_j^e} \right)_{A^e} \frac{\partial}{\partial s_j^e} \left(\left(\frac{\partial u}{\partial \boldsymbol{\nu}^e} \right)_{A^e} \right) w^e(x_1^e) d\sigma^e.
\end{aligned}$$

Proof. We have

$$\begin{aligned}
x_1^e &= \tau = \ln r \\
x_2^e &= \theta \\
x_3^e &= x_3. \tag{B.28}
\end{aligned}$$

and

$$\begin{aligned}
x_1^{v-e} &= \psi = \ln \tan \phi \\
x_2^{v-e} &= \theta \\
x_3^{v-e} &= \zeta = \ln x_3. \tag{B.29}
\end{aligned}$$

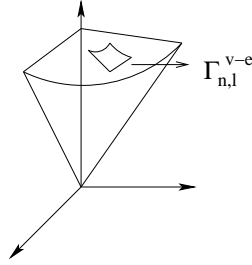


Figure B.4: Interior common boundary face $\Gamma_{u,k}^e = \Gamma_{n,l}^{v-e}$

Hence

$$\begin{aligned} x_1^e &= x_1^{v-e} + x_3^{v-e} = \psi + \zeta \\ x_2^e &= x_2^{v-e} \\ x_3^e &= e^{x_3^{v-e}} = e^\zeta. \end{aligned} \tag{B.30}$$

Clearly

$$\nabla_{x^{v-e}} u = J^e \nabla_{x^e} u. \tag{B.31}$$

Here

$$J^e = \begin{bmatrix} 1 & 0 & 0 \\ 0 & 1 & 0 \\ 1 & 0 & x_3 \end{bmatrix}. \tag{B.32}$$

Now if \mathbf{dx}^{v-e} is a tangent vector to a curve in x^{v-e} coordinates then its image in x^e coordinates is given by \mathbf{dx}^e where

$$\mathbf{dx}^e = (J^e)^T \mathbf{dx}^{v-e}. \tag{B.33}$$

Clearly the first fundamental form $(ds^{v-e})^2$ in x^{v-e} coordinates is

$$(ds^{v-e})^2 = (\mathbf{dx}^{v-e})^T (\mathbf{dx}^{v-e}) = (\mathbf{dx}^e)^T ((J^e)^{-1} (J^e)^{-T}) \mathbf{dx}^{v-e}. \tag{B.34}$$

Now

$$(J^e)^{-1} = \begin{bmatrix} 1 & 0 & 0 \\ 0 & 1 & 0 \\ -\frac{1}{x_3} & 0 & \frac{1}{x_3} \end{bmatrix}. \tag{B.35}$$

Hence

$$\begin{aligned} (ds^{v-e})^2 &= (dx_1^e)^2 + (dx_2^e)^2 + \frac{2}{x_3^2}(dx_3^e)^2 - \frac{2}{x_3}dx_1^edx_3^e \\ &= d\tau^2 + d\theta^2 + \frac{2}{x_3^2}dx_3^2 - \frac{2}{x_3}d\tau dx_3. \end{aligned} \quad (\text{B.36})$$

Moreover on $\tilde{\Gamma}_{n,l}^{v-e}$

$$d\sigma^{v-e} = d\tau d\theta$$

since

$$(ds^{v-e})^2 = d\tau^2 + d\theta^2$$

on $\tilde{\Gamma}_{n,l}^{v-e}$. Choose $\boldsymbol{\tau}_1^e = (1, 0, 0)^T$ and $\boldsymbol{\tau}_2^e = -(0, 1, 0)^T$. These are orthogonal unit vectors on $\tilde{\Gamma}_{u,k}^e$ since

$$(ds^e)^2 = d\tau^2 + d\theta^2 + dx_3^2. \quad (\text{B.37})$$

Define

$$\begin{aligned} \boldsymbol{\tau}_1^{v-e} &= (J^e)^{-T} \boldsymbol{\tau}_1^e, \text{ and} \\ \boldsymbol{\tau}_2^{v-e} &= -(J^e)^{-T} \boldsymbol{\tau}_2^e. \end{aligned} \quad (\text{B.38})$$

Let $\boldsymbol{\nu}^e = -(0, 0, 1)^T$ denote the unit normal vector to $\tilde{\Gamma}_{u,k}^e$. Let

$$\boldsymbol{m}^e = (1, 0, x_3)^T. \quad (\text{B.39})$$

Then

$$\boldsymbol{\nu}^{v-e} = (0, 0, 1)^T = (J^e)^{-T} \boldsymbol{m}^e \quad (\text{B.40})$$

is the unit normal to $\tilde{\Gamma}_{n,l}^{v-e}$. Finally let

$$\mathbf{ds}^e = (d\tau, d\theta, 0)^T$$

denote a tangent vector field on $\tilde{\Gamma}_{u,k}^e$. Define

$$ds^e = \sqrt{d\tau^2 + d\theta^2} \quad (\text{B.41})$$

$$\mathbf{ds}^{v-e} = (J^e)^{-T} \mathbf{ds}^e = (d\psi, d\theta, 0)^T \quad (\text{B.42})$$

$$ds^{v-e} = \sqrt{d\theta^2 + d\psi^2} = \sqrt{d\tau^2 + d\theta^2} = ds^e. \quad (\text{B.43})$$

Let

$$\mathbf{n}^e = \frac{(d\theta, -d\tau, 0)^T}{\sqrt{d\tau^2 + d\theta^2}} \quad (\text{B.44})$$

be the unit outward normal to $\partial\tilde{\Gamma}_{u,k}^e$. Then the unit outward normal \mathbf{n}^{v-e} to $\partial\tilde{\Gamma}_{n,l}^{v-e}$ is

$$\mathbf{n}^{v-e} = (J^e)^{-T} \mathbf{n}^e. \quad (\text{B.45})$$

Now

$$\begin{aligned} \left(\frac{\partial u}{\partial \mathbf{n}^{v-e}} \right)_{A^{v-e}} &= (\mathbf{n}^{v-e})^T A^{v-e} \nabla_{x^{v-e}} u \\ &= (\mathbf{n}^e)^T (J^e)^{-1} A^{v-e} J^e \nabla_{x^e} u \\ &= (\mathbf{n}^e)^T ((J^e)^{-1} (J^e)^{-T}) ((J^e)^T A^{v-e} J^e) \nabla_{x^e} u \\ &= (\mathbf{n}^e)^T \begin{bmatrix} 1 & 0 & -\frac{1}{x_3} \\ 0 & 1 & 0 \\ -\frac{1}{x_3} & 0 & \frac{2}{x_3^2} \end{bmatrix} A^e \nabla_{x^e} u \\ &= \frac{(d\theta, -d\tau, -\frac{d\theta}{x_3})^T}{\sqrt{d\tau^2 + d\theta^2}} A^e \nabla_{x^e} u. \end{aligned}$$

Here

$$\mathbf{n}^e = \frac{(d\theta, -d\tau, 0)^T}{\sqrt{d\theta^2 + d\tau^2}}.$$

It should be noted that $A^e = (J^e)^T A^{v-e} J^e$. Hence referring to Figure B.5

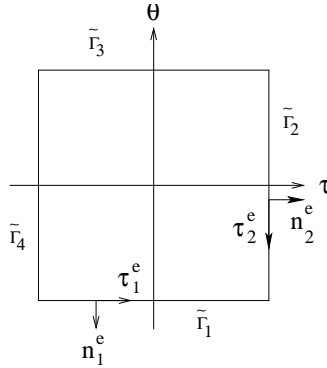


Figure B.5: The face $\tilde{\Gamma}_{u,k}^e$

$$\left(\frac{\partial u}{\partial \mathbf{n}_1^{v-e}} \right)_{A^{v-e}} = \left(\frac{\partial u}{\partial \tau_2^e} \right)_{A^e}, \quad (\text{B.46})$$

and

$$\left(\frac{\partial u}{\partial \mathbf{n}_2^{v-e}} \right)_{A^{v-e}} = \left(\frac{\partial u}{\partial \boldsymbol{\tau}_1^e} \right)_{A^e} + \frac{1}{x_3} \left(\frac{\partial u}{\partial \boldsymbol{\nu}^e} \right)_{A^e}. \quad (\text{B.47})$$

Moreover

$$\begin{aligned} \left(\frac{\partial u}{\partial \boldsymbol{\nu}^{v-e}} \right)_{A^{v-e}} &= \begin{bmatrix} 1 & 0 & x_3 \end{bmatrix} \begin{bmatrix} 1 & 0 & -\frac{1}{x_3} \\ 0 & 1 & 0 \\ -\frac{1}{x_3} & 0 & \frac{2}{x_3^2} \end{bmatrix} A^e \nabla_{x^e} u \\ &= \left[0, 0, \frac{1}{x_3} \right] A^e \nabla_{x^e} u \\ &= -\frac{1}{x_3} \left(\frac{\partial u}{\partial \boldsymbol{\nu}^e} \right)_{A^e}. \end{aligned} \quad (\text{B.48})$$

Now

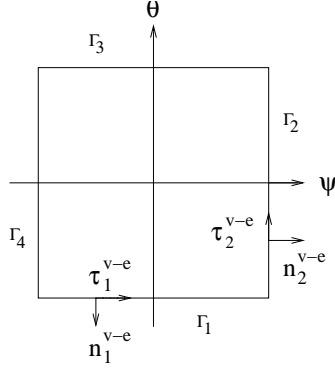


Figure B.6: The face $\tilde{\Gamma}_{n,l}^{v-e}$

$$\begin{aligned} &\oint_{\tilde{\Gamma}_{n,l}^{v-e}} e^{x_3^{v-e}} \left(\frac{\partial u}{\partial \mathbf{n}^{v-e}} \right)_{A^{v-e}} \left(\frac{\partial u}{\partial \boldsymbol{\nu}^{v-e}} \right)_{A^{v-e}} ds^{v-e} \\ &= \int_{\Gamma_1} x_3 \left(\frac{\partial u}{\partial \mathbf{n}_1^{v-e}} \right)_{A^{v-e}} \left(\frac{\partial u}{\partial \boldsymbol{\nu}^{v-e}} \right)_{A^{v-e}} d\psi \\ &\quad + \int_{\Gamma_2} x_3 \left(\frac{\partial u}{\partial \mathbf{n}_2^{v-e}} \right)_{A^{v-e}} \left(\frac{\partial u}{\partial \boldsymbol{\nu}^{v-e}} \right)_{A^{v-e}} d\theta \\ &\quad - \int_{\Gamma_3} x_3 \left(\frac{\partial u}{\partial \mathbf{n}_1^{v-e}} \right)_{A^{v-e}} \left(\frac{\partial u}{\partial \boldsymbol{\nu}^{v-e}} \right)_{A^{v-e}} d\psi \\ &\quad - \int_{\Gamma_4} x_3 \left(\frac{\partial u}{\partial \mathbf{n}_2^{v-e}} \right)_{A^{v-e}} \left(\frac{\partial u}{\partial \boldsymbol{\nu}^{v-e}} \right)_{A^{v-e}} d\theta \\ &= - \int_{\tilde{\Gamma}_1} \left(\frac{\partial u}{\partial \boldsymbol{\tau}_2^e} \right)_{A^e} \left(\frac{\partial u}{\partial \boldsymbol{\nu}^e} \right)_{A^e} d\tau \end{aligned}$$

$$\begin{aligned}
& - \int_{\tilde{\Gamma}_2} \left(\left(\frac{\partial u}{\partial \tau_1^e} \right)_{A^e} + \frac{1}{x_3} \left(\frac{\partial u}{\partial \nu^e} \right)_{A^e} \right) \left(\frac{\partial u}{\partial \nu^e} \right)_{A^e} d\theta \\
& + \int_{\tilde{\Gamma}_3} \left(\frac{\partial u}{\partial \tau_2^e} \right)_{A^e} \left(\frac{\partial u}{\partial \nu^e} \right)_{A^e} d\tau \\
& + \int_{\tilde{\Gamma}_4} \left(\left(\frac{\partial u}{\partial \tau_1^e} \right)_{A^e} + \frac{1}{x_3} \left(\frac{\partial u}{\partial \nu^e} \right)_{A^e} \right) \left(\frac{\partial u}{\partial \nu^e} \right)_{A^e} d\theta \\
& = - \oint_{\partial \tilde{\Gamma}_{u,k}^e} \left(\frac{\partial u}{\partial \mathbf{n}^e} \right)_{A^e} \left(\frac{\partial u}{\partial \nu^e} \right)_{A^e} ds^e \\
& - \int_{\tilde{\Gamma}_2} \frac{1}{x_3} \left(\frac{\partial u}{\partial \nu^e} \right)_{A^e}^2 d\theta + \int_{\tilde{\Gamma}_4} \frac{1}{x_3} \left(\frac{\partial u}{\partial \nu^e} \right)_{A^e}^2 d\theta
\end{aligned} \tag{B.49}$$

Now $\tau_1^{v-e} = (1, 0, 0)^T$ and $\tau_1^e = (J^e)^{-T} \tau_1^{v-e}$. Moreover $\tau_2^{v-e} = (0, 1, 0)^T$ and $\tau_2^e = -(J^e)^T \tau_2^{v-e}$.

Hence

$$\begin{aligned}
& 2 \int_{\tilde{\Gamma}_{n,l}^{v-e}} e^{x_3^{v-e}} \left(\frac{\partial u}{\partial \tau_1^{v-e}} \right)_{A^{v-e}} \frac{\partial}{\partial s_1^{v-e}} \left(\left(\frac{\partial u}{\partial \nu^{v-e}} \right)_{A^{v-e}} \right) d\sigma^{v-e} \\
& = -2 \int_{\tilde{\Gamma}_{u,k}^e} \left(\left(\frac{\partial u}{\partial \tau_1^e} \right)_{A^e} + \frac{1}{x_3} \left(\frac{\partial u}{\partial \nu^e} \right)_{A^e} \right) \frac{\partial}{\partial \tau} \left(\left(\frac{\partial u}{\partial \nu^e} \right)_{A^e} \right) d\tau d\theta \\
& = -2 \int_{\tilde{\Gamma}_{u,k}^e} \left(\frac{\partial u}{\partial \tau_1^e} \right)_{A^e} \frac{\partial}{\partial s_1^e} \left(\left(\frac{\partial u}{\partial \nu^e} \right)_{A^e} \right) d\sigma^e \\
& - \int_{\tilde{\Gamma}_2} \frac{1}{x_3} \left(\frac{\partial u}{\partial \nu^e} \right)_{A^e}^2 d\theta + \int_{\tilde{\Gamma}_4} \frac{1}{x_3} \left(\frac{\partial u}{\partial \nu^e} \right)_{A^e}^2 d\theta.
\end{aligned} \tag{B.50}$$

And

$$\begin{aligned}
& 2 \int_{\tilde{\Gamma}_{n,l}^{v-e}} e^{x_3^{v-e}} \left(\frac{\partial u}{\partial \tau_2^{v-e}} \right)_{A^{v-e}} \frac{\partial}{\partial s_2^{v-e}} \left(\left(\frac{\partial u}{\partial \nu^{v-e}} \right)_{A^{v-e}} \right) d\sigma^{v-e} \\
& = -2 \int_{\tilde{\Gamma}_{u,k}^e} \left(\frac{\partial u}{\partial \tau_2^e} \right)_{A^e} \frac{\partial}{\partial \theta} \left(\left(\frac{\partial u}{\partial \nu^e} \right)_{A^e} \right) d\tau d\theta \\
& = -2 \int_{\tilde{\Gamma}_{u,k}^e} \left(\frac{\partial u}{\partial \tau_2^e} \right)_{A^e} \frac{\partial}{\partial s_2^e} \left(\left(\frac{\partial u}{\partial \nu^e} \right)_{A^e} \right) d\sigma^e.
\end{aligned} \tag{B.51}$$

Combining (B.49), (B.50) and (B.51) we obtain the result. \square

B.3

Proof of Lemma 3.2.9

Lemma 3.2.9. *Let $\Gamma_{u,k}^e = \Gamma_{l,j}^r$. Then*

$$\rho_v^2 \sin^2(\phi_v) \oint_{\partial \Gamma_{l,j}^r} \left(\frac{\partial u}{\partial \mathbf{n}} \right)_A \left(\frac{\partial u}{\partial \boldsymbol{\nu}} \right)_A ds = - \oint_{\partial \tilde{\Gamma}_{u,k}^e} \left(\frac{\partial u}{\partial \boldsymbol{\nu}^e} \right)_{A^e} \left(\frac{\partial u}{\partial \mathbf{n}^e} \right)_{A^e} ds^e$$

and

$$\begin{aligned} & \rho_v^2 \sin^2(\phi_v) \left(\sum_{m=1}^2 \int_{\Gamma_{l,j}^r} \left(\frac{\partial u}{\partial \boldsymbol{\tau}_m} \right)_A \frac{\partial}{\partial s_m} \left(\frac{\partial u}{\partial \boldsymbol{\nu}} \right)_A d\sigma \right) \\ &= - \sum_{m=1}^2 \int_{\tilde{\Gamma}_{u,k}^e} \left(\frac{\partial u}{\partial \boldsymbol{\tau}_m^e} \right)_{A^e} \frac{\partial}{\partial s_m^e} \left(\frac{\partial u}{\partial \boldsymbol{\nu}^e} \right)_{A^e} d\sigma^e \end{aligned}$$

Proof. We have

$$\begin{aligned} x_1^e &= \tau = \ln r \\ x_2^e &= \theta \\ x_3^e &= x_3. \end{aligned} \tag{B.52}$$

Clearly,

$$\nabla_x u = R^e \nabla_{x^e} u \tag{B.53}$$

where

$$R^e = \begin{bmatrix} e^{-\tau} \cos \theta & -e^{-\tau} \sin \theta & 0 \\ e^{-\tau} \sin \theta & e^{-\tau} \cos \theta & 0 \\ 0 & 0 & 1 \end{bmatrix}. \tag{B.54}$$

Now if \mathbf{dx} is a tangent vector to a curve in x^v coordinates then its image in x^e coordinates is given by \mathbf{dx}^e where

$$\mathbf{dx}^e = (R^e)^T \mathbf{dx}. \tag{B.55}$$

Clearly, the first fundamental form $(ds)^2$ in x coordinates is

$$(ds)^2 = (\mathbf{dx})^T (\mathbf{dx}) = (\mathbf{dx}^e)^T (R^e)^{-1} (R^e)^{-T} \mathbf{dx}^e. \tag{B.56}$$

Now

$$(R^e)^{-1} = \begin{bmatrix} e^\tau \cos \theta & e^\tau \sin \theta & 0 \\ -e^\tau \sin \theta & e^\tau \cos \theta & 0 \\ 0 & 0 & 1 \end{bmatrix}. \tag{B.57}$$

Hence

$$(ds)^2 = e^{2\tau}(d\tau)^2 + e^{2\tau}(d\theta)^2 + (dx_3^e)^2. \quad (\text{B.58})$$

Moreover on $\Gamma_{l,j}^r$

$$d\sigma = e^\tau d\theta dx_3^e \quad (\text{B.59})$$

since

$$(ds)^2 = e^{2\tau}(d\theta)^2 + (dx_3^e)^2$$

on $\Gamma_{l,j}^r$. Choose $\boldsymbol{\tau}_1^e = (0, 1, 0)^T$ and $\boldsymbol{\tau}_2^e = (0, 0, 1)^T$. These are orthogonal unit tangent vectors on $\tilde{\Gamma}_{u,k}^e$ since $(ds)^2 = e^{2\tau}(d\tau)^2 + e^{2\tau}(d\theta)^2 + (dx_3^e)^2$.

Define

$$\begin{aligned} \boldsymbol{\tau}_1 &= e^{-\tau}(R^e)^{-T}\boldsymbol{\tau}_1^e, \\ \boldsymbol{\tau}_2 &= (R^e)^{-T}\boldsymbol{\tau}_2^e. \end{aligned} \quad (\text{B.60})$$

Let $\boldsymbol{\nu}^e = (1, 0, 0)^T$ denotes the unit normal vector on $\tilde{\Gamma}_{u,k}^e$. Then

$$\boldsymbol{\nu} = -e^{-\tau}(R^e)^{-T}\boldsymbol{\nu}^e$$

denotes the unit normal to $\Gamma_{l,j}^r$. Finally let

$$\mathbf{ds}^e = (0, d\theta, dx_3^e)$$

denotes a tangent vector field on $\tilde{\Gamma}_{u,k}^e$. Define

$$ds^e = \sqrt{(d\theta)^2 + (dx_3^e)^2}, \quad (\text{B.61})$$

$$\mathbf{ds} = (R^e)^{-T}\mathbf{ds}^e \quad (\text{B.62})$$

and

$$ds = \sqrt{e^{2\tau}(d\theta)^2 + (dx_3^e)^2}. \quad (\text{B.63})$$

Let

$$\mathbf{n}^e = \frac{(0, -dx_3^e, d\theta)^T}{\sqrt{(d\theta)^2 + (dx_3^e)^2}} \quad (\text{B.64})$$

be the outward unit normal to $\partial\tilde{\Gamma}_{u,k}^e$. Define

$$\mathbf{m}^e = \frac{(0, -e^{-\tau}dx_3^e, e^\tau d\theta)^T}{\sqrt{e^{2\tau}(d\theta)^2 + (dx_3^e)^2}}. \quad (\text{B.65})$$

Then

$$\mathbf{n} = (R^e)^{-T} \mathbf{m}^e \quad (\text{B.66})$$

is the outward unit normal to $\partial\Gamma_{l,j}^r$.

Now

$$\begin{aligned} \left(\frac{\partial u}{\partial \boldsymbol{\nu}} \right)_A &= \boldsymbol{\nu}^T A \nabla_x u \\ &= -e^{-\tau} (\boldsymbol{\nu}^e)^T (R^e)^{-1} A (R^e) \nabla_x^e u \\ &= -e^{-\tau} (\boldsymbol{\nu}^e)^T e^{-2\tau} ((R^e)^{-1} (R^e)^{-T}) A^e \nabla_x^e u. \end{aligned}$$

And

$$(\boldsymbol{\nu}^e)^T e^{-2\tau} ((R^e)^{-1} (R^e)^{-T}) = (\boldsymbol{\nu}^e)^T.$$

Hence we conclude that

$$\left(\frac{\partial u}{\partial \boldsymbol{\nu}} \right)_A = -e^{-\tau} \left(\frac{\partial u}{\partial \boldsymbol{\nu}^e} \right)_{A^e}. \quad (\text{B.67})$$

Also from (B.65)

$$\left(\frac{\partial u}{\partial \mathbf{n}} \right)_A = \mathbf{n}^T A \nabla_x u = ((\mathbf{m}^e)^T (R^e)^{-1} e^{-2\tau} (R^e)^{-T}) A^e \nabla_x^e u.$$

Clearly

$$((\mathbf{m}^e)^T (R^e)^{-1} e^{-2\tau} (R^e)^{-T}) = e^{-\tau} \frac{ds^e}{ds} (\mathbf{n}^e)^T.$$

Hence

$$\left(\frac{\partial u}{\partial \mathbf{n}} \right)_A ds = e^{-\tau} \left(\frac{\partial u}{\partial \mathbf{n}^e} \right)_{A^e} ds^e. \quad (\text{B.68})$$

Thus from (B.67) and (B.68) we get

$$\begin{aligned} \rho_v^2 \sin^2(\phi_v) \oint_{\partial\Gamma_{l,j}^r} \left(\frac{\partial u}{\partial \mathbf{n}} \right)_A \left(\frac{\partial u}{\partial \boldsymbol{\nu}} \right)_A ds \\ = -\rho_v^2 \sin^2(\phi_v) \oint_{\partial\tilde{\Gamma}_{u,k}^e} e^{-2\tau} \left(\frac{\partial u}{\partial \boldsymbol{\nu}^e} \right)_{A^e} \left(\frac{\partial u}{\partial \mathbf{n}^e} \right)_{A^e} ds^e \\ = -\oint_{\partial\tilde{\Gamma}_{u,k}^e} \left(\frac{\partial u}{\partial \boldsymbol{\nu}^e} \right)_{A^e} \left(\frac{\partial u}{\partial \mathbf{n}^e} \right)_{A^e} ds^e. \end{aligned} \quad (\text{B.69})$$

Using (B.60) it is easy to show that

$$\begin{aligned} \left(\frac{\partial u}{\partial \boldsymbol{\tau}_1} \right)_A &= e^{-\tau} \left(\frac{\partial u}{\partial \boldsymbol{\tau}_1^e} \right)_{A^e}, \\ \left(\frac{\partial u}{\partial \boldsymbol{\tau}_1} \right)_A &= e^{-2\tau} \left(\frac{\partial u}{\partial \boldsymbol{\tau}_1^e} \right)_{A^e} \end{aligned} \quad (\text{B.70})$$

Moreover using (B.67) we get

$$\begin{aligned}\frac{\partial}{\partial s_1} \left(\left(\frac{\partial u}{\partial \boldsymbol{\nu}} \right)_A \right) &= e^{-2\tau} \frac{\partial}{\partial s_1^e} \left(\left(\frac{\partial u}{\partial \boldsymbol{\nu}^e} \right)_{A^e} \right), \\ \frac{\partial}{\partial s_2} \left(\left(\frac{\partial u}{\partial \boldsymbol{\nu}} \right)_A \right) &= e^{-\tau} \frac{\partial}{\partial s_2^e} \left(\left(\frac{\partial u}{\partial \boldsymbol{\nu}^e} \right)_{A^e} \right).\end{aligned}\tag{B.71}$$

Combining (B.69), (B.70) and (B.71) we obtain the result. \square

Appendix C

C.1

Proof of Lemma 3.3.1

Lemma 3.3.1. *We can define a set of corrections $\{\eta_l^r\}_{l=1,\dots,N_r}$, $\{\eta_l^v\}_{l=1,\dots,N_v}$ for $v \in \mathcal{V}$, $\{\eta_l^{v-e}\}_{l=1,\dots,N_{v-e}}$ for $v-e \in \mathcal{V} - \mathcal{E}$ and $\{\eta_l^e\}_{l=1,\dots,N_e}$ for $e \in \mathcal{E}$ such that the corrected spectral element function p defined as*

$$\begin{aligned} p_l^r &= u_l^r + \eta_l^r && \text{for } l = 1, \dots, N_r, \\ p_l^v &= u_l^v + \eta_l^v && \text{for } l = 1, \dots, N_v \quad \text{and} \quad v \in \mathcal{V}, \\ p_l^{v-e} &= u_l^{v-e} + \eta_l^{v-e} && \text{for } l = 1, \dots, N_{v-e} \quad \text{and} \quad v-e \in \mathcal{V} - \mathcal{E}, \\ p_l^e &= u_l^e + \eta_l^e && \text{for } l = 1, \dots, N_e \quad \text{and} \quad e \in \mathcal{E}, \end{aligned}$$

is conforming and $p \in H_0^1(\Omega)$. i.e. $p \in H^1(\Omega)$ and p vanishes on $\Gamma^{[0]}$. Define

$$\begin{aligned} \mathcal{U}_{(1)}^{N,W}(\{\mathcal{F}_s\}) &= \sum_{l=1}^{N_r} \|s_l^r(x_1, x_2, x_3)\|_{1,\Omega_l^r}^2 + \sum_{v \in \mathcal{V}} \sum_{l=1}^{N_v} \|s_l^v(x_1^v, x_2^v, x_3^v) e^{x_3^v/2}\|_{1,\tilde{\Omega}_l^v}^2 \\ &+ \sum_{v-e \in \mathcal{V}-\mathcal{E}} \left(\sum_{l=1}^{N_{v-e}} \int_{\tilde{\Omega}_l^{v-e}} e^{x_3^{v-e}} \left(\sum_{i=1}^2 \left(\frac{\partial s_l^{v-e}}{\partial x_i^{v-e}} \right)^2 + \sin^2 \phi \left(\frac{\partial s_l^{v-e}}{\partial x_3^{v-e}} \right)^2 \right. \right. \\ &\left. \left. + (s_l^{v-e})^2 \right) dx^{v-e} + \sum_{l=1}^{N_{v-e}} \int_{\tilde{\Omega}_l^{v-e}} e^{x_3^{v-e}} (s_l^{v-e})^2 w^{v-e}(x^{v-e}) dx^{v-e} \right) \\ &+ \sum_{e \in \mathcal{E}} \left(\sum_{l=1}^{N_e} \int_{\tilde{\Omega}_l^e} \left(\sum_{i=1}^2 \left(\frac{\partial s_l^e}{\partial x_i^e} \right)^2 + e^{2\tau} \left(\frac{\partial s_l^e}{\partial x_3^e} \right)^2 + (s_l^e)^2 \right) dx^e \right. \\ &\left. + \sum_{l=1}^{N_e} \int_{\tilde{\Omega}_l^e} (s_l^e)^2 w^e(x_1^e) dx^e \right). \end{aligned} \tag{C.1}$$

Then the estimate

$$\mathcal{U}_{(1)}^{N,W}(\{\mathcal{F}_\eta\}) \leq C_W \mathcal{V}^{N,W}(\{\mathcal{F}_u\}) \tag{C.2}$$

holds. Here C_W is a constant, if the spectral element functions are conforming on the wirebasket WB of the elements, otherwise $C_W = C(\ln W)$, where C is a constant.

Proof. We first consider the case when the spectral element functions are conforming on the wirebasket. Consider an element $\Omega_l^r \subseteq \Omega^r$ which, for simplicity is assumed to be a hexahedral domain. Let Q denote the cube $(-1, 1)^3$ and $M_l^r(\lambda_1, \lambda_2, \lambda_3)$ denote an analytic mapping from Q to Ω_l^r . Let f_1 be the face corresponding to $\lambda_3 = -1$, f_2 the face corresponding to $\lambda_3 = 1$ and $[u(\lambda_1, \lambda_2)]|_{f_1}$ denote the jump in the value of u across the face f_1 so that $u_l^r(\lambda_1, \lambda_2) + 1/2 [u(\lambda_1, \lambda_2)]|_{f_1}$ = average value of u on the face f_1 . Similarly by $[u(\lambda_1, \lambda_2)]|_{f_2}$ we denote the jump in the value of u across the face f_2 so that $u_l^r(\lambda_1, \lambda_2) + 1/2 [u(\lambda_1, \lambda_2)]|_{f_2}$ = average value of u on the face f_2 .

Let f_3 be the face corresponding to $\lambda_2 = -1$ and f_4 the face corresponding to $\lambda_2 = 1$. We can now define $[u(\lambda_1, \lambda_3)]|_{f_3}$, the jump in u across the face f_3 , and $[u(\lambda_1, \lambda_3)]|_{f_4}$, the jump in u across the face f_4 . Finally, let f_5 denote the face corresponding to $\lambda_1 = -1$

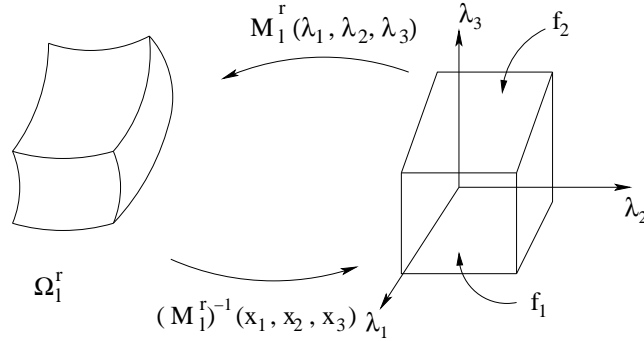


Figure C.1: The element Ω_l^r and the master cube.

and f_6 the face corresponding to $\lambda_1 = 1$. Once again, we define $[u(\lambda_2, \lambda_3)]|_{f_5}$, the jump in u across the face f_5 , and $[u(\lambda_2, \lambda_3)]|_{f_6}$, the jump in u across the face f_6 . Let us now define the correction

$$\begin{aligned} \nu_l^r(\lambda_1, \lambda_2, \lambda_3) = & \frac{(1 - \lambda_3)}{2} \frac{[u(\lambda_1, \lambda_2)]}{2} \Big|_{f_1} + \frac{(1 + \lambda_3)}{2} \frac{[u(\lambda_1, \lambda_2)]}{2} \Big|_{f_2} \\ & + \frac{(1 - \lambda_2)}{2} \frac{[u(\lambda_1, \lambda_3)]}{2} \Big|_{f_3} + \frac{(1 + \lambda_2)}{2} \frac{[u(\lambda_1, \lambda_3)]}{2} \Big|_{f_4} \\ & + \frac{(1 - \lambda_1)}{2} \frac{[u(\lambda_2, \lambda_3)]}{2} \Big|_{f_5} + \frac{(1 + \lambda_1)}{2} \frac{[u(\lambda_2, \lambda_3)]}{2} \Big|_{f_6}. \end{aligned} \quad (\text{C.3})$$

Then

$$\eta_l^r(x_1, x_2, x_3) = \nu_l^r((M_l^r)^{-1}(x_1, x_2, x_3)) .$$

Next, we define the corrections in the vertex neighbourhood Ω^v for $v \in \mathcal{V}$, the set of vertex neighbourhoods. Suppose Ω_l^v is not a corner element, nor does it have a face in common with a corner element. Then the correction $\eta_l^v(x_1^v, x_2^v, x_3^v)$ is defined in the same way as in the regular region.

If Ω_l^v is a corner element then define

$$\eta_l^v(x_1^v, x_2^v, x_3^v) \equiv 0.$$

If Ω_l^v is an element which has a face in common with a corner element, i.e.

$$\tilde{\Omega}_l^v = \{x^v : (\theta, \phi) \in S_j^v, \ln(\rho_1^v) < \chi < \ln(\rho_2^v)\}$$

then the corrected element function will assume the constant value h_v on the side $\chi = \ln(\rho_1^v)$. Hence the correction will assume the value $[u(\phi, \theta, \ln(\rho_1^v))]$ instead of $\frac{1}{2} [u(\phi, \theta, \ln(\rho_1^v))]$ on the side $\chi = \ln(\rho_1^v)$. In the vertex neighbourhood Ω^v the vertex coordinates are

$$\begin{aligned} x_1^v &= \phi \\ x_2^v &= \theta \\ x_3^v &= \chi = \ln \rho. \end{aligned}$$

Moreover

$$\int_{\Omega_l^v} |\nabla_x u_l^v|^2 dx = \int_{\tilde{\Omega}_l^v} \left(u_\phi^2 + \frac{1}{\sin^2 \phi} u_\theta^2 + (\rho u_\rho)^2 \right) \sin \phi d\rho d\phi d\theta.$$

Hence

$$\int_{\Omega_l^v} |\nabla_x u_l^v|^2 dx$$

is uniformly equivalent to

$$\int_{\tilde{\Omega}_l^v} e^{x_3^v} |\nabla_{x^v} u_l^v|^2 dx^v$$

for all $\Omega_l^v, v \in \mathcal{V}$.

Here we have used the fact that

$$0 < \phi_0 \leq \phi_v \leq \pi - \phi_0$$

for all $v \in \mathcal{V}$.

Next, we define the corrections in Ω^{v-e} , a vertex-edge neighbourhood, where $v - e \in \mathcal{V} - \mathcal{E}$, the set of vertex edge neighbourhoods. Let Ω_l^{v-e} be an element which is not a corner element, nor which has a face in common with a corner vertex-edge element. Then

$$\tilde{\Omega}_l^{v-e} = \{x^{v-e} : \psi_i^{v-e} < \psi < \psi_{i+1}^{v-e}, \theta_j^{v-e} < \theta < \theta_{j+1}^{v-e}, \zeta_k^{v-e} < \zeta < \zeta_{k+1}^{v-e}\}$$

with $2 \leq i, 2 \leq k$. If Ω_l^{v-e} is a corner element then $\eta_l^{v-e}(x^{v-e}) = 0$. Here

$$x_1^{v-e} = \psi = \ln(\tan \phi)$$

$$x_2^{v-e} = \theta$$

$$x_3^{v-e} = \zeta = \ln x_3 = \chi + \ln(\cos(\phi)).$$

We introduce local variables

$$\begin{aligned} y_1 &= x_1^{v-e} \\ y_2 &= x_2^{v-e} \\ y_3 &= \frac{x_3^{v-e}}{\sin(\phi_{i+1}^{v-e})}. \end{aligned}$$

Then Ω_l^{v-e} is mapped to a rectangular hexahedron $\tilde{\Omega}_l^{v-e}$ in x^{v-e} coordinates and to a long, thin hexahedron $\hat{\Omega}_l^{v-e}$ in the local y coordinates such that the length of the y_3 side becomes large as Ω_l^{v-e} approaches the edge of the domain Ω^{v-e} , as shown in Figure C.2. Clearly

$$\int_{\Omega_l^{v-e}} |\nabla_x u|^2 dx$$

is uniformly equivalent to

$$\int_{\hat{\Omega}_l^{v-e}} \left(u_\phi^2 + \frac{1}{\sin^2 \phi} u_\theta^2 + u_\chi^2 \right) e^\chi \sin \phi d\phi d\theta d\chi$$

for all $\Omega_l^{v-e} \subseteq \Omega^{v-e}$, $v - e \in \mathcal{V} - \mathcal{E}$. Here $\hat{\Omega}_l^{v-e}$ denotes the image of Ω_l^{v-e} in x^v coordinates.

Now

$$\nabla_{x^v} u = J^{v-e} \nabla_{x^{v-e}} u$$

where

$$J^{v-e} = \begin{bmatrix} \sec^2 \phi \cot \phi & 0 & -\tan \phi \\ 0 & 1 & 0 \\ 0 & 0 & 1 \end{bmatrix}$$

and

$$dx^v = \sin \phi \cos \phi \, dx^{v-e}.$$

Using the above we can show that

$$\int_{\Omega_l^{v-e}} |\nabla_x u|^2 \, dx$$

is uniformly equivalent to

$$\int_{\tilde{\Omega}_l^{v-e}} \left(\sum_{m=1}^2 \left(\frac{\partial u}{\partial x_m^{v-e}} \right)^2 + \sin^2 \phi \left(\frac{\partial u}{\partial x_3^{v-e}} \right)^2 \right) e^{x_3^{v-e}} \, dx^{v-e}$$

for all $\Omega_l^{v-e} \subseteq \Omega^{v-e}, v-e \in \mathcal{V} - \mathcal{E}$.

Hence

$$\int_{\Omega_l^{v-e}} |\nabla_x u|^2 \, dx$$

is uniformly equivalent to

$$\int_{\hat{\Omega}_l^{v-e}} e^{\sin(\phi_{i+1}^{v-e})y_3} \sin(\phi_{i+1}^{v-e}) |\nabla_y u|^2 \, dy.$$

Let f_1 denote the face $y_3 = \frac{\zeta_k}{\sin(\phi_{i+1}^{v-e})} = \kappa_k^i$ and f_2 the face $y_3 = \frac{\zeta_{k+1}}{\sin(\phi_{i+1}^{v-e})} = \kappa_{k+1}^i$.

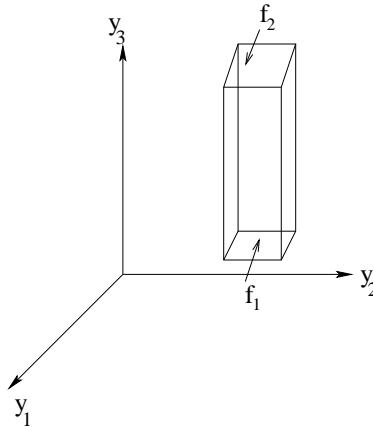


Figure C.2: Image of Ω_l^{v-e} in y -variables.

Let $[u(y_1, y_2)]|_{f_1}$ denote the jump in u across the face f_1 so that $u(y_1, y_2)|_{f_1} + 1/2[u(y_1, y_2)]|_{f_1}$ denotes the average value of u on the face f_1 . Similarly let $[u(y_1, y_2)]|_{f_2}$ denote the jump in the value of u across the face f_2 . We now define the correction

$$\nu_l^{v-e}(y_1, y_2, y_3) = \alpha_l^{v-e}(y_1, y_2, y_3) + \beta_l^{v-e}(y_1, y_2, y_3) + \gamma_l^{v-e}(y_1, y_2, y_3).$$

$\alpha_l^{v-e}(y_1, y_2, y_3)$ is first defined as follows:

Let

$$h_k^i = \min \left(1, \frac{\kappa_{k+1}^i - \kappa_k^i}{2} \right).$$

Let $r(y_3)$ be the function

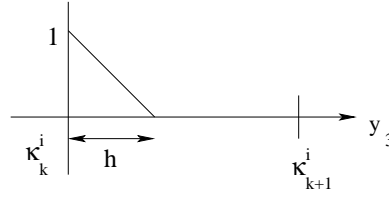


Figure C.3: The function $r(y_3)$.

$$r(y_3) = \begin{cases} \frac{(\kappa_k^i - y_3)}{h_k^i} + 1 & \text{for } \kappa_k^i \leq y_3 \leq \kappa_k^i + h_k^i \\ 0 & \text{for } \kappa_k^i + h_k^i \leq y_3 \leq \kappa_{k+1}^i. \end{cases} \quad (\text{C.4})$$

Let $s(y_3)$ be the function

$$s(y_3) = \begin{cases} 0 & \text{for } \kappa_k^i \leq y_3 \leq \kappa_{k+1}^i - h_k^i \\ \frac{y_3 - (\kappa_{k+1}^i - h_k^i)}{h_k^i} & \text{for } \kappa_{k+1}^i - h_k^i \leq y_3 \leq \kappa_{k+1}^i. \end{cases} \quad (\text{C.5})$$

Then we define the correction

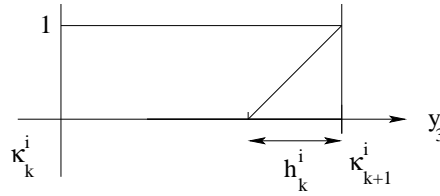


Figure C.4: The function $s(y_3)$.

$$\alpha_l^{v-e}(y_1, y_2, y_3) = 1/2[u(y_1, y_2)]|_{f_1} r(y_3) + 1/2[u(y_1, y_2)]|_{f_2} s(y_3).$$

If Ω_l^{v-e} is a corner element, i.e. the face f_1 corresponds to $x_3^{v-e} = \zeta_1^{v-e}$ then

$$\alpha_l^{v-e}(y_1, y_2, y_3) = [u(y_1, y_2)]|_{f_1} r(y_3) + 1/2[u(y_1, y_2)]|_{f_2} s(y_3).$$

Next, let f_3 denote the side $\theta = \theta_j^{v-e}$ and f_4 the side $\theta = \theta_{j+1}^{v-e}$. Let $[u(y_1, y_3)]|_{f_3}$ denote the jump across the side f_3 and $[u(y_1, y_3)]|_{f_4}$ the jump across the side f_4 . Define

$$\begin{aligned} \beta_l^{v-e}(y_1, y_2, y_3) &= \left(\frac{y_2 - \theta_{j+1}^{v-e}}{\theta_j^{v-e} - \theta_{j+1}^{v-e}} \right) \frac{[u(y_1, y_3)]}{2} \Big|_{f_3} \\ &+ \left(\frac{y_2 - \theta_j^{v-e}}{\theta_{j+1}^{v-e} - \theta_j^{v-e}} \right) \frac{[u(y_1, y_3)]}{2} \Big|_{f_4} \end{aligned}$$

It is assumed here that $\theta = \theta_j^{v-e}$ and $\theta = \theta_{j+1}^{v-e}$ do not correspond to a face of the domain Ω .

Finally, let f_5 denote the face $\psi = \psi_i^{v-e}$ and f_6 the face $\psi = \psi_{i+1}^{v-e}$. Define

$$\begin{aligned} \gamma_l^{v-e}(y_1, y_2, y_3) &= \left(\frac{y_1 - \psi_{i+1}^{v-e}}{\psi_i^{v-e} - \psi_{i+1}^{v-e}} \right) \frac{[u(y_2, y_3)]}{2} \Big|_{f_5} \\ &+ \left(\frac{y_1 - \psi_i^{v-e}}{\psi_{i+1}^{v-e} - \psi_i^{v-e}} \right) \frac{[u(y_2, y_3)]}{2} \Big|_{f_6} \end{aligned}$$

If $i = 1$ then the first term in the right hand side is multiplied by a factor of two.

Define the final correction as

$$\nu_l^{v-e}(y_1, y_2, y_3) = \alpha_l^{v-e}(y_1, y_2, y_3) + \beta_l^{v-e}(y_1, y_2, y_3) + \gamma_l^{v-e}(y_1, y_2, y_3).$$

Then

$$\eta_l^{v-e}(x^{v-e}) = \nu_l^{v-e} \left(x_1^{v-e}, x_2^{v-e}, \frac{x_3^{v-e}}{\sin(\phi_{i+1}^{v-e})} \right).$$

If Ω_l^{v-e} has a face in common with a corner element Ω_m^{v-e} then on the common face $\Gamma_{l,i}^{v-e}$ we define the correction $\eta_l^{v-e}(x^{v-e})$ so that the corrected value of the spectral element function $p_l^{v-e} = u_l^{v-e}(x^{v-e}) + \eta_l^{v-e}(x^{v-e})$ assumes the value of u_m^{v-e} on the common face $\Gamma_{l,i}^{v-e}$.

If Ω_m^{v-e} is a corner element then we define the correction $\eta_m^{v-e}(x^{v-e}) \equiv 0$.

Finally, we define the corrections in Ω^e , an edge neighbourhood where $e \in \mathcal{E}$, the set of edge neighbourhoods. Let Ω_l^e be an edge element. Then in Ω^e the edge coordinates are

$$x_1^e = \tau = \ln r$$

$$x_2^e = \theta$$

$$x_3^e = x_3.$$

Let $\tilde{\Omega}_l^e$ denote the image of Ω^e in x^e coordinates. Then

$$\tilde{\Omega}_l^e = \{x^e : \ln(r_j^e) < x_1^e < \ln(r_{j+1}^e), \theta_k^e < x_2^e < \theta_{k+1}^e, Z_n^e < x_3^e < Z_{n+1}^e\}.$$

Once again we introduce a set of local coordinates z in $\tilde{\Omega}_l^e$ defined as

$$\begin{aligned} z_1 &= x_1^e \\ z_2 &= x_2^e \\ z_3 &= \frac{x_3^e}{r_{j+1}^e}. \end{aligned}$$

Then $\tilde{\Omega}_l^e$ is mapped onto the hexahedron $\hat{\Omega}_l^e$ such that the length of the z_3 side becomes large as Ω_l^e approaches the edge of the domain.

Now

$$\int_{\Omega_u^e} |\nabla_x u|^2 dx = \int_{\tilde{\Omega}_l^e} \left(\left(\frac{\partial u}{\partial \tau} \right)^2 + \left(\frac{\partial u}{\partial \theta} \right)^2 + e^{2\tau} \left(\frac{\partial u}{\partial x_3} \right)^2 \right) d\tau d\theta dx_3.$$

Hence

$$\int_{\Omega_u^e} |\nabla_x u|^2 dx$$

is uniformly equivalent to

$$\int_{\hat{\Omega}_u^e} |\nabla_z u|^2 r_{j+1}^e dz.$$

Here u denotes the spectral element function defined on Ω_u^e . Now we can define corrections to the spectral element functions so that the corrected element functions are conforming as we have for vertex-edge elements.

Finally, a further set of corrections can be made so that the corrected element function $p(x) \in H_0^1(\Omega)$, i.e. p vanishes on $\Gamma^{[0]}$, the Dirichlet portion of the boundary $\partial\Omega$ of Ω . Moreover the estimate (C.1) holds.

We now briefly indicate how the corrections need to be defined in case the spectral element functions are nonconforming.

The corrections are first described for an element $\Omega_l^r \subseteq \Omega^r$, the regular region of Ω . Let $M_l^r(\lambda_1, \lambda_2, \lambda_3)$ denote the map from the cube $Q = (-1, 1)^3$ to Ω_l^r as shown in Figure C.1.

We first make a correction $\delta_l^r(\lambda_1, \lambda_2, \lambda_3) = \sum_{i=0}^1 \sum_{j=0}^1 \sum_{k=0}^1 a_{i,j,k} \lambda_1^i \lambda_2^j \lambda_3^k$ such that $(u_l^r + \delta_l^r)(n) = \bar{u}(n)$, where n denotes a node of $Q = (M_l^r)^{-1}(\Omega_l^r)$ and $\bar{u}(n)$ the average

value of u at the node n . Hence the corrected spectral element function is conforming at the nodes of Ω_l^r . Here we use the estimate

$$\|w\|_{L^\infty(R)}^2 \leq C \|w\|_{H^{3/2}(R)}^2$$

where R is a rectangle in the plane, each of whose sides is of length $= \Theta(1)$.

Next, we define a correction $\epsilon_l^r(\lambda_1, \lambda_2, \lambda_3)$ such that if t is a point on a side S of $Q = (M_l^r)^{-1}(\Omega_l^r)$ then $(u_l^r + \delta_l^r + \epsilon_l^r)(t) = \overline{u + \delta}(t)$ where $\overline{u + \delta}(t)$ denotes the average value of $u + \delta$ at t . It should be noted that $\epsilon_l^r(t) = 0$ if t is a node of Q . Consider for example the side corresponding to $\lambda_1 = -1$, $\lambda_2 = -1$, $-1 < \lambda_3 < 1$ and let the correction corresponding to the side be $g(\lambda_3)$. Then the contribution of the correction for this side to ϵ_l^r would be $\frac{(1-\lambda_1)}{2} \frac{(1-\lambda_2)}{2} g(\lambda_3)$. The contributions of the corrections for other sides would be similarly defined and ϵ_l^r would be the sum of all these contributions. Here we use the estimate

$$\|w\|_{H^1(S)}^2 \leq C \ln W \|w\|_{H^{3/2}(R)}^2$$

where R is a rectangle in the plane, each of whose sides is of length $\Theta(1)$, and S is a side of the rectangle R . Moreover w is a polynomial of degree W in each of its two arguments.

Now $u_l^r + \delta_l^r + \epsilon_l^r$, would be conforming on the portion of the wirebasket contained in Ω^r , the regular region of Ω . We shall next make corrections in Ω^v for $v \in \mathcal{V}$, Ω^{v-e} for $v - e \in \mathcal{V} - \mathcal{E}$ and Ω^e for $e \in \mathcal{E}$, so that the corrected spectral element functions are conforming on the wire basket of the elements contained in Ω . Once this has been done a further set of corrections can be made so that the corrected spectral element functions would be conforming on the faces as well as the wire basket and vanish on the Dirichlet portion of the boundary $\Gamma^{[0]}$ of $\partial\Omega$ as has already been described. The corrections $\delta_l^v + \epsilon_l^v$ that need to be made in the vertex neighbourhood Ω^v of Ω so that $u_l^v + \delta_l^v + \epsilon_l^v$ would be conforming on the portion of the wirebasket contained in Ω^v are very similar to those described for the regular region Ω^r of Ω and hence are not discussed any further. We now describe the corrections $\delta_l^{v-e} + \epsilon_l^{v-e}$ that need to be made in the vertex-edge neighbourhood Ω^{v-e} of Ω so that $u_l^{v-e} + \delta_l^{v-e} + \epsilon_l^{v-e}$ would be conforming on the portion of the wirebasket contained in Ω^{v-e} .

Let Ω_l^{v-e} be an element in the vertex-edge neighbourhood Ω^{v-e} , and let $\widehat{\Omega}_l^{v-e}$ be its

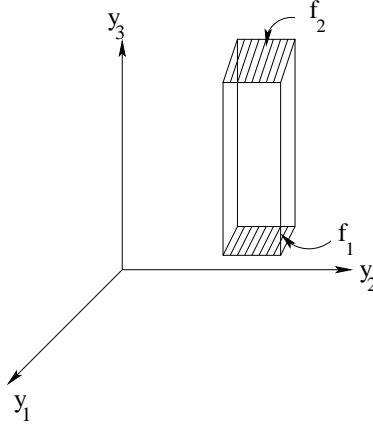
Figure C.5: The element $\hat{\Omega}_l^{v-e}$.

image in y coordinates where

$$\begin{aligned} y_1 &= \psi = \ln(\tan \phi) \\ y_2 &= \theta \\ y_3 &= \frac{\zeta}{\sin(\phi_{i+1}^{v-e})} = \frac{\ln(x_3)}{\sin(\phi_{i+1}^{v-e})}. \end{aligned}$$

Then the length of the y_3 side becomes large as the elements approach the edge of the domain Ω . We define

$$\sigma_1(y_1, y_2) = \sum_{i,j=0,1} h_{i,j}^{(1)} y_1^i y_2^j,$$

a bilinear function of y_1 and y_2 so that

$$u_l^{v-e}(y_1, y_2, y_3) + \sigma_1(y_1, y_2)|_{f_1} = w_1(y_1, y_2)$$

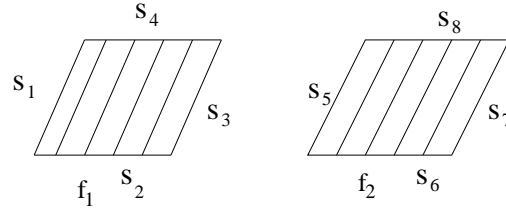
is conforming at the nodes of the face f_1 . Here $w_1(y_1, y_2)$ assumes the average value of the spectral element functions at the nodes of f_1 .

In the same way we define

$$\sigma_2(y_1, y_2) = \sum_{i,j=0,1} h_{i,j}^{(2)} y_1^i y_2^j,$$

a bilinear function of y_1 and y_2 , so that

$$u_l^{v-e}(y_1, y_2, y_3) + \sigma_2(y_1, y_2)|_{f_2} = w_2(y_1, y_2)$$

Figure C.6: Faces f_1 and f_2 .

is conforming at the nodes of the face f_2 . The correction $\delta_l^{v-e}(y_1, y_2, y_3)$ is then given by

$$\delta_l^{v-e}(y_1, y_2, y_3) = \sigma_1(y_1, y_2)r(y_3) + \sigma_2(y_1, y_2)s(y_3) .$$

Here $r(y_3)$ and $s(y_3)$ are defined in (C.4) and (C.5).

Let

$$\nu_1(y_1, y_2) = \sum_{i=0}^W \sum_{j=0}^W o_{i,j}^{(1)} y_1^i y_2^j$$

be a polynomial of degree N in y_1 and y_2 separately such that

$$u_l^{v-e}(y_1, y_2, y_3) + \delta_l^{v-e}(y_1, y_2, y_3) + \nu_1(y_1, y_2)$$

is conforming at the sides of the face f_1 .

In the same way we define

$$\nu_2(y_1, y_2) = \sum_{i=0}^W \sum_{j=0}^W o_{i,j}^{(2)} y_1^i y_2^j$$

such that

$$u_l^{v-e}(y_1, y_2, y_3) + \delta_l^{v-e}(y_1, y_2, y_3) + \nu_2(y_1, y_2)$$

is conforming at the sides of the face f_2 .

Define

$$\omega_1(y_1, y_2, y_3) = \nu_1(y_1, y_2)r(y_3) + \nu_2(y_1, y_2)s(y_3).$$

Here $r(y_3)$ and $s(y_3)$ are defined in (C.4) and (C.5).

Now $u_l^{v-e} + \delta_l^{v-e} + \omega_1$ is conforming on the face f_1 and f_2 . We can define corrections $\sigma_9(y_3)$, $\sigma_{10}(y_3)$, $\sigma_{11}(y_3)$ and $\sigma_{12}(y_3)$ such that

$$(u_l^{v-e} + \delta_l^{v-e} + \omega_1)(y_1, y_2, y_3) + \sigma_i(y_3)$$

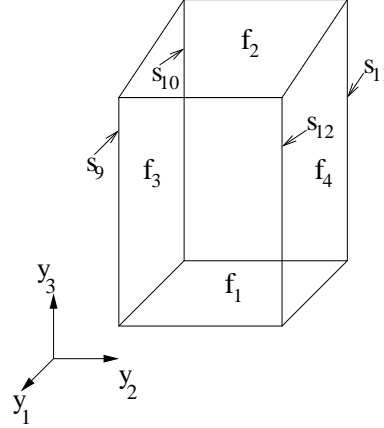


Figure C.7: Sides $s_i, i = 1, \dots, 12$ and faces $f_i, i = 1, \dots, 6$ of a typical element in vertex-edge neighbourhood.

is conforming on the sides s_i as shown in Figure C.7. Note that $\sigma_i(y_3)$ is zero at the end points of the side s_i . On the face f_3 define $l_3(y_1, y_3)$ to be a linear function of y_1 which assumes the value $\sigma_i(y_3)$ on the side s_i for $i = 9, 10$. Similarly on the face f_4 define $l_4(y_1, y_3)$ to be a linear function of y_1 which assumes the value $\sigma_i(y_3)$ on the side s_i for $i = 11, 12$. We now define $\omega_2(y_1, y_2, y_3)$ to be a linear function of y_2 such that ω_2 assumes the value $l_3(y_1, y_3)$ on the face f_3 and the value $l_4(y_1, y_3)$ on the face f_4 . The correction $\beta_l^{v-e}(y_1, y_2, y_3)$ is then given by

$$\beta_l^{v-e}(y_1, y_2, y_3) = \delta_l^{v-e}(y_1, y_2, y_3) + \omega_1(y_1, y_2, y_3) + \omega_2(y_1, y_2, y_3).$$

□

C.2

Proof of Theorem 3.3.1

Theorem 3.3.1. *The following estimate for the spectral element functions holds*

$$\mathcal{U}_{(1)}^{N,W}(\{\mathcal{F}_u\}) \leq K_{N,W} \mathcal{V}^{N,W}(\{\mathcal{F}_u\}). \quad (\text{C.6})$$

Here $K_{N,W} = CN^4$, when the boundary conditions are mixed and $K_{N,W} = C(\ln W)^2$ when the boundary conditions are Dirichlet.

If the spectral element functions vanish on the wirebasket WB of the elements then $K_{N,W} = C(\ln W)^2$, where C is a constant.

Proof. Let p denote the corrected spectral element function defined in Lemma 3.3.1 and

$$B(p, \lambda) = \int_{\Omega} \left(\sum_{i,j=1}^3 a_{i,j} p_{x_i} \lambda_{x_j} + \sum_{i=1}^3 b_i p_{x_i} \lambda + cp \lambda \right) dx \quad (\text{C.7})$$

be a bilinear form for $p, \lambda \in H_0^1(\Omega)$. Here $H_0^1(\Omega)$ denotes the subspace of functions $\subseteq H^1(\Omega)$ which vanish on $\Gamma^{[0]}$. Moreover there is a constant K such that

$$K \|q\|_{H^1(\Omega)}^2 \leq B(q, q) \quad (\text{C.8})$$

for all $q \in H_0^1(\Omega)$.

Now

$$B(p, \lambda) = B_{\text{regular}}(p, \lambda) + B_{\text{vertices}}(p, \lambda) + B_{\text{vertex-edge}}(p, \lambda) + B_{\text{edges}}(p, \lambda). \quad (\text{C.9})$$

Here

$$B_{\text{regular}}(p, \lambda) = \sum_{l=1}^{N_r} B(p, \lambda)_{\Omega_l^r}$$

and

$$B(p, \lambda)_{\Omega_l^r} = \int_{\Omega_l^r} \sum_{i,j=1}^3 \left(a_{i,j} p_{x_i} \lambda_{x_j} + \sum_{i=1}^3 b_i p_{x_i} \lambda + cp \lambda \right) dx.$$

The other terms are similarly defined.

Now

$$p_l^r = u_l^r + \eta_l^r.$$

Hence

$$B(p, \lambda)_{\Omega_l^r} = B(u_l^r, \lambda)_{\Omega_l^r} + B(\eta_l^r, \lambda)_{\Omega_l^r}.$$

Integrating by parts we obtain,

$$B(u_l^r, \lambda)_{\Omega_l^r} = \int_{\Omega_l^r} L u_l^r \lambda \, dx + \int_{\partial \Omega_l^r} \left(\frac{\partial u_l^r}{\partial \boldsymbol{\nu}} \right)_A \lambda \, d\sigma.$$

Hence

$$\begin{aligned} B_{\text{regular}}(p, p) &= \sum_{l=1}^{N_r} \int_{\Omega_l^r} L u_l^r p \, dx + \sum_{\Gamma_{l,i}^r \subseteq \Omega^r} \int_{\Gamma_{l,i}^r} \left(\frac{\partial u}{\partial \boldsymbol{\nu}} \right)_A p \, d\sigma \\ &\quad + \sum_{\Gamma_{l,i}^r \subseteq \partial \Omega^r} \int_{\Gamma_{l,i}^r} \left(\frac{\partial u}{\partial \boldsymbol{\nu}} \right)_A p \, d\sigma + \sum_{l=1}^{N_r} B(\eta_l^r, p)_{\Omega_l^r}. \end{aligned} \quad (\text{C.10})$$

Now

$$B_{vertices}(p, \lambda) = \sum_{v \in \mathcal{V}} \sum_{l=1}^{N_v} B(p, \lambda)_{\Omega_l^v}.$$

Clearly

$$B(p, \lambda)_{\Omega_l^v} = B(u_l^v, \lambda)_{\Omega_l^v} + B(\eta_l^v, \lambda)_{\Omega_l^v}.$$

Once more using integration by parts

$$B(u_l^v, \lambda)_{\Omega_l^v} = \int_{\tilde{\Omega}_l^v} L^v u(x^v) \lambda e^{\chi/2} \sqrt{\sin \phi} dx^v + \int_{\partial \tilde{\Omega}_l^v} \left(\frac{\partial u_l^v}{\partial \boldsymbol{\nu}^v} \right)_{A^v} \lambda e^{\chi} \sin \phi d\sigma^v.$$

Hence

$$\begin{aligned} B_{vertices}(p, p) &= \sum_{v \in \mathcal{V}} \left(\sum_{l=1}^{N_v} \int_{\tilde{\Omega}_l^v} L^v u(x^v) \lambda e^{\chi/2} \sqrt{\sin \phi} dx^v \right. \\ &\quad + \sum_{\Gamma_{l,i}^v \subseteq \Omega^v} \int_{\tilde{\Gamma}_{l,i}^v} \left[\left(\frac{\partial u}{\partial \boldsymbol{\nu}^v} \right)_{A^v} \right] p e^{\chi} \sin \phi d\sigma^v \\ &\quad \left. + \sum_{\Gamma_{l,i}^v \subseteq \partial \Omega^v} \int_{\tilde{\Gamma}_{l,i}^v} \left(\frac{\partial u}{\partial \boldsymbol{\nu}^v} \right)_{A^v} p e^{\chi} \sin \phi d\sigma^v + \sum_{l=1}^{N_v} B(\eta_l^v, p)_{\Omega_l^v} \right). \end{aligned} \quad (C.11)$$

Now if $\Gamma_{l,i}^v$ is a face of Ω_l^v and $\Gamma_{j,k}^r$ is a face of Ω_j^r such that $\Gamma_{l,i}^v = \Gamma_{j,k}^r$ then

$$\int_{\Gamma_{j,k}^r} \left(\frac{\partial u_l^r}{\partial \boldsymbol{\nu}^r} \right)_{A^v} p d\sigma = - \int_{\Gamma_{l,i}^v} \left(\frac{\partial u_l^v}{\partial \boldsymbol{\nu}^v} \right)_{A^v} p e^{\chi} \sin \phi d\sigma^v. \quad (C.12)$$

Next

$$B_{vertex-edge}(p, \lambda) = \sum_{v-e \in \mathcal{V}-\mathcal{E}} \sum_{l=1}^{N_{v-e}} B(p, \lambda)_{\Omega_l^{v-e}}.$$

And

$$B(p, \lambda)_{\Omega_l^{v-e}} = B(u_l^{v-e}, \lambda)_{\Omega_l^{v-e}} + B(\eta_l^{v-e}, \lambda)_{\Omega_l^{v-e}}.$$

Integration by parts gives

$$\begin{aligned} B(u_l^{v-e}, \lambda)_{\Omega_l^{v-e}} &= \int_{\tilde{\Omega}_l^{v-e}} L^{v-e} u(x^{v-e}) \lambda (x^{v-e}) e^{\zeta/2} dx^{v-e} \\ &\quad + \int_{\partial \tilde{\Omega}_l^{v-e}} \left(\frac{\partial u}{\partial \boldsymbol{\nu}^{v-e}} \right)_{A^{v-e}} \lambda e^{\zeta} d\sigma^{v-e}. \end{aligned}$$

Hence

$$\begin{aligned}
B_{vertex-edge}(p, p) &= \sum_{v-e \in \mathcal{V}-\mathcal{E}} \left(\sum_{l=1}^{N_{v-e}} \int_{\tilde{\Omega}_l^{v-e}} L^{v-e} u(x^{v-e}) p(x^{v-e}) e^{\zeta/2} dx^{v-e} \right. \\
&\quad + \sum_{\Gamma_{l,i}^{v-e} \subseteq \Omega^{v-e}} \int_{\tilde{\Gamma}_{l,i}^{v-e}} \left[\left(\frac{\partial u}{\partial \boldsymbol{\nu}^{v-e}} \right)_{A^{v-e}} \right] p e^\chi d\sigma^{v-e} \\
&\quad + \sum_{\Gamma_{l,i}^{v-e} \subseteq \partial\Omega^{v-e}} \int_{\tilde{\Gamma}_{l,i}^{v-e}} \left(\frac{\partial u}{\partial \boldsymbol{\nu}^{v-e}} \right)_{A^{v-e}} p e^\chi d\sigma^{v-e} \\
&\quad \left. + \sum_{l=1}^{N_{v-e}} B(\eta_l^{v-e}, p)_{\Omega_l^{v-e}} \right). \tag{C.13}
\end{aligned}$$

Now if $\Gamma_{m,j}^v = \Gamma_{l,i}^{v-e}$ then

$$\int_{\tilde{\Gamma}_{m,j}^v} \left(\frac{\partial u}{\partial \boldsymbol{\nu}^v} \right)_{A^v} p e^\chi \sin \phi d\sigma^v = - \int_{\tilde{\Gamma}_{l,i}^{v-e}} \left(\frac{\partial u}{\partial \boldsymbol{\nu}^{v-e}} \right)_{A^{v-e}} p e^\zeta d\sigma^{v-e}. \tag{C.14}$$

Finally

$$B_{edges}(p, \lambda) = \sum_{e \in \mathcal{E}} \sum_{l=1}^{N_e} B(p, \lambda)_{\Omega_l^e}.$$

Here

$$B(p, \lambda)_{\Omega_l^e} = B(u_l^e, \lambda)_{\Omega_l^e} + B(\eta_l^e, \lambda)_{\Omega_l^e}.$$

Integrating by parts we obtain

$$B(u_l^e, \lambda)_{\Omega_l^e} = \int_{\tilde{\Omega}_l^e} L^e u(x^e) \lambda dx^e + \int_{\partial \tilde{\Omega}_l^e} \left(\frac{\partial u}{\partial \boldsymbol{\nu}^e} \right)_{A^e} \lambda d\sigma^e.$$

Hence

$$\begin{aligned}
B_{edges}(p, p) &= \sum_{e \in \mathcal{E}} \left(\sum_{l=1}^{N_e} \int_{\tilde{\Omega}_l^e} L^e u(x^e) p dx^e \right. \\
&\quad + \sum_{\Gamma_{l,i}^e \subseteq \Omega^e} \int_{\tilde{\Gamma}_{l,i}^e} \left[\left(\frac{\partial u}{\partial \boldsymbol{\nu}^e} \right)_{A^e} \right] p d\sigma^e + \sum_{\Gamma_{l,i}^e \subseteq \partial\Omega^e} \int_{\tilde{\Gamma}_{l,i}^e} \left(\frac{\partial u}{\partial \boldsymbol{\nu}^e} \right)_{A^e} p d\sigma^e \\
&\quad \left. + \sum_{l=1}^{N_e} B(\eta_l^e, p)_{\Omega_l^e} \right). \tag{C.15}
\end{aligned}$$

Let $\Gamma_{l,i}^{v-e} = \Gamma_{m,j}^e$. Then it can be shown that

$$\int_{\tilde{\Gamma}_{l,i}^{v-e}} \left(\frac{\partial u}{\partial \boldsymbol{\nu}^{v-e}} \right)_{A^{v-e}} p e^\zeta d\sigma^{v-e} = - \int_{\tilde{\Gamma}_{m,j}^e} \left(\frac{\partial u}{\partial \boldsymbol{\nu}^e} \right)_{A^e} p d\sigma^e \tag{C.16}$$

Also if $\Gamma_{m,j}^e = \Gamma_{n,k}^r$ then

$$\int_{\tilde{\Gamma}_{m,j}^e} \left(\frac{\partial u}{\partial \boldsymbol{\nu}^e} \right)_{A^e} p d\sigma^e = - \int_{\Gamma_{n,k}^r} \left(\frac{\partial u}{\partial \boldsymbol{\nu}} \right)_A p d\sigma \quad (\text{C.17})$$

Now

$$\begin{aligned} B(p, p)_\Omega &= B_{\text{regular}}(p, p) + B_{\text{vertices}}(p, p) + B_{\text{vertex-edges}}(p, p) \\ &\quad + B_{\text{edges}}(p, p). \end{aligned} \quad (\text{C.18})$$

Substituting (C.10)–(C.17) into the above we obtain

$$B(p, p)_\Omega \leq cd \mathcal{V}^{N,W}(\{F_u\}) + 1/d \mathcal{G}(p). \quad (\text{C.19})$$

In the above

$$\begin{aligned} \mathcal{G}(p) &= \|p(x)\|_{1,\Omega^r}^2 + \sum_{v \in \mathcal{V}} \|p(x^v) e^{x_3^{v-e}/2}\|_{1,\tilde{\Omega}^v}^2 + \sum_{v-e \in \mathcal{V}-\mathcal{E}} \int_{\tilde{\Omega}^{v-e}} \left(\sum_{i=1}^2 \left(\frac{\partial p(x^{v-e})}{\partial x_i^{v-e}} \right)^2 \right. \\ &\quad \left. + \sin^2 \phi \left(\frac{\partial p(x^{v-e})}{\partial x_3^{v-e}} \right)^2 + (p(x^{v-e}))^2 \right) e^{x_3^{v-e}} w^{v-e}(x_1^{v-e}) dx^{v-e} \\ &\quad + \sum_{e \in \mathcal{E}} \int_{\tilde{\Omega}^e} \left(\sum_{i=1}^2 \left(\frac{\partial p(x^e)}{\partial x_i^e} \right)^2 + e^{2\tau} \left(\frac{\partial p(x^e)}{\partial x_3^e} \right)^2 + (p(x^e))^2 \right) w^e(x_1^e) dx^e. \end{aligned} \quad (\text{C.20})$$

Now

$$K \|p\|_{H^1(\Omega)}^2 \leq B(p, p).$$

Moreover if the spectral element functions are not conforming on the wirebasket WB then

$$\mathcal{G}(p) \leq C_{N,W} \|p\|_{H^1(\Omega)}^2. \quad (\text{C.21})$$

Here $C_{N,W} = EN^2$ if the boundary conditions are mixed and $C_{N,W} = E$ if the boundary conditions are Dirichlet. Choosing $d = \frac{2EN^2}{K}$ in (C.19) gives

$$B(p, p)_\Omega \leq \frac{c}{K} C_{N,W} \mathcal{V}^{N,W}(\{\mathcal{F}_u\}).$$

Hence combining the above and (C.20) gives

$$\mathcal{G}(p) \leq \frac{2c}{K^2} (C_{N,W})^2 N^4 \mathcal{V}^{N,W}(\{\mathcal{F}_u\}). \quad (\text{C.22})$$

Now (C.1) and (C.22) yields (C.6).

Finally, we consider the case when the spectral element functions are conforming on the wirebasket WB and vanish on it. Then p vanishes on the wirebasket. Consider $p(x^e)$ on $\tilde{\Omega}_l^e$. Here

$$\tilde{\Omega}_l^e = \{x^e : \ln(r_i^e) < x_1^e < \ln(r_{i+1}^e), \theta_j < x_2^e < \theta_{j+1}, Z_k^e < x_3^e < Z_{k+1}^e\} .$$

Now if $s(y_1, y_2)$ is a polynomial of degree W in each of its arguments on the unit square S which vanishes at one of the vertices of S then using a *scaling* argument as in § 3.4 of [87] we obtain

$$\int_S (s(y))^2 dy \leq F(\ln W) \int_S \left(\left(\frac{\partial s}{\partial y_1} \right)^2 + \left(\frac{\partial s}{\partial y_2} \right)^2 \right) dy .$$

Hence, since $p(x_1^e, x_2^e, \cdot)$ is a polynomial of degree W in x_1^e and x_2^e

$$\int_{\tilde{\Omega}_l^e} (p(x^e))^2 dx^e \leq F(\ln W) \int_{\tilde{\Omega}_l^e} \left(\sum_{i=1}^2 \left(\frac{\partial p(x^e)}{\partial x_i^e} \right)^2 + e^{2\tau} \left(\frac{\partial p(x^e)}{\partial x_3^e} \right)^2 \right) dx^e .$$

And so it can be shown that

$$\mathcal{G}(p) \leq F \ln W \|p\|_{H^1(\Omega)}^2 . \quad (\text{C.23})$$

Choosing $d = \frac{1}{\frac{K}{2F \ln W}}$ in (C.19) gives

$$\mathcal{G}(p) \leq \frac{2cF^2}{K^2} (\ln W)^2 \mathcal{V}^{N,W}(\{\mathcal{F}_u\}) . \quad (\text{C.24})$$

Now combining (C.1) and (C.24) yields (C.6). □

Appendix D

D.1

Proof of Lemma 3.4.1

Lemma 3.4.1. *Let Ω_m^r and Ω_p^r be elements in the regular region Ω^r of Ω and $\Gamma_{m,i}^r$ be a face of Ω_m^r and $\Gamma_{p,j}^r$ be a face of Ω_p^r such that $\Gamma_{m,i}^r = \Gamma_{p,j}^r$. Then for any $\epsilon > 0$ there exists a constant C_ϵ such that for W large enough*

$$\left| \int_{\partial\Gamma_{m,i}^r} \left(\left(\frac{\partial u_m^r}{\partial \boldsymbol{\nu}} \right)_A \left(\frac{\partial u_m^r}{\partial \mathbf{n}} \right)_A - \left(\frac{\partial u_p^r}{\partial \boldsymbol{\nu}} \right)_A \left(\frac{\partial u_p^r}{\partial \mathbf{n}} \right)_A \right) ds \right| \leq C_\epsilon (\ln W)^2 \sum_{k=1}^3 \| [u_{x_k}] \|_{1/2, \Gamma_{m,i}^r}^2 + \epsilon \sum_{1 \leq |\alpha| \leq 2} \left(\| D_x^\alpha u_m^r \|_{0, \Omega_m^r}^2 + \| D_x^\alpha u_p^r \|_{0, \Omega_p^r}^2 \right). \quad (\text{D.1})$$

Proof. Let $\Gamma_{m,i}^r$ be the image of the mapping M_m^r from Q to Ω_m^r corresponding to $\lambda_3 = -1$ and $\Gamma_{p,j}^r$, the image of the mapping M_p^r from Q to Ω_p^r corresponding to $\lambda_3 = 1$. Then $\Gamma_{m,i}^r$ is the image of the square $S = (-1, 1)^2$ under these mappings. However the proof remains valid if it is the image of T , the master triangle, too.

Now

$$\int_{\partial\Gamma_{m,i}^r} \left(\frac{\partial u}{\partial \boldsymbol{\nu}} \right)_A \left(\frac{\partial u}{\partial \mathbf{n}} \right)_A ds = \int_S \sum_{i,j=1}^3 \alpha_{i,j} \frac{\partial u}{\partial x_i} \frac{\partial u}{\partial x_j} ds. \quad (\text{D.2})$$

Here the element of arc length ds in the right hand side denotes either $d\lambda_1$ or $d\lambda_2$.

Moreover $\alpha_{i,j}$ is an analytic function of its arguments. Now

$$\frac{\partial u_m^r}{\partial x_i} = \sum_{j=1}^3 \beta_{i,j} \frac{\partial u_m^r}{\partial \lambda_j}$$

where $\beta_{i,j}$ is an analytic function of $\lambda = (\lambda_1, \lambda_2, \lambda_3)$.

Let $\hat{\beta}_{i,j}$ be the projection of $\beta_{i,j}$ into the space of polynomials of degree W in $H^3(Q)$.

Then for any $m > 0$

$$\| \beta_{i,j} - \hat{\beta}_{i,j} \|_{1,\infty,Q} \leq \frac{C_m}{W^m} \quad (\text{D.3})$$

as $W \rightarrow \infty$.

Define $\left(\frac{\partial u_m^r}{\partial x_i} \right)^a$, an approximate representation for $\frac{\partial u_m^r}{\partial x_i}$, by

$$\left(\frac{\partial u_m^r}{\partial x_i} \right)^a = \sum_{j=1}^3 \hat{\beta}_{i,j} \frac{\partial u_m^r}{\partial \lambda_j}.$$

Moreover $\left(\frac{\partial u_m^r}{\partial x_i}\right)^a$ is a polynomial of degree $2W$ in each of its arguments λ_1, λ_2 and λ_3 .

Now

$$\left\| \frac{\partial u_m^r}{\partial x_i} - \left(\frac{\partial u_m^r}{\partial x_i} \right)^a \right\|_{0,\partial S} \leq \frac{C}{W^4} \sum_{j=1}^3 \left\| \frac{\partial u_m^r}{\partial \lambda_j} \right\|_{0,\partial S} \leq \frac{C}{W^5} \sum_{j=1}^3 \left\| \frac{\partial u_m^r}{\partial \lambda_j}(\lambda) \right\|_{5/4,Q}$$

by the trace theorem for Sobolev spaces.

Hence

$$\left\| \frac{\partial u_m^r}{\partial x_i} - \left(\frac{\partial u_m^r}{\partial x_i} \right)^a \right\|_{0,\partial S} \leq \frac{C}{W^4} \sum_{1 \leq |\alpha| \leq 2} (\|D_\lambda^\alpha u_m^r\|_{0,Q}^2)^{1/2}. \quad (\text{D.4})$$

Here we have used the inverse inequality for differentiation

$$\left\| \frac{\partial u_m^r}{\partial \lambda_i}(\lambda) \right\|_{5/4,Q} \leq KW \left\| \frac{\partial u_m^r}{\partial \lambda_i}(\lambda) \right\|_{1,Q}.$$

Now

$$\left\| \frac{\partial u_m^r}{\partial x_i} \right\|_{0,\partial S}^2 \leq C \sum_{i=1}^3 \left\| \frac{\partial u_m^r}{\partial \lambda_i} \right\|_{0,\partial S}^2.$$

Moreover (see [87]),

$$\left\| \frac{\partial u_m^r}{\partial x_i} \right\|_{0,\partial S}^2 \leq C(\ln W) \sum_{1 \leq |\alpha| \leq 2} \|D_\lambda^\alpha u_m^r\|_{0,Q}^2. \quad (\text{D.5a})$$

In the same way it can be shown that

$$\left\| \left(\frac{\partial u_m^r}{\partial x_i} \right)^a \right\|_{0,\partial S}^2 \leq C(\ln W) \sum_{1 \leq |\alpha| \leq 2} \|D_\lambda^\alpha u_m^r\|_{0,Q}^2. \quad (\text{D.5b})$$

Now

$$\int_{\partial \Gamma_{m,i}^r} \left(\frac{\partial u_m^r}{\partial \boldsymbol{\nu}} \right)_A \left(\frac{\partial u_m^r}{\partial \mathbf{n}} \right)_A ds = \int_{\partial S} \sum_{i,j=1}^3 \alpha_{i,j} \left(\frac{\partial u_m^r}{\partial x_i} \right) \left(\frac{\partial u_m^r}{\partial x_j} \right) ds.$$

Using (D.4) and (D.5) gives

$$\begin{aligned} & \left| \int_{\partial S} \sum_{i,j=1}^3 \alpha_{i,j} \left(\left(\frac{\partial u_m^r}{\partial x_i} \right)^a \left(\frac{\partial u_m^r}{\partial x_j} \right)^a - \frac{\partial u_m^r}{\partial x_i} \frac{\partial u_m^r}{\partial x_j} \right) ds \right| \\ & \leq C \left(\sum_{i,j=1}^3 \left\| \left(\frac{\partial u_m^r}{\partial x_i} \right)^a \right\|_{0,\partial S} \left\| \left(\frac{\partial u_m^r}{\partial x_j} \right)^a - \left(\frac{\partial u_m^r}{\partial x_j} \right) \right\|_{0,\partial S} \right. \\ & \quad \left. + \sum_{i,j=1}^3 \left\| \left(\frac{\partial u_m^r}{\partial x_j} \right) \right\|_{0,\partial S} \left\| \left(\frac{\partial u_m^r}{\partial x_i} \right)^a - \left(\frac{\partial u_m^r}{\partial x_i} \right) \right\|_{0,\partial S} \right) \\ & \leq C \frac{\sqrt{\ln W}}{W^4} \sum_{1 \leq |\alpha| \leq 2} \|D_\lambda^\alpha u_m^r\|_{0,Q}^2. \end{aligned} \quad (\text{D.6})$$

In the same way it can be shown that

$$\begin{aligned} & \left| \int_{\partial S} \sum_{i,j=1}^3 \alpha_{i,j} \left(\left(\frac{\partial u_p^r}{\partial x_i} \right)^a \left(\frac{\partial u_p^r}{\partial x_j} \right)^a - \left(\frac{\partial u_p^r}{\partial x_i} \right) \left(\frac{\partial u_p^r}{\partial x_j} \right) \right) ds \right| \\ & \leq C \frac{\sqrt{\ln W}}{W^4} \sum_{1 \leq |\alpha| \leq 2} \|D_\lambda^\alpha u_p^r\|_{0,Q}^2. \end{aligned} \quad (D.7)$$

Hence

$$\begin{aligned} & \left| \int_{\partial S} \sum_{i,j=1}^3 \alpha_{i,j} \left(\left(\frac{\partial u_m^r}{\partial x_i} \right) \left(\frac{\partial u_m^r}{\partial x_j} \right) - \left(\frac{\partial u_p^r}{\partial x_i} \right) \left(\frac{\partial u_p^r}{\partial x_j} \right) \right) ds \right| \\ & \leq \left| \int_{\partial S} \sum_{i,j=1}^3 \alpha_{i,j} \left(\left(\frac{\partial u_m^r}{\partial x_i} \right)^a \left(\frac{\partial u_m^r}{\partial x_j} \right)^a - \left(\frac{\partial u_p^r}{\partial x_i} \right)^a \left(\frac{\partial u_p^r}{\partial x_j} \right)^a \right) ds \right| \\ & + \frac{C\sqrt{\ln W}}{W^4} \left(\sum_{1 \leq |\alpha| \leq 2} (\|D_\lambda^\alpha u_m^r\|_{0,Q}^2 + \|D_\lambda^\alpha u_p^r\|_{0,Q}^2) \right). \end{aligned} \quad (D.8)$$

Now

$$\begin{aligned} & \left| \int_{\partial S} \sum_{i,j=1}^3 \alpha_{i,j} \left(\left(\frac{\partial u_m^r}{\partial x_i} \right)^a \left(\frac{\partial u_m^r}{\partial x_j} \right)^a - \left(\frac{\partial u_p^r}{\partial x_i} \right)^a \left(\frac{\partial u_p^r}{\partial x_j} \right)^a \right) ds \right| \\ & \leq C \left[\sum_{i,j=1}^3 \left(\left\| \left(\frac{\partial u_m^r}{\partial x_i} \right)^a \right\|_{0,\partial S} \left\| \left(\frac{\partial u_m^r}{\partial x_j} \right)^a - \left(\frac{\partial u_p^r}{\partial x_j} \right)^a \right\|_{0,\partial S} \right. \right. \\ & \quad \left. \left. + \left\| \left(\frac{\partial u_p^r}{\partial x_j} \right)^a \right\|_{0,\partial S} \left\| \left(\frac{\partial u_m^r}{\partial x_i} \right)^a - \left(\frac{\partial u_p^r}{\partial x_i} \right)^a \right\|_{0,\partial S} \right) \right] \end{aligned}$$

Hence for any $\epsilon > 0$ there is a constant C_ϵ such that

$$\begin{aligned} & \left| \int_{\partial S} \sum_{i,j=1}^3 \alpha_{i,j} \left(\left(\frac{\partial u_m^r}{\partial x_i} \right)^a \left(\frac{\partial u_m^r}{\partial x_j} \right)^a - \left(\frac{\partial u_p^r}{\partial x_i} \right)^a \left(\frac{\partial u_p^r}{\partial x_j} \right)^a \right) ds \right| \\ & \leq C_\epsilon (\ln W) \left(\sum_{i,j=1}^3 \left\| \left(\frac{\partial u_m^r}{\partial x_i} \right)^a - \left(\frac{\partial u_p^r}{\partial x_i} \right)^a \right\|_{0,\partial S}^2 \right) \\ & + \epsilon/3 \left(\sum_{1 \leq |\alpha| \leq 2} (\|D_\lambda^\alpha u_m^r\|_{0,Q}^2 + \|D_\lambda^\alpha u_p^r\|_{0,Q}^2) \right). \end{aligned} \quad (D.9)$$

Here we have used the estimate (D.5)

$$\left\| \left(\frac{\partial u_m^r}{\partial x_i} \right)^a \right\|_{0,\partial S}^2 \leq C (\ln W) \left(\sum_{1 \leq |\alpha| \leq 2} \|D_\lambda^\alpha u_m^r\|_{0,Q}^2 \right).$$

and

$$\left\| \left(\frac{\partial u_p^r}{\partial x_i} \right)^a \right\|_{0,\partial S}^2 \leq C(\ln W) \left(\sum_{1 \leq |\alpha| \leq 2} \|D_\lambda^\alpha u_p^r\|_{0,Q}^2 \right).$$

Now as in [87]

$$\left\| \left(\frac{\partial u_m^r}{\partial x_i} \right)^a - \left(\frac{\partial u_p^r}{\partial x_i} \right)^a \right\|_{0,\partial S}^2 \leq C(\ln W) \left(\left\| \left(\frac{\partial u_m^r}{\partial x_i} \right)^a - \left(\frac{\partial u_p^r}{\partial x_i} \right)^a \right\|_{1/2,S}^2 \right) \quad (\text{D.10})$$

since $\left(\frac{\partial u_m^r}{\partial x_i} \right)$ and $\left(\frac{\partial u_p^r}{\partial x_i} \right)$ are polynomials of degree $2W$ in each of their arguments.

Now combining (D.9) and (D.10) gives

$$\begin{aligned} & \left| \int_{\partial S} \sum_{i,j=1}^3 \alpha_{i,j} \left(\left(\frac{\partial u_m^r}{\partial x_i} \right)^a \left(\frac{\partial u_m^r}{\partial x_j} \right)^a - \left(\frac{\partial u_p^r}{\partial x_i} \right)^a \left(\frac{\partial u_p^r}{\partial x_j} \right)^a \right) ds \right| \\ & \leq C_\epsilon (\ln W)^2 \left(\sum_{i,j=1}^3 \left\| \left(\frac{\partial u_m^r}{\partial x_i} \right)^a - \left(\frac{\partial u_p^r}{\partial x_i} \right)^a \right\|_{1/2,S}^2 \right) \\ & \quad + \epsilon/3 \left(\sum_{1 \leq |\alpha| \leq 2} (\|D_\lambda^\alpha u_m^r\|_{0,Q}^2 + \|D_\lambda^\alpha u_p^r\|_{0,Q}^2) \right). \end{aligned} \quad (\text{D.11})$$

Next

$$\begin{aligned} \left\| \left(\frac{\partial u_m^r}{\partial x_i} \right)^a - \left(\frac{\partial u_p^r}{\partial x_i} \right)^a \right\|_{1/2,S} & \leq \sum_{j=1}^3 \left\| (\beta_{i,j} - \hat{\beta}_{i,j}) \frac{\partial u_m^r}{\partial \lambda_j} \right\|_{1/2,S} \\ & \leq \sum_{j=1}^3 \left\| (\beta_{i,j} - \hat{\beta}_{i,j}) \right\|_{1,\infty,S} \left\| \frac{\partial u_m^r}{\partial \lambda_j} \right\|_{1/2,S}. \end{aligned}$$

Hence

$$\left\| \left(\frac{\partial u_m^r}{\partial x_i} \right)^a - \left(\frac{\partial u_p^r}{\partial x_i} \right)^a \right\|_{1/2,S}^2 \leq \frac{C}{W^8} \left(\sum_{1 \leq |\alpha| \leq 2} \|D_\lambda^\alpha u_m^r\|_{0,Q}^2 \right). \quad (\text{D.12a})$$

In the same way it can be shown that

$$\left\| \left(\frac{\partial u_p^r}{\partial x_i} \right)^a - \left(\frac{\partial u_p^r}{\partial x_i} \right)^a \right\|_{1/2,S}^2 \leq \frac{C}{W^8} \left(\sum_{1 \leq |\alpha| \leq 2} \|D_\lambda^\alpha u_p^r\|_{0,Q}^2 \right). \quad (\text{D.12b})$$

Combining (D.11) and (D.12) and choosing W large enough gives

$$\begin{aligned} & \left| \int_{\partial S} \sum_{i,j=1}^3 \alpha_{i,j} \left(\left(\frac{\partial u_m^r}{\partial x_i} \right)^a \left(\frac{\partial u_m^r}{\partial x_j} \right)^a - \left(\frac{\partial u_p^r}{\partial x_i} \right)^a \left(\frac{\partial u_p^r}{\partial x_j} \right)^a \right) ds \right| \\ & \leq C_\epsilon (\ln W)^2 \left(\sum_{i=1}^3 \left\| \frac{\partial u_m^r}{\partial x_i} - \frac{\partial u_p^r}{\partial x_i} \right\|_{1/2,S}^2 \right) + 2\epsilon/3 \left(\sum_{1 \leq |\alpha| \leq 2} \|D_\lambda^\alpha u_p^r\|_{0,Q}^2 \right). \end{aligned} \quad (\text{D.13})$$

Now substituting (D.13) into (D.8) and choosing W large enough yields

$$\begin{aligned} & \left| \int_{\partial S} \sum_{i,j=1}^3 \alpha_{i,j} \left(\left(\frac{\partial u_m^r}{\partial x_i} \right) \left(\frac{\partial u_m^r}{\partial x_j} \right) - \left(\frac{\partial u_p^r}{\partial x_i} \right) \left(\frac{\partial u_p^r}{\partial x_j} \right) \right) ds \right| \\ & \leq C_\epsilon (\ln W)^2 \left(\sum_{i=1}^3 \left\| \frac{\partial u_m^r}{\partial x_i} - \frac{\partial u_p^r}{\partial x_i} \right\|_{1/2,S}^2 \right) + \epsilon \left(\sum_{1 \leq |\alpha| \leq 2} \|D_\lambda^\alpha u_p^r\|_{0,Q}^2 \right). \end{aligned} \quad (\text{D.14})$$

And so the required result (D.1) follows. \square

D.2

Proof of Lemma 3.4.2

Lemma 3.4.2. *Let Ω_m^r and Ω_p^r be elements in the regular region Ω^r of Ω and $\Gamma_{m,i}^r$ be a face of Ω_m^r and $\Gamma_{p,j}^r$ be a face of Ω_p^r such that $\Gamma_{m,i}^r = \Gamma_{p,j}^r$. Then for any $\epsilon > 0$ there exists a constant C_ϵ such that for W large enough*

$$\begin{aligned} & \left| \sum_{j=1}^2 \left(\int_{\Gamma_{m,i}^r} \left(\frac{\partial u_m^r}{\partial \tau_j} \right)_A \frac{\partial}{\partial s_j} \left(\frac{\partial u_m^r}{\partial \nu} \right)_A - \int_{\Gamma_{p,j}^r} \left(\frac{\partial u_p^r}{\partial \tau_j} \right)_A \frac{\partial}{\partial s_j} \left(\frac{\partial u_p^r}{\partial \nu} \right)_A \right) d\sigma \right| \\ & \leq C_\epsilon (\ln W)^2 \sum_{k=1}^3 \| [u_{x_k}] \|_{1/2, \Gamma_{p,j}^r}^2 \\ & \quad + \epsilon \sum_{1 \leq |\alpha| \leq 2} \left(\|D_x^\alpha u_m^r\|_{0, \Omega_m^r}^2 + \|D_x^\alpha u_p^r\|_{0, \Omega_p^r}^2 \right). \end{aligned} \quad (\text{D.15})$$

Proof. It is enough to show that

$$\begin{aligned} & \left| \int_{\Gamma_{m,i}^r} \left(\left(\frac{\partial u_m^r}{\partial \tau_j} \right)_A \frac{\partial}{\partial s_j} \left(\frac{\partial u_m^r}{\partial \nu} \right)_A - \left(\frac{\partial u_p^r}{\partial \tau_j} \right)_A \frac{\partial}{\partial s_j} \left(\frac{\partial u_p^r}{\partial \nu} \right)_A \right) d\sigma \right| \\ & \leq C_\epsilon (\ln W)^2 \sum_{k=1}^3 \| [u_{x_k}] \|_{1/2, \Gamma_{p,j}^r}^2 \\ & \quad + \epsilon \sum_{1 \leq |\alpha| \leq 2} \left(\|D_x^\alpha u_m^r\|_{0, \Omega_m^r}^2 + \|D_x^\alpha u_p^r\|_{0, \Omega_p^r}^2 \right) \end{aligned} \quad (\text{D.16})$$

for $j = 1$.

Let $\Gamma_{m,i}^r$ be the image of the mapping M_m^r from Q to Ω_m^r corresponding to $\lambda_3 = -1$ and $\Gamma_{p,j}^r$, the image of the mapping M_p^r from Q to Ω_p^r corresponding to $\lambda_3 = 1$. Then $\Gamma_{m,i}^r$ is the image of the square $S = (-1, 1)^2$ under these mappings. However the proof

remains valid if it is the image of T , the master triangle, too.

Now

$$\begin{aligned} & \int_{\Gamma_{m,i}^r} \left\{ \left(\frac{\partial u}{\partial \boldsymbol{\tau}_1} \right)_A \frac{\partial}{\partial s_1} \left(\frac{\partial u}{\partial \boldsymbol{\nu}} \right)_A \right\} d\sigma \\ &= \sum_{j=1}^2 \sum_{i,k=1}^3 \int_S \left\{ \left(a_{i,j} \frac{\partial u}{\partial x_i} \right) \frac{\partial}{\partial \lambda_j} \left(b_k \frac{\partial u}{\partial x_k} \right) \right\} d\lambda_1 d\lambda_2 \end{aligned} \quad (\text{D.17})$$

where $a_{i,j}(\lambda_1, \lambda_2)$ and $b_k(\lambda_1, \lambda_2)$ are analytic functions of λ_1 and λ_2 .

Now as in Lemma 3.4.1, let $\hat{a}_{i,j}(\lambda_1, \lambda_2)$ and $\hat{b}_k(\lambda_1, \lambda_2)$ be the projections of $a_{i,j}(\lambda_1, \lambda_2)$ and $b_k(\lambda_1, \lambda_2)$ into the space of polynomials of degree W in $H^3(S)$. Moreover, let $\left(\frac{\partial u_m^r}{\partial x_i} \right)^a$, $\left(\frac{\partial u_p^r}{\partial x_i} \right)^a$ be the approximations to $\frac{\partial u_m^r}{\partial x_i}$ and $\frac{\partial u_p^r}{\partial x_i}$ defined in Lemma 3.4.1. Then $\left(\frac{\partial u_m^r}{\partial x_i} \right)^a$ and $\left(\frac{\partial u_p^r}{\partial x_i} \right)^a$ are polynomials of degree $2W$ in each of the variables λ_1, λ_2 and λ_3 .

Now

$$\begin{aligned} & \left| \int_S \left(a_{i,j} \left(\frac{\partial u_m^r}{\partial x_i} \right) \frac{\partial}{\partial \lambda_j} \left(b_k \frac{\partial u_m^r}{\partial x_k} \right) - \hat{a}_{i,j} \left(\frac{\partial u_m^r}{\partial x_i} \right) \frac{\partial}{\partial \lambda_j} \left(\hat{b}_k \frac{\partial u_m^r}{\partial x_k} \right) \right) d\lambda_1 d\lambda_2 \right| \\ & \leq \left| \int_S (a_{i,j} - \hat{a}_{i,j}) \frac{\partial u_m^r}{\partial x_i} \frac{\partial}{\partial \lambda_j} \left(b_k \frac{\partial u_m^r}{\partial x_k} \right) d\lambda_1 d\lambda_2 \right| \\ & \quad + \left| \int_S \hat{a}_{i,j} \frac{\partial u_m^r}{\partial x_i} \frac{\partial}{\partial \lambda_j} \left((b_k - \hat{b}_k) \frac{\partial u_m^r}{\partial x_k} \right) d\lambda_1 d\lambda_2 \right| \\ & \leq \frac{C}{W^4} \sum_{l,m=1}^3 \left\| \frac{\partial u_m^r}{\partial \lambda_l} \right\|_{0,S} \left(\left\| \frac{\partial u_m^r}{\partial \lambda_m} \right\|_{0,S} + \left\| \frac{\partial^2 u_m^r}{\partial \lambda_m \partial \lambda_j} \right\|_{0,S} \right) \\ & \leq \frac{C}{W^4} \sum_{l=1}^3 \left\| \frac{\partial u_m^r}{\partial \lambda_l} \right\|_{7/4,Q}^2. \end{aligned} \quad (\text{D.18})$$

To obtain the above inequality we have used the trace theorem for Sobolev spaces. Hence by the inverse inequality for differentiation

$$\begin{aligned} & \left| \int_S \left(a_{i,j} \left(\frac{\partial u_m^r}{\partial x_i} \right) \frac{\partial}{\partial \lambda_j} \left(b_k \frac{\partial u_m^r}{\partial x_k} \right) - \hat{a}_{i,j} \left(\frac{\partial u_m^r}{\partial x_i} \right) \frac{\partial}{\partial \lambda_j} \left(\hat{b}_k \frac{\partial u_m^r}{\partial x_k} \right) \right) d\lambda_1 d\lambda_2 \right| \\ & \leq \frac{C}{W} \sum_{1 \leq |\alpha| \leq 2} \|D_\lambda^\alpha u_m^r\|_{2,Q}^2. \end{aligned} \quad (\text{D.19})$$

Combining (D.17) and (D.19) gives

$$\begin{aligned}
& \left| \int_S \left(a_{i,j} \frac{\partial u_m^r}{\partial x_i} \frac{\partial}{\partial \lambda_j} \left(b_k \frac{\partial u_m^r}{\partial x_k} \right) - a_{i,j} \frac{\partial u_p^r}{\partial x_i} \frac{\partial}{\partial \lambda_j} \left(b_k \frac{\partial u_p^r}{\partial x_k} \right) \right) d\lambda_1 d\lambda_2 \right| \\
& \leq \left| \int_S \left(\hat{a}_{i,j} \frac{\partial u_m^r}{\partial x_i} \frac{\partial}{\partial \lambda_j} \left(\hat{b}_k \frac{\partial u_m^r}{\partial x_k} \right) - \hat{a}_{i,j} \left(\frac{\partial u_p^r}{\partial x_i} \right) \frac{\partial}{\partial \lambda_j} \left(\hat{b}_k \frac{\partial u_p^r}{\partial x_k} \right) \right) d\lambda_1 d\lambda_2 \right| \\
& + \frac{C}{W} \left(\sum_{1 \leq |\alpha| \leq 2} \left(\|D_\lambda^\alpha u_m^r\|_{2,Q}^2 + \|D_\lambda^\alpha u_p^r\|_{2,Q}^2 \right) \right). \tag{D.20}
\end{aligned}$$

Next

$$\begin{aligned}
& \left| \int_S \left(\hat{a}_{i,j} \frac{\partial u_m^r}{\partial x_i} \frac{\partial}{\partial \lambda_j} \left(\hat{b}_k \frac{\partial u_m^r}{\partial x_k} \right) - \hat{a}_{i,j} \left(\frac{\partial u_m^r}{\partial x_i} \right)^a \frac{\partial}{\partial \lambda_j} \left(\hat{b}_k \left(\frac{\partial u_m^r}{\partial x_k} \right)^a \right) \right) d\lambda_1 d\lambda_2 \right| \\
& \leq \left| \int_S \hat{a}_{i,j} \frac{\partial u_m^r}{\partial x_i} \frac{\partial}{\partial \lambda_j} \left(\hat{b}_k \left(\frac{\partial u_m^r}{\partial x_k} - \left(\frac{\partial u_m^r}{\partial x_k} \right)^a \right) \right) d\lambda_1 d\lambda_2 \right| \\
& + \left| \int_S \hat{a}_{i,j} \left(\left(\frac{\partial u_m^r}{\partial x_i} \right)^a - \frac{\partial u_m^r}{\partial x_i} \right) \frac{\partial}{\partial \lambda_j} \left(\left(\frac{\partial u_m^r}{\partial x_k} \right)^a \right) d\lambda_1 d\lambda_2 \right| \\
& \leq C \left(\left\| \frac{\partial u_m^r}{\partial x_i} \right\|_{0,S} \left\| \frac{\partial}{\partial \lambda_j} \left(\frac{\partial u_m^r}{\partial x_k} - \left(\frac{\partial u_m^r}{\partial x_k} \right)^a \right) \right\|_{0,S} \right) \\
& + \left\| \left(\frac{\partial u_m^r}{\partial x_i} \right)^a - \frac{\partial u_m^r}{\partial x_i} \right\|_{0,S} \left\| \frac{\partial}{\partial \lambda_j} \left(\left(\frac{\partial u_m^r}{\partial x_k} \right)^a \right) \right\|_{0,S} \right). \tag{D.21}
\end{aligned}$$

Now

$$\left\| \frac{\partial u_m^r}{\partial x_i} \right\|_{0,S} \leq C \sum_{|\alpha| \leq 1} \|D_\lambda^\alpha u_m^r\|_{1,Q}. \tag{D.22}$$

and

$$\left\| \frac{\partial}{\partial \lambda_j} \left(\frac{\partial u_m^r}{\partial x_k} - \left(\frac{\partial u_m^r}{\partial x_k} \right)^a \right) \right\|_{0,S} \leq \frac{C}{W^4} \sum_{1 \leq |\alpha| \leq 2} \|D_\lambda^\alpha u_m^r\|_{0,S}. \tag{D.23}$$

Hence

$$\left\| \frac{\partial}{\partial \lambda_j} \left(\frac{\partial u_m^r}{\partial x_k} - \left(\frac{\partial u_m^r}{\partial x_k} \right)^a \right) \right\|_{0,S} \leq \frac{C}{W^4} \sum_{|\alpha|=1} \|D_\lambda^\alpha u_m^r\|_{2,Q}. \tag{D.24}$$

Here we have used the trace theorem for Sobolev spaces.

Now using the inverse inequality for differentiation in (D.24) gives

$$\left\| \frac{\partial}{\partial \lambda_j} \left(\frac{\partial u_m^r}{\partial x_k} - \left(\frac{\partial u_m^r}{\partial x_k} \right)^a \right) \right\|_{0,S} \leq \frac{C}{W^2} \sum_{1 \leq |\alpha| \leq 2} \|D_\lambda^\alpha u_m^r\|_{1,Q}. \tag{D.25}$$

Combining (D.22) and (D.25) gives

$$\left\| \frac{\partial u_m^r}{\partial x_i} \right\|_{0,S} \left\| \frac{\partial}{\partial \lambda_j} \left(\frac{\partial u_m^r}{\partial x_k} - \left(\frac{\partial u_m^r}{\partial x_k} \right)^a \right) \right\|_{0,S} \leq \frac{C}{W^2} \sum_{1 \leq |\alpha| \leq 2} \|D_\lambda^\alpha u_m^r\|_{0,Q}. \quad (\text{D.26})$$

Next

$$\left\| \left(\frac{\partial u_m^r}{\partial x_i} \right)^a - \frac{\partial u_m^r}{\partial x_i} \right\|_{0,S} \leq \frac{C}{W^4} \sum_{|\alpha|=1} \|D_\lambda^\alpha u_m^r\|_{0,S}.$$

Hence by the trace theorem for Sobolev spaces

$$\left\| \left(\frac{\partial u_m^r}{\partial x_i} \right)^a - \frac{\partial u_m^r}{\partial x_i} \right\|_{0,S} \leq \frac{C}{W^4} \sum_{1 \leq |\alpha| \leq 2} \|D_\lambda^\alpha u_m^r\|_{0,Q}. \quad (\text{D.27})$$

And

$$\left\| \frac{\partial}{\partial \lambda_j} \left(\left(\frac{\partial u_m^r}{\partial x_k} \right)^a \right) \right\|_{0,S} \leq C \sum_{1 \leq |\alpha| \leq 2} \|D_\lambda^\alpha u_m^r\|_{0,S}.$$

Using the trace theorem and inverse inequality for differentiation gives

$$\left\| \frac{\partial}{\partial \lambda_j} \left(\left(\frac{\partial u_m^r}{\partial x_k} \right)^a \right) \right\|_{0,S} \leq CW^3 \sum_{1 \leq |\alpha| \leq 2} \|D_\lambda^\alpha u_m^r\|_{0,Q}. \quad (\text{D.28})$$

Combining (D.27) and (D.28) we obtain

$$\begin{aligned} & \left\| \left(\frac{\partial u_m^r}{\partial x_i} \right)^a - \frac{\partial u_m^r}{\partial x_i} \right\|_{0,S} \left\| \frac{\partial}{\partial \lambda_j} \left(\left(\frac{\partial u_m^r}{\partial x_k} \right)^a \right) \right\|_{0,S} \\ & \leq \frac{C}{W} \left(\sum_{1 \leq |\alpha| \leq 2} \|D_\lambda^\alpha u_m^r\|_{0,Q}^2 \right). \end{aligned} \quad (\text{D.29})$$

Substituting (D.26) and (D.29) into (D.21) yields

$$\begin{aligned} & \left| \int_S \left(\hat{a}_{i,j} \frac{\partial u_m^r}{\partial x_i} \frac{\partial}{\partial \lambda_j} \left(\hat{b}_k \frac{\partial u_m^r}{\partial x_k} \right) - \hat{a}_{i,j} \left(\frac{\partial u_m^r}{\partial x_i} \right)^a \frac{\partial}{\partial \lambda_j} \left(\hat{b}_k \left(\frac{\partial u_m^r}{\partial x_k} \right)^a \right) \right) d\lambda_1 d\lambda_2 \right| \\ & \leq \frac{C}{W} \left(\sum_{1 \leq |\alpha| \leq 2} \|D_\lambda^\alpha u_m^r\|_{0,Q}^2 \right). \end{aligned} \quad (\text{D.30a})$$

In the same way it can be shown that

$$\begin{aligned} & \left| \int_S \left(\hat{a}_{i,j} \frac{\partial u_p^r}{\partial x_i} \frac{\partial}{\partial \lambda_j} \left(\hat{b}_k \frac{\partial u_p^r}{\partial x_k} \right) - \hat{a}_{i,j} \left(\frac{\partial u_p^r}{\partial x_i} \right)^a \frac{\partial}{\partial \lambda_j} \left(\hat{b}_k \left(\frac{\partial u_p^r}{\partial x_k} \right)^a \right) \right) d\lambda_1 d\lambda_2 \right| \\ & \leq \frac{C}{W} \left(\sum_{1 \leq |\alpha| \leq 2} \|D_\lambda^\alpha u_p^r\|_{0,Q}^2 \right). \end{aligned} \quad (\text{D.30b})$$

Combining (D.20) and (D.30) gives

$$\begin{aligned}
& \left| \int_S \left(a_{i,j} \frac{\partial u_m^r}{\partial x_i} \frac{\partial}{\partial \lambda_j} \left(b_k \frac{\partial u_m^r}{\partial x_k} \right) - a_{i,j} \frac{\partial u_p^r}{\partial x_i} \frac{\partial}{\partial \lambda_j} \left(b_k \left(\frac{\partial u_p^r}{\partial x_k} \right) \right) \right) d\lambda_1 d\lambda_2 \right| \\
& \leq \left| \int_S \left(\hat{a}_{i,j} \left(\frac{\partial u_m^r}{\partial x_i} \right)^a \frac{\partial}{\partial \lambda_j} \left(\hat{b}_k \left(\frac{\partial u_m^r}{\partial x_k} \right)^a \right) \right. \right. \\
& \quad \left. \left. - \hat{a}_{i,j} \left(\frac{\partial u_p^r}{\partial x_i} \right)^a \frac{\partial}{\partial \lambda_j} \left(\hat{b}_k \left(\frac{\partial u_p^r}{\partial x_k} \right)^a \right) \right) d\lambda_1 d\lambda_2 \right| \\
& \quad + \frac{C}{W} \left(\sum_{1 \leq |\alpha| \leq 2} (\|D_x^\alpha u_m^r\|_{0,Q}^2 + \|D_x^\alpha u_p^r\|_{0,Q}^2) \right). \tag{D.31}
\end{aligned}$$

Clearly

$$\begin{aligned}
& \left| \int_S \left(\hat{a}_{i,j} \left(\frac{\partial u_m^r}{\partial x_i} \right)^a \frac{\partial}{\partial \lambda_j} \left(\hat{b}_k \left(\frac{\partial u_m^r}{\partial x_k} \right)^a \right) \right. \right. \\
& \quad \left. \left. - \hat{a}_{i,j} \left(\frac{\partial u_p^r}{\partial x_i} \right)^a \frac{\partial}{\partial \lambda_j} \left(\hat{b}_k \left(\frac{\partial u_p^r}{\partial x_k} \right)^a \right) \right) d\lambda_1 d\lambda_2 \right| \\
& \leq \left| \int_S \hat{a}_{i,j} \left(\frac{\partial u_m^r}{\partial x_i} \right)^a \frac{\partial}{\partial \lambda_j} \left(\hat{b}_k \left(\left(\frac{\partial u_m^r}{\partial x_k} \right)^a - \left(\frac{\partial u_p^r}{\partial x_k} \right)^a \right) \right) d\lambda_1 d\lambda_2 \right| \\
& \quad + \left| \int_S \left(\hat{a}_{i,j} \left(\left(\frac{\partial u_m^r}{\partial x_i} \right)^a - \left(\frac{\partial u_p^r}{\partial x_i} \right)^a \right) \frac{\partial}{\partial \lambda_j} \left(\hat{b}_k \left(\frac{\partial u_p^r}{\partial x_k} \right)^a \right) \right) d\lambda_1 d\lambda_2 \right|. \tag{D.32}
\end{aligned}$$

Now if $e(\lambda_1, \lambda_2)$ and $f(\lambda_1, \lambda_2)$ are polynomials of degree W in λ_1 and λ_2 then using Theorem 4.1 of [37]

$$\left| \int_S e(\lambda_1, \lambda_2) \frac{\partial}{\partial \lambda_j} (f(\lambda_1, \lambda_2)) d\lambda_1 d\lambda_2 \right| \leq C(\ln W) \|e\|_{1/2,S} \|f\|_{1/2,S}. \tag{D.33}$$

The estimate (D.32) remains valid if we replace the square S by the master triangle T .

Hence for any $\eta > 0$ there is a constant C such that

$$\begin{aligned}
& \left| \int_S \hat{a}_{i,j} \left(\frac{\partial u_m^r}{\partial x_i} \right)^a \frac{\partial}{\partial \lambda_j} \left(\hat{b}_k \left(\left(\frac{\partial u_m^r}{\partial x_k} \right)^a - \left(\frac{\partial u_p^r}{\partial x_k} \right)^a \right) \right) d\lambda_1 d\lambda_2 \right| \\
& \leq \frac{C}{\eta} (\ln W)^2 \left\| \hat{b}_k \left(\left(\frac{\partial u_m^r}{\partial x_k} \right)^a - \left(\frac{\partial u_p^r}{\partial x_k} \right)^a \right) \right\|_{1/2,S}^2 + \eta \left\| \hat{a}_{i,j} \left(\frac{\partial u_m^r}{\partial x_i} \right)^a \right\|_{1/2,S}^2 \\
& \leq K \left(\frac{1}{\eta} (\ln W)^2 \left\| \left(\left(\frac{\partial u_m^r}{\partial x_k} \right)^a - \left(\frac{\partial u_p^r}{\partial x_k} \right)^a \right) \right\|_{1/2,S}^2 + \eta \left\| \left(\frac{\partial u_m^r}{\partial x_i} \right)^a \right\|_{1/2,S}^2 \right). \tag{D.34}
\end{aligned}$$

Here we have used the estimate

$$\|gh\|_{1/2,S} \leq C \|g\|_{1,\infty,S} \|h\|_{1/2,S}. \tag{D.35}$$

Now

$$\begin{aligned} \left\| \left(\frac{\partial u_m^r}{\partial x_k} \right)^a - \left(\frac{\partial u_p^r}{\partial x_k} \right)^a \right\|_{1/2,S}^2 &\leq \left(\left\| \frac{\partial u_m^r}{\partial x_k} - \frac{\partial u_p^r}{\partial x_k} \right\|_{1/2,S}^2 + \left\| \frac{\partial u_p^r}{\partial x_k} - \left(\frac{\partial u_p^r}{\partial x_k} \right)^a \right\|_{1/2,S}^2 \right. \\ &\quad \left. + \left\| \frac{\partial u_m^r}{\partial x_k} - \left(\frac{\partial u_m^r}{\partial x_k} \right)^a \right\|_{1/2,S}^2 \right). \end{aligned} \quad (\text{D.36})$$

By the trace theorem for Sobolev spaces

$$\left\| \frac{\partial u_p^r}{\partial x_k} - \left(\frac{\partial u_p^r}{\partial x_k} \right)^a \right\|_{1/2,S} \leq C \left\| \frac{\partial u_p^r}{\partial x_k} - \left(\frac{\partial u_p^r}{\partial x_k} \right)^a \right\|_{1,Q} \quad (\text{D.37})$$

and

$$\left\| \frac{\partial u_p^r}{\partial x_k} - \left(\frac{\partial u_p^r}{\partial x_k} \right)^a \right\|_{1,Q} \leq \frac{C}{W^4} \left(\sum_{1 \leq |\alpha| \leq 2} \|D_\lambda^\alpha u_p^r\|_{1,Q} \right). \quad (\text{D.38})$$

Substituting (D.37) and (D.38) into (D.36) gives

$$\begin{aligned} \left\| \left(\frac{\partial u_m^r}{\partial x_k} \right)^a - \left(\frac{\partial u_p^r}{\partial x_k} \right)^a \right\|_{1/2,S}^2 &\leq C \left\| \frac{\partial u_m^r}{\partial x_k} - \frac{\partial u_p^r}{\partial x_k} \right\|_{1/2,S}^2 \\ &\quad + \frac{K}{W^8} \left(\sum_{1 \leq |\alpha| \leq 2} \|D_x^\alpha u_p^r\|_{0,\Omega_p^r}^2 + \|D_x^\alpha u_m^r\|_{0,\Omega_m^r}^2 \right). \end{aligned} \quad (\text{D.39})$$

Next by the trace theorem for Sobolev spaces

$$\left\| \left(\frac{\partial u_m^r}{\partial x_i} \right)^a \right\|_{1/2,S}^2 \leq C \left\| \left(\frac{\partial u_m^r}{\partial x_i} \right)^a \right\|_{1,Q}$$

and

$$\left\| \left(\frac{\partial u_m^r}{\partial x_i} \right)^a \right\|_{1,Q} \leq C \left\| \frac{\partial u_m^r}{\partial x_i} \right\|_{1,Q} + \frac{C}{W^4} \left(\sum_{1 \leq |\alpha| \leq 2} \|D_x^\alpha u_m^r\|_{1,Q} \right).$$

Hence

$$\left\| \left(\frac{\partial u_m^r}{\partial x_i} \right)^a \right\|_{1/2,S} \leq C \left(\sum_{1 \leq |\alpha| \leq 2} \|D_x^\alpha u_m^r\|_{\Omega_m^r} \right). \quad (\text{D.40})$$

Substituting (D.39) and (D.40) into (D.34) for any $\eta > 0$

$$\begin{aligned} &\left| \int_S \hat{a}_{i,j} \left(\frac{\partial u_m^r}{\partial x_i} \right)^a \frac{\partial}{\partial \lambda_j} \left(\hat{b}_k \left(\left(\frac{\partial u_m^r}{\partial x_k} \right)^a - \left(\frac{\partial u_p^r}{\partial x_k} \right)^a \right) \right) d\lambda_1 d\lambda_2 \right| \\ &\leq K \left(\frac{(\ln W)^2}{\eta} \left\| \frac{\partial u_m^r}{\partial x_k} - \frac{\partial u_p^r}{\partial x_k} \right\|_{1/2,S}^2 + \eta \left(\sum_{1 \leq |\alpha| \leq 2} \|D_x^\alpha u_m^r\|_{0,\Omega_m^r}^2 \right) \right) \end{aligned} \quad (\text{D.41})$$

by choosing W large enough.

In the same way it can be shown that

$$\begin{aligned} & \left| \int_S \hat{a}_{i,j} \left(\left(\frac{\partial u_m^r}{\partial x_i} \right)^a - \left(\frac{\partial u_p^r}{\partial x_i} \right)^a \right) \frac{\partial}{\partial \lambda_j} \left(\hat{b}_k \left(\frac{\partial u_p^r}{\partial x_k} \right)^a \right) d\lambda_1 d\lambda_2 \right| \\ & \leq K \left(\frac{(\ln W)^2}{\eta} \left\| \frac{\partial u_m^r}{\partial x_k} - \frac{\partial u_p^r}{\partial x_k} \right\|_{1/2,S}^2 + \eta \left(\sum_{1 \leq |\alpha| \leq 2} \|D_x^\alpha u_p^r\|_{0,\Omega_m^r}^2 \right) \right). \end{aligned} \quad (D.42)$$

Substituting (D.41) and (D.42) into (D.31) and combining it with (D.32) gives

$$\begin{aligned} & \left| \int_S \left(a_{i,j} \frac{\partial u_m^r}{\partial x_i} \frac{\partial}{\partial \lambda_j} \left(b_k \frac{\partial u_m^r}{\partial x_k} \right) - a_{i,j} \frac{\partial u_p^r}{\partial x_i} \frac{\partial}{\partial \lambda_j} \left(b_k \frac{\partial u_p^r}{\partial x_k} \right) \right) d\lambda_1 d\lambda_2 \right| \\ & \leq K \left(\frac{(\ln W)^2}{\eta} \left(\sum_{k=1}^3 \| [u_{x_k}] \|_{1/2,\Gamma_{p,j}^r}^2 \right) \right. \\ & \quad \left. + \eta \left(\sum_{1 \leq |\alpha| \leq 2} (\|D_x^\alpha u_m^r\|_{0,Q}^2 + \|D_x^\alpha u_p^r\|_{0,Q}^2) \right) \right). \end{aligned} \quad (D.43)$$

Now choosing $\epsilon = K\eta$, (D.15) follows. \square

D.3

Proof of Lemma 3.4.3

Lemma 3.4.3. *Let Ω_m^e and Ω_p^e be elements in the edge neighbourhood Ω^e of Ω and $\Gamma_{m,i}^e$ be a face of Ω_m^e and $\Gamma_{p,j}^e$ be a face of Ω_p^e such that $\Gamma_{m,i}^e = \Gamma_{p,j}^e$ and $\mu(\tilde{\Gamma}_{m,i}^e) < \infty$. Then for any $\epsilon > 0$ there exists a constant C_ϵ such that for W large enough*

$$\begin{aligned} & \left| \oint_{\partial \tilde{\Gamma}_{m,i}^e} \left(\left(\frac{\partial u_m^e}{\partial \mathbf{n}^e} \right)_{A^e} \left(\frac{\partial u_m^e}{\partial \boldsymbol{\nu}^e} \right)_{A^e} - \left(\frac{\partial u_p^e}{\partial \mathbf{n}^e} \right)_{A^e} \left(\frac{\partial u_p^e}{\partial \boldsymbol{\nu}^e} \right)_{A^e} \right) ds^e \right| \\ & \leq C_\epsilon (\ln W)^2 \left(\| [u_{x_1}^e] \|_{\tilde{\Gamma}_{m,i}^e}^2 + \| [u_{x_2}^e] \|_{\tilde{\Gamma}_{m,i}^e}^2 + \| G_{m,i}^e[u_{x_3}^e] \|_{\tilde{\Gamma}_{m,i}^e}^2 \right) \end{aligned} \quad (D.44a)$$

$$\begin{aligned} & + \epsilon \sum_{k=m,p} \left(\int_{\tilde{\Omega}_k^e} \left(\sum_{i,j=1,2} \left(\frac{\partial^2 u_k^e}{\partial x_i^e \partial x_j^e} \right)^2 + e^{2\tau} \sum_{i=1}^2 \left(\frac{\partial^2 u_k^e}{\partial x_k^e \partial x_3^e} \right)^2 + e^{4\tau} \left(\frac{\partial^2 u_k^e}{(\partial x_3^e)^2} \right)^2 \right. \right. \\ & \quad \left. \left. + \sum_{i=1}^2 \left(\frac{\partial u_k^e}{\partial x_i^e} \right)^2 + e^{2\tau} \left(\frac{\partial u_k^e}{\partial x_3^e} \right)^2 \right) w^e(x_1^e) dx^e \right). \end{aligned} \quad (D.44b)$$

Here C_ϵ is a constant which depend on ϵ but is uniform for all $\tilde{\Gamma}_{m,i}^e \subseteq \tilde{\Omega}^e$, and $G_{m,i}^e =$

$$\sup_{x^e \in \tilde{\Gamma}_{m,i}^e} (e^\tau).$$

If $\mu(\tilde{\Gamma}_{m,i}^e) = \infty$ then for any $\epsilon > 0$ for W, N large enough

$$\left| \oint_{\partial \tilde{\Gamma}_{m,i}^e} \left(\left(\frac{\partial u_m^e}{\partial \mathbf{n}^e} \right)_{A^e} \left(\frac{\partial u_m^e}{\partial \boldsymbol{\nu}^e} \right)_{A^e} - \left(\frac{\partial u_p^e}{\partial \mathbf{n}^e} \right)_{A^e} \left(\frac{\partial u_p^e}{\partial \boldsymbol{\nu}^e} \right)_{A^e} \right) ds^e \right| \leq \epsilon \left(\int_{\tilde{\Omega}_m^e} (u_m^e)^2 w^e(x_1^e) dx^e + \int_{\tilde{\Omega}_m^e} (u_m^e)^2 w^e(x_1^e) dx^e \right) \quad (\text{D.44c})$$

provided $W = O(e^{N^\alpha})$ with $\alpha < 1/2$.

Proof. In the edge neighbourhood Ω^e the system of coordinates used are

$$\begin{aligned} x_1^e &= \tau \\ x_2^e &= \theta \\ x_3^e &= x_3. \end{aligned} \quad (\text{D.45a})$$

There are two cases to be considered. the first case is when

$$\tilde{\Gamma}_{m,i}^e = \{x^e : \alpha_0 < x_1^e < \alpha_1, \beta_0 < x_2^e < \beta_1, x_3^e = \gamma_0\}.$$

We introduce local variables

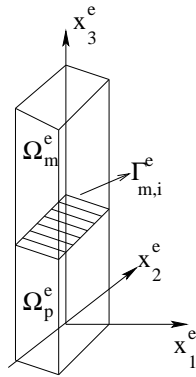


Figure D.1: A common face in the interior of the edge neighbourhood in $x_1^e - x_2^e$ plane.

$$\begin{aligned} z_1 &= x_1^e \\ z_2 &= x_2^e \\ z_3 &= \frac{x_3^e}{G_{m,i}^e}. \end{aligned} \quad (\text{D.45b})$$

Now

$$\begin{aligned} \left(\frac{\partial u}{\partial x_1^e} \right)_{A^e} &= \begin{bmatrix} 1 & 0 & 0 \end{bmatrix} A^e \begin{bmatrix} \frac{\partial u}{\partial x_1^e} \\ \frac{\partial u}{\partial x_2^e} \\ \frac{\partial u}{\partial x_3^e} \end{bmatrix} \\ &= \begin{bmatrix} 1 & 0 & 0 \end{bmatrix} \begin{bmatrix} 1 & 0 & 0 \\ 0 & 1 & 0 \\ 0 & 0 & \frac{1}{G_{m,i}^e} \end{bmatrix} A^e \begin{bmatrix} 1 & 0 & 0 \\ 0 & 1 & 0 \\ 0 & 0 & \frac{1}{G_{m,i}^e} \end{bmatrix} \begin{bmatrix} \frac{\partial u}{\partial z_1} \\ \frac{\partial u}{\partial z_2} \\ \frac{\partial u}{\partial z_3} \end{bmatrix} \end{aligned}$$

Hence we obtain

$$\left(\frac{\partial u}{\partial x_1^e} \right)_{A^e} = \left(\frac{\partial u}{\partial z_1} \right)_{\hat{A}^e} \quad (\text{D.46a})$$

$$\left(\frac{\partial u}{\partial x_2^e} \right)_{A^e} = \left(\frac{\partial u}{\partial z_2} \right)_{\hat{A}^e} \quad (\text{D.46b})$$

$$\left(\frac{\partial u}{\partial x_3^e} \right)_{A^e} = G_{m,i}^e \left(\frac{\partial u}{\partial z_3} \right)_{\hat{A}^e}. \quad (\text{D.46c})$$

Here using (3.76)

$$\hat{A}^e = (\hat{S}^e)^T A \hat{S}^e \quad (\text{D.47a})$$

where

$$\hat{S}^e = \begin{bmatrix} \cos \theta & -\sin \theta & 0 \\ \sin \theta & \cos \theta & 0 \\ 0 & 0 & \frac{e^\tau}{G_{m,i}^e} \end{bmatrix}. \quad (\text{D.47b})$$

Hence \hat{A}^e and its derivatives with respect to z are uniformly bounded in $\hat{\Omega}_m^e$ and $\hat{\Omega}_p^e$. Here $\hat{\Omega}_m^e$ and $\hat{\Omega}_p^e$ are the images of Ω_m^e and Ω_p^e in z variables respectively. Now

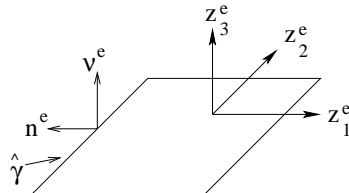


Figure D.2: $\hat{\gamma}$, image of $\tilde{\gamma}$, in z -coordinates.

$$\begin{aligned}
& \int_{\tilde{\gamma}} \left(\left(\frac{\partial u_m^e}{\partial \mathbf{n}^e} \right)_{A^e} \left(\frac{\partial u_m^e}{\partial \boldsymbol{\nu}^e} \right)_{A^e} - \left(\frac{\partial u_p^e}{\partial \mathbf{n}^e} \right)_{A^e} \left(\frac{\partial u_p^e}{\partial \boldsymbol{\nu}^e} \right)_{A^e} \right) ds^e \\
&= \int_{\tilde{\gamma}} \left(\left(\frac{\partial u_m^e}{\partial x_1^e} \right)_{A^e} \left(\frac{\partial u_m^e}{\partial x_3^e} \right)_{A^e} - \left(\frac{\partial u_p^e}{\partial x_1^e} \right)_{A^e} \left(\frac{\partial u_p^e}{\partial x_3^e} \right)_{A^e} \right) dx_2^e \\
&= G_{m,i}^e \int_{\hat{\gamma}} \left(\left(\frac{\partial u_m^e}{\partial z_1} \right)_{\hat{A}^e} \left(\frac{\partial u_m^e}{\partial z_3} \right)_{\hat{A}^e} - \left(\frac{\partial u_p^e}{\partial z_1} \right)_{\hat{A}^e} \left(\frac{\partial u_p^e}{\partial z_3} \right)_{\hat{A}^e} \right) dz_2. \quad (\text{D.48})
\end{aligned}$$

Here $\hat{\gamma}$ is the image of $\tilde{\gamma}$ in z coordinates as shown in Figure D.2.

Proceeding as in Lemma 3.4.1 we can prove using the representation (D.48) that for any $\eta > 0$ there exists a constant C_η , which depends on η , but is uniform for all $\tilde{\Gamma}_{m,i}^e \subseteq \tilde{\Omega}^e$ such that

$$\begin{aligned}
& \left| \int_{\partial \tilde{\Gamma}_{m,i}^e} \left(\left(\frac{\partial u_m^e}{\partial \mathbf{n}^e} \right)_{A^e} \left(\frac{\partial u_m^e}{\partial \boldsymbol{\nu}^e} \right)_{A^e} - \left(\frac{\partial u_p^e}{\partial \mathbf{n}^e} \right)_{A^e} \left(\frac{\partial u_p^e}{\partial \boldsymbol{\nu}^e} \right)_{A^e} \right) ds^e \right| \\
&\leq G_{m,i}^e \left(C_\eta (\ln W)^2 \sum_{k=1}^3 \| [u_{z_k}] \|_{1/2, \tilde{\Gamma}_{m,i}^e}^2 \right. \\
&\quad \left. + \eta \left(\sum_{1 \leq |\alpha| \leq 2} \left(\| D_z^\alpha u_m^e \|_{0, \hat{\Omega}_m^e}^2 + \| D_z^\alpha u_p^e \|_{0, \hat{\Omega}_p^e}^2 \right) \right) \right). \quad (\text{D.49})
\end{aligned}$$

Here $\hat{\Gamma}_{m,i}^e$ is the image of $\Gamma_{m,i}^e$ in z coordinates and $\hat{\Omega}_m^e$ and $\hat{\Omega}_p^e$ are the images of Ω_m^e and Ω_p^e in z coordinates. And by a proper choice of η in (D.49) we obtain (D.44).

The other case to be considered is when the boundary $\tilde{\Gamma}_{m,i}^e$ corresponds to

$$\tilde{\Gamma}_{m,i}^e = \{x^e : \alpha_0 < x_1^e < \alpha_1, x_2^e = \beta_0, \gamma_0 < x_3^e < \gamma_1\}.$$

The case when

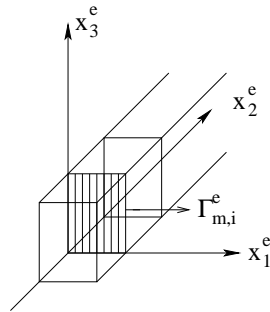


Figure D.3: A common face in the interior of the edge neighbourhood in $x_1^e - x_3^e$ plane.

$$\tilde{\Gamma}_{m,i}^e = \{x^e : x_1^e = \alpha_0, \beta_0 < x_2^e < \beta_1, \gamma_0 < x_3^e < \gamma_1\}$$

is essentially the same and hence is omitted.

Now

$$\begin{aligned}
 & \int_{\tilde{\gamma}} \left(\left(\frac{\partial u_m^e}{\partial \mathbf{n}^e} \right)_{A^e} \left(\frac{\partial u_m^e}{\partial \boldsymbol{\nu}^e} \right)_{A^e} - \left(\frac{\partial u_p^e}{\partial \mathbf{n}^e} \right)_{A^e} \left(\frac{\partial u_p^e}{\partial \boldsymbol{\nu}^e} \right)_{A^e} \right) ds^e \\
 &= \int_{\tilde{\gamma}} \left(\left(\frac{\partial u_m^e}{\partial x_1^e} \right)_{A^e} \left(\frac{\partial u_m^e}{\partial x_2^e} \right)_{A^e} - \left(\frac{\partial u_p^e}{\partial x_1^e} \right)_{A^e} \left(\frac{\partial u_p^e}{\partial x_2^e} \right)_{A^e} \right) dx_3^e \\
 &= G_{m,i}^e \int_{\hat{\gamma}} \left(\left(\frac{\partial u_m^e}{\partial z_1} \right)_{\hat{A}^e} \left(\frac{\partial u_m^e}{\partial z_2} \right)_{\hat{A}^e} - \left(\frac{\partial u_p^e}{\partial z_1} \right)_{\hat{A}^e} \left(\frac{\partial u_p^e}{\partial z_2} \right)_{\hat{A}^e} \right) dz_3. \quad (\text{D.50})
 \end{aligned}$$

Here $\hat{\gamma}$ is the image of $\tilde{\gamma}$ in z coordinates as shown in Figure D.4.

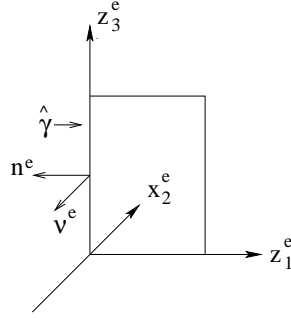


Figure D.4: $\hat{\gamma}$, image of $\tilde{\gamma}$, in z -coordinates.

Let $\hat{\Omega}_m^e$ and $\hat{\Omega}_p^e$ be the images of Ω_m^e and Ω_p^e in z coordinates. Then $\hat{\Omega}_m^e$ and $\hat{\Omega}_p^e$ are

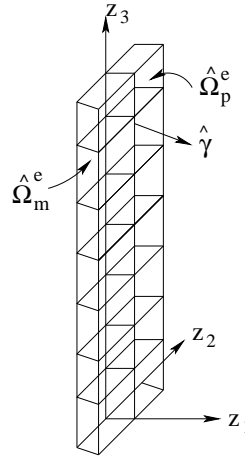


Figure D.5: Division of $\hat{\Omega}_m^e$ into smaller rectangles.

long thin rectangles in z coordinates with the length in the z_3 direction $= \Theta \left(\frac{1}{G_{m,i}^e} \right)$. We divide these rectangles into $\Theta \left(\frac{1}{G_{m,i}^e} \right)$ rectangles as shown in the Figure D.5, where each rectangle has length in the z_3 direction $= \Theta(1)$.

Proceeding as in Lemma 3.4.1 we can prove using the representation (D.50) that

$$\begin{aligned} & \left| \int_{\partial \tilde{\Gamma}_{m,i}^e} \left(\left(\frac{\partial u_m^e}{\partial \mathbf{n}^e} \right)_{A^e} \left(\frac{\partial u_m^e}{\partial \boldsymbol{\nu}^e} \right)_{A^e} - \left(\frac{\partial u_p^e}{\partial \mathbf{n}^e} \right)_{A^e} \left(\frac{\partial u_p^e}{\partial \boldsymbol{\nu}^e} \right)_{A^e} \right) ds^e \right| \\ & \leq G_{m,i}^e \left(C_\eta (\ln W)^2 \sum_{k=1}^3 \| [u_{z_k}] \|_{1/2, \tilde{\Gamma}_{m,i}^e}^2 \right. \\ & \quad \left. + \eta \left(\sum_{1 \leq |\alpha| \leq 2} \left(\| D_z^\alpha u_m^e \|_{0, \tilde{\Omega}_m^e}^2 + \| D_z^\alpha u_p^e \|_{0, \tilde{\Omega}_p^e}^2 \right) \right) \right). \end{aligned} \quad (\text{D.51})$$

Here $\hat{\Gamma}_{m,i}^e$ is the image of $\Gamma_{m,i}^e$ in z coordinates and $\hat{\Omega}_m^e$ and $\hat{\Omega}_p^e$ are the images of Ω_m^e and Ω_p^e in z coordinates. Now by a proper choice of η in (D.51) we obtain (D.44). \square

D.4

Proof of Lemma 3.4.4

Lemma 3.4.4. *Let Ω_m^e and Ω_p^e be elements in the edge neighbourhood Ω^e of Ω and $\Gamma_{m,i}^e$ be a face of Ω_m^e and $\Gamma_{p,j}^e$ be a face of Ω_p^e such that $\Gamma_{m,i}^e = \Gamma_{p,j}^e$ and $\mu(\tilde{\Gamma}_{m,i}^e) < \infty$. Then for any $\epsilon > 0$ there exists a constant C_ϵ such that for W large enough*

$$\begin{aligned} & \left| \int_{\tilde{\Gamma}_{m,i}^e} \sum_{l=1}^2 \left(\left(\frac{\partial u_m^e}{\partial \boldsymbol{\tau}_l^e} \right)_{A^e} \frac{\partial}{\partial s_l^e} \left(\left(\frac{\partial u_m^e}{\partial \boldsymbol{\nu}^e} \right)_{A^e} \right) - \left(\frac{\partial u_p^e}{\partial \boldsymbol{\tau}_l^e} \right)_{A^e} \frac{\partial}{\partial s_l^e} \left(\left(\frac{\partial u_p^e}{\partial \boldsymbol{\nu}^e} \right)_{A^e} \right) \right) d\sigma^e \right| \\ & \leq C_\epsilon (\ln W)^2 \left(\| [u_{x_1}^e] \|_{\tilde{\Gamma}_{m,i}^e}^2 + \| [u_{x_2}^e] \|_{\tilde{\Gamma}_{m,i}^e}^2 + \| G_{m,i}^e [u_{x_3}^e] \|_{\tilde{\Gamma}_{m,i}^e}^2 \right) \\ & \quad + \epsilon \sum_{k=m,p} \left(\int_{\tilde{\Omega}_k^e} \left(\sum_{i,j=1,2} \left(\frac{\partial^2 u_k^e}{\partial x_i^e \partial x_j^e} \right)^2 + e^{2\tau} \sum_{i=1}^2 \left(\frac{\partial^2 u_k^e}{\partial x_i^e \partial x_3^e} \right)^2 + e^{4\tau} \left(\frac{\partial^2 u_k^e}{(\partial x_3^e)^2} \right)^2 \right. \right. \\ & \quad \left. \left. + \sum_{i=1}^2 \left(\frac{\partial u_k^e}{\partial x_i^e} \right)^2 + e^{2\tau} \left(\frac{\partial u_k^e}{\partial x_3^e} \right)^2 \right) w^e(x_1^e) dx^e \right). \end{aligned} \quad (\text{D.52a})$$

If $\mu(\tilde{\Gamma}_{m,i}^e) = \infty$ then for any $\epsilon > 0$ for W, N large enough

$$\begin{aligned} & \left| \int_{\tilde{\Gamma}_{m,i}^e} \sum_{l=1}^2 \left(\left(\frac{\partial u_m^e}{\partial \boldsymbol{\tau}_l^e} \right)_{A^e} \frac{\partial}{\partial s_l^e} \left(\left(\frac{\partial u_m^e}{\partial \boldsymbol{\nu}^e} \right)_{A^e} \right) - \left(\frac{\partial u_p^e}{\partial \boldsymbol{\tau}_l^e} \right)_{A^e} \frac{\partial}{\partial s_l^e} \left(\left(\frac{\partial u_p^e}{\partial \boldsymbol{\nu}^e} \right)_{A^e} \right) \right) d\sigma^e \right| \\ & \leq \epsilon \left(\int_{\tilde{\Omega}_m^e} (u_m^e)^2 w^e(x_1^e) dx^e + \int_{\tilde{\Omega}_m^e} (u_m^e)^2 w^e(x_1^e) dx^e \right) \end{aligned} \quad (\text{D.52b})$$

provided $W = O(e^{N^\alpha})$ with $\alpha < 1/2$.

Proof. Let us first consider the case when

$$\tilde{\Gamma}_{m,i}^e = \{x^e : \alpha_0 < x_1^e < \alpha_1, \beta_0 < x_2^e < \beta_1, x_3^e = \gamma_0\}$$

which corresponds to Figure D.1.

Now using (D.47)

$$\begin{aligned} & \int_{\tilde{\Gamma}_{m,i}^e} \sum_{l=1}^2 \left(\left(\frac{\partial u_m^e}{\partial \tau_l^e} \right)_{A^e} \frac{\partial}{\partial s_l^e} \left(\left(\frac{\partial u_m^e}{\partial \nu^e} \right)_{A^e} \right) \right. \\ & \quad \left. - \left(\frac{\partial u_p^e}{\partial \tau_l^e} \right)_{A^e} \frac{\partial}{\partial s_l^e} \left(\left(\frac{\partial u_p^e}{\partial \nu^e} \right)_{A^e} \right) \right) d\sigma^e \\ &= \int_{\tilde{\Gamma}_{m,i}^e} \sum_{l=1}^2 \left(\left(\frac{\partial u_m^e}{\partial x_l^e} \right)_{A^e} \frac{\partial}{\partial x_l^e} \left(\left(\frac{\partial u_m^e}{\partial x_3^e} \right)_{A^e} \right) \right. \\ & \quad \left. - \left(\frac{\partial u_p^e}{\partial x_l^e} \right)_{A^e} \frac{\partial}{\partial x_l^e} \left(\left(\frac{\partial u_p^e}{\partial x_3^e} \right)_{A^e} \right) \right) dx_1^e dx_2^e \\ &= G_{m,i}^e \int_{\hat{\Gamma}_{m,i}^e} \sum_{l=1}^2 \left(\left(\frac{\partial u_m^e}{\partial z_l} \right)_{\hat{A}^e} \frac{\partial}{\partial z_l} \left(\left(\frac{\partial u_m^e}{\partial z_3} \right)_{\hat{A}^e} \right) \right. \\ & \quad \left. - \left(\frac{\partial u_p^e}{\partial z_l} \right)_{\hat{A}^e} \frac{\partial}{\partial z_l} \left(\left(\frac{\partial u_p^e}{\partial z_3} \right)_{\hat{A}^e} \right) \right) dz_1 dz_2. \end{aligned} \quad (\text{D.53})$$

Proceeding as in Lemma 3.4.2 we can prove using the representation (D.53) that for any $\eta > 0$ there exists a constant C_η , which depends on η , but is uniform for all $\tilde{\Gamma}_{m,i}^e \subseteq \tilde{\Omega}^e$ such that

$$\begin{aligned} & \int_{\tilde{\Gamma}_{m,i}^e} \sum_{l=1}^2 \left(\left(\frac{\partial u_m^e}{\partial \tau_l^e} \right)_{A^e} \frac{\partial}{\partial s_l^e} \left(\left(\frac{\partial u_m^e}{\partial \nu^e} \right)_{A^e} \right) - \left(\frac{\partial u_p^e}{\partial \tau_l^e} \right)_{A^e} \frac{\partial}{\partial s_l^e} \left(\left(\frac{\partial u_p^e}{\partial \nu^e} \right)_{A^e} \right) \right) d\sigma^e \\ & \leq G_{m,i}^e \left(C_\eta (\ln W)^2 \sum_{k=1}^3 \| [u_{z_k}] \|_{1/2, \hat{\Gamma}_{m,i}^e}^2 \right. \\ & \quad \left. + \eta \left(\sum_{1 \leq |\alpha| \leq 2} \left(\| D_z^\alpha u_m^e \|_{0, \hat{\Omega}_m^e}^2 + \| D_z^\alpha u_p^e \|_{0, \hat{\Omega}_p^e}^2 \right) \right) \right). \end{aligned} \quad (\text{D.54})$$

And by a proper choice of η in (D.54) we obtain (D.52).

The next case we consider is when the boundary $\tilde{\Gamma}_{m,i}^e$ corresponds to

$$\tilde{\Gamma}_{m,i}^e = \{x^e : \alpha_0 < x_1^e < \alpha_1, x_2^e = \beta_0, \gamma_0 < x_3^e < \gamma_1\}.$$

The boundary $\tilde{\Gamma}_{m,i}^e$ is shown in Figure D.3. Now

$$\begin{aligned} & \int_{\tilde{\Gamma}_{m,i}^e} \sum_{l=1}^2 \left(\left(\frac{\partial u_m^e}{\partial \tau_l^e} \right)_{A^e} \frac{\partial}{\partial s_l^e} \left(\left(\frac{\partial u_m^e}{\partial \nu^e} \right)_{A^e} \right) - \left(\frac{\partial u_p^e}{\partial \tau_l^e} \right)_{A^e} \frac{\partial}{\partial s_l^e} \left(\left(\frac{\partial u_p^e}{\partial \nu^e} \right)_{A^e} \right) \right) d\sigma^e \\ &= \int_{\tilde{\Gamma}_{m,i}^e} \left(\left(\frac{\partial u_m^e}{\partial x_1^e} \right)_{A^e} \frac{\partial}{\partial x_1^e} \left(\left(\frac{\partial u_m^e}{\partial x_2^e} \right)_{A^e} \right) - \left(\frac{\partial u_p^e}{\partial x_1^e} \right)_{A^e} \frac{\partial}{\partial x_1^e} \left(\left(\frac{\partial u_p^e}{\partial x_2^e} \right)_{A^e} \right) \right) dx_1^e dx_3^e \\ &+ \int_{\tilde{\Gamma}_{m,i}^e} \left(\left(\frac{\partial u_m^e}{\partial x_3^e} \right)_{A^e} \frac{\partial}{\partial x_3^e} \left(\left(\frac{\partial u_m^e}{\partial x_2^e} \right)_{A^e} \right) - \left(\frac{\partial u_p^e}{\partial x_3^e} \right)_{A^e} \frac{\partial}{\partial x_3^e} \left(\left(\frac{\partial u_p^e}{\partial x_2^e} \right)_{A^e} \right) \right) dx_1^e dx_3^e. \end{aligned}$$

Hence

$$\begin{aligned} & \int_{\tilde{\Gamma}_{m,i}^e} \sum_{l=1}^2 \left(\left(\frac{\partial u_m^e}{\partial \tau_l^e} \right)_{A^e} \frac{\partial}{\partial s_l^e} \left(\left(\frac{\partial u_m^e}{\partial \nu^e} \right)_{A^e} \right) \right. \\ & \quad \left. - \left(\frac{\partial u_p^e}{\partial \tau_l^e} \right)_{A^e} \frac{\partial}{\partial s_l^e} \left(\left(\frac{\partial u_p^e}{\partial \nu^e} \right)_{A^e} \right) \right) d\sigma^e \\ &= G_{m,i}^e \left(\int_{\tilde{\Gamma}_{m,i}^e} \left(\left(\frac{\partial u_m^e}{\partial z_1} \right)_{\hat{A}^e} \frac{\partial}{\partial z_1} \left(\left(\frac{\partial u_m^e}{\partial z_2} \right)_{\hat{A}^e} \right) \right. \right. \\ & \quad \left. \left. - \left(\frac{\partial u_p^e}{\partial z_1} \right)_{\hat{A}^e} \frac{\partial}{\partial z_1} \left(\left(\frac{\partial u_p^e}{\partial z_2} \right)_{\hat{A}^e} \right) \right) dz_1 dz_3 \right. \\ & \quad \left. + \int_{\tilde{\Gamma}_{m,i}^e} \left(\left(\frac{\partial u_m^e}{\partial z_3} \right)_{\hat{A}^e} \frac{\partial}{\partial z_3} \left(\left(\frac{\partial u_m^e}{\partial z_2} \right)_{\hat{A}^e} \right) \right. \right. \\ & \quad \left. \left. - \left(\frac{\partial u_p^e}{\partial z_3} \right)_{\hat{A}^e} \frac{\partial}{\partial z_3} \left(\left(\frac{\partial u_p^e}{\partial z_2} \right)_{\hat{A}^e} \right) \right) dz_1 dz_3 \right). \end{aligned} \quad (D.55)$$

Proceeding as in Lemma 3.4.2 we can prove using the representation (D.55) that for any $\eta > 0$ there exists a constant C_η , which depends on η , but is uniform for all $\tilde{\Gamma}_{m,i}^e \subseteq \tilde{\Omega}^e$ such that

$$\begin{aligned} & \left| \int_{\tilde{\Gamma}_{m,i}^e} \sum_{l=1}^2 \left(\left(\frac{\partial u_m^e}{\partial \tau_l^e} \right)_{A^e} \frac{\partial}{\partial s_l^e} \left(\left(\frac{\partial u_m^e}{\partial \nu^e} \right)_{A^e} \right) - \left(\frac{\partial u_p^e}{\partial \tau_l^e} \right)_{A^e} \frac{\partial}{\partial s_l^e} \left(\left(\frac{\partial u_p^e}{\partial \nu^e} \right)_{A^e} \right) \right) d\sigma^e \right| \\ & \leq G_{m,i}^e \left(C_\eta (\ln W)^2 \sum_{k=1}^3 \| [u_{z_k}] \|_{1/2, \hat{\Gamma}_{m,i}^e}^2 \right. \\ & \quad \left. + \eta \left(\sum_{1 \leq |\alpha| \leq 2} \left(\| D_z^\alpha u_m^e \|_{0, \hat{\Omega}_m^e}^2 + \| D_z^\alpha u_p^e \|_{0, \hat{\Omega}_p^e}^2 \right) \right) \right). \end{aligned} \quad (D.56)$$

Now by a proper choice of η , (D.52) follows. \square

D.5

Proof of Lemma 3.5.1

Lemma 3.5.1. *Let $\Gamma_{m,j}^r$ be part of the boundary of the element Ω_m^r which lies on the $x_2 - x_3$ axis. Define the contributions from $\Gamma_{m,j}^r$ by*

$$\begin{aligned} (BT)_{m,j}^r &= \rho_v^2 \sin^2(\phi_v) \left(- \oint_{\partial\Gamma_{m,j}^r} \left(\frac{\partial u}{\partial \mathbf{n}} \right)_A \left(\frac{\partial u}{\partial \boldsymbol{\nu}} \right)_A ds \right. \\ &\quad \left. + 2 \int_{\Gamma_{m,j}^r} \sum_{j=1}^2 \left(\frac{\partial u}{\partial \boldsymbol{\tau}_j} \right)_A \frac{\partial}{\partial s_j} \left(\left(\frac{\partial u}{\partial \boldsymbol{\nu}} \right)_A \right) d\sigma \right). \end{aligned} \quad (\text{D.57})$$

If Dirichlet boundary conditions are imposed on $\Gamma_{m,j}^r$ then

$$\begin{aligned} |(BT)_{m,j}^r| &\leq C_\epsilon (\ln W)^2 \|u_m^r\|_{3/2, \Gamma_{m,j}^r}^2 + K_\epsilon \sum_{|\alpha|=1} \|D_x^\alpha u_m^r\|_{0, \Omega_m^r}^2 \\ &\quad + \epsilon \sum_{|\alpha|=2} \|D_x^\alpha u_m^r\|_{0, \Omega_m^r}^2. \end{aligned} \quad (\text{D.58})$$

If Neumann boundary conditions are imposed on $\Gamma_{m,j}^r$ then

$$|(BT)_{m,j}^r| \leq C_\epsilon (\ln W)^2 \left\| \left(\frac{\partial u_m^r}{\partial \boldsymbol{\nu}} \right)_A \right\|_{1/2, \Gamma_{m,j}^r}^2 + \epsilon \sum_{1 \leq |\alpha| \leq 2} \|D_x^\alpha u_m^r\|_{2, \Omega_m^r}^2. \quad (\text{D.59})$$

Proof. In case the boundary conditions on the face corresponding to the $x_2 - x_3$ axis are Neumann we can show that for any $\epsilon > 0$

$$|(BT)_{m,j}^r| \leq C_\epsilon (\ln W)^2 \left\| \left(\frac{\partial u_m^r}{\partial \boldsymbol{\nu}} \right)_A \right\|_{1/2, \Gamma_{m,j}^r}^2 + \epsilon \sum_{1 \leq |\alpha| \leq 2} \|D_x^\alpha u_m^r\|_{2, \Omega_m^r}^2. \quad (\text{D.60})$$

We now need to examine the case when Dirichlet boundary conditions are imposed on the face corresponding to the $x_2 - x_3$ plane.

We may choose

$$\begin{aligned} \boldsymbol{\tau}_1 &= (0, 0, 1), \\ \boldsymbol{\tau}_2 &= (0, 1, 0), \\ \boldsymbol{\nu} &= (-1, 0, 0). \end{aligned} \quad (\text{D.61})$$

Now

$$\begin{aligned} A\boldsymbol{\tau}_1 &= \alpha_{11}\boldsymbol{\tau}_1 + \alpha_{12}\boldsymbol{\tau}_2 + \alpha_{13}A\boldsymbol{\nu} \\ A\boldsymbol{\tau}_2 &= \alpha_{21}\boldsymbol{\tau}_1 + \alpha_{22}\boldsymbol{\tau}_2 + \alpha_{23}A\boldsymbol{\nu} \end{aligned} \quad (\text{D.62})$$

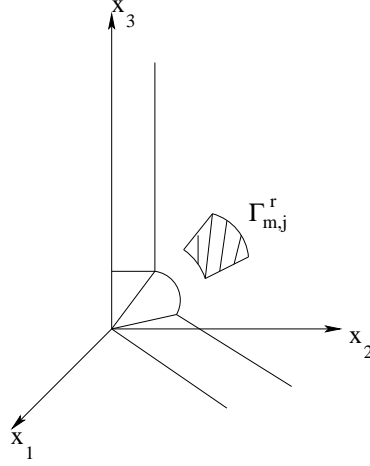


Figure D.6: The face $\Gamma_{m,j}^r$ of the boundary element Ω_m^r .

Here

$$\alpha_{13} = \frac{\boldsymbol{\nu}^t A \boldsymbol{\tau}_1}{\boldsymbol{\nu}^t A \boldsymbol{\nu}}, \quad \alpha_{23} = \frac{\boldsymbol{\nu}^t A \boldsymbol{\tau}_2}{\boldsymbol{\nu}^t A \boldsymbol{\nu}}, \quad (\text{D.63})$$

and

$$\begin{aligned} \alpha_{11} &= \boldsymbol{\tau}_1^t A \boldsymbol{\tau}_1 - \frac{(\boldsymbol{\nu}^t A \boldsymbol{\tau}_1)^2}{\boldsymbol{\nu}^t A \boldsymbol{\nu}}, & \alpha_{12} &= \boldsymbol{\tau}_2^t A \boldsymbol{\tau}_1 - \frac{(\boldsymbol{\nu}^t A \boldsymbol{\tau}_1)(\boldsymbol{\nu}^t A \boldsymbol{\tau}_2)}{\boldsymbol{\nu}^t A \boldsymbol{\nu}}, \\ \alpha_{21} &= \boldsymbol{\tau}_1^t A \boldsymbol{\tau}_2 - \frac{(\boldsymbol{\nu}^t A \boldsymbol{\tau}_2)(\boldsymbol{\nu}^t A \boldsymbol{\tau}_1)}{\boldsymbol{\nu}^t A \boldsymbol{\nu}}, & \alpha_{22} &= \boldsymbol{\tau}_2^t A \boldsymbol{\tau}_2 - \frac{(\boldsymbol{\nu}^t A \boldsymbol{\tau}_2)^2}{\boldsymbol{\nu}^t A \boldsymbol{\nu}}. \end{aligned}$$

Hence we conclude that

$$\begin{aligned} \left(\frac{\partial u}{\partial \boldsymbol{\tau}_1} \right)_A &= \alpha_{11} \frac{\partial u}{\partial \boldsymbol{\tau}_1} + \alpha_{12} \frac{\partial u}{\partial \boldsymbol{\tau}_2} + \alpha_{13} \left(\frac{\partial u}{\partial \boldsymbol{\nu}} \right)_A \\ \left(\frac{\partial u}{\partial \boldsymbol{\tau}_2} \right)_A &= \alpha_{21} \frac{\partial u}{\partial \boldsymbol{\tau}_1} + \alpha_{22} \frac{\partial u}{\partial \boldsymbol{\tau}_2} + \alpha_{23} \left(\frac{\partial u}{\partial \boldsymbol{\nu}} \right)_A. \end{aligned} \quad (\text{D.64})$$

Thus

$$\begin{aligned} & 2 \int_{\Gamma_{m,j}^r} \sum_{k=1}^2 \left(\frac{\partial u}{\partial \boldsymbol{\tau}_k} \right)_A \frac{\partial}{\partial s_k} \left(\frac{\partial u}{\partial \boldsymbol{\nu}} \right)_A d\sigma \\ &= 2 \int_{\Gamma_{m,j}^r} \left(\sum_{k,l=1}^2 \alpha_{k,l} \left(\frac{\partial u}{\partial \boldsymbol{\tau}_l} \right) \frac{\partial}{\partial s_k} \left(\frac{\partial u}{\partial \boldsymbol{\nu}} \right)_A \right) d\sigma \\ &+ 2 \int_{\Gamma_{m,j}^r} \left(\alpha_{13} \left(\frac{\partial u}{\partial \boldsymbol{\nu}} \right)_A \frac{\partial}{\partial s_1} \left(\frac{\partial u}{\partial \boldsymbol{\nu}} \right)_A + \alpha_{23} \left(\frac{\partial u}{\partial \boldsymbol{\nu}} \right)_A \frac{\partial}{\partial s_2} \left(\frac{\partial u}{\partial \boldsymbol{\nu}} \right)_A \right) d\sigma. \end{aligned} \quad (\text{D.65})$$

Now

$$\begin{aligned}
& 2 \int_{\Gamma_{m,j}^r} \left(\alpha_{13} \left(\frac{\partial u}{\partial \boldsymbol{\nu}} \right)_A \frac{\partial}{\partial s_1} \left(\frac{\partial u}{\partial \boldsymbol{\nu}} \right)_A + \alpha_{23} \left(\frac{\partial u}{\partial \boldsymbol{\nu}} \right)_A \frac{\partial}{\partial s_2} \left(\frac{\partial u}{\partial \boldsymbol{\nu}} \right)_A \right) d\sigma \\
&= \int_{\Gamma_{m,j}^r} \left(\frac{\partial}{\partial s_1} \left(\alpha_{13} \left(\frac{\partial u}{\partial \boldsymbol{\nu}} \right)_A^2 \right) + \frac{\partial}{\partial s_2} \left(\alpha_{23} \left(\frac{\partial u}{\partial \boldsymbol{\nu}} \right)_A^2 \right) \right) d\sigma \\
&- \int_{\Gamma_{m,j}^r} \left(\frac{\partial}{\partial s_1} (\alpha_{13}) + \frac{\partial}{\partial s_2} (\alpha_{23}) \right) \left(\frac{\partial u}{\partial \boldsymbol{\nu}} \right)_A^2 d\sigma. \tag{D.66}
\end{aligned}$$

Using the divergence theorem we conclude that

$$\begin{aligned}
& 2 \int_{\Gamma_{m,j}^r} \left(\alpha_{13} \left(\frac{\partial u}{\partial \boldsymbol{\nu}} \right)_A \frac{\partial}{\partial s_1} \left(\frac{\partial u}{\partial \boldsymbol{\nu}} \right)_A + \alpha_{23} \left(\frac{\partial u}{\partial \boldsymbol{\nu}} \right)_A \frac{\partial}{\partial s_2} \left(\frac{\partial u}{\partial \boldsymbol{\nu}} \right)_A \right) d\sigma \\
&= \int_{\partial \Gamma_{m,j}^r} \{ (\mathbf{n} \cdot \boldsymbol{\tau}_1) \alpha_{13} + (\mathbf{n} \cdot \boldsymbol{\tau}_2) \alpha_{23} \} \left(\frac{\partial u}{\partial \boldsymbol{\nu}} \right)_A^2 ds \\
&- \int_{\Gamma_{m,j}^r} \left(\frac{\partial}{\partial s_1} (\alpha_{13}) + \frac{\partial}{\partial s_2} (\alpha_{23}) \right) \left(\frac{\partial u}{\partial \boldsymbol{\nu}} \right)_A^2 d\sigma. \tag{D.67}
\end{aligned}$$

Here \mathbf{n} denotes the unit outward normal to $\partial \Gamma_{m,j}^r$.

Now

$$\begin{aligned}
\{ (\mathbf{n} \cdot \boldsymbol{\tau}_1) \alpha_{13} + (\mathbf{n} \cdot \boldsymbol{\tau}_2) \alpha_{23} \} &= \frac{(\mathbf{n} \cdot \boldsymbol{\tau}_1) \boldsymbol{\nu}^t A \boldsymbol{\tau}_1 + (\mathbf{n} \cdot \boldsymbol{\tau}_2) \boldsymbol{\nu}^t A \boldsymbol{\tau}_2}{\boldsymbol{\nu}^t A \boldsymbol{\nu}} \\
&= \frac{\boldsymbol{\nu}^t A \{ (\mathbf{n} \cdot \boldsymbol{\tau}_1) \boldsymbol{\tau}_1 + (\mathbf{n} \cdot \boldsymbol{\tau}_2) \boldsymbol{\tau}_2 \}}{\boldsymbol{\nu}^t A \boldsymbol{\nu}} = \frac{\boldsymbol{\nu}^t A \mathbf{n}}{\boldsymbol{\nu}^t A \boldsymbol{\nu}}.
\end{aligned}$$

Hence

$$\int_{\partial \Gamma_{m,j}^r} \{ (\mathbf{n} \cdot \boldsymbol{\tau}_1) \alpha_{13} + (\mathbf{n} \cdot \boldsymbol{\tau}_2) \alpha_{23} \} \left(\frac{\partial u}{\partial \boldsymbol{\nu}} \right)_A^2 ds = \int_{\partial \Gamma_{m,j}^r} \frac{\boldsymbol{\nu}^t A \mathbf{n}}{\boldsymbol{\nu}^t A \boldsymbol{\nu}} \left(\frac{\partial u}{\partial \boldsymbol{\nu}} \right)_A^2 ds. \tag{D.68}$$

Thus

$$\begin{aligned}
& 2\rho_v^2 \sin^2(\phi_v) \int_{\Gamma_{m,j}^r} \sum_{k=1}^2 \left(\frac{\partial u}{\partial \boldsymbol{\tau}_k} \right)_A \frac{\partial}{\partial s_k} \left(\frac{\partial u}{\partial \boldsymbol{\nu}} \right)_A d\sigma \\
&= \rho_v^2 \sin^2(\phi_v) \left(\int_{\Gamma_{m,j}^r} \left(\sum_{k,l=1}^2 2\alpha_{k,l} \left(\frac{\partial u}{\partial \boldsymbol{\tau}_l} \right)_A \frac{\partial}{\partial s_k} \left(\frac{\partial u}{\partial \boldsymbol{\nu}} \right)_A \right) d\sigma \right. \\
&- \left. \int_{\Gamma_{m,j}^r} \left(\sum_{k=1}^2 \frac{\partial}{\partial s_k} (\alpha_{k3}) \right) \left(\frac{\partial u}{\partial \boldsymbol{\nu}} \right)_A^2 d\sigma + \int_{\partial \Gamma_{m,j}^r} \frac{\boldsymbol{\nu}^t A \mathbf{n}}{\boldsymbol{\nu}^t A \boldsymbol{\nu}} \left(\frac{\partial u}{\partial \boldsymbol{\nu}} \right)_A^2 ds \right). \tag{D.69}
\end{aligned}$$

We now examine the term

$$\rho_v^2 \sin^2(\phi_v) \left(- \oint_{\partial \Gamma_{m,j}^r} \left(\frac{\partial u}{\partial \mathbf{n}} \right)_A \left(\frac{\partial u}{\partial \boldsymbol{\nu}} \right)_A ds \right). \tag{D.70}$$

Now

$$\left(\frac{\partial u}{\partial \mathbf{n}}\right)_A = \gamma_{11} \frac{\partial u}{\partial \boldsymbol{\tau}_1} + \gamma_{12} \frac{\partial u}{\partial \boldsymbol{\tau}_2} + \gamma_{13} \left(\frac{\partial u}{\partial \boldsymbol{\nu}}\right)_A.$$

Here

$$\begin{aligned} \gamma_{13} &= \frac{\boldsymbol{\nu}^t A \mathbf{n}}{\boldsymbol{\nu}^t A \boldsymbol{\nu}}, \\ \gamma_{11} &= \boldsymbol{\tau}_1^t A \mathbf{n} - \frac{(\boldsymbol{\nu}^t A \mathbf{n})(\boldsymbol{\nu}^t A \boldsymbol{\tau}_1)}{\boldsymbol{\nu}^t A \boldsymbol{\nu}}, \\ \gamma_{12} &= \boldsymbol{\tau}_2^t A \mathbf{n} - \frac{(\boldsymbol{\nu}^t A \mathbf{n})(\boldsymbol{\nu}^t A \boldsymbol{\tau}_2)}{\boldsymbol{\nu}^t A \boldsymbol{\nu}}. \end{aligned} \quad (\text{D.71})$$

Hence

$$\begin{aligned} &\rho_v^2 \sin^2(\phi_v) \left(- \oint_{\partial \Gamma_{m,j}^r} \left(\frac{\partial u}{\partial \mathbf{n}}\right)_A \left(\frac{\partial u}{\partial \boldsymbol{\nu}}\right)_A ds \right) \\ &= \rho_v^2 \sin^2(\phi_v) \left(- \oint_{\partial \Gamma_{m,j}^r} \sum_{k=1}^2 \gamma_{1,k} \frac{\partial u}{\partial \boldsymbol{\tau}_k} \left(\frac{\partial u}{\partial \boldsymbol{\nu}}\right)_A ds \right. \\ &\quad \left. - \oint_{\partial \Gamma_{m,j}^r} \left(\frac{\boldsymbol{\nu}^t A \mathbf{n}}{\boldsymbol{\nu}^t A \boldsymbol{\nu}}\right) \left(\frac{\partial u}{\partial \boldsymbol{\nu}}\right)_A^2 ds \right). \end{aligned} \quad (\text{D.72})$$

Combining (D.69) and (D.72) we obtain

$$(BT)_{m,j}^r = \rho_v^2 \sin^2(\phi_v) \left(\int_{\Gamma_{m,j}^r} \left(\sum_{k,l=1}^2 2\alpha_{k,l} \frac{\partial u}{\partial \boldsymbol{\tau}_l} \frac{\partial}{\partial s_k} \left(\frac{\partial u}{\partial \boldsymbol{\nu}}\right)_A \right) d\sigma \right. \quad (\text{D.73})$$

$$\left. - \int_{\Gamma_{m,j}^r} \left(\sum_{k=1}^2 \frac{\partial}{\partial s_k} (\alpha_{k3}) \right) \left(\frac{\partial u}{\partial \boldsymbol{\nu}}\right)_A^2 d\sigma - \oint_{\partial \Gamma_{m,j}^r} \sum_{k=1}^2 \gamma_{1,k} \frac{\partial u}{\partial \boldsymbol{\tau}_k} \left(\frac{\partial u}{\partial \mathbf{n}}\right)_A ds \right). \quad (\text{D.74})$$

Using (D.73) we can show that

$$\begin{aligned} \|(BT)_{m,j}^r\| &\leq C_\epsilon (\ln W)^2 \|u_m^r\|_{3/2, \Gamma_{m,j}^r}^2 + \epsilon/2 \sum_{1 \leq |\alpha| \leq 2} \|D_x^\alpha u_m^r\|_{0, \Omega_m^r}^2 \\ &\quad + K |u_m^r|_{1, \Gamma_{m,j}^r}^2. \end{aligned} \quad (\text{D.74})$$

Now

$$|u_m^r|_{1, \Gamma_{m,j}^r}^2 \leq K_\epsilon |u_m^r|_{1, \Omega_m^r}^2 + \epsilon/2 |u_m^r|_{2, \Omega_m^r}^2. \quad (\text{D.75})$$

Hence

$$\begin{aligned} \|(BT)_{m,j}^r\| &\leq C_\epsilon (\ln W)^2 \|u_m^r\|_{3/2, \Gamma_{m,j}^r}^2 + K_\epsilon \sum_{|\alpha|=1} \|D_x^\alpha u_m^r\|_{0, \Omega_m^r}^2 \\ &\quad + \epsilon \sum_{|\alpha|=2} \|D_x^\alpha u_m^r\|_{0, \Omega_m^r}^2. \end{aligned} \quad (D.76)$$

□

D.6

Proof of Lemma 3.5.2

Lemma 3.5.2. *Let $\Gamma_{m,j}^e$ be part of the boundary of the element Ω_m^e which lies on the $x_2 - x_3$ axis. Define the contributions from $\Gamma_{m,j}^e$ by*

$$\begin{aligned} (BT)_{m,j}^e &= - \oint_{\partial \tilde{\Gamma}_{m,j}^e} \left(\frac{\partial u}{\partial \mathbf{n}^e} \right)_{A^e} \left(\frac{\partial u}{\partial \boldsymbol{\nu}^e} \right)_{A^e} ds^e \\ &\quad - 2 \int_{\tilde{\Gamma}_{m,j}^e} \sum_{l=1}^2 \left(\frac{\partial u}{\partial \boldsymbol{\tau}_l^e} \right)_{A^e} \frac{\partial}{\partial s_l^e} \left(\left(\frac{\partial u}{\partial \boldsymbol{\nu}^e} \right)_{A^e} \right) d\sigma^e. \end{aligned} \quad (D.77)$$

If Dirichlet boundary conditions are imposed on $\Gamma_{m,j}^e$ and $\mu(\tilde{\Gamma}_{m,j}^e) < \infty$ then for any $\epsilon > 0$ there exists constants C_ϵ, K_ϵ such that for W large enough

$$\begin{aligned} |(BT)_{m,j}^e| &\leq C_\epsilon (\ln W)^2 \left(\|u_m^e\|_{0, \tilde{\Gamma}_{m,j}^e}^2 + \left\| \left(\frac{\partial u_m^e}{\partial x_1^e} \right) \right\|_{\tilde{\Gamma}_{m,j}^e}^2 + \left\| G_{m,j}^e \left(\frac{\partial u_m^e}{\partial x_3^e} \right) \right\|_{\tilde{\Gamma}_{m,j}^e}^2 \right) \\ &\quad + K_\epsilon \int_{\tilde{\Omega}_m^e} \left(\sum_{i=1}^2 \left(\frac{\partial u_m^e}{\partial x_i^e} \right)^2 + e^{2\tau} \left(\frac{\partial u_m^e}{\partial x_3^e} \right)^2 \right) dx^e + \epsilon \int_{\tilde{\Omega}_m^e} \left(\sum_{i,j=1,2} \left(\frac{\partial^2 u_m^e}{\partial x_i^e \partial x_j^e} \right)^2 \right. \\ &\quad \left. + e^{2\tau} \sum_{i=1}^2 \left(\frac{\partial^2 u_m^e}{\partial x_i^e \partial x_3^e} \right)^2 + e^{4\tau} \left(\frac{\partial^2 u_m^e}{(\partial x_3^e)^2} \right)^2 \right) dx^e. \end{aligned} \quad (D.78)$$

If Neumann boundary conditions are imposed on $\Gamma_{m,j}^e$ and $\mu(\tilde{\Gamma}_{m,j}^e) < \infty$ then for any $\epsilon > 0$ there exists a constant C_ϵ such that

$$\begin{aligned} |(BT)_{m,j}^e| &\leq C_\epsilon (\ln W)^2 \left\| \left(\frac{\partial u}{\partial \boldsymbol{\nu}^e} \right)_{A^e} \right\|_{\tilde{\Gamma}_{m,j}^e}^2 + \epsilon \left(\int_{\tilde{\Omega}_m^e} \left(\sum_{i,j=1}^2 \left(\frac{\partial^2 u_m^e}{\partial x_i^e \partial x_j^e} \right)^2 \right. \right. \\ &\quad \left. \left. + e^{2\tau} \sum_{i=1}^2 \left(\frac{\partial^2 u_m^e}{\partial x_i^e \partial x_3^e} \right)^2 + e^{4\tau} \left(\frac{\partial^2 u_m^e}{(\partial x_3^e)^2} \right)^2 + \sum_{i=1}^2 \left(\frac{\partial u_m^e}{\partial x_i^e} \right)^2 \right. \right. \\ &\quad \left. \left. + e^{2\tau} \left(\frac{\partial u_m^e}{\partial x_3^e} \right)^2 \right) dx^e \right). \end{aligned} \quad (D.79)$$

If $\mu(\tilde{\Gamma}_{m,j}^e) = \infty$ then for any $\epsilon > 0$ for N, W large enough

$$|(BT)_{m,j}^e| \leq \epsilon \int_{\tilde{\Omega}_m^e} (u_m^e)^2 w^e(x_1^e) dx^e$$

provided $W = O(e^{N^\alpha})$ for $\alpha < 1/2$.

Proof. In the edge neighbourhood the coordinates used are

$$\begin{aligned} x_1^e &= \tau \\ x_2^e &= \theta \\ x_3^e &= x_3. \end{aligned} \tag{D.80}$$

We introduce the variables as in (D.45)

$$\begin{aligned} z_1 &= x_1^e \\ z_2 &= x_2^e \\ z_3 &= \frac{x_3^e}{G_{m,i}^e}. \end{aligned} \tag{D.81}$$

Let us examine the term

$$\begin{aligned} (BT)_{m,j}^e &= -2 \int_{\tilde{\Gamma}_{m,j}^e} \sum_{l=1}^2 \left(\frac{\partial u}{\partial \tau_l^e} \right)_{A^e} \frac{\partial}{\partial s_l^e} \left(\frac{\partial u}{\partial \nu^e} \right)_{A^e} d\sigma^e \\ &\quad + \oint_{\partial \tilde{\Gamma}_{m,j}^e} \left(\frac{\partial u}{\partial \mathbf{n}^e} \right)_{A^e} \left(\frac{\partial u}{\partial \nu^e} \right)_{A^e} ds^e. \end{aligned} \tag{D.82}$$

If the boundary conditions are Neumann we can prove as in Lemma 3.4.4 that

$$\begin{aligned} |(BT)_{m,j}^e| &\leq C_\epsilon (\ln W)^2 \left\| \left(\frac{\partial u_m^e}{\partial \nu^e} \right)_{\tilde{A}^e} \right\|_{\tilde{\Gamma}_{m,j}^e}^2 \\ &\quad + \epsilon \left(\int_{\tilde{\Omega}_m^e} \sum_{i,j=1,2} \left(\frac{\partial^2 u_m^e}{\partial x_i^e \partial x_j^e} \right)^2 + e^{2\tau} \sum_{i=1}^2 \left(\frac{\partial^2 u_m^e}{\partial x_i^e \partial x_3^e} \right)^2 + e^{4\tau} \left(\frac{\partial^2 u_m^e}{(\partial x_3^e)^2} \right)^2 \right. \\ &\quad \left. + \sum_{i=1}^2 \left(\frac{\partial u_m^e}{\partial x_i^e} \right)^2 + e^{2\tau} \left(\frac{\partial u_m^e}{\partial x_3^e} \right)^2 \right) w^e(x_1^e) dx^e. \end{aligned} \tag{D.83}$$

Let us now examine the case when the boundary conditions are Dirichlet.

Now choose

$$\begin{aligned} \tau_1^e &= (1, 0, 0) \\ \tau_2^e &= (0, 0, 1) \\ \nu^e &= (0, -1, 0). \end{aligned} \tag{D.84}$$

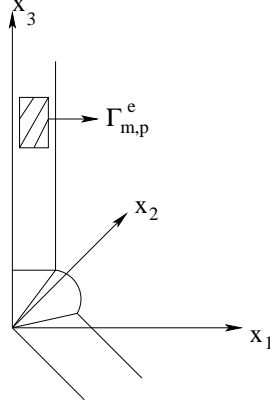


Figure D.7: The face $\Gamma_{m,p}^e$ of the boundary element Ω_m^e .

Moreover

$$\begin{aligned} A^e \boldsymbol{\tau}_1^e &= \alpha_{11}^e \boldsymbol{\tau}_1^e + \alpha_{12}^e \boldsymbol{\tau}_2^e + \alpha_{13}^e A^e \boldsymbol{\nu}^e, \\ A^e \boldsymbol{\tau}_2^e &= \alpha_{21}^e \boldsymbol{\tau}_1^e + \alpha_{22}^e \boldsymbol{\tau}_2^e + \alpha_{23}^e A^e \boldsymbol{\nu}^e. \end{aligned} \quad (\text{D.85a})$$

Here

$$\begin{aligned} \alpha_{13}^e &= \frac{(\boldsymbol{\nu}^e)^t A^e \boldsymbol{\tau}_1^e}{(\boldsymbol{\nu}^e)^t A^e \boldsymbol{\nu}^e}, \quad \alpha_{23}^e = \frac{(\boldsymbol{\nu}^e)^t A^e \boldsymbol{\tau}_2^e}{(\boldsymbol{\nu}^e)^t A^e \boldsymbol{\nu}^e}, \\ \alpha_{11}^e &= (\boldsymbol{\tau}_1^e)^t A^e \boldsymbol{\tau}_1^e - \frac{((\boldsymbol{\nu}^e)^t A^e \boldsymbol{\tau}_1^e)^2}{(\boldsymbol{\nu}^e)^t A^e \boldsymbol{\nu}^e}, \\ \alpha_{12}^e &= (\boldsymbol{\tau}_2^e)^t A^e \boldsymbol{\tau}_1^e - \frac{((\boldsymbol{\nu}^e)^t A^e \boldsymbol{\tau}_1^e)((\boldsymbol{\nu}^e)^t A^e \boldsymbol{\tau}_2^e)}{(\boldsymbol{\nu}^e)^t A^e \boldsymbol{\nu}^e}, \\ \alpha_{21}^e &= (\boldsymbol{\tau}_1^e)^t A^e \boldsymbol{\tau}_2^e - \frac{((\boldsymbol{\nu}^e)^t A^e \boldsymbol{\tau}_2^e)((\boldsymbol{\nu}^e)^t A^e \boldsymbol{\tau}_1^e)}{(\boldsymbol{\nu}^e)^t A^e \boldsymbol{\nu}^e}, \\ \alpha_{22}^e &= (\boldsymbol{\tau}_2^e)^t A^e \boldsymbol{\tau}_2^e - \frac{((\boldsymbol{\nu}^e)^t A^e \boldsymbol{\tau}_2^e)^2}{(\boldsymbol{\nu}^e)^t A^e \boldsymbol{\nu}^e}. \end{aligned} \quad (\text{D.85b})$$

Now

$$\left(\frac{\partial u}{\partial \mathbf{n}^e} \right)_{A^e} = \gamma_{11}^e \left(\frac{\partial u}{\partial \boldsymbol{\tau}_1^e} \right) + \gamma_{12}^e \left(\frac{\partial u}{\partial \boldsymbol{\tau}_2^e} \right) + \gamma_{13}^e \left(\frac{\partial u}{\partial \boldsymbol{\nu}^e} \right)_{A^e}. \quad (\text{D.86a})$$

Here

$$\begin{aligned} \gamma_{13}^e &= \frac{(\boldsymbol{\nu}^e)^t A^e \mathbf{n}^e}{(\boldsymbol{\nu}^e)^t A^e \boldsymbol{\nu}^e}, \\ \gamma_{11}^e &= (\boldsymbol{\tau}_1^e)^t A^e \mathbf{n}^e - \frac{((\boldsymbol{\nu}^e)^t A^e \mathbf{n}^e)((\boldsymbol{\nu}^e)^t A^e \boldsymbol{\tau}_1^e)}{(\boldsymbol{\nu}^e)^t A^e \boldsymbol{\nu}^e}, \\ \gamma_{12}^e &= (\boldsymbol{\tau}_2^e)^t A^e \mathbf{n}^e - \frac{((\boldsymbol{\nu}^e)^t A^e \mathbf{n}^e)((\boldsymbol{\nu}^e)^t A^e \boldsymbol{\tau}_2^e)}{(\boldsymbol{\nu}^e)^t A^e \boldsymbol{\nu}^e}. \end{aligned} \quad (\text{D.86b})$$

Then it can be shown that

$$\begin{aligned}
 (BT)^e_{m,j} = & \left(\int_{\tilde{\Gamma}_{m,j}^e} \left(\sum_{k,l=1}^2 2\alpha_{k,l}^e \frac{\partial u}{\partial \tau_l^e} \frac{\partial}{\partial s_k^e} \left(\frac{\partial u}{\partial \nu^e} \right)_{A^e} \right) d\sigma^e \right. \\
 & - \int_{\tilde{\Gamma}_{m,j}^e} \left(\sum_{k=1}^2 \frac{\partial}{\partial s_k^e} (\alpha_{k3}^e) \right) \left(\frac{\partial u}{\partial \nu^e} \right)_{A^e}^2 d\sigma^e \\
 & \left. - \oint_{\partial \tilde{\Gamma}_{m,j}^e} \sum_{k=1}^2 \gamma_{1,k}^e \frac{\partial u}{\partial \tau_k^e} \left(\frac{\partial u}{\partial \mathbf{n}^e} \right)_{A^e} ds^e \right). \quad (D.87)
 \end{aligned}$$

Now

$$\begin{aligned}
 \alpha_{13}^e &= \frac{(\nu^e)^t A^e \tau_1^e}{(\nu^e)^t A^e \nu^e}, \quad \alpha_{23}^e = \frac{(\nu^e)^t A^e \tau_2^e}{(\nu^e)^t A^e \nu^e}, \\
 \alpha_{11}^e &= (\tau_1^e)^t A^e \tau_1^e - \frac{((\nu^e)^t A^e \tau_1^e)^2}{(\nu^e)^t A^e \nu^e}, \\
 \alpha_{12}^e &= (\tau_2^e)^t A^e \tau_1^e - \frac{((\nu^e)^t A^e \tau_1^e)((\nu^e)^t A^e \tau_2^e)}{(\nu^e)^t A^e \nu^e}, \\
 \alpha_{21}^e &= \alpha_{12}^e, \quad \alpha_{22}^e = (\tau_2^e)^t A^e \tau_2^e - \frac{((\nu^e)^t A^e \tau_2^e)^2}{(\nu^e)^t A^e \nu^e}. \quad (D.88)
 \end{aligned}$$

Hence

$$\begin{aligned}
 (\text{I}) &= \int_{\tilde{\Gamma}_{m,j}^e} \left(\sum_{k,l=1}^2 2\alpha_{k,l}^e \frac{\partial u}{\partial \tau_l^e} \frac{\partial}{\partial s_k^e} \left(\left(\frac{\partial u}{\partial \nu^e} \right)_{A^e} \right) \right) d\sigma^e \\
 &= - \int_{\tilde{\Gamma}_{m,j}^e} 2 \left(\alpha_{1,1}^e \frac{\partial u}{\partial x_1^e} \frac{\partial}{\partial x_1^e} \left(\left(\frac{\partial u}{\partial x_2^e} \right)_{A^e} \right) + \alpha_{1,2}^e \frac{\partial u}{\partial x_3^e} \frac{\partial}{\partial x_1^e} \left(\left(\frac{\partial u}{\partial x_2^e} \right)_{A^e} \right) \right. \\
 &\quad \left. + \alpha_{2,1}^e \frac{\partial u}{\partial x_1^e} \frac{\partial}{\partial x_3^e} \left(\left(\frac{\partial u}{\partial x_2^e} \right)_{A^e} \right) + \alpha_{2,2}^e \frac{\partial u}{\partial x_3^e} \frac{\partial}{\partial x_3^e} \left(\left(\frac{\partial u}{\partial x_2^e} \right)_{A^e} \right) \right) dx_1^e dx_3^e \\
 &= -2G_{m,j}^e \int_{\hat{\Gamma}_{m,j}^e} \left(\alpha_{1,1}^e \frac{\partial u}{\partial z_1} \frac{\partial}{\partial z_1} \left(\left(\frac{\partial u}{\partial z_2} \right)_{\hat{A}^e} \right) + \frac{\alpha_{1,2}^e}{G_{m,j}^e} \frac{\partial u}{\partial z_3} \frac{\partial}{\partial z_1} \left(\left(\frac{\partial u}{\partial z_2} \right)_{\hat{A}^e} \right) \right. \\
 &\quad \left. + \frac{\alpha_{2,1}^e}{G_{m,j}^e} \frac{\partial u}{\partial z_1} \frac{\partial}{\partial z_3} \left(\left(\frac{\partial u}{\partial z_2} \right)_{\hat{A}^e} \right) + \frac{\alpha_{2,2}^e}{(G_{m,j}^e)^2} \frac{\partial u}{\partial z_3} \frac{\partial}{\partial z_3} \left(\left(\frac{\partial u}{\partial z_2} \right)_{\hat{A}^e} \right) \right) dz_1 dz_3. \quad (D.89)
 \end{aligned}$$

Here $\hat{\Gamma}_{m,j}^e$ denotes the image of $\Gamma_{m,j}^e$ in z coordinates.

Now from (3.79), (3.80) and (D.88) $\alpha_{1,1}^e$, $\frac{\alpha_{1,2}^e}{G_{m,j}^e}$, $\frac{\alpha_{2,1}^e}{G_{m,j}^e}$ and $\frac{\alpha_{2,2}^e}{(G_{m,j}^e)^2}$ are bounded and have bounded derivatives in z coordinates.

Therefore

$$\begin{aligned} |(\text{I})| &\leq \left(C_\epsilon (\ln W)^2 \left(\left\| \frac{\partial u_m^e}{\partial z_1} \right\|_{1/2, \hat{\Gamma}_{m,j}^e}^2 + \left\| \frac{\partial u_m^e}{\partial z_3} \right\|_{1/2, \hat{\Gamma}_{m,j}^e}^2 \right) \right. \\ &\quad \left. + \epsilon \left(\sum_{1 \leq |\alpha| \leq 2} \|D_z^\alpha u_m^e\|_{0, \hat{\Omega}_m^e}^2 \right) \right) G_{m,j}^e. \end{aligned} \quad (\text{D.90})$$

Next, we examine

$$\begin{aligned} (\text{II}) &= - \int_{\hat{\Gamma}_{m,j}^e} \left(\sum_{k=1}^2 \frac{\partial}{\partial s_k^e} (\alpha_{k3}^e) \right) \left(\frac{\partial u}{\partial \boldsymbol{\nu}^e} \right)_{A^e}^2 d\sigma^e \\ &= -G_{m,j}^e \int_{\hat{\Gamma}_{m,j}^e} \left(\left(\frac{\partial}{\partial z_1} \alpha_{1,3}^e \right) \left(\frac{\partial u}{\partial z_2} \right)_{\hat{A}^e}^2 \right. \\ &\quad \left. + \frac{1}{G_{m,j}^e} \left(\frac{\partial}{\partial z_3} \alpha_{2,3}^e \right) \left(\frac{\partial u}{\partial z_2} \right)_{\hat{A}^e}^2 \right) dz_1 dz_3. \end{aligned} \quad (\text{D.91})$$

Now $\alpha_{1,3}^e$ and $\frac{\alpha_{2,3}^e}{G_{m,j}^e}$ are bounded and have uniformly bounded derivatives in z coordinates.

Hence

$$|(\text{II})| \leq K G_{m,j}^e |u_m^e|_{1, \hat{\Gamma}_m^e}^2 \leq G_{m,j}^e \left(K_\epsilon |u_m^e|_{1, \hat{\Omega}_m^e}^2 + \epsilon |u_m^e|_{2, \hat{\Omega}_m^e}^2 \right). \quad (\text{D.92})$$

Finally, we examine

$$(\text{III}) = \oint_{\partial \hat{\Gamma}_{m,j}^e} \sum_{k=1}^2 \gamma_{1,k}^e \frac{\partial u}{\partial \boldsymbol{\tau}_k^e} \left(\frac{\partial u}{\partial \boldsymbol{n}^e} \right)_{A^e} ds^e. \quad (\text{D.93})$$

Consider

$$(\text{IIIa}) = \int_{\tilde{\gamma}} \sum_{k=1}^2 \gamma_{1,k}^e \frac{\partial u}{\partial \boldsymbol{\tau}_k^e} \left(\frac{\partial u}{\partial \boldsymbol{n}^e} \right)_{A^e} ds^e.$$

Now $\boldsymbol{n}^e = \boldsymbol{\tau}_2^e$ and so from (D.86b)

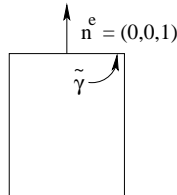


Figure D.8: The edge $\tilde{\gamma}$.

$$\begin{aligned}\gamma_{11}^e &= \left((\boldsymbol{\tau}_1^e)^t A^e \boldsymbol{\tau}_2^e - \frac{((\boldsymbol{\nu}^e)^t A^e \boldsymbol{\tau}_2^e)((\boldsymbol{\nu}^e)^t A^e \boldsymbol{\tau}_1^e)}{(\boldsymbol{\nu}^e)^t A^e \boldsymbol{\nu}^e} \right), \\ \gamma_{12}^e &= \left((\boldsymbol{\tau}_2^e)^t A^e \boldsymbol{\tau}_2^e - \frac{((\boldsymbol{\nu}^e)^t A^e \boldsymbol{\tau}_2^e)((\boldsymbol{\nu}^e)^t A^e \boldsymbol{\tau}_2^e)}{(\boldsymbol{\nu}^e)^t A^e \boldsymbol{\nu}^e} \right).\end{aligned}\quad (\text{D.94})$$

Hence

$$\begin{aligned}(\text{IIIa}) &= \int_{\hat{\gamma}} \left(\gamma_{11}^e \left(\frac{\partial u}{\partial z_1} \right) \left(\frac{\partial u}{\partial z_2} \right)_{\hat{A}^e} + \frac{\gamma_{12}^e}{G_{m,j}^e} \left(\frac{\partial u}{\partial z_3} \right) \left(\frac{\partial u}{\partial z_2} \right)_{\hat{A}^e} \right) dz_1 \\ &= G_{m,j}^e \int_{\hat{\gamma}} \left(\frac{\gamma_{11}^e}{G_{m,j}^e} \left(\frac{\partial u}{\partial z_1} \right) \left(\frac{\partial u}{\partial z_2} \right)_{\hat{A}^e} + \frac{\gamma_{12}^e}{(G_{m,j}^e)^2} \left(\frac{\partial u}{\partial z_3} \right) \left(\frac{\partial u}{\partial z_2} \right)_{\hat{A}^e} \right) dz_1.\end{aligned}$$

Now from (3.79), (3.80) and (D.94), $\frac{\gamma_{11}^e}{G_{m,j}^e}$ and $\frac{\gamma_{12}^e}{(G_{m,j}^e)^2}$ are bounded and have uniformly bounded derivatives in z coordinates.

And so we can show that

$$\begin{aligned}|(\text{IIIa})| &\leq G_{m,j}^e \left(C_\epsilon (\ln W)^2 \left(\left\| \frac{\partial u_m^e}{\partial z_1} \right\|_{1/2, \hat{\Gamma}_{m,j}^e}^2 + \left\| \frac{\partial u_m^e}{\partial z_3} \right\|_{1/2, \hat{\Gamma}_{m,j}^e}^2 \right) \right. \\ &\quad \left. + \epsilon \sum_{1 \leq |\alpha| \leq 2} \|D_z^\alpha u_m^e\|_{0, \hat{\Omega}_m^e}^2 \right).\end{aligned}\quad (\text{D.95})$$

Next, consider

$$(\text{IIIb}) = \int_{\hat{\gamma}} \sum_{k=1}^2 \gamma_{1,k}^e \frac{\partial u}{\partial \boldsymbol{\tau}_k^e} \left(\frac{\partial u}{\partial \boldsymbol{n}^e} \right)_{A^e} ds^e.$$

Now $\boldsymbol{n}^e = \boldsymbol{\tau}_1^e$ and so from (D.86b)

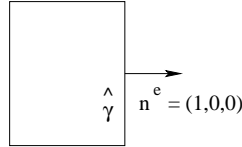


Figure D.9: The edge $\hat{\gamma}$.

$$\begin{aligned}\gamma_{11}^e &= \left((\boldsymbol{\tau}_1^e)^t A^e \boldsymbol{\tau}_1^e - \frac{((\boldsymbol{\nu}^e)^t A^e \boldsymbol{\tau}_1^e)((\boldsymbol{\nu}^e)^t A^e \boldsymbol{\tau}_1^e)}{(\boldsymbol{\nu}^e)^t A^e \boldsymbol{\nu}^e} \right), \\ \gamma_{12}^e &= \left((\boldsymbol{\tau}_2^e)^t A^e \boldsymbol{\tau}_1^e - \frac{((\boldsymbol{\nu}^e)^t A^e \boldsymbol{\tau}_1^e)((\boldsymbol{\nu}^e)^t A^e \boldsymbol{\tau}_2^e)}{(\boldsymbol{\nu}^e)^t A^e \boldsymbol{\nu}^e} \right).\end{aligned}\quad (\text{D.96})$$

Hence

$$(\text{IIIb}) = G_{m,j}^e \int_{\hat{\gamma}} \left(\gamma_{11}^e \left(\frac{\partial u}{\partial z_1} \right) \left(\frac{\partial u}{\partial z_1} \right)_{\hat{A}^e} + \frac{\gamma_{12}^e}{G_{m,j}^e} \left(\frac{\partial u}{\partial z_3} \right) \left(\frac{\partial u}{\partial z_1} \right)_{\hat{A}^e} \right) dz_3.$$

Now from (3.79), (3.80) and (D.96), γ_{11}^e and $\frac{\gamma_{12}^e}{G_{m,j}^e}$ are bounded and have uniformly bounded derivatives in z coordinates.

So we can show that

$$\begin{aligned} |(\text{IIIb})| &\leq G_{m,j}^e \left(C_\epsilon (\ln W)^2 \left(\left\| \frac{\partial u_m^e}{\partial z_1} \right\|_{1/2, \hat{\Gamma}_{m,j}^e}^2 + \left\| \frac{\partial u_m^e}{\partial z_3} \right\|_{1/2, \hat{\Gamma}_{m,j}^e}^2 \right) \right. \\ &\quad \left. + \epsilon \sum_{1 \leq |\alpha| \leq 2} \|D_z^\alpha u_m^e\|_{0, \hat{\Omega}_m^e}^2 \right). \end{aligned} \quad (\text{D.97})$$

Combining (D.90), (D.92), (D.95) and (D.97), we obtain

$$\begin{aligned} |(BT)_{m,j}^e| &\leq G_{m,j}^e \left(C_\epsilon (\ln W)^2 \left(\left\| \frac{\partial u_m^e}{\partial z_1} \right\|_{1/2, \hat{\Gamma}_{m,j}^e}^2 + \left\| \frac{\partial u_m^e}{\partial z_3} \right\|_{1/2, \hat{\Gamma}_{m,j}^e}^2 \right) \right. \\ &\quad \left. + K_\epsilon \sum_{|\alpha|=1} \|D_z^\alpha u_m^e\|_{0, \hat{\Omega}_m^e}^2 + \epsilon \sum_{|\alpha|=2} \|D_z^\alpha u_m^e\|_{0, \hat{\Omega}_m^e}^2 \right). \end{aligned} \quad (\text{D.98})$$

From this the result follows. \square

Bibliography

- [1] R.A. Adams (1975): *Sobolev Spaces*, Academic Press, New York.
- [2] G. Anagnostou (1991): *Non-conforming sliding spectral element method for the unsteady incompressible Navier-Stokes equations*, Ph.D. thesis, Massachusetts Institute of Technology.
- [3] B. Andersson, U. Falk, I. Babuška and T. Von-Petersdorff (1995): Reliable stress and fracture mechanics analysis of complex components using a $h - p$ version of FEM, *Int. J. Numer. Meth. Eng.*, 38, 2135.
- [4] D.N. Arnold, F. Brezzi, B. Cockburn and D. Marini (2000): The development of discontinuous Galerkin methods. In *Discontinuous Galerkin methods: Theory, computation and applications* (ed. B. Cockburn, G.E. Karniadakis and C.W. Shu), p. 89. Springer, Germany.
- [5] D.N. Arnold, F. Brezzi, B. Cockburn and D. Marini (2002): Unified analysis of discontinuous Galerkin methods for elliptic problems, *SIAM J. Numer. Anal.*, 39, 1794.
- [6] A.K. Aziz and I. Babuška (1972): *The Mathematical Foundations of the Finite Element Method with Applications to Partial Differential Equations*, Academic Press, New York.
- [7] I. Babuška (1994): On the h, p and $h - p$ version of the finite element method, *Tatra Mountains Math. Publ.*, 4, 5-18.

-
- [8] I. Babuška and B. Guo (1986): The $h - p$ Version of the finite element method, Part I: The basic approximation results, *Comp. Mech.*, 1, 21-41.
 - [9] I. Babuška and B. Guo (1986): The $h - p$ Version of the finite element method, Part II: General results and Applications, *Comp. Mech.*, 1, 203-220.
 - [10] I. Babuška and B. Guo (1988): Regularity of the solutions of elliptic problems with piecewise analytic data, Part I: Boundary value problems for linear elliptic equation of second order, *SIAM J. Math. Anal.* Vol. 19, No. 1, 172.
 - [11] I. Babuška and B. Guo (1988): The $h - p$ version of the finite element method on domains with curved boundaries, *SIAM J. Num. Anal.*, Vol 25, 837.
 - [12] I. Babuška and B. Guo (1995): The $h - p$ version of the finite element method in R^3 .
 - [13] I. Babuška and B. Guo (1996): Approximation properties of the $h - p$ version of the finite element method, *Comp. Methods Appl. Mech. Engrg*, 133, 319-346.
 - [14] I. Babuška and B. Guo (1997): Regularity of the solutions for elliptic problems on non-smooth domains in R^3 , Part I: Countably Normed spaces on polyhedral domains; *Proc. of the Royal Society of Edinburgh*, 127A, 77-126.
 - [15] I. Babuška and B. Guo (1997): Regularity of the solutions for elliptic problems on non-smooth domains in R^3 , Part II: Regularity in neighbourhoods of edges; *Tech. Note BN-1182, IPST, University of Maryland, College Park, Proc. of the Royal Society of Edinburgh*, 127A, 517-545.
 - [16] I. Babuška and B. Guo: Regularity of the solutions for elliptic problems on non-smooth domains in R^3 , Part III: Regularity in neighbourhoods of vertices. To appear in *Proc. of the Royal Society of Edinburgh*.
 - [17] I. Babuška and S.H. Oh (1990): The p -version of the Finite Element Method for Domains with Corners and for Infinite Domains, *Numer. Meth. PDEs.*, Vol. 6, pp 371-392.

-
- [18] I. Babuška, B. Guo, B. Andersson, H.S. Oh and J.M. Melenk (1996): Finite element methods for solving problems with singular solutions, *J. Comp. Appl. Math.*, Vol. 74, 51-70.
 - [19] I. Babuška and M. Suri (1994): The p and $h-p$ version of the finite element method, basic principles and properties, *SIAM review*, Vol. 36, No. 4, 578-632.
 - [20] I. Babuška, T. Von-Petersdorff and B. Andersson (1994): Numerical treatment of vertex singularities and intensity factors for mixed boundary value problems for the Laplace equation in \mathbb{R}^3 , *SIAM J. Numer. Anal.*, 31, 1265.
 - [21] A.E. Beagles and J.R. Whiteman (1985): Treatment of a reentrant vertex in three dimensional Poisson problem, *Singularities and constructive methods for their treatment*, edited by Grisvard et al, Lecture Note No. 1121, Springer-Verlag.
 - [22] C. Bernardi, Y. Maday, C. Mavriplis and A.T. Patera (1989): The mortar element method applied to spectral discretizations, In *Finite element analysis in fluids, seventh international conference on finite element methods in flow problems* (ed. T. J. Chung and G. R. Karr). UAH Press, Huntsville, TX.
 - [23] C. Bernardi and Y. Maday (1999): Spectral methods. In *Handbook of Numerical Analysis V*, ed. P.G. Ciarlet and J.L. Lions. Amsterdam: Elsevier Sciences.
 - [24] J.P. Boyd (2001): *Chebyshev and Fourier Spectral Methods*, 2nd edn. (Dover, New York).
 - [25] E.N. Blinova (1944): Hydrodynamic theory of pressure and temperature waves and center of action of the atmosphere, Trans. No. 113 (Regional Control Office, Second Weather Region, Patterson Field, OH).
 - [26] P.B. Bochev, M.D. Gunzburger (2009): *Least-Squares Finite Element Methods*, Springer.
 - [27] C. Canuto, M.Y. Hussaini, A. Quarteroni, T.A. Zang (1987): *Spectral methods in fluid dynamics*, Springer, New York.

-
- [28] C. Canuto, M.Y. Hussaini, A. Quarteroni, T.A. Zang (2006): Spectral methods, Fundamentals in single domains; Scientific computaion, Springer.
- [29] C. Canuto, M.Y. Hussaini, A. Quarteroni, T.A. Zang (2007): Spectral methods, Evolution to Complex geometries and applications to fluid dynamics, Scientific computaion, Springer.
- [30] R.W. Clough (1960): The Finite Element Method in Plane Stress Analysis, Proceedings of 2nd ASCE Conference on Electronic Computation, Pittsburgh, PA, September 89.
- [31] B. Cockburn, G.E. Karniadakis and C.W. Shu (2000): The development of discontinuous Galerkin methods, In *Discontinuous Galerkin methods: theory, computation and applications* (ed. B. Cockburn, G.E. Karniadakis and C.W. Shu), p. 3, Springer, Germany.
- [32] M. Costabel and M. Dauge (1993): General asymptotics of solutions of second-order elliptic boundary value problems I and II, *Proc. R. Soc. Edin.*, 123A, 109.
- [33] M. Dauge (1988): Elliptic boundary value problems in corner domains-Smoothness and asymptotics of solutions, Lecture Notes in Mathematics 1341. Springer-Verlag, Heidelberg.
- [34] L. Demkowicz, J.T. Oden, W. Rachowicz and O. Hardy (1989): Toward a universal $h - p$ adaptive finite element strategy, Part I: Constrained approximations and data structure, *Comp. Meth. Appl. Mech. Eng.*, 77, 79.
- [35] P. Dutt and S. Bedekar (2001): Spectral Methods for Hyperbolic Initial Boundary Value Problems on Parallel Computers, *Jour. Comp. Appl. Math.*, 134, pp 165-190.
- [36] P. Dutt, P. Biswas and G. N. Raju (2008): Preconditioners for spectral element methods for elliptic and parabolic problems, *Journal of Computational and Applied Mathematics*, Vol. 215, Issue 1, 152-166.

-
- [37] P. Dutt, S. Tomar and B.V.R. Kumar (2002): Stability estimates for $h - p$ spectral element methods for elliptic problems, Proc. Indian Acad. Sci. (Math Sci.) Vol. 112, No. 4, 601-639.
- [38] P. Dutt and S. Tomar (2003): Stability estimates for $h - p$ spectral element methods for general elliptic problems on curvilinear domains, Proc. Indian Acad. Sci. (Math. Sci.) Vol.113, No.4, 395-429.
- [39] P.K. Dutt, N. Kishore Kumar and C.S. Upadhyay (2007): Non-conforming $h - p$ spectral element methods for elliptic problems, Proc. Indian Acad. Sci. (Math. Sci.) Vol. 117, No. 1, 109-145.
- [40] E. Eliassen, B. Machenhauer and E. Rasmussen (1970): 'On a Numerical Method for Integration of the Hydrodynamical Equations with a Spectral Representation of the Horizontal Fields', Rep. No. 2 (Institut for Teoretisk Meteorologi, Univ. Copenhagen).
- [41] B.A. Finlayson and L.E. Scriven (1966): The Method of Weighted Residuals: A Review, Appl. Mech. Rev., 19, pp 735-748.
- [42] R.A. Frazer, W.P. Jones and S.W. Skan (1937): *Approximation to Functions and to the Solution of Differential Equations*, Rep. and Mem. 1799 (Aeronautical Research Council, London).
- [43] B. Galerkin (1915): Rods and plates: Series occurring in various questions concerning the elastic equilibrium of rods and plates, Vestn. Inzhen., 19, pp 897-908.
- [44] D. Gottlieb and S.A. Orszag (1986): Numerical analysis of spectral methods, Theory and applications, SIAM.
- [45] P. Grisvard : Singularities des problèmes aux limites dans polyèdres, Exposé no. VIII, Ecole Polytechnique Centre de Mathematique, France.
- [46] P. Grisvard (1985): Elliptic problems in nonsmooth domains, Monographs and Studies in Mathematics 24, Pitman Advanced Publishing Program, Boston, MA.

-
- [47] P. Grisvard (1976): Behavior of the solutions of an elliptic boundary value problem in a polyhedral domain, Numerical solution of PDEs, edited by B. Hubbard, pp 207-274.
- [48] W. Gui and I. Babuska (1986): The h, p and $h - p$ versions of the finite element method for one dimensional problem, Part I: The error analysis of the p version, Part II: The error analysis of the h and $h - p$ versions, Part III: The adaptive $h - p$ version; Numer. Math., 49, 577-683.
- [49] B. Guo (1994): The $h - p$ Version of the finite element method for solving boundary value problems in polyhedral domains, In *Boundary value problems and integral equations in non smooth domains*, volume 167 of *Lecture Notes in Pure and Appl. Math.*, pages 101-120. eds. M. Costabel, M. Dauge, C. Nicaise and Marcel Dekker Inc.
- [50] B. Guo (1995): Optimal finite element approaches for elasticity problems on non-smooth domains in R^3 , Computational Mechanics's 95, Vol. 1, 427-432, eds. S.N. Atluri, G. Yawaga and T.A. Cruse, Springer.
- [51] B. Guo (1996): $h - p$ version of the finite element method in R^3 : Theory and algorithm, In *ICOSAHOM 95: Proceedings of the third international conference on spectral and higher order methods* (ed. A.V. Ilin and L.R. Scott), Houston, TX, June 5, 1995, p. 487-500, Houston Journal of Mathematics, 1996.
- [52] B. Guo and S.H. Oh (1995): The method of auxiliary mapping for the finite element solutions of elliptic partial differential equations on non-smooth domains in R^3 . Available at <http://home.cc.umanitoba.ca/~guo/publication.htm>.
- [53] Bo-nan Jiang (1998): *Least-Squares Finite Element Method: Theory and Applications in Computational Fluid Dynamics and Electromagnetics*, Springer-Verlag, New York.
- [54] L.V. Kantorovic (1934): On a new method of approximate solution of partial differential equations, Dokl. Akad. Nauk SSSR 4, pp 532-536 (in Russian).

-
- [55] G. Karniadakis and J. Sherwin (1999): Spectral/ h - p Element Methods for CFD, Oxford University Press.
 - [56] S. Kesavan (1998): *Topics in Functional Analysis and Applications*, Wiley Eastern.
 - [57] V.A. Kondratiev (1967): Boundary value problems for elliptic equations in domains with conical or angular points, *Trans. Moscow Math. Soc.*, 16, 227.
 - [58] V.A. Kondratiev (1970): The smoothness of a solution of Dirichlet's problem for second order elliptic equations in a region with a piecewise smooth boundary, *Differentsial'nye Uravneniya*, 6(10), 1831-1843. *Differential Equations*, 6, 1392-1401.
 - [59] H.O. Kreiss and J. Oliger (1972): Comparison of accurate methods for the integration of hyperbolic equations, *Tellus*, 24, pp 199-215.
 - [60] N.K. Kumar, P.K. Dutt and C.S. Upadhyay (2009): Nonconforming spectral/ $h - p$ element methods for elliptic systems, *Journal of Numerical Mathematics*, Vol. 17, Issue 2, pp 119-142.
 - [61] N. Kishore Kumar, G. Naga Raju (2010): Least-squares $h - p$ /spectral element method for elliptic problems, *Applied Numerical Mathematics*, Vol. 60, 38-54.
 - [62] C. Lanczos (1938): Trigonometric interpolation of empirical and analytical functions, *J. Math. Phys.*, 67, pp 123-199.
 - [63] S.J. Lee, H.S. Oh, J.H. Yun (2001): Extension of the method of auxiliary mapping for three-dimensional elliptic boundary value problems, *Int. J. Numer. Math. Engg.*, 50, pp 1103-1129.
 - [64] J.L. Lions and E. Magenes (1972): Non-homogeneous boundary value problems and applications, Vol II; Springer Verlag, Berlin, Heidelberg, New York.
 - [65] T.R. Lucas and S.H. Oh (1993): The method of auxiliary mappings in the finite element solutions of elliptic boundary value problems containing boundary or corner singularities, *Journal of Computational Physics*, 108, pp 327-342.

-
- [66] C. Mavriplis (1989): *Non-conforming discretizations and a posteriori error estimators for adaptive spectral element techniques*, Ph.D. thesis, Massachusetts Institute of Technology.
- [67] J.T. Oden, L. Demkowicz, W. Rachowicz and T. Westermann (1989): Toward a universal $h-p$ adaptive finite element strategy, Part II: A posteriori error estimation. *Comp. Meth. Appl. Mech. Eng.*, 77, 113.
- [68] S.H. Oh and I. Babuška (1992): The p -version of the finite element method for the elliptic problems with interfaces, *Computer Methods in Applied Mechanics and Engineering*, 97, pp 211-232.
- [69] S.H. Oh and I. Babuška (1995): The method of auxiliary mapping for the finite element solutions of elasticity problems containing singularities, *Journal of Computational Physics*, 121, pp 193-212.
- [70] S.A. Orszag (1969): Numerical methods for the simulation of turbulence, *Phys. Fluids Suppl. II.* 12, pp 250-257.
- [71] S.A. Orszag (1972): Comparison of pseudospectral and spectral approximation, *Stud. Appl. Math.*, 51, pp 253-259.
- [72] S.A. Orszag (1980): Spectral methods for problems in complex geometries, *J. Comput. Phys.*, 37, pp 70-92.
- [73] D. Pathria and G.E. Karniadakis (1995): Spectral element methods for elliptic problems in non-smooth domains, *Journal of Computational Physics*, 122, 83-95.
- [74] M. Proot (2003): *The least-squares spectral element method*, Ph.D. thesis, Delft University of Technology, The Netherlands.
- [75] M. Proot and M.I. Gerritsma (2002): Least-squares spectral elements applied to the Stokes problem, *J. Comput. Phys.*, 181, pp 454-477.

-
- [76] W. Rachowicz, J.T. Oden and L. Demkowicz (1989): Toward a universal $h - p$ adaptive finite element strategy, Part III: Design of $h - p$ meshes. *Comp. Meth. Appl. Mech. Eng.*, 77, 181.
- [77] D. Schötzau, C. Schwab and T.P. Wihler (2009): hp -DGFEM for second order elliptic problems in polyhedra, I: Stability and Quasioptimality on Geometric Meshes, Research Report No. 2009-28, ETH, Zürich.
- [78] D. Schötzau, C. Schwab and T.P. Wihler (2009): hp -DGFEM for second order elliptic problems in polyhedra, II: Exponential Convergence, Research Report No. 2009-29, ETH, Zürich.
- [79] Ch. Schwab (1998): p and $h - p$ Finite element methods, Clarendon Press, Oxford.
- [80] I. Silberman (1954): Planetary waves in the atmosphere, *J. Meteorol*, 11, pp 27-34.
- [81] B. Szabó and I. Babuska (1991): *Finite element analysis*, Wiley, New york.
- [82] B. Szabó and Z. Yosibash (1996): Superconvergent extraction of flux intensity factors and first derivatives from finite element solutions, *Comp. Meth. Appl. Mech. Eng.*, 129, 349.
- [83] J.C. Slater (1934): Electronic energy bands in metal. *Phys. Rev.*, 45, pp 794-801.
- [84] S.K. Tomar, P.Dutt and B.V.Ratish Kumar (2002): An Efficient and Exponentially Accurate Parallel $h - p$ Spectral Element Method for Elliptic Problems on Polygonal Domains - The Dirichlet Case, Lecture Notes in Computer Science 2552, High Performance Computing, Springer Verlag.
- [85] S.K. Tomar (2002): $h - p$ spectral element methods for elliptic problems on non-smooth domains using parallel computers, Ph.D. Thesis, IIT Kanpur, India, 2001. Reprint available as Tec. Rep. no. 1631, Faculty of Mathematical Sciences, University of Twente, The Netherlands. <http://www.math.utwente.nl/publications>.

- [86] S.K. Tomar (2006): $h - p$ Spectral element methods for elliptic problems over non-smooth domains using parallel computers, *Computing* 78, 117-143.
- [87] Toselli, Widlund (2005): Domain decomposition methods-Algorithms and theory, Springer series in computational mathematics.
- [88] H. Walden and R.B. Kellogg (1977): Numerical determination of the fundamental eigenvalue for the Laplace operator in a spherical domain, *J. Eng. Math.*, 11, pp 299-318.
- [89] Wolfgang Kuhnel (2005): Differential Geometry, Curves-Surfaces-Manifolds, Student mathematical library, vol. 96, AMS.
- [90] Z. Yosibash (1997): Numerical analysis of edge singularities in three-dimensional elasticity, *Int. J. Numer. Meth. Eng.*, 40, 4611.
- [91] Z. Yosibash (2000): Computing singular solutions of elliptic boundary value problems in polyhedral domains using p -FEM, *Appl. Numer. Math.*, 33, 71.
- [92] Z. Yosibash and B. Szabó (1995): Numerical analysis of singularities in two dimensions, Part 1: Computation of eigenpairs, *Int. J. Numer. Meth. Eng.*, 38, 2055.
- [93] O.C. Zienkiewicz, Y.K. Cheung (1967): *The Finite Element Method in Structural and Continuum Mechanics*, McGraw-Hill, London.

This figure "logobw.jpg" is available in "jpg" format from:

<http://arxiv.org/ps/1110.2316v1>